JUN 2 6 1933

U. S. DEPARTMENT OF COMMERCE

BUREAU OF STANDARDS JOURNAL OF RESEARCH

Vol. 10 APRIL, 1933 No. 4

CONTENTS

RP. No.	TITLE AND AUTHOR	Page
540.	Infra-red spectra of neon, argon, and krypton. William F. Meggers and C. J. Humphreys	427
541.	Photographic reversal by desensitizing dyes. Burt H. Carroll and C. M. Kretchman	449
542.	1, 1-dimethylcyclopentane and 2-methylhexane in a midcontinent petroleum. Johannes H. Bruun and Mildred M. Hicks-Bruun	465
543.	The combination of silk and wool with positive and negative ions. Milton Harris	475
544.	The preparation and crystallization of pure ether-soluble rubber hydrocarbon: Composition, melting point, and optical properties. W. H. Smith, Charles Proffer Saylor, and Henry J. Wing	479
545.	Wind pressure on a model of the Empire State Building. Hugh L. Dryden and George C. Hill	493
546.	Standard states for bomb calorimetry. Edward W. Washburn	525
547.	The influence of pH on the deterioration of vegetable-tanned leather by sulphuric acid. R. C. Bowker and E. L. Wallace	559
548.	An apparatus for magnetic testing at high magnetic forces. Raymond L. Sanford and Evert G. Bennett	567

Bureau of Standards Journal of Research

CONTENTS OF RECENT NUMBERS

October, 1932 (Vol. 9, No. 4)

RP482. The synthesis, purification, and certain physical constants of the normal hydrocarbons from pentane to dodecane, of *n*-amyl bromide and of *n*-nonyl bromide. B. J. Mair. Price 5 cents.

RP483. A study of some ceramic bodies of low absorption maturing at temperatures below 1,000° C. R. F. Geller and D. N. Evans. Price 5 cents.

RP484. The determination of magnesia in phosphate rock. James I. Hoffman. Price 5 cents.

RP485. Collisions of the first and second kind in the positive column of cæsium discharge. F. L. Mohler. Price 5 cents.

RP486. The areas and tensile properties of deformed concrete-reinforcement bars. A. H. Stang, L. R. Sweetman, and C. Gough. Price 5 cents.

RP487. A calorimetric method for determining the intrinsic energy of a gas as a function of the pressure. Edward W. Washburn. Price 5 cents.

RP488. The photographic emulsion: Variables in sensitization by dyes. Burt H. Carroll and Donald Hubbard. Price 5 cents.

RP489. A method for the separation of rhodium from iridium and the gravimetric determination of these metals. Raleigh Gilchrist. Price 5 cents.

RP490. The isoelectric point of silk. Milton Harris. Price 5 cents.

RP491. Effective applied voltage as an indicator of the radiation emitted by an X-ray tube. Lauriston S. Taylor, George Singer, and C. F. Stoneburner. Price 5 cents.

RP492. Column curves and stress-strain diagrams. William R. Osgood. Price 5 cents.

November, 1932 (Vol. 9, No. 5)

RP493. The variation with angle of emission of the radiation from metals bombarded by slow electrons. C. Boeckner. Price 5 cents.

RP494. Nitrogen content of some standard sample steels. J. G. Thompson and E. H. Hamilton. Price 5 cents.

RP495. Analytical methods for the determination of levulose in crude products. R. F. Jackson, J. A. Mathews, and W. D. Chase. Price 5 cents.

RP496. Determination of alumina and silica in steel by the hydrochloric acid residue method. J. G. Thompson and J. S. Acken. Price 5 cents.

RP497. An analysis of lanthanum spectra La I, La II, La III. Henry Norris Russell and William F. Meggers. Price 10 cents.

RP498. Analysis of weighted silk. Ralph T. Mease. Price 5 cents.

RP499. The heat of formation of hydrogen chloride and some related thermo-dynamic data. Frederick D. Rossini. Price 5 cents.

RP500. Thermal expansion of lead. Peter Hidnert and W. T. Sweeney. Price 5 cents.

December, 1932 (Vol. 9, No. 6)

RP501. Isolation of the three xylenes from an Oklahoma petroleum. Joseph D. White and F. W. Rose, jr. Price 5 cents.

RP502. Characteristic equations of vacuum and gas-filled tungsten-filament lamps. L. E. Barbrow and J. Franklin Meyer. Price 5 cents.

RP503. The calorimetric determination of the intrinsic energy of gases as a function of the pressure. Data on oxygen and its mixtures with carbon dioxide to 40 atmospheres, at 28° C. Frederick D. Rossini and Mikkel Frandsen. Price 5 cents.

RP504. Shear tests of reinforced brick masonry beams. D. E. Parsons, A. H. Stang, and J. W. McBurney. Price 5 cents.

RP505. The measurement of low-voltage X-ray intensities. Lauriston S. Taylor and C. F. Stoneburner. Price 5 cents.

RP506. A multi-range potentiometer and its application to the measurement of small temperature differences. H. B. Brooks and A. W. Spinks. Price 5 cents.

RP507. The density of some soda-lime-silica glasses as a function of the composition. F. W Glaze, J. C. Young, and A. N. Finn. Price 5 cents.

RP508. Coiled-filament resistance thermometers. C. H. Meyers. Price 5 cents.

RP509. Deflection of cosmic rays by a magnetic field. L. F. Curtiss. Price 5 cents.

RP510. The system: CaO-B_2O_3. Elmer T. Carlson.

RP511. A metal-connected glass electrode. M. R. Thompson. Price 5 cents.

Research papers, where price is given, are already available, and others will be available in the near future as separates for purchase from the Superintendent of Documents, United States Government Printing Office, Washington, D. C

U. S. DEPARTMENT OF COMMERCE
DANIEL C. ROPER, Secretary
BUREAU OF STANDARDS
LYMAN J. BRIGGS, Acting Director

BUREAU OF STANDARDS JOURNAL OF RESEARCH

April, 1933
Vol. 10, No. 4

UNITED STATES
GOVERNMENT PRINTING OFFICE
WASHINGTON : 1933

For sale by the Superintendent of Documents, Washington, D. C. - - Price 25 cents; $2.50 per year on subscription

For a partial list of previous research papers appearing in BUREAU OF STANDARDS JOURNAL OF RESEARCH see pages 2 and 3 of the cover

INFRA-RED SPECTRA OF NEON, ARGON, AND KRYPTON

By William F. Meggers and C. J. Humphreys

ABSTRACT

The first spectra of neon, argon, and krypton have been photographed in the infra-red (7,600 to 12,200 A) with two new Eastman emulsions having P and Q types of sensitization with sensitivity maxima at 8,600 and 9,700 A, respectively. The sources were Geissler tubes operated with uncondensed high-voltage a. c. discharges, and the spectrographs were concave gratings of 21 feet radius. About 200 infra-red lines have been photographed in the spectrum of each of the noble gases and analysis has resulted in the confirmation and extension of the tables of spectral terms. Several new hydrogen-like terms from *f*-type electrons have been found in each spectrum, and the 3d terms lacking in the A I and Kr I spectra have all been identified. Many of the new lines can be accurately computed from relative terms and such calculated values may serve as preliminary standards of wave lengths in the infra-red.

CONTENTS

	Page
I. Introduction	427
II. Wave-length measurements	428
III. Results	429
1. Neon	429
2. Argon	437
3. Krypton	443

I. INTRODUCTION

Neutral atoms of the noble gases are characterized by spectra of exceptional utility and rare beauty. Geissler tubes containing these gases at low pressure when excited by moderate electrical discharges, emit spectral lines of high homogeneity which have been demonstrated to be reproducible within 1 part in 50,000,000. These lines are favorably regarded as standards of wave length, and are extensively used in spectroscopy and metrology. It is not unlikely that one of these lines may ultimately be chosen as the most practical and permanent primary standard of length, especially if an even-numbered isotope can be segregated so that the strongest lines will be free from hyperfine structure.

From a theoretical viewpoint the first spectra of the noble gases are of special interest because they arise in each case from a "closed shell" configuration of electrons, and unlike other complex spectra they are found to consist of extended series of relatively simple types (S,P,D,F terms) and low multiplicities (singlets and triplets). Evidence of a gradual transition from *sl* to *jj* electron coupling as the atomic complexity increases adds interest to a comparison of the spectral structures of all the noble gases.

Both practical and theoretical considerations have been responsible for intensive investigations of the noble gas spectra, and especially for efforts to extend observations to the region of greater wave lenghts. Except for a relatively small number of lines in the extreme ultra-violet, each of these spectra exhibits several group series beginning in the red or infra-red and converging to limits in the near ultra-violet or in the visible region. The fact that many of the intrinsically strongest lines of these spectra occur in the infra-red accounts for the

successful photography of a considerable proportion of them even with relatively insensitive materials. Thus the most energetic infra-red lines of Ne, A, Kr, and Xe had already been detected photographically to about 1 μ with dicyanine or neocyanine sensitized plates when about a year ago the vastly superior infra-red sensitizers, mesocyanine and xenocyanine, were discovered. As soon as the new photographic plates became available for spectrography, the spectroscopy section of this bureau applied them to explorations of infra-red emission spectra, including those characteristic of the noble gases. Preliminary results on this group were reported [1] at a meeting of the American Physical Society last April. In the meantime the observations have been repeated and extended, and details have been published for two of these elements, viz, He [2] and Xe.[3] Data for the intermediate gases, Ne, A, and Kr, are now presented, they consist of wave-length measurements, estimated intensities and series classifications of infra-red lines in the wave length interval 7,600 to 12,200 A. These results are to be regarded as preliminary or exploratory; they were obtained with spectrographs of moderate dispersion, but the accuracy of measurement is sufficient for purposes of spectral structure analysis, and for the determination of retardations in future interferometric comparisons. Wave lengths corresponding to the stronger lines are being measured with increased precision by the Fabry-Perot interferometer method and will be presented in a subsequent paper on standard wave lengths in the infra-red. In the meantime values computed from accurately fixed relative terms may serve as proper standards in this range, since the accuracy of such calculated values may be expected to exceed that of the preliminary observations.

The spark spectra of the heavier noble gases are also rich in infra-red lines, but their description is reserved for later publication.

II. WAVE-LENGTH MEASUREMENTS

Geissler tubes of glass purchased from Robert Goetze in Leipzig served as sources of radiation. Each tube has two cylindrical electrode bulbs connected by a capillary of 11 cm length and about 1 mm bore, the viewing end of which is inclosed in a thin-walled glass bulb of 2.5 cm diameter. Such tubes can be viewed either side on or end on, the latter being preferred on account of increased intensity.[4] In the experiments here reported the tube was always mounted with its capillary on the axis of the spectrograph with the viewing end directed toward the slit, the capillary bore being imaged on the slit with a condensing lens.

The tubes were filled with exceptionally pure gases at sufficient pressure to insure relatively long life in spite of gradual gas disappearance accompanying electrode sputtering. To produce the first spectrum the tube was operated with uncondensed electrical discharges from a. c. transformers, the current through the tube being about 20 ma. Under these conditions no spark lines appeared in the spectral interval under investigation. Spectrochemical analysis revealed a trace of O in the Ne, no impurities in the A, a small amount of A and Xe in the Kr and a trace of Kr in the Xe.

---

[1] W. F. Meggers and C. J. Humphreys, Phys. Rev., vol. 40, p. 1040, 1932.
[2] W. F. Meggers and G. H. Dieke, B. S. Jour. Research, vol. 9 (RP462), p. 121, 1932.
[3] C. J. Humphreys and W. F. Meggers, B. S. Jour. Research, vol. 10, (RP521) p. 139, 1933.
[4] End-on use of these sources is objectionable in interferometry on account of self-reversal phenomena then appearing on lines involving normal or metastable states.

The spectrograms were made with two concave diffraction gratings of 21 feet radius of curvature, each mounted in parallel light from a mirror of similar radius.[5] One grating has 20,000 lines per inch and the other 7,500 lines per inch, their scales in the first-order red spectrum are 3.7 and 10.2 A/mm, respectively. The larger dispersion was applied to the interval 7,600 to 9,200 A, while the smaller scale was used over the entire range 7,600 to 12,200 A. On each spectrogram the spectrum of the iron arc was recorded in the second and third orders of the grating alongside the spectrum of the noble gas which was photographed in the first order with a red glass filter in front of the slit to remove overlapping higher orders. Wave-length measurements were then made relative to international standards in the iron spectrum, doubling or trebling their values to obtain effective standards in the infra-red range. The final scale of these measurements was adjusted slightly to bring it into accord with preliminary values derived from interferometer comparisons of the stronger lines. Wave-length measurements from the larger scale spectrograms should not contain errors exceeding one or two hundredths of an angstrom unit, but the remainer may have an average error two or three times as large.

Exposure times were usually 16 to 24 hours, but one 48-hour exposure was made for each gas in order to record as many lines as possible beyond 11,000 A where the photographic sensitivity is very low. Under these conditions the stronger lines were tremendously overexposed, and were accompanied by numerous Rowland ghosts from which the wave length of the parent line could be derived with higher accuracy than from measurements of the greatly widened primary image. All such ghosts were removed from the final lists. Lyman ghosts [6] were sought but only one was found, a line observed for Kr at 12,282 A being interpreted as (7/5–1/1,500) 8,776.75 A.

Photographic plates with P and Q types of sensitizing as prepared by the research laboratory of the Eastman Kodak Co.[7] were employed. These plates are sensitized to infra-red radiation with new dyes which have been named mesocyanine and xenocyanine. The former has a relatively narrow sensitizing band with a strong maximum at 8,600 A, while the latter has a much broader band with a maximum action at wave length 9,700 A. The P-type plates were used in the interval 7,600 to 9,200 A, and the Q-type in the range 8,500 to 12,200 A. Both types of plates were hypersensitized by bathing from 1 to 5 minutes in a dilute ammonia solution, rinsing in alcohol, and drying in a current of air. After exposure they were developed for 5 minutes in Eastman's X-ray developer at a temperature of about 18° C.

III. RESULTS

1. NEON

Paschen's [8] description and analysis of the spectrum of neon has served as a model for the remaining noble gases. A special notation which was proposed by Paschen to represent the spectral terms of neon has been retained in describing the first spectrum of the remaining gases of this group. A translation into the notation now in general use, while highly desirable, is not feasible at present, because of the

[5] W. F. Meggers and Kelvin Burns, B. S. Sci. Papers, vol. 18 (S441), p. 191, 1922.
[6] W. F. Meggers and C. C. Kiess, J. Opt. Soc. Am. and Rev. Sci. Inst., vol. 6, p. 417, 1922.
[7] C. E. K. Mees, J. Opt. Soc. Am. vol. 22, p. 204, 1932. Addendum, April, 1932.
[8] F. Paschen, Ann. der Physik, vol. 60, p. 405, 1919.

overlapping of the multiplets, the fact that the Landé interval rule and theoretical Zeeman effects are usually violated in these spectra, and on account of ambiguities in the correlation of levels with their series limits. Nothing was added to the results for neon until Gremmer[9] found some new lines by exposing neocyanine plates 36 to 60 hours. These additional lines fixed, by means of new combinations, four 2s terms for which only series interpolated values could be given by Paschen. Altogether Gremmer added 27 classified lines to the infra-red between 7,944.22 and 9,665.40 A. By employing an efficient spectograph, an intense source, and very long exposures, Rasmussen[10] recorded on neocyanine plates 7 new lines in the neon spectrum (10,296 to 11,178 A), which were classified as 2p–2s combinations.

The infra-red spectrum of neon was investigated with a spectrometer, thermopile, and galvanometer by Hardy[11], who observed 30 lines ranging in wave length from 9,667.6 to 18,552 A. We have recorded 16 of these lines photographically, the last one being 12,066.4 A, and have adopted Hardy's values for the remainder, with a correction of −2.6 A applied to them, since the lines observed by both methods differ by this amount on the average. Comparison of galvanometer deflections with estimated photographic intensities gives a rough calibration of the spectral sensitivity of a xenocyanine plate; at 11,000 A the sensitivity is less than one-tenth that of the maximum near 9,700 A and at 12,000 A it has declined to less than one one-thousandth.

Complete results now available for the infra-red spectrum of neon are presented in Table 1, where the intensity, observed wave length, vacuum wave number, symbolic-term difference, and numerical-term difference appear in successive columns. Wave lengths given to 3 decimals are quoted from Paschen's publication; they represent interferometer measurements of high precision. The vacuum wave numbers were taken from Kayser's[12] table for wave lengths up to 10,000 A, beyond which they were obtained by computing the reciprocal of the wave lengths corrected to vacuum values with the aid of the atmospheric dispersion formula of Meggers and Peters.[13]

TABLE 1.—*Infra-red spectrum of neon*

Intensity	λ_{air} I. A.	ν_{vac} cm^{-1} observed	Term combination	ν_{vac} cm^{-1} calculated
Hardy	Hardy			
1	18, 549	5, 389. 7	$3d_1'$–4W	5, 390
1	18, 430	5, 424. 5	$3s_1'''$–4V	5, 425. 2
2	18, 386. 4	5, 437. 32	$3s_1'''$–4T	5, 437. 2
			$3s_1''''$–4U	5, 438. 1
1	18, 306. 4	5, 461. 08	$3d_3$–4Y	5, 462. 02
3	18, 271. 4	5, 471. 54	$3d_5$–4Z	5, 471
1	18, 078. 4	5, 529. 96	$3d_5$–4X	5, 528. 50
1	17, 165. 4	5, 824. 08	$2p_1$–$2s_4$	5, 825. 25
2	15, 234. 4	6, 562. 28	$2p_1$–$2s_2$	6, 563. 85
1	13, 219. 4	7, 562. 58	$2p_2$–$2s_5$	7, 562. 69

[9] W. Gremmer, Zeitschr. f. Phys., vol. 50, p. 716, 1928.
[10] E. Rasmussen, Dissertation, Copenhagen, 1932.
[11] J. D. Hardy, Phys. Rev., vol. 38, p. 2162, 1931.
[12] H. Kayser, Tabelle der Schwingungszahlen, Leipzig, 1925.
[13] W. F. Meggers and C. G. Peters, B. S. Sci. Papers, vol. 14 (S327), p. 722, 1918.

TABLE 1.—*Infra-red spectrum of neon*—Continued

Intensity	λ_{air} I. A.	ν_{vac} cm^{-1} observed	Term combination	ν_{vac} cm^{-1} calculated
Hardy	Hardy			
2	12, 912. 4	7, 742. 40	$2p_4$–$2s_5$	7, 742. 63
0. 3	12, 767. 4	7, 830. 30	$2p_5$–$2s_5$	7, 829. 03
2	12, 690. 1	7, 877. 99	$2p_3$–$2s_4$	7, 878. 54
1	12, 594. 8	7, 937. 64	$2p_4$–$2s_4$	7, 937. 47
1	12, 458. 4	8, 024. 52	$2p_5$–$2s_4$	8, 023. 87
B. S.	B. S.			
1	12, 066. 4	8, 285. 21	$2p_6$–$2s_5$	8, 285. 28
1	11, 985. 1	8, 341. 40	$2p_3$–$2s_3$	8, 341. 53
3	11, 789. 0	8, 480. 17	$2p_6$–$2s_4$	8, 480. 12
4	11, 766. 9	8, 496. 10	$2p_3$–$2s_2$	8, 496. 13
1	11, 688. 1	8, 553. 37	$2p_1$–$3d_5$	8, 553. 485
3	11, 614. 20	8, 607. 80	$2p_5$–$2s_3$	8, 607. 87
2	11, 536. 35	8, 665. 89	$2p_1$–$3d_2$	8, 665. 865
4	11, 525. 10	8, 674. 34	$2p_7$–$2s_4$	8, 674. 38
8	11, 522. 83	8, 676. 05	$2p_4$–$2s_2$	8, 676. 07
4	11, 499. 27	8, 762. 41	$2p_5$–$2s_2$	8, 762. 47
5	11, 390. 50	8, 776. 85	$2p_8$–$2s_5$	8, 776. 92
15	11, 177. 51	8, 944. 09	$2p_9$–$2s_5$	8, 944. 10
30	11, 143. 04	8, 971. 76	$2p_8$–$2s_4$	8, 971. 76
1	11, 120. 3	8, 990. 11	$2s_2$–$4p_8$	8, 990. 16
3	11, 049. 6	9, 047. 63	$2s_5$–$4p_6$	9, 047. 60
2	11, 044. 1	9, 052. 13	$2s_2$–$4p_1$	9, 052. 43
2	11, 020. 8	9, 071. 27	$2s_4$–$4p_3$	9, 071. 32
3	10, 888. 4	9, 181. 57	$3d_1'$–6Z	9, 181. 6
2	10, 886. 1	9, 183. 51	$3d_1''$–6Z	9, 183. 4
200	10, 844. 47	9, 218. 77	$2p_6$–$2s_2$	9, 218. 72
4	10, 830. 33	9, 230. 80		
2	10, 819. 9	9, 239. 70	$3s_1''$–6U	9, 239. 92
1	10, 814. 7	9, 244. 1	$3d_2$–6Y	9, 244. 2
2	10, 808. 1	9, 249. 8	$3s_1'''$–6U	9, 249. 68
2	10, 806. 3	9, 251. 3	$3s_1''''$–6U	9, 251. 24
100	10, 798. 02	9, 258. 42	$2p_7$–$2s_3$	9, 258. 38
2	10, 780. 40	9, 273. 56	$3d_3$–7Y	9, 273. 6
3	10, 766. 03	9, 285. 93	$3d_1'$–6W	9, 285. 93
4	10, 763. 98	9, 287. 70	$3d_1''$–6W	9, 287. 70
1?	10, 760. 4	9, 290. 8	$3d_4$–6Z	9, 290. 9
1?	10, 758. 2	9, 292. 7	$3d_4'$–6Z	9, 292. 7
3	10, 690. 35	9, 351. 67	$3d_5$–6X	9, 351. 64
1	10, 673. 7	9, 366. 3	$3d_6$–6X	9, 366. 28
30	10, 620. 63	9, 413. 01	$2p_7$–$2s_2$	9, 412. 98
300	10, 562. 38	9, 564. 97	$2p_1$–$3s_1'$	9, 464. 941
3	10, 432. 53	9, 582. 77	$2s_4$–$4p_4$	9, 582. 82
80	10, 295. 40	9, 710. 41	$2p_8$–$2s_2$	9, 710. 36
1	10, 267. 0	9, 737. 28		
7	10, 245. 70	9, 757. 51	$2s_5$–$4p_2$	9, 757. 56
2	10, 224. 6	9, 777. 65	$2s_5$–$4p_4$	9, 777. 66
2	10, 210. 73	9, 790. 93	$2s_4$–$4p_1$	9, 791. 03
3	10, 091. 53	9, 906. 59	$3s_1'''$–8W	9, 906. 5
1	10, 057. 6	9, 940. 0		
2	10, 038. 9	9, 958. 5	$3d_1'$–6U	9, 958. 47
2	10, 037. 1	9, 960. 3	$3d_1''$–6U	9, 960. 24

TABLE 1.—*Infra-red spectrum of neon*—Continued

Intensity	λ_{air} I. A.	ν_{vac} cm^{-1} observed	Term combination	ν_{vac} cm^{-1} calculated
B. S.	B. S.			
4	10, 008. 55	9, 988. 72	$3d_1'$–7Y	9, 988. 68
30	10, 007. 31	9, 989. 96	$3d_1'$–7Z	9, 989. 94
20	10, 005. 54	9, 991. 72	$3d_1''$–7Z	9, 991. 71
1	10, 000. 9	9, 996. 4		
2	9, 974. 2	10, 023. 1	$3d_2$–6U	10, 023. 27
6	9, 963. 55	10, 033. 84	$3s_1'$–7U	10, 033. 82
15	9, 947. 94	10, 049. 58	$3s_1''$–7U	10, 049. 54
2	9, 944. 9	10, 052. 6	$3d_3$–6U	10, 052. 68
7h	9, 944. 1	10, 053. 5	$3d_2$–7Y	10, 053. 48
15	9, 938. 35	10, 059. 28	$3s_1'''$–7U	10, 059. 30
10	9, 936. 83	10, 060. 81	$3s_1''''$–7U	10, 060. 86
4	9, 918. 52	10, 079. 39	$3d_3$–7X	10, 079. 40
20	9, 915. 13	10, 082. 83	$3d_3$–7Y	10, 082. 89
30	9, 902. 31	10, 095. 89	$3d_1'$–7W	10, 095. 88
40	9, 900. 58	10, 097. 64	$3d_1''$–7W	10, 097. 65
2	9, 899. 06	10, 099. 20	$3d_4$–7Z	10, 099. 21
3	9, 897. 30	10, 101. 00	$3d_4$–7Z	10, 101. 04
2	9, 875. 90	10, 122. 88	$3d_1''$–$6p_5$	10, 122. 7
20	9, 837. 47	10, 162. 43	$3d_5$–7X	10, 162. 37
5	9, 823. 42	10, 176. 97	$3d_2$–$6p_1$	10, 176. 90
1	9, 807. 0	10, 194. 0		
2	9, 788. 1	10, 213. 7	$2s_2$–$5p_{10}$	10, 213. 58
2	9, 760. 57	10, 242. 50		
1	9, 744. 2	10, 259. 7		
1	9, 741. 3	10, 262. 9	$3d_6$–$7p_{10}$?	10, 263. 4
1	9, 728. 2	10, 276. 6	$3s_1''$–9W	10, 276. 74
1	9, 724. 8	10, 280. 2	$2s_2$–$5p_8$	10, 280. 16
3	9, 702. 40	10, 303. 90	$3d_5$–$6p_4$	10, 303. 8
1, 000	9, 665. 426	10, 343. 33	$2p_{10}$–$2s_5$	10, 343. 34
3	9, 658. 5	10, 350. 7		
1	9, 642. 2	10, 368. 2	$2s_3$–$5p_{10}$	10, 368. 18
2	9, 620. 8	10, 391. 3		
5	9, 592. 19	10, 422. 29		
3	9, 584. 79	10, 430. 34		
2	9, 573. 99	10, 442. 10	$2s_2$–$5p_3$	10, 442. 22
300	9, 547. 40	10, 471. 18	$2p_2$–$3d_6$	10, 471. 128
500	9, 534. 17	10, 485. 71	$2p_2$–$3d_5$	10, 485. 770
5?+g	9, 508. 4	10, 514. 1	$3d_1''$–8Z	10, 513. 82
3	9, 506. 59	10, 516. 14		
2	9, 497. 9	10, 525. 8		
500	9, 486. 68	10, 538. 21	$2p_{10}$–$2s_4$	10, 538. 18
2h	9, 467. 8	10, 559. 2	$3s_1'$–8U	10, 559. 1
300	9, 459. 21	10, 568. 81	$2p_2$–$3d_3$	10, 568. 744
1	9, 454. 0	10, 574. 6	$3s_1''$–8U	10, 574. 8
10	9, 452. 08	10, 576. 78	$3d_2$–8Z?	10, 576. 85
3	9, 445. 26	10, 584. 42	$3d_2$–8Y $3s_1'''$–8U	10, 584. 41 10, 584. 5
2	9, 443. 8	10, 586. 1	$3s_1''''$–8U	10, 586. 1
40	9, 432. 94	10, 598. 24	$2p_2$–$3d_2$	10, 598. 150
500	9, 425. 38	10, 606. 74	$2p_3$–$3d_5$	10, 606. 782

TABLE 1.—*Infra-red spectrum of neon*—Continued

Intensity	λ_{air} I. A.	ν_{vac} cm^{-1} observed	Term combination	ν_{vac} cm^{-1} calculated
B. S.	B. S.			
4	9, 412. 32	10, 621. 46	$3d_4$–8Z	10, 621. 32
6	9, 410. 75	10, 623. 23	$3d_4'$–8Z	10, 623. 15
8	9, 405. 75	10, 628. 88	$3d_4$–8Y	10, 628. 88
2	9, 393. 8	10, 642. 4		
5	9, 377. 2	10, 661. 2	$2p_2$–$3d_1''$	10, 661. 187
200	9, 373. 28	10, 665. 70	$2p_4$–$3d_5$	10, 665. 711
3	9, 353. 3	10, 688. 5	$3d_5$–8X	10, 688. 48
2	9, 340. 5	10, 703. 1	$3d_6$–8X	10, 703. 12
1?	9, 335. 0	10, 709. 4	$3d_3$–8W	10, 709. 5
600	9, 326. 52	10, 719. 17	$2p_3$–$3d_2$	10, 719. 162
300	9, 313. 98	10, 733. 61	$2p_4$–$3d_4$	10, 733. 621
150	9, 310. 58	10, 737. 52	$2p_5$–$3d_6$	10, 737. 467
600	9, 300. 85	10, 748. 76	$2p_4$–$3d_3$	10, 748. 685
100	9, 275. 53	10, 778. 10	$2p_4$–$3d_2$	10, 778. 091
1	9, 237. 4	10, 822. 6		
200	9, 226. 67	10, 835. 17	$2p_5$–$3d_3$	10, 835. 083
200	9, 221. 59	10, 841. 14	$2p_4$–$3d_1''$	10, 841. 128
400	9, 220. 05	10, 842. 95	$2p_4$–$3d_1'$	10, 842. 893
1?	9, 214. 5	10, 849. 5	$3d_1'$–1, 378. 6	10, 849. 5
2	9, 212. 9	10, 851. 4	$3d_1''$–1,378.6	10, 851. 3
600	9, 201. 76	10, 864. 51	$2p_5$–$3d_2$	10, 864. 489
1?	9, 193. 8	10, 873. 9	$3d_1''$–$7p_5$	10, 874. 0
3	9, 191. 8	10, 876. 3		
600	9, 148. 68	10, 927. 54	$2p_5$–$3d_1''$	10, 927. 526
1	9, 123. 2	10, 958. 1	$3d_4$–1, 378. 6	10, 958. 7
20	9, 121. 14	10, 960. 54	$3d_4'$–1, 378.6	10, 960. 5
1?	9, 115. 3	10, 967. 6	$3d_3$–9Y	10, 967. 6
1	9, 111. 8	10, 971. 8		
3	9, 103. 53	10, 981. 74	$3d_4$–9Z	10, 981. 74
1	9, 102. 1	10, 983. 5	$3d_4'$–9Z	10, 983. 57
3	9, 094. 9	10, 992. 1		
1	9, 088. 5	10, 999. 9		
1	9, 078. 2	11, 012. 4		
8	9, 073. 04	11, 018. 64	$2s_4$–$5p_8$	11, 018. 66
2	9, 069. 7	11, 022. 7		
1	9, 062. 6	11, 031. 3		
1	9, 061. 5	11, 032. 7		
6	9, 052. 54	11, 043. 60	$2s_4$–$5p_7$	11, 043. 52
3	9, 049. 06	11, 047. 84	$2s_4$–$5p_6$	11, 047. 88
1	9, 046. 8	11, 050. 6	$3d_5$–9Y	11, 050. 6
2	9, 045. 4	11, 052. 3		
3	9, 039. 0	11, 060. 1	$3d_2$–9W	11, 060. 09
6	9, 036. 98	11, 062. 61	$2s_2$–$5p_4$	11, 062. 72
200	8, 988. 58	11, 122. 18	$2p_{10}$–$2s_3$	11, 122. 18
2	8, 968. 6	11, 146. 9	$2s_5$–$5p_{10}$	11, 147. 02
3	8, 962. 34	11, 154. 74	$2s_2$–$5p_1$	11, 154. 83
7	8, 948. 12	11, 172. 47	$3d_5$–9W	11, 172. 47
6	8, 941. 47	11, 180. 78	$2s_4$–$5p_3$	11, 180. 82
10	8, 929. 24	11, 196. 09	$2s_5$–$5p_9$	11, 196. 03
2	8, 927. 4	11, 198. 4	$2s_3$–$5p_2$	11, 198. 49

TABLE 1.—*Infra-red spectrum of neon*—Continued

Intensity	λ_{air} I. A.	ν_{vac} cm^{-1} observed	Term combination	ν_{vac} cm^{-1} calculated
B. S.	B. S.			
300	8, 919. 50	11, 208. 31	$2p_5$–$3d_5$	11, 208. 353
3	8, 915. 44	11, 213. 42	$2s_5$–$5p_8$	11, 213. 60
3	8, 913. 0	11, 216. 5		
2	8, 895. 6	11, 238. 4	$2s_5$–$5p_7$	11, 238. 36
10	8, 892. 22	11, 242. 70	$2s_5$–$5p_6$	11, 242. 72
500	8, 865. 76	11, 276. 25	$2p_{10}$–$2s_2$	11, 276. 263
100	8, 865. 33	11, 276. 80	$2p_6$–$3d_4$	11, 276. 78
700	8, 853. 88	11, 291. 39	$2p_6$–$3d_3$	11, 291. 327
2	8, 842. 1	11, 306. 4		
50	8, 830. 92	11, 320. 74	$2p_6$–$3d_2$	11, 320. 733
6	8, 820. 36	11, 334. 30		
30	8, 792. 51	11, 370. 20	$2p_2$–$3s_1''''$	11, 370. 185
1, 000	8, 783. 78	11, 381. 50	$2p_2$–$3s_1'''$	11, 381. 505
50	8, 782. 01	11, 383. 79	$2p_6$–$3d_1''$	11, 383. 770
1, 200	8, 780. 65	11, 385. 56	$2p_6$–$3d_1'$	11, 385. 535
150	8, 778. 75	11, 388. 02	$2p_7$–$3d_6$	11, 387. 977
400	8, 771. 70	11, 397. 17	$2p_3$–$3s_1'$	11, 397. 226
15	8, 767. 55	11, 402. 57	$2p_7$–$3d_5$	11, 402. 619
200	8, 704. 15	11, 485. 62	$2p_7$–$3d_3$	11, 485. 593
500	8, 681. 94	11, 515. 00	$2p_7$–$3d_2$	11, 514. 999
500	8, 679. 51	11, 518. 23	$2p_3$–$3s_1'$	11, 518. 238
400	8, 654. 51	11, 550. 17	$2p_4$–$3s_1''''$	11, 550. 126
1, 500	8, 654. 380	11, 551. 673	$2p_4$–$3s_1'''$	11, 551. 687
300	8, 647. 05	11, 561. 46	$2p_4$–$3s_1''$	11, 561. 446
50	8, 635. 31	11, 577. 18	$2p_4$–$3s_1'$	11, 577. 167
600	8, 634. 668	11, 578. 044	$2p_7$–$3d_1''$	11, 578. 036
400	8, 591. 266	11, 636. 535	$2p_5$–$3s_1''''$	11, 636. 524
60	8, 582. 91	11, 647. 86	$2p_5$–$3s_1''$	11, 647. 844
100	8, 571. 36	11, 663. 56	$2p_5$–$3s_1'$	11, 663. 565
60	8, 544. 70	11, 699. 95	$2p_8$–$3d_5$	11, 699. 996
500	8, 495. 359	11, 767. 904	$2p_8$–$3d_4$	11, 767. 906
80	8, 484. 45	11, 783. 03	$2p_8$–$3d_3$	11, 782. 970
150	8, 463. 37	11, 812. 38	$2p_8$–$3d_2$	11, 812. 376
400	8, 418. 447	11, 875. 416	$2p_8$–$3d_1''$	11, 875. 413
100	8, 417. 18	11, 877. 20	$2p_8$–$3d_1'$	11, 877. 178
800	8, 377. 630	11, 933. 274	$2p_9$–$3d_4'$	11, 933. 260
200	8, 376. 41	11, 935. 02	$2p_9$–$3d_4$	11, 935. 088
150	8, 365. 75	11, 950. 22	$2p_9$–$3d_3$	11, 950. 152
150	8, 301. 54	12, 042. 65	$2p_9$–$3d_1''$	12, 042. 595
600	8, 300. 338	12, 044. 396	$2p_9$–$3d_1'$	12, 044. 360
80	8, 267. 11	12, 092. 81	$2p_6$–$3s_1''''$	12, 092. 768
250	8, 266. 092	12, 094. 293	$2p_6$–$3s_1'''$	12, 094. 329
150	8, 259. 392	12, 104. 105	$2p_5$–$3s_1''$	12, 104. 088
30	8, 248. 70	12, 119. 80	$2p_6$–$3s_1'$	12, 119. 809
300	8, 136. 423	12, 287. 039	$2p_7$–$3s_1''''$	12, 287. 034
60	8, 128. 93	12, 298. 36	$2p_7$–$3s_1''$	12, 298. 354
100	8, 118. 554	12, 314. 088	$2p_7$–$3s_1'$	12, 314. 075
2	8, 093. 08	12, 352. 84	$2s_4$–$6p_3$	12, 352. 85
200	8, 082. 460	12, 369. 074	$1s_2$–$2p_{10}$	12, 369. 077
1	8, 076. 06	12, 378. 88	$2s_2$–$6p_1$	12, 378. 92

TABLE 1.—*Infra-red spectrum of neon*—Continued

Intensity	λ_{air} I. A.	ν_{vac} cm^{-1} observed	Term combination	ν_{vac} cm^{-1} calculated
B. S.	B. S.			
2	8, 041. 79	12, 431. 63	$2s_5$–$6p_9$	12, 431. 77
2	8, 024. 11	12, 459. 02	$2s_5$–$6p_6$	12, 459. 16
20	7, 944. 16	12, 584. 41	$2p_8$–$3s_1''''$	12, 584. 411
200	7, 943. 193	12, 585. 938	$2p_8$–$3s_1'''$	12, 585. 972
70	7, 937. 00	12, 595. 76	$2p_8$–$3s_1''$	12, 595. 731
40	7, 927. 13	12, 611. 44	$2p_8$–$3s_1'$	12, 611. 452
1	7, 840. 04	12, 751. 53	$2p_9$–$3s_1''''$	12, 751. 593
30	7, 839. 08	12, 753. 10	$2p_9$–$3s_1'''$	12, 753. 154
7	7, 833. 06	12, 762. 90	$2p_9$–$3s_1''$	12, 762. 913
10	7, 724. 63	12, 942. 05	$2p_1$–$3s_4$	12, 942. 039
(Paschen)	(Paschen)			
0. 5	2, 994. 410	33, 385. 84	$1s_4$–4V	33, 385. 9
1	2, 994. 250	33, 387. 63	$1s_4$–4U	33, 387. 5
2	2, 957. 293	33, 804. 85	$1s_5$–4U	33, 804. 9
0. 5	2, 957. 148	33, 806. 50	$1s_5$–4T	33, 806. 5
3	2, 755. 82	36, 276. 2	$1s_5$–5U	36, 276. 2

Wave lengths exceeding 12,066.4 A are quoted from Hardy's paper, with a correction of −2.6 A. Analysis of these data showed that a large majority of the 200 infra-red lines observed for neon could be accounted for as combinations of established terms, thus confirming the identity of these terms. About 60 faint lines between 9,100 and 10,900 A appear to represent combinations of $3d$ terms with higher members of f-type series, and most of these lines have been so classified. Only two terms of this type, $4x$ and $4y$ were known heretofore. Hardy states that "the lines in the region around 1.8 μ are apparently due to combinations between the $3d$ levels and the x and y groups, and although the wave lengths have been checked as well as possible the agreement with the calculated frequencies from the known terms does not check very well with the experimental values." Our interpretation of these lines accounts for only two of them as combinations $3d$–$4x, y$ while the remainder appear to be combinations $3d$–$4z, u, v, w, t$, thus adding five new f-type terms. Three of the latter, $4u, v, t$ are first members of non-Ritzian series and are checked by combinations with $1s$ terms which represent previously unclassified lines in the ultra-violet, now presented at the end of Table 1. The infra-red data are insufficient to establish any of the 5 f terms with certainty, but their approximate values can be obtained from interpolation.

In order to facilitate the comparison of results in Table 1 with the identified spectral terms of neon the latter are collected in Table 2. These data have not been presented in this condensed form heretofore.

TABLE 2.—*Terms in the Ne I spectrum*

Electron	j	Term, Paschen notation	$m=$ 1	2	3	4	5	6	7	8	9	10	11	12	13
s	2	s_5	39, 887. 610	15, 328. 31	8, 101. 291	5, 004. 811	3, 396. 713	2, 456. 121	1, 858. 065	1, 454. 136	1, 169. 614	960. 902	803. 40		
	1	s_4	39, 470. 160	15, 133. 47	8, 016. 679	4, 962. 103	3, 372. 371	2, 439. 967	1, 848. 546	1, 447. 593	1, 164. 914	957. 058	800. 659		
	0	s_3	39, 110. 808	14, 549. 47	7, 323. 132	4, 223, 467	2, 616. 576	1, 675. 101	1, 077. 331	674. 195	403. 51				
	1	s_2	38, 040. 731	14, 394. 87	7, 272. 964	4, 201. 806	2, 605. 422	1, 667. 672	1, 072. 452	670. 006	400. 011				
p	1	p_{10}		25, 671. 654	11, 411. 490	6, 479. 926	4, 181. 293	2, 920. 09	2, 156. 5						
	3	p_9		24, 272. 411	11, 098. 710	6, 370. 29	4, 132. 28	2, 896. 54	2, 142. 4	1, 647. 2	1, 306. 2				
	2	p_8		24, 105. 229	11, 030. 293	6, 338. 150	4, 114. 714	2, 885. 75	2, 137. 8	1, 642. 6					
	1	p_7		23, 807. 852	10, 916. 780	6, 289. 812	4, 089. 950	2, 871. 44	2, 126. 25	1, 638. 0	1, 299. 2	1, 057. 5			
	2	p_6		23, 613. 586	10, 891. 040	6, 280. 708	4, 085. 59	2, 869. 15	2, 126. 25	1, 638. 0	1, 299. 2	1, 057. 5			
	1	p_5		23, 157. 342	10, 272. 127	5, 573. 896	3, 344. 458	2, 107. 1	1, 355. 8	864. 0					
	2	p_4		23, 070. 944	10, 220. 817	5, 550. 650	3, 332. 150	2, 101. 4	1, 356. 0						
	0	p_2		23, 012. 015	10, 528. 095	6, 062. 146	3, 952. 655	2, 780. 615	2, 015. 951	1, 602. 1					
	1	p_3		22, 891. 003	10, 221. 687	5, 570. 750	3, 350. 981	2, 126. 25							
	0	p_1		20, 958. 718	9, 643. 510	5, 342. 445	3, 240. 040	2, 015. 95	1, 264. 31	747. 9	422. 9	232. 8	115. 4		
d	3	d_1'			12, 228. 051	6, 880. 789	4, 402. 564	3, 056. 202	2, 243. 920	1, 718. 220	1, 357. 220	1, 099. 190	908. 168	762. 926	646. 478
	2	d_1''			12, 229. 816	6, 881. 853	4, 403. 132	3, 056. 560	2, 244. 170	1, 718. 368	1, 357. 326	1, 099. 246	808. 489	763. 290	
	1	d_2			12, 292. 853	6, 902. 485	4, 412. 438	3, 061. 514	2, 246. 577	1, 720. 345	1, 358. 594	1, 100. 153			
	2	d_3			12, 322. 259	6, 917. 919	4, 420. 888	3, 066. 464	2, 248. 114	1, 722. 661	1, 360. 060	1, 101. 547	909. 370	764. 337	649. 298
	4	d_4'			12, 339. 151	6, 929. 461	4, 427. 771	3, 070. 961	2, 254. 011	1, 724. 341	1, 361. 571	1, 102. 311	910. 561	764. 961	651. 371
	3	d_4			12, 337. 323	6, 928. 369	4, 427. 148	3, 070. 547	2, 253. 703	1, 724. 170	1, 361. 431	1, 102. 214	910. 56	764. 96	651. 29
	1	d_5			12, 405. 233	6, 954. 126	4, 441. 035	3, 078. 128	2, 257. 525	1, 727. 573	1, 363. 532	1, 103. 978	911. 541	765. 843	651. 944
	0	d_6			12, 419. 875	6, 961. 797	4, 446. 443	3, 081. 236	2, 260. 272	1, 729. 075	1, 364. 545	1, 104. 860	912. 032		
	1	s_1'			11, 493. 777	6, 121. 687	3, 633. 432	2, 284. 565	1, 468. 399	940. 428	578. 638	319. 942			
	2	s_2''			11, 509. 498	6, 132. 505	3, 640. 106	2, 287. 288	1, 471. 002	942. 297	579. 982	320. 977			
	3	s_1'''			11, 519. 257	6, 133. 562	3, 639. 752	2, 287. 022	1, 470. 822	942. 209	579. 922	320. 899			
	2	s_1''''			11, 520. 818	6, 134. 473	3, 640. 473	2, 289. 452	1, 471. 550	942. 349	579. 931	320. 931			
f	1	X				6, 876. 73		3, 053. 59	2, 242. 86	1, 716. 75					
	2	Y				6, 860. 24	(4, 390)	3, 048. 71	2, 239. 39	1, 708. 44	1, 354. 6				
	3	Z				6, 851		3, 046. 4	2, 238. 11	1, 716. 00	1, 355. 58				
	2	W				6, 838		2, 942. 14	2, 132. 17	1, 612. 8	1, 232. 76				
	1	V				6, 084. 3									
	2	U				6, 082. 7	(3, 612)	2, 269. 58	1, 459. 97	934. 7					
	3	T				6, 081. 1									

2. ARGON

An extensive description and analysis of the first spectrum of argon was published by Meissner [14] who found the structure of this sprectum very similar to that of neon. Several groups of terms ($2s$, $3d$, etc.) could not be established because their strongest combinations lay out of range of Meissner's observations in the infra-red. Gremmer [15] observed 36 new lines in the infra-red, but only 8 of these were explained by Meissner's terms, and 9 of them are not present on our spectrograms.

Important additions to the data for argon were made by Rasmussen [16] who succeeded, with an efficient spectrograph, an intense light source, and very long exposures to neocyanine plates, in recording infra-red lines to 10,683.4 A. The $2s$ terms, 5 of the $3d$ terms, and several additional f terms were identified from these observations.

TABLE 3.—*Infra-red spectrum of argon*

Intensity	λ_{air} I. A.	ν_{vac} cm^{-1} observed	Term combination	ν_{vac} cm^{-1} calculated
Paschen	Paschen			
4	13, 719. 9	7, 287. 3	$2p_9$–$3d_4'$	7, 287. 60
4	13, 504. 6	7, 402. 9	$2p_8$–$3d_4$	7, 403. 12
31	12, 499	7, 998. 5	$2p_9$–$2s_5$	8, 005. 65
B. S.	B. S.			
1	11, 720. 0	8, 530. 1	$2p_8$–$3d_2$	8, 530. 29
2	11, 668. 9	8, 567. 44	$2p_6$–$3s_1''$	8, 567. 56
5	11, 488. 1	8, 702. 31	$1s_2$–$2p_{10}$	8, 702. 20
2	11, 441. 7	8, 737. 59	$2p_6$–$2s_2$	8, 737. 50
1	11, 393. 53	8, 774. 52	$2p_7$–$2s_3$	8, 774. 30
2	11, 106. 41	9, 001. 35	$3d_1'$–5U	9, 001. 19
5	11, 078. 87	9, 023. 72	$2p_8$–$3s_1''''$	9, 023. 67
5	10, 950. 73	9, 129. 31	$2p_6$–$3s_1'$	9, 129. 31
2	10, 892. 39	9, 178. 21	$2p_9$–$3s_1''''$	9, 178. 24
10	10, 880. 92	9, 187. 88	$2p_8$–$3s_1''$	9, 187. 78
1	10, 860. 95	9, 204. 78	$2p_8$–$3s_1'''$	9, 204. 69
4	10, 773. 33	9, 279. 64	$2p_7$–$3s_1'$	9, 279. 60
2	10, 770. 33	9, 282. 22	$3d_4''$–5Y	9, 282. 17
6	10, 759. 12	9, 291. 90	$3d_4''$–5U	9, 291. 97
5	10, 733. 88	9, 313. 74	$3s_1'''$–5W	9, 313. 81
1	10, 722. 1	9, 323. 98	$2p_{10}$–$3d_1''$	9, 324. 00
4	10, 712. 76	9, 332. 11	$3s_1''$–5Z	9, 332. 13
8	10, 700. 97	9, 342. 39	$2p_9$–$3s_1''$	9, 342. 35
3	10, 683. 40	9, 357. 76	$2p_8$–$2s_2$	9, 357. 72
40	10, 681. 80	9, 359. 16	$2p_9$–$3s_1'''$	9, 359. 36
100	10, 673. 61	9, 366. 35	$2p_{10}$–$2s_5$	9, 366. 37
10	10, 529. 31	9, 494. 70	$3s_1''''$–5W	9, 494. 83
30	10, 506. 48	9, 515. 33	$3d_3$–4Z	9, 515. 46
100	10, 478. 09	9, 541. 11	$2p_{10}$–$2s_4$	9, 541. 11
300	10, 470. 09	9, 548. 41	$1s_3$–$2p_{10}$	9, 548. 36
1	10, 357. 6	9, 652. 1	$3d_5$–$4p_5$	9, 652. 27
60	10, 332. 76	9, 675. 31	$3d_4$–5V	9, 675. 34

[14] K. W. Meissner, Zeitschr. f. Phys., vol. 37, p. 238, 1926; vol. 39, p. 172, 1926; vol. 40, p. 839, 1927.
[15] W. Gremmer, Zeitschr. f. Phys., vol. 50, p. 721, 1928.
[16] E. Rasmussen, Zeitschr. f. Phys., vol. 75, p. 695, 1932.

TABLE 3.—*Infra-red spectrum of argon*—Continued

Intensity	λ_{air} I. A.	ν_{vac} cm^{-1} observed	Term combination	ν_{vac} cm^{-1} calculated
B. S.	B. S.			
2	10, 319. 62	9, 687. 62	$3d_4$–5Y	9, 687. 76
20	10, 309. 15	9, 697. 47	$3d_4$–5U	9, 697. 58
1	10, 266. 79	9, 737. 48	$2s_5$–$5p_9$	9, 737. 40
10	10, 254. 04	9, 749. 58	$2p_5$–$3s_1'$	9, 749. 53
1	10, 208. 7	9, 792. 88	$2s_5$–$5p_6$	9, 793. 32
1	10, 206. 9	9, 794. 6	$3d_1''$–$5p_8$	9, 794. 77
1	10, 171. 2	9, 828. 98	$3d_1''$–$5p_7$	9, 828. 99
30	10, 163. 45	9, 836. 49	$3d_5$–4Z	9, 836. 44
4	10, 104. 82	9, 893. 56	$3d_2$–6X	9, 893. 53
8	10, 094. 32	9, 903. 85	$3d_2$–6Y	9, 903. 99
50	10, 069. 04	9, 928. 71	$2p_1$–$4d_5$	9, 928. 76
150	10, 052. 10	9, 945. 45	$3d_4'$–5V	9, 945. 43
2	10, 039. 75	9, 957. 68	$3d_4'$–5Y?	9, 957. 85
40	10, 029. 70	9, 967. 65	$3d_4'$–5U	9, 967. 65
3	10, 007. 61	9, 989. 66	$3d_2$–5Z	9, 989. 62
1	9, 994. 94	10, 002. 32	$3s_1''''$–$5p_4$	10, 002. 54
20	9, 951. 88	10, 045. 60	$2p_{10}$–$3d_2$	10, 045. 58
1	9, 937. 80	10, 059. 83	$3s_1''$–7Y	10, 060. 20
6	9, 882. 18	10, 161. 45	$3s_1'$–6Z	10, 116. 34
1	9, 815. 22	10, 185. 47	$3d_4$–$5p_9$	10, 185. 36
4	9, 800. 92	10, 200. 33	$3d_4$–$5p_8$	10, 200. 36
1, 000	9, 784. 49	10, 217. 46	$1s_2$–$2p_8$	10, 217. 49
1	9, 774. 79	10, 227. 60	$3s_1''''$–7U	10, 227. 86
8	9, 677. 80	10, 330. 10	$3d_1'$–6V	10, 329. 97
6	9, 673. 39	10, 334. 80	$3d_1'$–6Y	10, 334. 79
50	9, 666. 86	10, 341. 79	$3d_1'$–6U	10, 341. 62
1, 500	9, 657. 76	10, 351. 53	$1s_4$–$2p_{10}$	10, 351. 44
4	9, 595. 09	10, 419. 14	$3d_1'$–5W	10, 419. 01
1	9, 593. 67	10, 420. 68	$3d_1'$–5Z	10, 420. 42
5	9, 561. 60	10, 455. 63	$3d_4'$–$5p_9$	10, 455. 45
4	9, 555. 2	10, 462. 6	$3d_3$–$4p_4$	10, 462. 42
2	9, 547. 73	10, 470. 83	$3d_3$–$4p_2$	10, 470. 61
3	9, 486. 02	10, 538. 94	$2p_{10}$–$3s_1''''$	10, 538. 96
50	9, 478. 39	10, 547. 42	$3d_3$–5X	10, 547. 33
100	9, 459. 09	10, 568. 94	$3d_3$–5Y	10, 569. 17
2	9, 446. 57	10, 582. 95	$2s_5$–6Y	10, 583. 20
3	9, 408. 66	10, 625. 59	$3d_4''$–6Y	10, 625. 57
20	9, 402. 69	10, 632. 34	$3d_4''$–6U	10, 632. 40
5	9, 377. 63	10, 660. 64	$3s_1'''$–6Z $3s_1'''$–6W	10, 661. 18 10, 660. 84
4	9, 362. 50	10, 677. 98	$3s_1''$–6Z $3s_1''$–6W	10, 678. 09 10, 677. 75
200	9, 354. 22	10, 687. 43	$1s_2$–$2p_7$	10, 687. 42
3	9, 340. 59	10, 703. 03	$2p_{10}$–$3s_1''$	10, 703. 07
8	9, 334. 80	10, 709. 67	$3d_2$–7X $3d_4''$–5W	10, 709. 67 10, 709. 79
1	9, 333. 32	10, 711. 36	$3d_4''$–5Z	10, 711. 20
2	9, 328. 08	10, 717. 38	$3d_2$–7Y	10, 717. 69
2	9, 322. 84	10, 723. 40		
100	9, 291. 58	10, 759. 48	$2p_{10}$–$2s_3$	10, 759. 52
1	9, 242. 17	10, 817. 00	$3d_5$–$4p_3$	10, 817. 16

TABLE 3.—*Infra-red spectrum of argon*—Continued

Intensity	λ_{air} I. A.	ν_{vac} cm^{-1} observed	Term combination	ν_{vac} cm^{-1} calculated
B. S,	B. S.			
1, 000	9, 224. 49	10, 837. 73	$1s_2$–$2p_6$	10, 837. 71
5h	9, 221. 08	10, 841. 74	$3s_1''''$–6W	10, 841. 86
50	9, 198. 61	10, 868. 23	$3d_3$–5X	10, 868. 31
150	9, 194. 68	10, 872. 87	$2p_{10}$–$2s_2$	10, 873. 01
6	9, 180. 17	10, 890. 06	$3d_5$–5Y	10, 890. 15
500	9, 122. 95	10, 958. 36	$1s_5$–$2p_{10}$	10, 958. 28
1	9, 111. 3	10, 972. 4	$3d_3$–$4p_1$	10, 972. 54
60	9, 075. 42	11, 015. 75	$2p_2$–$4d_3$	11, 015. 64
50	9, 073. 34	11, 018. 28	$3d_6$–5X	11, 018. 44
40	9, 066. 77	11, 026. 26	$3d_4$–6V	11, 026. 34
2	9, 057. 51	11, 037. 53	$2p_1$–$3s_4$	11, 037. 54
4h	9, 057. 23	11, 037. 88	$3d_4$–6U	11, 037. 99
10	8, 994. 09	11, 115. 36	$3d_4$–5W	11, 115. 38
1	8, 992. 84	11, 116. 91	$3d_4$–5Z	11, 116. 79
3	8, 988. 20	11, 122. 65	$3d_3$–$5p_6$	11, 122. 69
2	8, 970. 98	11, 144. 00	$3d_1'$–7V	11, 143. 96
2	8, 967. 39	11, 148. 46	$3d_1'$–7Y	11, 148. 49
10	8, 964. 48	11, 152. 08	$3d_1'$–7U	11, 152. 04
40	8, 962. 19	11, 154. 93	$2p_2$–$4d_5$	11, 154. 97
1	8, 895. 42	11, 238. 66	$3d_2$–8X	11, 238. 81
1	8, 891. 70	11, 243. 36	$3d_2$–8Y	11, 243. 94
4	8, 874. 84	11, 264. 72	$2p_{10}$–$3s_1'$	11, 264. 82
150	8, 849. 97	11, 296. 37	$3d_4'$–6V	11, 296. 43
1	8, 846. 17	11, 301. 23	$3d_4'$–6Y	11, 301. 25
20	8, 840. 82	11, 308. 07	$3d_6$–6U	11, 308. 08
3	8, 840. 39	11, 308. 61		
1	8, 819. 37	11, 335. 57	$3d_2$–6Z	11, 335. 58
3	8, 805. 16	11, 353. 86	$3d_3$–$5p_{10}$?	11, 354. 45
100	8, 799. 13	11, 361. 64	$2p_3$–$4d_5$	11, 361. 69
30	8, 784. 59	11, 380. 44	$2p_4$–$4d_6$	11, 380. 35
200	8, 761. 72	11, 410. 12	$2p_2$–$4d_3$	11, 410. 19
1	8, 741. 26	11, 436. 86	$3d_3$–$5p_7$	11, 436. 97
3	8, 739. 51	11, 439. 15	$3d_1''$–7Y	11, 439. 27
20	8, 736. 63	11, 442. 92	$3d_1''$–7U	11, 442. 82
2	8, 736. 19	11, 443. 50	$3d_5$–$5p_6$	11, 443. 67
5	8, 713. 79	11, 472. 91	$3s_1'''$–7Z	11, 472. 92
3	8, 700. 95	11, 489. 84	$3s_1''$–7Z	11, 489. 83
2	8, 690. 12	11, 504. 16	$3d_6$–$5p_{10}$	11, 504. 55
60	8, 678. 43	11, 519. 66	$2p_4$–$4d_5$	11, 519. 68
400	8, 667. 94	11, 533. 60	$1s_3$–$2p_7$	11, 533. 58
1	8, 642. 89	11, 567. 03	$3d_5$–$5p_5$	11, 567. 10
100	8, 620. 47	11, 597. 11	$2p_5$–$4d_5$	11, 597. 10
150	8, 605. 78	11, 616. 91	$2p_3$–$4d_3$	11, 616. 91
4	8, 579. 49	11, 652. 51	$3s_1''''$–7W	11, 652. 5
5	8, 578. 06	11, 654. 45	$1s_2$–$2p_5$	11, 654. 45

TABLE 3.—*Infra-red spectrum of argon*—Continued

Intensity	λ_{air} I. A.	ν_{vac} cm^{-1} observed	Term combination	ν_{vac} cm^{-1} calculated
B. S.	B. S.			
1	8, 565. 13	11, 672. 04	$3d_1'$–8V	11, 672. 00
1	8, 563. 38	11, 674. 43	$3d_1'$–8Y	11, 674. 74
3	8, 561. 38	11, 677. 16	$3d_1'$–8U	11, 677. 09
2, 000	8, 521. 442	11, 731. 884	$1s_2$–$2p_4$	11, 731. 87
2	8, 496. 64	11, 766. 13	$3d_1'$–6Z	11, 766. 38
			$3d_1'$–6W	11, 766. 04
40	8, 490. 30	11, 774. 92	$2p_4$–$4d_3$	11, 744. 90
20	8, 443. 44	11, 840. 27	$3d_4$–7V	11, 840. 33
1	8, 440. 26	11, 844. 73	$3d_4$–7Y	11, 844. 86
6	8, 437. 71	11, 848. 30	$3d_4$–7U	11, 848. 41
2, 500	8, 424. 648	11, 866. 675	$1s_4$–$2p_8$	11, 866. 73
3, 000	8, 408. 213	11, 889. 870	$1s_2$–$2p_3$	11, 889. 86
20	8, 399. 35	11, 902. 42	$3d_3$–6X	11, 902. 11
80	8, 392. 28	11, 912. 44	$3d_3$–6Y	11, 912. 57
60	8, 384. 73	11, 923. 17	$2p_3$–$4d_4$	11, 923. 17
3	8, 367. 03	11, 948. 39	$2p_2$–$4d_1''$	11, 948. 49
1	8, 355. 30	22, 965. 17	$3d_1''$–8Y	11, 965. 52
4	8, 353. 50	11, 967. 75	$3d_1''$–8U	11, 967. 87
20	8, 332. 21	11, 998. 32	$3d_3$–5Z	11, 998. 20
1	8, 305. 02	12, 037. 60	$3d_1'$–9Y	12, 037. 6
1	8, 303. 79	12, 039. 39	$3d_1'$–9U	12, 039. 39
8	8, 291. 88	12, 056. 68	$3d_4''$–6W	12, 056. 82
1, 500	8, 264. 524	12, 096. 589	$1s_2$–$2p_2$	12, 096. 58
50	8, 255. 07	12, 110. 44	$3d_4'$–7V	12, 110. 42
4	8, 249. 58	12, 118. 50	$3d_4'$–7U	12, 118. 50
6	8, 224. 72	12, 155. 13	$2p_3$–$4d_1''$	12, 155. 21
20	8, 203. 42	12, 186. 69	$2p_2$–$3s_5$	12, 186. 74
20	8, 178. 96	12, 223. 14	$3d_5$–6X	12, 223. 09
40	8, 178. 84	12, 223. 32		
10	8, 171. 95	12, 233. 62	$3d_5$–6Y	12, 233. 55
2	8, 166. 21	12, 242. 22		
3	8, 151. 86	12, 263. 77	$2p_2$–$3s_4$	12, 263. 75
10	8, 143. 50	12, 276. 36	$2p_3$–$4d_1'$	12, 276. 36
2	8, 127. 30	12, 300. 83		
50	8, 119. 18	12, 313. 13	$2p_4$–$4d_1''$	12, 313. 20
4, 000	8, 115. 309	12, 319. 006	$1s_5$–$2p_9$	12, 319. 00
2, 000	8, 103. 692	12, 336. 665	$1s_4$–$2p_7$	12, 336. 66
20	8, 094. 06	12, 351. 35	$2p_2$–$4d_2$	12, 351. 34
5	8, 082. 93	12, 368. 35	$3d_4$–8V	12, 368. 36
20	8, 079. 68	12, 373. 32	$3d_5$–6X	12, 373. 19
			$3d_4$–8U	12, 373. 46
20	8, 066. 60	12, 393. 39	$2p_3$–$3s_5$	12, 393. 46
1	8, 058. 53	12, 405. 80		
100	8, 053. 32	12, 413. 83	$2p_6$–$4d_5$	12, 413. 84
50	8, 046. 13	12, 424. 92	$2p_7$–$4d_6$	12, 424. 80
20	8, 037. 23	12, 438. 68	$2p_1$–$3s_2$	12, 438. 70
2	8, 021. 9	12, 462. 4	$3d_4$–6W	12, 462. 41

TABLE 3.—*Infra-red spectrum of argon*—Continued

Intensity	λ_{air} I.A.	ν_{vac} cm^{-1} observed	Term combination	ν_{vac} cm^{-1} calculated
B. S.	B. S.			
800	8, 014. 785	12, 473. 515	$1s_5$–$2p_8$	12, 473. 57
600	8, 006. 157	12, 486. 957	$1s_4$–$2p_6$	12, 486. 95
3	7, 965. 08	12, 551. 35	$2p_4$–$3s_5$	12, 551. 45
2	7, 960. 84	12, 558. 04	$2p_3$–$4d_2$	12, 558. 06
10	7, 956. 99	12, 564. 12	$2p_7$–$4d_5$	12, 564. 13
400	7, 948. 176	12, 578. 048	$1s_3$–$2p_4$	12, 578. 03
20	7, 916. 45	12, 628. 45	$2p_4$–$3s_4$	12, 628. 46
4	7, 910. 23	12, 638. 40	$3d_4'$–8V	12, 638. 35
1	7, 906. 91	12, 643. 69	$3d_4'$–8U	12, 643. 55
100	7, 891. 10	12, 669. 02	$2p_6$–$4d_3$	12, 669. 06
40	7, 868. 20	12, 705. 90	$2p_5$–$3s_4$	12, 705. 88
15	7, 861. 91	12, 716. 06	$2p_4$–$4d_2$	12, 716. 05
2	7, 860. 44	12, 718. 44	$3d_5$–7X	12, 718. 26
8	7, 855. 73	12, 726. 06	$3d_5$–7Y	12, 726. 27
1	7, 853. 29	12, 730. 02	$3d_4$–9V	12, 730. 04
10	7, 814. 33	12, 793. 49	$2p_5$–$4d_2$	12, 793. 47
30	7, 798. 55	12, 819. 37	$2p_7$–$4d_3$	12, 819. 35
200	7, 724. 210	12, 942. 749	$1s_3$–$2p_2$	12, 942. 74
200	7, 723. 759	12, 943. 507	$1s_5$–$2p_7$	12, 943. 50
20	7, 704. 81	12, 975. 34	$2p_6$–$4d_4$	12, 975. 32
2	7, 690. 10	13, 000. 16	$3d_4'$–9V	13, 000. 13
50	7, 670. 04	13, 034. 16	$2p_8$–$4d_5$	13, 034. 06
4	7, 667. 03	13, 039. 28	$3d_5$–7X	13, 039. 24
2	7, 662. 3	13, 047. 3	$3d_5$–7Y	13, 047. 25
500	7, 635. 107	13, 093. 795	$1s_5$–$2p_6$	13, 093. 79
50	7, 628. 86	13, 104. 52	$2p_2$–$4s_1''''$	13, 104. 44
30	7, 618. 33	13, 122. 63	$2p_2$–$4s_1''$	13, 122. 58

Our results for the infra-red lines in the first spectrum of argon are displayed in Table 3, which is constructed exactly like Table 1. Analysis of these new data has yielded improved values for the four $2s$ terms, has identified all 12 of the $3d$ terms, and extended the f-type sequences, so that the recognition of energy states for neutral argon may now be regarded as complete. The $2s$ terms were evaluated from combinations with Meissner's $2p$ terms, the d terms from Meissner's f and p terms, and the new f terms were based upon combinations with the derived d terms. All of the known spectral terms of the A I spectrum are collected in Table 4, which is similar to Table 2.

Radiometric investigation of this spectrum should reveal many intense lines which may be expected from combinations of known terms, but which lie beyond the present limit of photographic detection. Three such lines were observed by Paschen [17] many years ago, their wave lengths (corrected to the I. A. scale) and probable classifications appear at the head of Table 3.

[17] F. Paschen, Ann. d. Phys. (4), vol. 27, p. 537, 1908.

TABLE 4.—*Terms in the A I spectrum*

Electron	j	Term, Paschen notation	m= 1	2	3	4	5	6	7	8	9	10	11	12	13
s	2	s_5	33, 967. 70	13, 643. 05	7, 428. 30	4, 671. 41	3, 208. 24	2, 339. 84	1, 781. 51	1, 402. 07	1, 132. 11	933. 22	782. 70		
	1	s_4	33, 360. 86	13, 468. 31	7, 351. 29	4, 632. 09	3, 229. 21	2, 328. 75	1, 779. 56	1, 396. 01	1, 127. 17				
	0	s_3	32, 557. 78	12, 249. 90	6, 014. 82	3, 238. 44	1, 776. 73	908. 49							
	1	s_2	31, 711. 62	12, 136. 41	5, 950. 13	3, 229. 21	1, 758. 19	899. 88							
p	1	p_{10}		23, 009. 42	10, 451. 43	6, 042. 50	3, 938. 95	2, 799. 70	2, 071. 83	1, 605. 92	1, 267. 17	1, 038. 82			
	3	p_9		21, 648. 70	10, 168. 70	5, 944. 94	3, 905. 65	2, 762. 38	2, 057. 31	1, 591. 58					
	2	p_8		21, 494. 13	10, 112. 12	5, 919. 48	3, 890. 65	2, 754. 70	2, 051. 60	1, 586. 42					
	1	p_7		21, 024. 20	9, 960. 10	5, 854. 19	3, 856. 43	2, 735. 10	2, 038. 79	1, 579. 91	1, 258. 13				
	2	p_6		20, 873. 91	9, 927. 84	5, 840. 46	3, 849. 73	2, 730. 41	2, 036. 53	1, 577. 61	1, 257. 65				
	0	p_5		20, 057. 17	9, 548. 47	5, 641. 13	3, 726. 30	2, 672. 00	1, 988. 81	1, 549. 49	1, 222. 38	1, 009. 72	841. 44		
	1	p_4		19, 979. 75	8, 703. 94	4, 510. 00	2, 467. 81	1, 327. 71							
	2	p_3		19, 821. 76	8, 642. 38	4, 476. 24	2, 452. 93	1, 319. 48							
	1	p_2		19, 615. 04	8, 651. 83	4, 501. 81	2, 460. 37	1, 334. 11							
	0	p_1		18, 388. 83	8, 240. 51	4, 320. 86	2, 361. 52	1, 279. 98	587. 23						
d	3	d_1'			13, 394. 64	7, 545. 4	4, 781. 81	3, 279. 03	2, 396. 35	1, 817. 83	1, 430. 78	1, 154. 08	948. 33		
	2	d_1''			13, 685. 42	7, 666. 55	4, 829. 28	3, 284. 65	2, 419. 50	1, 820. 18	1, 440. 06	1, 165. 78	949. 02	798. 56	
	1	d_2			12, 963. 84	7, 263. 70	4, 597. 22	3, 175. 53	2, 323. 11	1, 779. 56					
	2	d_3			14, 972. 42	8, 204. 85	5, 024. 56		2, 507. 57		1, 473. 54	1, 178. 80	951. 68	808. 88	690. 69
	4	d_4'			14, 361. 10	8, 087. 81	5, 075. 38	3, 458. 28	2, 501. 59	1, 891. 62	1, 479. 81				
	3	d_4			14, 091. 01	7, 898. 59	4, 951. 29	3, 339. 54	2, 461. 97	1, 842. 03	1, 459. 46	1, 178. 94	956. 92	806. 22	684. 43
	1	d_5			15, 293. 40	8, 460. 07	5, 178. 63	3, 643. 51	2, 556. 59	1, 975. 62	1, 498. 39	1, 212. 87	1, 011. 98	818. 80	698. 52
	0	d_6			15, 443. 50	8, 599. 40	5, 317. 39	3, 602. 55	2, 584. 77	1, 948. 52	1, 516. 41	1, 215. 82	996. 85		
	1	s_1'			11, 744. 60	6, 099. 53	3, 302. 90	1, 828. 46							
	2	s_1''			12, 306. 35	6, 492. 46	3, 738. 54	2, 045. 03	1, 205. 00	522. 72					
	3	s_1'''			12, 289. 44	6, 357. 99	3, 554. 04	1, 961. 50	1, 021. 95						
	2	s_1''''			12, 470. 46	6, 510. 60	3, 605. 97	1, 998. 09	1, 058. 32						
f	1	X				6, 922. 91	4, 425. 09	3, 070. 31	2, 254. 16	1, 725. 03					
	2	Y				6, 881. 55	4, 403. 25	3, 059. 85	2, 246. 15	1, 719. 90					
	2	Z				5, 456. 96	2, 974. 22	1, 628. 26	816. 52						
	3	U					4, 393. 45	3, 053. 02	2, 242. 60	1, 717. 55	1, 355. 25				
	4	V					4, 415. 67	3, 064. 67	2, 250. 68	1, 722. 65	1, 360. 97				
	3	W					2, 975. 63	1, 628. 60	817. 9						

3. KRYPTON

The first spectrum of krypton was analyzed simultaneously by Gremmer [18] and by Meggers, de Bruin, and Humphreys.[19] Our preliminary description and analysis was extended [20] two years later, when the number of observed and classified lines was doubled. Gremmer [21] then reported his own analysis to be in perfect agreement with ours if a revised interpretation be given to six of our levels. Up to this time eight of the $3d$ terms were still lacking. With long exposures Rasmussen [22] recorded additional lines mainly in the red and infra-red which led to the identification of five of the missing $3d$ terms, an extension of the terms and a few minor changes among the higher terms.

TABLE 5.—*Infra-red spectrum of krypton*

Intensity	λ_{air} I. A.	ν_{vac} cm^{-1} observed	Term combination	ν_{vac} cm^{-1} calculated
1	12, 124	8, 245. 9	$1s_2$–$2p_5$	8, 246. 153
1?	11, 996. 8	8, 333. 28	$3d_3$–4Y?	8, 333. 64
5	11, 819. 3	8, 458. 43	$2p_{10}$–$2s_6$?	8, 458. 43
1	11, 611. 7	8, 609. 65	$2s_4$–5Y	8, 609. 56
5	11, 457. 4	8, 725. 60	$2p_{10}$–$2s_4$	8, 725. 60
3	11, 259. 0	8, 879. 35	$3d_5$–4X	8, 879. 48
6	11, 257. 7	8, 880. 38	$3d_5$–4Z	8, 880. 28
3	11, 187. 0	8, 936. 50	$3d_5$–4Y	8, 936. 30
20	10, 874. 84	9, 193. 02	$3d_6$–4X	9, 193. 02
5	10, 699. 2	9, 343. 93	$3d_4'$–$4p_9$	9, 343, 62
3	10, 626. 5	9, 407. 86	$3d_1'$–5U	9, 407. 80
5	10, 608. 37	9, 423. 94	$3d_1'$–5Y	9, 424. 32
30	10, 592. 97	9, 437. 64	$3d_1'$–5W	9, 437. 71
1	10, 575. 48	9, 453. 25	$3d_3$–$4p_8$	9, 453. 07
1	10, 486. 28	9, 533. 66	$3d_3$–$4p_7$	9, 533. 60
5	10, 458. 56	9, 558. 93	$3d_3$–$4p_6$	9, 558. 97
10	10, 374. 44	9, 636. 44	$3d_1''$–5Y	9, 636. 15
100	10, 360. 37	9, 649. 52	$3d_1''$–5W	9, 649. 54
2	10, 322. 88	9, 684. 56	$2p_3$–$5d_6$	9, 684. 47
80	10, 296. 93	9, 708. 97	$2p_5$–$4d_5$	9, 708. 904
2	10, 273. 6	9, 831. 02	$2p_2$–$5d_5$	9, 831. 00
10	10, 147. 68	9, 851. 77	$2p_2$–$5d_3$	9, 851. 75
30	10, 120. 96	9, 877. 78	$2p_3$–$5d_3$	9, 877. 77
10	10, 077. 66	9, 920. 22	$3d_5$–$4p_{10}$	9, 920. 29
10	10, 065. 96	9, 931. 75	$2p_2$–$5d_4$	9, 931. 739
2	10, 054. 86	9, 942. 72	$2s_4$–6Z	9, 942. 53
3	10, 038. 65	9, 958. 77	$2s_4$–6Y?	9, 958. 18
1	9, 989. 3	10, 008. 0	$2p_4$–$5d_6$	10, 007. 70
3	9, 917. 60	10, 080. 32	$2p_6$–$5d_5$	10, 080. 25
4	9, 916. 37	10, 081. 57	$3d_1'$–$5p_6$	10, 081. 47

[18] W. Gremmer, Zeitschr. f. Phys., vol. 54, p. 199, 1929.
[19] W. F. Meggers, T. L. de Bruin, and C. J. Humphreys, B. S. Jour. of Research, vol. 3 (RP89), p. 129, 1929.
[20] W. F. Meggers, T. L. de Bruin, and C. J. Humphreys, B. S. Jour. of Research, vol. 7 (RP364), p. 643, 1931.
[21] W. Gremmer, Zeitschr. f. Phys., vol. 73, p. 620, 1932.
[22] E. Rasmussen, Zeitschr. f. Phys., vol. 73, p. 779, 1932.

TABLE 5.—*Infra-red spectrum of krypton*—Continued

Intensity	λ_{air} I. A.	ν_{vac} cm^{-1} observed	Term combination	ν_{vac} cm^{-1} calculated
2	9, 897. 08	10, 101. 22	$2p_2$–$5d_1'$	10, 101. 18
4	9, 862. 95	10, 136. 18	$3d_5$–$4p_7$	10, 136. 26
500	9, 856. 24	10, 143. 08	$2p_6$–$3s_1''''$	10, 143. 06
5	9, 838. 33	10, 161. 54	$3d_5$–$4p_6$	10, 161. 63
2h	9, 810. 27	10, 190. 61	$3d_2$–6X	10, 190. 60
3	9, 794. 89	10, 206. 60	$3d_2$–6Y	10, 206. 61
2	9, 768. 69	10, 233. 98	$3d_6$–$4p_{10}$	10, 233. 83
2, 000	9, 751. 74	10, 251. 77	$1s_4$–$2p_{10}$	10, 251. 750
50	9, 743. 11	10, 260. 85	$3d_4$–5U	10, 260. 80
2h	9, 727. 51	10, 277. 31	$3d_4$–5Y	10, 277. 32
1	9, 722. 78	10, 282. 30	$3d_1''$–$5p_7$	10, 281. 85
15	9, 714. 85	10, 290. 70	$3d_4$–5W	10, 290. 71
50	9, 704. 22	10, 301. 97	$2p_7$–$3s_1''''$	10, 302. 01
10	9, 687. 83	10, 319. 40	$2p_6$–$3s_1''$	10, 319. 35
2	9, 682. 26	10, 325. 34	$3d_5$–$4p_5$	10, 325. 32
1	9, 669. 03	10, 339. 47	$2p_3$–$5d_2$	10, 339. 64
3	9, 615. 63	10, 396. 88	$2p_4$–$5d_1''$	10, 396. 89
1	9, 607. 2	10, 406. 0		
30	9, 540. 89	10, 478. 33	$2p_7$–$3s_1''$	10, 478. 30
1	9, 532. 3	10, 487. 8	$2p_1$–$6d_5$	10, 487. 87
20	9, 450. 88	10, 578. 13	$2p_6$–$3s_1'''$	1p, 578. 09
100	9, 362. 03	10, 678. 52	$2p_6$–$4d_5$	10, 678. 428
100	9, 352. 23	10, 689. 61	$3d_4'$–5U	10, 689. 72
1	9, 337. 9	10, 706. 1	$3d_4'$–5Y	10, 706. 24
10	9, 326. 03	10, 719. 74	$3d_4'$–5W	10, 719. 63
1	9, 299. 40	10, 750. 43	$3d_3$–$3p_4$	10, 750. 58
1	9, 287. 87	10, 763. 78	$3d_1'$–6U	10, 763. 85
2	9, 279. 9	10, 773. 0	$3d_1'$–6Y	10, 772. 94
8	9, 273. 02	10, 781. 02	$3d_1'$–6W	10, 781. 04
10	9, 270. 96	10, 783. 41	$3d_3$–5Z	10, 783. 41
1	9, 262. 69	10, 793. 04	$3d_3$–5X	10, 793. 04
30	9, 243. 54	10, 815. 40		
1	9, 243. 00	10, 816. 03	$3d_3$–5Y	10, 815. 97
1	9, 234. 16	10, 826. 39	$3d_3$–$3p_3$	10, 826. 50
1	9, 224. 83	10, 837. 34	$2p_7$–$4d_5$	10, 837. 372
2	9, 188. 69	10, 879. 96	$3d_3$–$3p_2$	10, 880. 09
20	9, 122. 49	10, 958. 91	$2p_8$–$3s_1''''$	10, 959. 02
20	9, 111. 69	10, 971. 90	$2p_9$–$3s_1''''$	10, 972. 00
1	9, 100. 58	10, 985. 30	$3d_1''$–6Y	10, 984. 77
4h	9, 094. 33	10, 992. 85	$3d_1''$–6W	10, 992. 87
3	9, 044. 47	11, 053. 45	$2p_5$–$3s_1'$	11, 053. 49
30	8, 999. 19	11, 109. 06	$2p_7$–$4d_6$	11, 109. 076
1?	8, 978. 5	11, 134. 6	$3d_3$–$3p_1$?	11, 133. 89
50	8, 977. 99	11, 135. 20	$2p_8$–$3s_1''$	11, 135. 31
10	8, 967. 53	11, 148. 29	$2p_9$–$3s_1''$	11, 148. 29
2, 000	8, 928. 6934	11, 196. 7764	$1s_5$–$2p_{10}$	11, 196. 776
2	8, 925. 3	11, 201. 0		
4	8, 870. 32	11, 270. 46		
3	8, 842. 46	11, 305. 97	$3d_4'$–$5p_9$	11, 305. 63
20	8, 805. 78	11, 353. 06	$3d_5$–$3p_4$	11, 353. 24

TABLE 5.—*Infra-red spectrum of krypton*—Continued

Intensity	λ_{air} I. A.	ν_{vac} cm^{-1} observed	Term combination	ν_{vac} cm^{-1} calculated
30	8, 780. 25	11, 386. 07	$3d_5$–5Z	11, 386. 07
6, 000	8, 776. 7498	11, 390. 6150	$1s_4$–$2p_8$	11, 390. 615
50	8, 774. 05	11, 394. 12	$2p_8$–$3s_1'''$	11, 394. 05
4	8, 773. 00	11, 395. 48	$3d_5$–5X	11, 395. 70
150	8, 764. 09	11, 407. 08	$2p_9$–$3s_1'''$	11, 407. 03
30	8, 755. 20	11, 418. 65	$3d_5$–5Y	11, 418. 63
2	8, 747. 29	11, 428. 97	$3d_5$–$3p_3$	11, 429. 16
3	8, 746. 43	11, 430. 10	$2p_2$–$6d_3$	11, 430. 17
1	8, 742. 49	11, 435. 25	$2p_1$–$7d_5$	11, 435. 27
8	8, 726. 54	11, 456. 15	$2p_3$–$6d_3$	11, 456. 19
1	8, 722. 17	11, 461. 76	$3d_3$–$5p_7$	11, 461. 85
2	8, 713. 62	11, 473. 14	$3d_3$–$5p_6$	11, 473. 16
40	8, 697. 50	11, 494. 40	$2p_8$–$4d_5$	11, 494. 389
2	8, 673. 48	11, 526. 23	$2p_2$–$6d_4$	11, 526. 30
8	8, 651. 49	11, 555. 66	$2p_5$–$4d_2$	11, 555. 57
1	8, 632. 81	11, 580. 54	$3d_1'$–7U	11, 580. 58
1	8, 631. 5	11, 582. 3	$2p_2$–$6d_1''$	11, 582. 39
1h	8, 628. 70	11, 586. 05	$3d_1'$–7Y	11, 586. 06
4h	8, 624. 82	11, 591. 26	$3d_1'$–7W	11, 591. 35
40	8, 605. 85	11, 616. 81	$3d_4$–6U	11, 616. 85
1	8, 599. 4	11, 625. 5	$3d_4$–6Y	11, 625. 94
10	8, 593. 1	11, 634. 05	$3d_4$–6W	11, 634. 04
20	8, 569. 02	11, 666. 74	$3d_6$–$3p_4$	11, 666. 78
50	8, 560. 89	11, 677. 82	$2p_5$–$3s_4$	11, 677. 83
40	8, 537. 93	11, 709. 23	$3d_6$–5X	11, 709. 24
3, 000	8, 508. 8736	11, 749. 2128	$1s_2$–$2p_4$	11, 749 213
30	8, 498. 21	11, 763. 96	$2p_6$–$2s_2$	11, 763. 975
2	8, 477. 20	11, 793. 11	$2p_6$–$4d_4$	11, 793. 139
2h	8, 469. 96	11, 803. 19	$3d_1''$–7W	11, 803. 18
100	8, 412. 45	11, 883. 89	$2p_6$–$4d_3$	11, 883. 903
15	8, 384. 90	11, 922. 93	$2p_7$–$2s_2$	11, 922. 919
5	8, 375. 93	11, 935. 70		
1	8, 332. 73	11, 997. 58	$3d_5$–$5p_{10}$	11, 997. 67
2	8, 321. 09	12, 014. 36		
10	8, 303. 20	12, 040. 24	$2p_6$–$4d_1''$	12, 040. 15
20	8, 301. 39	12, 042. 87	$2p_7$–$4d_3$	12, 042. 847
5, 000	8, 298. 1091	12, 047. 6312	$1s_4$–$2p_7$	12, 047. 632
4h	8, 287. 56	12, 062. 96	$3d_4'$–6W	12, 062. 96
1, 500	8, 281. 05	12, 072. 45	$1s_2$–$2p_3$	12, 072. 446
100	8, 272. 36	12, 085. 13	$2p_6$–$4d_1'$	12, 085. 16
3, 000	8, 263. 2412	12, 098. 4676	$1s_2$–$2p_2$	12, 098. 465
10h	8, 228. 89	12, 148. 97	$3d_3$–6X	12, 148. 58
6	8, 222. 69	12, 158. 13	$2p_2$–$4s_1'$	12, 158. 08
80	8, 218. 40	12, 164. 48	$3d_3$–6Y	12, 164. 59
1	8, 210. 1	12, 176. 8	$2p_2$–$4s_1''$	12, 176. 91
40	8, 206. 62	12, 181. 94	$2p_7$–$3s_1'$	12, 181. 96
20	8, 205. 22	12, 184. 02	$2p_3$–$4s_1'$	12, 184. 10
50	8, 195. 07	12, 199. 11	$2p_7$–$4d_1''$	12, 199. 10
2	8, 192. 4	12, 203. 1	$2p_3$–$4s_1''$	12, 202. 93
3, 000	8, 190. 0570	12, 206. 5759	$1s_4$–$2p_6$	12, 206. 576

TABLE 5.—*Infra-red spectrum of krypton*—Continued

Intensity	λ_{air} I. A.	ν_{vac} cm^{-1} observed	Term combination	ν_{vac} cm^{-1} calculated
15	8, 144. 96	12, 274. 16	$2p_{10}$–$3s_1''$	12, 274. 18
60	8, 132. 98	12, 292. 24	$2p_2$–$4s_1'''$	12, 292. 40
6, 000	8, 112. 9023	12, 322. 6615	$1s_5$–$2p_9$	12, 322. 662
4, 000	8, 104. 3660	12, 335. 6408	$1s_5$–$2p_8$	12, 335. 641
500	8, 104. 02	12, 336. 17	$2p_9$–$4d_4'$	12, 336. 17
1, 500	8, 059. 5053	12, 404. 3030	$1s_3$–$2p_4$	12, 404. 302
8*h*	8, 040. 50	12, 433. 62	$3d_4$–7U	12, 433. 58
1	8, 039. 8	12, 434. 7		
2*h*	8, 033. 52	12, 444. 43	$3d_4$–7W	12, 444. 35
5	7, 993. 12	12, 507. 32	$2p_4$–$4s_1'$	12, 507. 33
2	7, 990. 78	12, 510. 99		
100	7, 982. 42	12, 524. 08	$2p_6$–$3s_5$	12, 524. 142
30	7, 981. 82	12, 525. 05	$2p_6$–$4d_2$	12, 525. 09
20	7, 981. 19	15, 526. 02	$2p_4$–$4s_1''$	12, 526. 16
1	7, 962. 62	12, 555. 23	$3d_3$–$6p_6$	12, 555. 12
2	7, 957. 67	12, 563. 04	$2p_2$–$7d_1'$	12, 562. 92
20	7, 946. 99	12, 579. 92	$2p_8$–$2s_2$	12, 579. 936
2	7, 938. 34	12, 593. 63	$2p_3$–$7d_3$	12, 593. 62
180	7, 928. 602	12, 609. 100	$2p_8$–$4d_4$	12, 609. 100
40	7, 920. 47	12, 622. 05	$2p_9$–$4d_4$	12, 622. 079
200	7, 913. 443	12, 633. 254	$2p_{10}$–$4d_5$	12, 633. 254
30	7, 904. 62	12, 647. 35	$2p_6$–$3s_4$	12, 647. 35
10	7, 882. 36	12, 683. 07	$2p_7$–$3s_5$	12, 683. 086
30	7, 881. 76	12, 684. 03	$2p_7$–$4d_2$	12, 684. 04
2	7, 871. 93	12, 699. 88	$2p_8$–$4d_3$	12, 699. 864
20	7, 863. 91	12, 712. 81	$2p_9$–$4d_3$	12, 712. 843
800	7, 854. 823	12, 727. 535	$1s_3$–$2p_3$	12, 727. 535
4	7, 840. 40	12, 750. 96	$3d_5$–6X	12, 751. 24
8*h*	7, 840. 01	12, 751. 58	$3d_5$–6Z	12, 751. 60
2*h*	7, 830. 21	12, 767. 54	$3d_5$–6Y	12, 767. 25
50	7, 806. 52	12, 806. 29	$2p_7$–$3s_4$	12, 806. 30
2	7, 786. 66	12, 838. 95	$2p_8$–$3s_1'$	12, 838. 97
40	7, 776. 28	12, 856. 09	$2p_8$–$4d_1''$	12, 856. 11
5*h*	7, 772. 40	12, 862. 50	$3d'_4$–7U	12, 862. 50
5	7, 768. 43	12, 869. 08	$2p_9$–$4d_1''$	12, 869. 09
1	7, 765. 89	12, 873. 29	$3d'_4$–7W	12, 873. 27
3	7, 749. 16	12, 901. 08	$2p_8$–$4d_1'$	12, 901. 12
150	7, 746. 831	12, 904. 958	$2p_{10}$–$4d_6$	12, 904. 958
40	7, 741. 39	12, 914. 03	$2p_9$–$4d_1'$	12, 914. 10
1*h*	7, 712. 0	12, 963. 2	$3d_4$–8U	12, 963. 7
1*h*	7, 709. 0	12, 968. 3	$3d_3$–7Z	12, 968. 1
2*h*	7, 703. 41	12, 977. 70	$3d_3$–7Y	12, 977. 71
1, 200	7, 694. 5401	12, 992. 6577	$1s_5$–$2p_7$	12, 992. 658
1, 000	7, 685. 2472	13, 008. 3682	$1s_3$–$2p_1$	13, 008. 368
4	7, 652. 16	13, 064. 62	$3d_6$–6X	13, 064. 78
4, 000	7, 601. 5465	13, 151. 6027	$1s_5$–$2p_6$	13, 151. 602

TABLE 6.—*Terms of the Kr I spectrum*

Electron	j	Term, Paschen notation	m = 1	2	3	4	5	6	7	8	9	10	11
s	2	s_5	32, 943. 165	13, 287. 96?	7, 267. 421	4, 589. 89	3, 162. 96	2, 306. 57	1, 760. 51	1, 387. 08			
	1	s_4	31, 998. 139	13, 020. 79	7, 144. 21	4, 541. 83	3, 135. 59	2, 295. 92	1, 744. 08	1, 374. 03			
	0	s_3	27, 723. 281										
	1	s_2	27, 068. 192	8, 027. 588									
p	1	p_{10}		21, 746. 389	10, 027. 695	5, 909. 57	3, 832. 19	2, 734. 83	2, 042. 48				
	3	p_9		20, 620. 503	9, 799. 251	5, 773. 85	3, 811. 84	2, 705. 35	2, 019. 12	1, 564. 98			
	2	p_8		20, 607. 524	9, 793. 745	5, 774. 13	3, 809. 12	2, 705. 06					
	1	p_7		19, 950. 507	9, 601. 415	5, 693. 60	3, 765. 35	2, 680. 06					
	2	p_6		19, 791. 563	9, 552. 277	5, 668. 23	3, 754. 04	2, 672. 08	1, 998. 84	1, 550. 40			
	0	p_5		18, 822. 039	9, 153. 252	5, 504. 54	3, 618. 73	2, 606. 77	1, 958. 67	1, 524. 57			
	1	p_4		15, 318. 979	4, 476. 620								
	1	p_3		14, 995. 746	4, 400. 695								
	2	p_2		14, 969. 727	4, 347. 112								
	0	p_1		14, 059. 824	4, 093. 310								
d	3	d_1'			13, 835. 55	7, 706. 40	4, 868. 55	3, 335. 88	2, 406. 81	1, 835. 85	1, 440. 83	1, 160. 56	
	2	d_1''			14, 047. 38	7, 751. 41	4, 922. 09	3, 387. 34	2, 418. 23	1, 843. 46	1, 447. 56		
	1	d_2			13, 269. 22	7, 266. 47	4, 656. 11	3, 226. 14	2, 400. 86	1, 810. 54			
	2	d_3			15, 227. 20	7, 907. 660	5, 117. 98	3, 539. 56	2, 402. 13	1, 867. 81	1, 469. 52	1, 183. 77	
	4	d_4'			15, 117. 47	8, 284. 33	5, 136. 010	3, 480. 96	2, 511. 28	1, 896. 05	1, 481. 82	1, 189. 70	976. 20
	3	d_4			14, 688. 55	7, 998. 424	5, 037. 988	3, 443. 43	2, 444. 00		1, 464. 48	1, 178. 05	968. 00
	1	d_5			15, 829. 86	9, 113. 135	5, 238. 73	3, 571. 95	2, 624. 55	1, 911. 91	1, 486. 34	1, 196. 75	
	0	d_6			16, 143. 40	8, 841. 431	5, 311. 28	3, 583. 95	2, 579. 23	1, 981. 54	1, 502. 47	1, 206. 59	
	1	s_1'			7, 768. 55	2, 811. 65							
	2	s_1''			9, 472. 21	2, 792. 82							
	3	s_1'''			9, 213. 47	2, 677. 33							
	2	s_1''''			9, 648. 50								
f	1	X				6, 950. 38	4, 334. 16	3, 078. 62	2, 259. 64	1, 727. 10	1, 364. 65	1, 105. 03	
	2	Y				6, 893. 56	4, 411. 23	3, 062. 61	2, 249. 49	1, 722. 3			
	2	Z				6, 949. 58	4, 443. 79	3, 078. 26	2, 259. 1				
		U					4, 427. 75	3, 071. 70	2, 254. 97	1, 724. 8	1, 362. 4	1, 102. 82	
		W					4, 397. 84	3, 064. 51	2, 244. 20	1, 715. 3			

The present investigation of the infra-red spectrum of krypto with mesocyanine and xenocyanine plates yields 200 lines, more tha half of which have never been observed before. Analysis of thes data brings the discovery of spectral terms nearer completion an firmly establishes the nature of some terms previously known bu misinterpreted on account of unobserved combinations. The correc tions suggested by Gremmer are justified, and most of the extension and revisions of terms by Rasmussen are confirmed. The results fo the observed and classified lines of krypton are presented in Table in the same manner as they were shown for neon and argon in Table 1 and 3, respectively. Wave lengths given to more than 2 decima places are quoted from the interferometer measurements by Humph reys.[23] Such values fix the relative values of combining terms ver accurately and thus permit the calculation of other wave lengths wit somewhat higher precision than can be claimed for ordinary gratin measurements. A complete list of the Kr I terms now available i given in Table 6, which is comparable with Tables 2 and 4 for Ne and A I spectra, respectively. The $2s_4$ term at 13,020.79 is checke by double-electron (s–f) transitions, but no such combinations wer observed for the $2s_5$ term, which was placed at 13,287.96 on the assump tion that the otherwise unclassified line at 8,458.43 A represented th transition $2p_{10}$–$2s_5$.

Radiometric investigation of this spectrum is recommended to thos equipped to undertake it because many of the expected combination of known terms still lie beyond the range of present photographi materials.

WASHINGTON, November 26, 1932.

[23] C. J. Humphreys, B. S. Jour. of Research, vol. 5 (R P 245), p. 1041; 1930.

PHOTOGRAPHIC REVERSAL BY DESENSITIZING DYES

By Burt H. Carroll and C. M. Kretchman

ABSTRACT

Latent image on a photographic plate which has been exposed, then bathed in solution of a desensitizing dye, may be destroyed by a second exposure to light of the proper wave length. Quantitative measurements of the variation of density with wave length were made on plates treated with five desensitizing dyes. In three cases it was also possible to make indirect determinations of the spectral distribution of energy absorbed by the dyed silver bromide; less complete data are available for the other two. There is good correlation between reversal and energy absorption. Where the absorption by silver bromide and by the dye are sufficiently separated in wave length, there are maxima corresponding to each. The Herschel effect in the absence of dyes was negligible, and there is no evidence that it is increased by the dyes. It was demonstrated that safranine may produce either reversal or normal sensitization depending only on the bromide ion concentration. Characteristic curves of the process were made by time scale exposures. The evidence supports the hypothesis that the process is an oxidation, and is the reverse of ordinary sensitization chemically as well as photographically.

CONTENTS

	Page
I. Spectral sensitivity of the reversal process	449
II. Effects of bromide and dye concentrations	458
III. Discussion	461

I. SPECTRAL SENSITIVITY OF THE REVERSAL PROCESS

Positive images of passable gradation may be produced by the following process, the sensitivity being about one-tenth that of a lantern-slide plate so that camera exposures are possible. The plate or film is given a moderate uniform exposure; then bathed in a solution of any one of many desensitizing dyes, preferably with the addition of soluble bromide, dried, and again exposed. The latent image formed by the first exposure is destroyed by the second, and a positive image is formed on normal development. The process is characterized by sensitivity to a wide range of wave lengths, and in many cases the relative sensitivity to the longer wave lengths may be greater than in a good panchromatic emulsion, although the absolute value is much less.

This phenomenon was first observed by Waterhouse,[1] but our knowledge [2] of it is very largely due to the extensive experiments of Lüppo-Cramer, which are now summarized in the latest edition of Eder's Handbuch der Photographie.[3] While as a pictorial process it is of very little value, its mechanism is of considerable interest because of its possible bearing on the mechanisms of sensitization and desensitization, and of other reversal phenomena.

The primary object of the experiments to be described in this communication was to determine the relation of the spectral sensitivity of the process to the spectral absorption of the dye which is used. As

[1] Waterhouse, Proc. Roy. Soc. London, vol. 29, p. 186, 1875.

[2] No attempt will be made in this paper to give complete references to the extensive literature of dye reversal and the Herschel effect.

[3] Vol. 2, pt. 1, Grundlagen der photographische Negativverfahren; vol. 3, pt. 3, Sensibilisierung und Desensibilisierung.

already mentioned, the longer wave lengths are usually effective. Lüppo-Cramer has come to the conclusion that the process is essentially the same as the Herschel effect (reversal by red and infra-red radiation on preexposed plates, in the absence of dyes) and that the spectral absorption of the dye "plays only a secondary rôle if at all." Experiments by Mauz,[4] which were made at Lüppo-Cramer's suggestion, were considered as confirming this conclusion. On the other hand, in earlier experiments by one of the writers [5] the maximum reversal corresponded to the maximum absorption by the dye with considerable regularity after allowing for a displacement to the red of about 50 mμ, like that found in ordinary sensitization.

In this process, results depend on the experimental conditions even more than in normal photography. As it was desired to find the region or regions of maximum sensitivity, the diffraction spectrum was used for exposure because the change of energy with wave length is much less than in a prism instrument. It was essential to avoid overexposure. It is well known that by sufficient exposure it is possible to record a continuous spectrum on an unsensitized emulsion as far as 0.6 to 0.7 μ, even though the sensitivity in this region is negligible for practical purposes. Stray light in even the best instruments may also give the appearance of continuous sensitivity if the exposure is excessive.

The best apparatus available was a small spectrograph having a concave reflection grating mounted in parallel light, giving a dispersion of 5 mμ/mm. A Tungsarc lamp was used as the light source. The intensity is quite high, test exposures on fast panchromatic emulsions being made at one twenty-fifth to one-half second, and the stray light is much less than with a transmission grating. This apparatus has been previously used for experiments with methods of spectral sensitization.[6] While the use of the grating spectrograph avoids the great concentration of energy in the longer wave lengths produced by a prism instrument with an incandescent source, the energy from the Tungsarc lamp (color temperature about 3,000° K.) increases so rapidly with wave length that the exposure of the plates to the red end of the spectrum was several times as great as to the blue end.

The test plates were given the white light exposure in a special exposure box, which had been tested photographically for uniformity of illumination. They were then bathed with the mixed solution of desensitizing dye and soluble bromide, swabbed with moist cotton to remove the surplus solution, and dried in a rack designed so that there was unobstructed flow of air over the entire surface of the plate. There are liable to be local irregularities in these plates under the best conditions, and unless the drying is quite uniform, quantitative work is likely to become impossible. The spectrograph exposures were made directly after drying. After the second exposure they were brush developed for four minutes at 20° C. in metolhydroquinone, using the Eastman D–11 formula.

Most of the experiments were done with an experimental pure bromide emulsion. (No. 4–97–2), having a Bureau of Standards speed of 25 and a γ of 0.8 for the above development. This emulsion was used because it was possible to observe the Herschel effect on it under the

[4] E. Mauz, Zeit. f. wiss. Phot., vol. 27, p. 49, 1929.
[5] B. H. Carroll, J. Phys. Chem., vol. 29, p. 693, 1925.
[6] Carroll and Hubbard, B. S. Jour. Research, vol. 4 (RP173), p. 693, 1930.

ame conditions as the dye reversal; pure bromide emulsions are gen-rally best for this purpose, as they have a minimum of normal ensitivity to the red.

Densities were measured by a physical photometer improvised from Fabry-Buisson microphotometer. The illuminating system was sed to focus a narrow line of light on the plate, and the transmission easured from the deflection of a galvanometer connected directly o a caesium photoelectric cell receiving only radiation transmitted y the plate. Within the range used, the accuracy of the assumption hat the deflection was proportional to transmission was of the order f 5 per cent. The photometer obviously is accurate only for low ensities, but these were the most important in the reversal work. Densities measured in this way are higher than those determined nder diffuse illumination. The wave-length scale was supplied y exposures of the helium spectrum; these could not be superposed n all the reversal plates because the sensitivity was too low, but he scale could be reproduced to 0.2 mm on the plate which is quite ufficient.

The dyes used were as nearly as practicable the same as those used y Mauz.[7] Pinakryptol green and yellow were obtained from the . G. Farbenindustrie. Fuchsin (pararosaniline) and safranine were Kahlbaum products, believed to be Nos. 646 and 841, respectively, n the Colour Index; phenosafranine was not available, but the tolu-afranine is so closely related that no important difference is to be nticipated. Some experiments were also made with the parent dye f the pinakryptol series, 2-*m*-nitrostyrrylquinoline dimethyl sul-hate, for comparison with those described by Lüppo-Cramer on pages 284–285 of Eder's Handbuch, vol. 3, p. 3. This material was ynthesized by the research laboratory of the Eastman Kodak Co., rom *m*-nitrobenzaldehyde and quinaldine dimethylsulphate at our equest; we wish here to acknowledge their generous assistance.

In the previous experiments by Carroll,[8] and by Mauz,[9] the spectral ensitivities of the plates were compared simply with the absorptions f aqueous solutions of the dyes; data for the latter were obtained either from the literature or by relatively crude measurements. We are indebted to Dr. K. S. Gibson and Miss Mabel E. Brown, of the olorimetry section of this bureau, for quantitative data on the spec-tral absorptions of the dye solutions used in these experiments. It is more satisfactory, however, to know the absorption of the dyed silver bromide, which is the actual absorbing system in the plates. Eder [10] has proved in this way that the maxima of absorption and sensitization actually correspond for some of the sensitizing dyes. Apparatus for transmission measurements on highly diffusing materials like photographic plates was not available, but the absorption maxima were located by measuring the spectral reflection. Silver bromide was prepared by precipitation from equivalent solutions of silver nitrate and potassium bromide, washed five times by decantation, then agitated with approximately 1:5,000 solutions of each of the four dyes, plus a trace of potassium bromide. The silver bromide was considerably peptized by the dyes. The mixture was allowed to stand overnight, and the supernatant solution carefully decanted

[7] See footnote 4, p. 450.
[8] See footnote 5, p. 450.
[9] See footnote 4, p. 450.
[10] Eder, Photographie mit Bromsilber-Gelatine (1903 edition), p. 151.

from the silver bromide, which was then suspended in distilled wate
This process was repeated twice to eliminate dye not adsorbed to th
silver bromide. The final suspension was coated on small pieces
glass, previously coated with a thin gelatin substratum, and drie
The reflection of these samples was measured in diffuse illuminatio
by the colorimetry section. The blackening of the silver bromi
under the intense illumination in the spectrophotometer gave co
siderable difficulty, but error from this source was very largely reduce
by rapid readings on a number of samples, measurements being mad
both on increasing and decreasing wave length. It was, howeve
impossible to make satisfactory measurements on the sample dye
with pinakryptol green, with its relatively broad and flat absorptio
bands. All values are relative to the reflectance of a diffusing surfac
of magnesium oxide, used as a nonselective standard.

Comparison of spectral absorption and spectral sensitivity for eac
of the dyes may be made from the data presented in Figures 1 to
In each of these figures the densities of plates after spectrograp
exposures are plotted (in solid lines) as ordinates, against wave length
as abscissæ. A minimum of density obviously corresponds to a ma
imum of reversal, and vice versa. The data for spectral absorptio
are given by the broken lines. Curve 1 in each figure represents th
absorbancy (minus log transmittancy) for an aqueous solution of th
corresponding dye, at a concentration chosen so as to give a range
logarithms comparable to the other curves. In each case there is
maximum of reversal corresponding to the maximum of absorption b
the dye, but displaced by 40 to 60 mμ toward the longer wave lengths
In Figure 2 the maximum reversal at 465 mμ obviously corresponds t
the principal absorption band of the dye at 430 mμ; the change of slop
from 590 to 650 mμ indicates that a faint secondary maximum corre
sponding to the absorption band at 580 mμ is superposed on the mai
curve. The reversal curve for plates bathed with fuchsin (fig. 3) an
safranine (fig. 4) have minimum densities at about 420 mμ in addition
to those at 610 and 580 mμ, respectively, which may be attributed t
the dyes. There is no absorption by fuchsin or safranine in the regio
of 360 to 380 mμ to account for these minima at 420 to 430 mμ. Th
quantitative measurements of spectral absorption by these solution
were carried to 390 mμ without any indication of a second maximum
at shorter wave lengths, and approximate photographic tests failed t
show any significant absorption between 400 and 310 mμ. We ar
therefore forced to the conclusion that the minima around 420 m
correspond to absorption by the silver bromide itself; this conclusio
will be discussed more fully later in the paper.

Curve 2 in Figures 1, 3, and 4 represents the spectral reflectio
of silver bromide dyed with the corresponding dyes; the data ar
plotted as minus log reflectance, so that a maximum in the curv
corresponds to minimum reflectance and maximum absorption. I
will be noted that the maxima of these curves are displaced approxi-
mately 20 mμ toward the longer wave lengths from the maxima o
absorption in solution. In the case of silver bromide dyed with
pinakryptol yellow, the dye and the silver bromide absorb in the
same spectral region, so that the two components of reflection can
not be distinguished.

Curve 3 in Figures 1, 3, and 4 represents on a logarithmic scale the
variation with wave length in the energy radiated by a black body at

000° K. The curves in the three figures are displaced vertically y varying amounts to fit the scales of the figures. The color temerature of a Tungsarc lamp is not over 3,000°, and possibly nearer 900°. The relative energy incident on the plates may, as a first pproximation, be taken as equal to this, since nothing in the spectroraph or illuminating system introduces appreciable selective absorpon or reflection in the visible region.

Curve 4 approximates the relative energy absorbed at each wave ngth from a source of 3,000° color temperature by a material of e reflectance represented by curve 2. In making this calculation, e transmission by the dyed silver bromide was taken as negligible

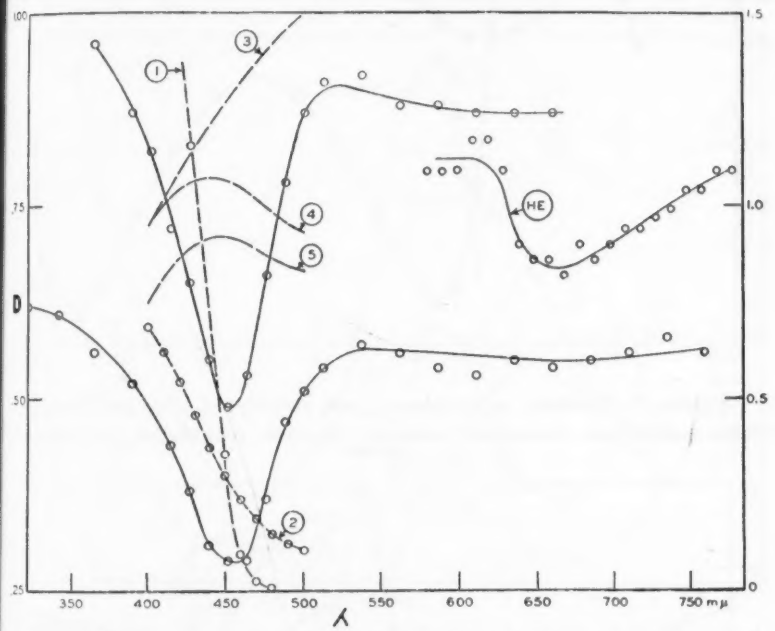

FIGURE 1.—*Reversal on plates bathed with pinakryptol yellow and bromide*

Solid lines represent densities of plates, on left-hand ordinate scale. The curve marked *H E* is for the Herschel effect on a pure bromide emulsion without dye; 1.5 has been subtracted from all densities to bring the curve on the same plot with the others. Dashed curves (right-hand ordinate scale) are: (1) Absorbancy (minus log transmittancy) of pinakryptol yellow solution, 1.0 g per liter, in 1 cm thickness; (2) minus log reflectence of silver bromide dyed with pinakryptol yellow; (3) log relative spectral energy distribution of a black body at 3,000° K.; (4) log spectral distribution of energy absorbed from a source such as (3) by silver bromide dyed with pinakryptol yellow; and (5) log quanta absorbed under these conditions

and the absorption as (1 − reflectance); the absorption was multiplied by the relative energy for this wave length, and the logarithm of this quantity plotted. The transmission was not measureable with the available apparatus, but appeared to be not over 10 per cent for the samples actually used for measurement of reflectance. Curve 5 in each of the figures was obtained by dividing the energy absorbed at each wave length by the frequency of the radiation (the inverse of the wave length). This procedure gives the relative number of quanta of energy absorbed. The logarithm of the number was plotted. As curves 3, 4, and 5 all express only relative values, plotted on a logarithmic scale, they have been shifted vertically so as to produce

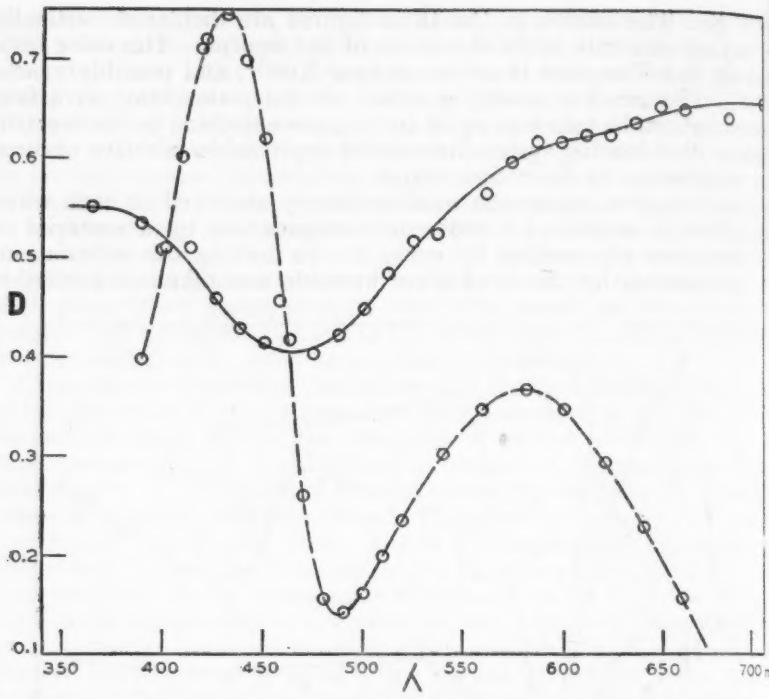

FIGURE 2.—*Reversal on plate bathed with pinakryptol green and bromide*

Solid line, density of plate. Dashed line, absorbancy of pinakryptol green solution, 1 cm thickness, 0.02 per liter

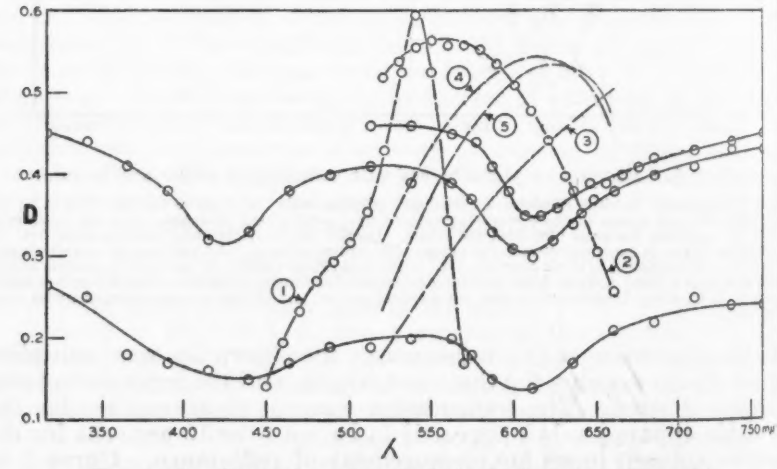

FIGURE 3.—*Reversal on plates bathed with fuchsin and bromide*

Solid lines represent densities of plates; upper curve made with red filter over slit of spectrograph. Dashed curves: (1) Absorbancy of fuchsin solution, 0.0024 g per liter, in 1 cm thickness; (2) minus log reflectance of silver bromide dyed with fuchsin; (3) log relative spectral energy distribution of a black body at 3,000° K.; (4) log spectral distribution ofenergy absorbed from a source such as (3) by silver bromide dyed with fuchsin; and (5) log quanta absorbed under these conditions

the minimum confusion in the figures. As a first approximation, the extent of a given photochemical reaction produced by different frequencies not too widely separated may be expected to be proportional to the number of quanta absorbed at each frequency. There are in many cases very large deviations from this theoretical prediction, the higher frequencies (shorter wave lengths) tending to be the more effective, but in the absence of more definite knowledge the effect of varying frequency on a reaction should be compared with the number of quanta absorbed by the material which is believed to be chemically activated by the radiation.

Considering the region covered by curve 5 in Figures 1, 3, and 4, it is obvious that there is excellent correspondence between the reversal

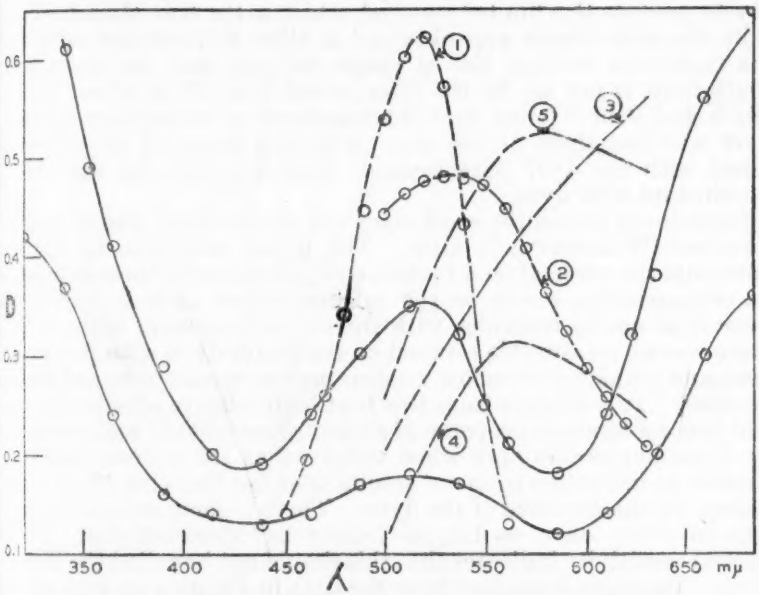

FIGURE 4.—*Reversal on plates bathed with safranine and bromide*

Solid lines represent densities of plates. Dashed curves: (1) Absorbancy of safranine solution, 1 cm thickness, 0.008 g per liter; (2) minus log reflectance of silver bromide dyed with safranine; (3) log relative spectral energy distribution of a black body at 3,000° K.; (4) log spectral distribution of energy absorbed from a source such as (3) by silver bromide dyed with safranine; and (5) log quanta absorbed under these conditions

and the energy quanta absorbed by the dye on the silver bromide. The maxima fall together within the limits of error of the determinations. Figure 2 shows that the relation between reversal and the absorbancy of dye solution is the same for pinakryptol green as for the other dyes. The inevitable conclusion from these data is that the spectral sensitivity of the reversal process depends on the absorption by the dye as directly as does spectral sensitization of the ordinary type. This confirms the earlier work by one of us.[11] It is in direct contradiction to Lüppo-Cramer's conclusion, which we shall be able to show is the result of the misleading impression of spectral sensitivity which may be given by inspection of exposures through filters.

In Figures 3 and 4, there are marked minima of density around 420 to 430 mμ, which are obviously the result of light absorbed by the

[11] Footnote 5, p. 450.

silver bromide itself. The combination of absorption which increases with decreasing wave length and energy incident on the plate in amounts increasing with increasing wave length determines the location of maximum absorption and hence of maximum reversal. In Figures 1 and 2, this maximum of reversal is shifted to 450 and 465 mμ, respectively, by the absorption of the dye superposed on that of the silver bromide.

In Figure 1, the curve marked *H E* represents the density of a plate coated with pure bromide emulsion which, after the first uniform exposure, had been bathed in 1 per cent potassium bromide solution without dye, then dried and exposed in the spectrograph using a red filter over the slit to eliminate the second order spectrum and stray light of short wave lengths. An exposure of 2½ hours was necessary to produce this limited reversal, which is the true Herschel effect, while the other curves were obtained in 4½ or 13½ minutes using dyes. The maximum reversal lies at about 660 mμ, and the short wavelength limit is not set by the filter, which cuts off at about 590 mμ. Hilsch and Pohl [12] found that the maximum of absorption by photosilver was just short of 700 mμ. A similar Herschel effect was obtained with the 4–97 pure bromide emulsion used for the reversal experiments with dyes.

Ten-minute exposures were made on all the dyed plates with the same red (Wratten "A") filter. The upper solid line in Figure 3 represents the reversal on a fuchsin-dyed plate under these conditions; the corresponding result on the safranine-dyed plate is omitted because it so nearly coincides with the shorter exposure without filter. There was no measurable reversal on the plates dyed with pinakryptol green and pinakryptol yellow, confirming the results obtained without the filter. It is evident from this that high relative sensitivity to red light is not a common property of all emulsions treated with desensitizing dyes, but occurs only when the dye has the proper absorption. There is no indication from our results that the Herschel effect was increased by the presence of the dyes. There is some sensitivity to red light in every case, as Lüppo-Cramer has demonstrated, but the spectral sensitivity indicates that this should not be called the Herschel effect. Its origin is evident from the data in Figure 5 on long spectrograph exposures. Process plates were given the usual uniform exposure to white light, then bathed with pinakryptol green, pinakryptol yellow and 2-*m*-nitro-styrrylquinoline dimethylsulphate, each at a dilution of 1:5,000 in bromide solution, dried, and exposed in the spectrograph for five minutes without filter, and one hour with the minus blue filter (absorbing radiation of wave length less than 500 mμ) over the slit. Curves 1 and 2 show clearly that as the exposure was increased, the region of reversal on the pinakryptol yellow bathed plate extended into the red without indication of a second maximum. The behavior of the plate bathed with pinakryptol green (curve 3) was similar, but there are indications of a secondary maximum about 640 mμ corresponding to the secondary maximum of absorption of the dye.

The reversal obtained with 2-*m*-nitrostyrrylquinoline dimethylsulphate, one of the simplest dyes of the pinakryptol series, is of particular interest because Lüppo-Cramer [13] has used this as evidence that the reversal effect is independent of the spectral absorption of

[12] Hilsch and Pohl, Proc. 8th. Int. Cong. Phot., p. 29, 1931.
[13] Lüppo-Cramer, reference 3 "Sensibilisierung und Desensibilisierung," pp. 284–285, and Figure 53.

the dye. The 5-minute exposure without filter on the plate treated with this dye produced a reversal which would be represented by a curve quite close to (1) in Figure 5. Examination of curve 4 shows that the slope on the long wave length side is steeper than that of curve 2, made with pinakryptol yellow. This is to be expected, since absorption by 2-*m*-nitrostyrrylquinoline dimethylsulphate was found to be very slight at wave lengths over 400 mμ; the spectral sensitivity was therefore determined almost entirely by the absorption of the silver bromide.

On visual inspection of the plates made with this material the reversal could be detected to over 700 mμ, but could not be measured

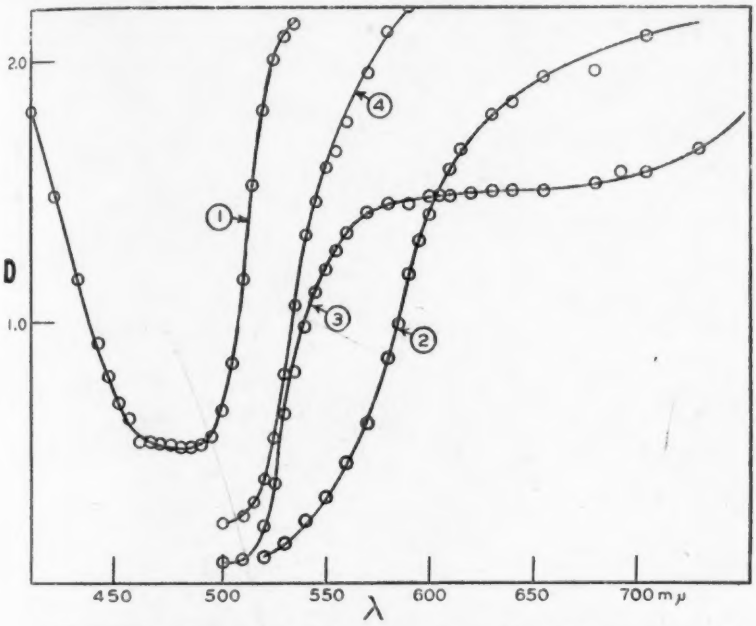

FIGURE 5.—*Reversal on plates given long spectrograph exposures*

Curve 1, 5-minute exposure; curves 2, 3, and 4, 60-minute exposures with minus blue filter in front of slit of spectrograph. Curves 1 and 2, plate bathed with pinakryptol yellow and bromide; curve 3, plate bathed with pinakryptol green and bromide; and curve 4, plate bathed with 2-*m*-nitrostyrrylquinoline dimethylsulphate and bromide.

with any accuracy on the microphotometer because it involved small changes in relatively high densities. Another piece of the same plate used for curve 4 (fig. 5) was exposed behind an Eder-Hecht wedge for two and one-half minutes at 30 cm from a 75-watt, gas-filled lamp. The result is reproduced in Figure 6; the similarity to Lüppo-Cramer's results (reproduced in his fig. 53) is obvious. The wedge and filter exposure appears to indicate a relative sensitivity to the longer wave lengths which is not confirmed by the quantitative measurements on the spectrograph exposures. The answer appears to lie in what Lüppo-Cramer has called the "time effect," the marked failure of the reciprocity law for this process in the sense that the photographic effect falls off much less rapidly than the intensity. This shows in the original of the Eder-Hecht exposure as an extraordinarily long

and flat "toe" of the characteristic curve. The consequence is that intensity differences, as judged from the threshold of photographic effect, tend to be equalized and the filter strips on the Eder-Hecht wedge are printed for a distance out of proportion to the relative spectral sensitivity.

II. EFFECT OF BROMIDE AND DYE CONCENTRATIONS

The curves of Figure 7 represent the results of an experiment which we believe to have considerable theoretical significance. Process

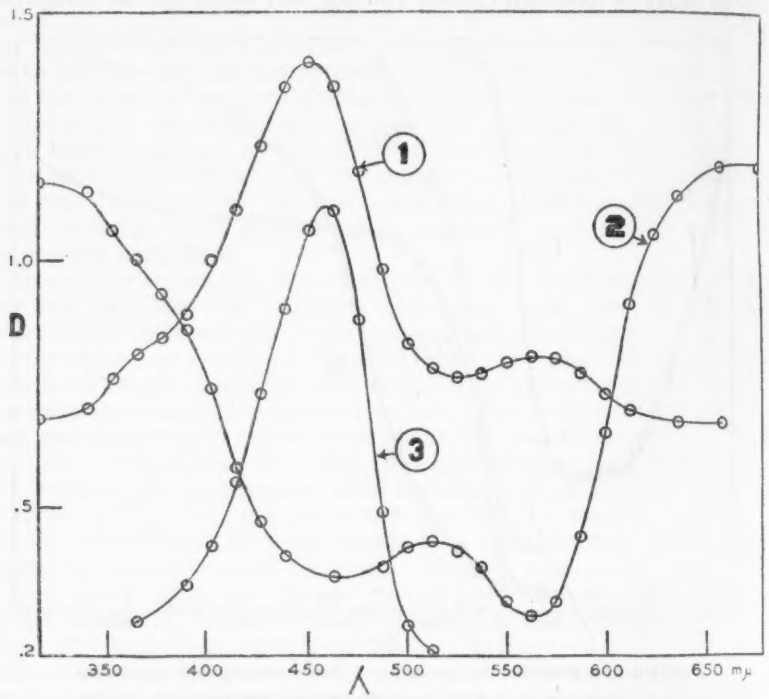

FIGURE 7.—*Densities of plates after spectrograph exposures*

(1) Preexposed, washed, bathed with solution of safranine in pure water, and dried before spectrograph exposure; (2) preexposed, bathed with solution of safranine and potassium bromide, and dried before spectrograph exposure; and (3) plate of same emulsion, untreated

plates were given suitable preexposures. They were then cut in halves. One half of each was washed for five minutes in running water to remove all soluble bromide, then bathed in a 1: 30,000 solution of safranine in distilled water, dried, and exposed in the spectrograph. The other half was bathed in a 1: 30,000 solution of safranine in 1 per cent KBr solution, then dried and exposed in the spectrograph. All plates were given a series of spectrograph exposures. Curve 1 in Figure 7 represents a plate given 4-second preexposure, washed and bathed in safranine without bromide, and exposed 30 seconds in the spectrograph. Curve 2 is for a plate given 8-second preexposure, bathed in safranine plus bromide, and exposed 90 seconds in the spectrograph. Spectral sensitivity was not dependent on the exposure times; densities for the above values were

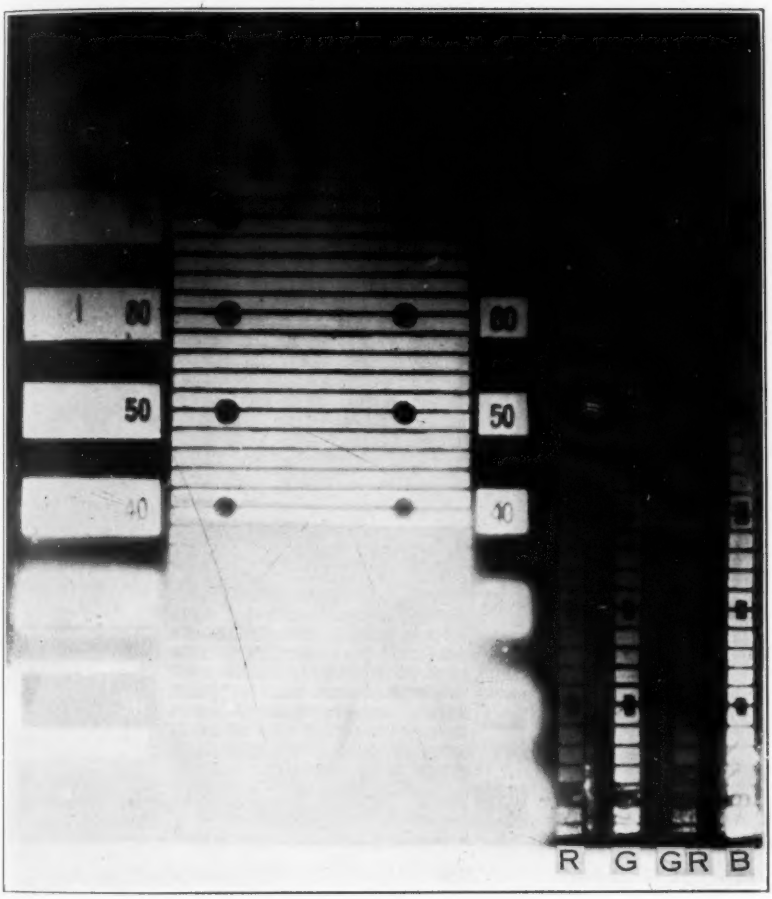

FIGURE 6.—*Process plate given uniform exposure to white light, then bathed in a mixed solution of 2-m-nitrostyrrylquinoline dimethylsulphate and potassium bromide, dried, and exposed again to incandescent light through an Eder-Hecht wedge*

Letters on the narrow strips to the right have the following significance: *R*, red filter; *G*, yellow; *GR*, green; *B*, blue.

UNIV. OF MICH.

chosen as the most suitable for plotting together. Curve 3 in Figure 7 is for an untreated plate of the same kind exposed in the spectrograph for 1 second, without preexposure.

Curve 1 has a maximum of density at 565 mμ; curve 2 has a minimum of density at the same wave length. The maximum at 565 mμ in curve 1 obviously indicates sensitization in the ordinary sense by safranine (in spite of its marked desensitizing properties, this dye is described in the 1903 edition of Eder as "a moderately good green sensitizer"). The corresponding minimum in curve 2 demonstrates beyond question that the reversal process is also brought about by light absorbed by the dye. The energy acquired in this way may either form or destroy latent image, depending on the conditions in the emulsion, the silver (or bromide) ion concentration being the variable involved in this experiment.

The maxima in curves 1 and 3, and minimum in curve 2 at 450 to 460 mμ [13] demonstrate that the same relation holds for radiation absorbed by the silver halide itself as for that absorbed by the dye. Under normal conditions, it is used to form latent image, but in the presence of both dye and soluble bromide it instead destroys image already existing. A maximum of reversal in this region can be detected in Figure 2 of Mauz's paper illustrating exposures on fuchsin bathed plates.

The dye reversal process has generally been associated in the literature, with the longer wave lengths, but there are other illustrations of reversal by radiation absorbed by the silver halide. This is the case for solarization [14] and for reversal on plates which have been converted to iodide.[15]

Further evidence on the nature of the reversal process was obtained from a different type of experiment. Lüppo-Cramer [16] has given characteristic curves of dye reversal with varying concentrations of dye. These curves were made with an intensity scale, and in view of the marked anomalies of the process with regard to intensity it seemed worth while to repeat them with the time scale, which might be simpler to interpret. The experiments were made with safranine on process plates. After constant preexposure, the plates were bathed in solutions of the dye at a dilution of one part of dye to 15, 30, 60, 120, 240, and 480 $\times$ 10^3 parts of 1 per cent KBr solution. These dilutions are indicated by the corresponding numbers on the curves of Figure 8. All plates were dried together, then given a nonintermittent sector wheel exposure (0.11 to 30 seconds) to the light from a 500 c. p. "Point-o-lite" lamp at 0.9 m, with a Wratten Minus Blue filter. A second set of plates was exposed 2 to 512 seconds. The combined curves from three test strips for each of the two exposures are plotted in Figure 8 as changes in density from the unexposed portion of the plate. The reproducibility of these curves was relatively poor, although the individual curves for each set of conditions were smooth; the probable error in location of each curve is of the order of 0.2 in density.

The curves for dilutions of 30 to 480 $\times$ 10^3 fall into a regular progression, the reversal beginning after longer and longer exposure as the

[13] On the pure bromide emulsion used for the exposures recorded in Figure 4, the corresponding minimum lay at 420 to 430 mμ. The shift is explained by the presence of 3 per cent silver iodide in the silver halide of the process emulsion used for Figure 7.
[14] Reference 5, p. 450.
[15] Renwick, J. Soc. Chem. Ind., vol. 39, p. 156 T, 1920.
[16] Lüppo-Cramer Phot. Ind., vol. 25, p. 1099, 1927. Zeit. f. wiss. Phot., vol. 26, p. 345, 1929.

dilution increases. The most unexpected feature of the data is the formation of a negative image in the early stages of exposure at the highest dilutions, preceding the reversal. This has been observed by Lüppo-Cramer [17] in a few cases of exposures with the intensity scale. With the intensity scale, the reversal may be followed by a negative image (at the highest intensities). This has frequently been observed by Lüppo-Cramer, and confirmed in this laboratory;

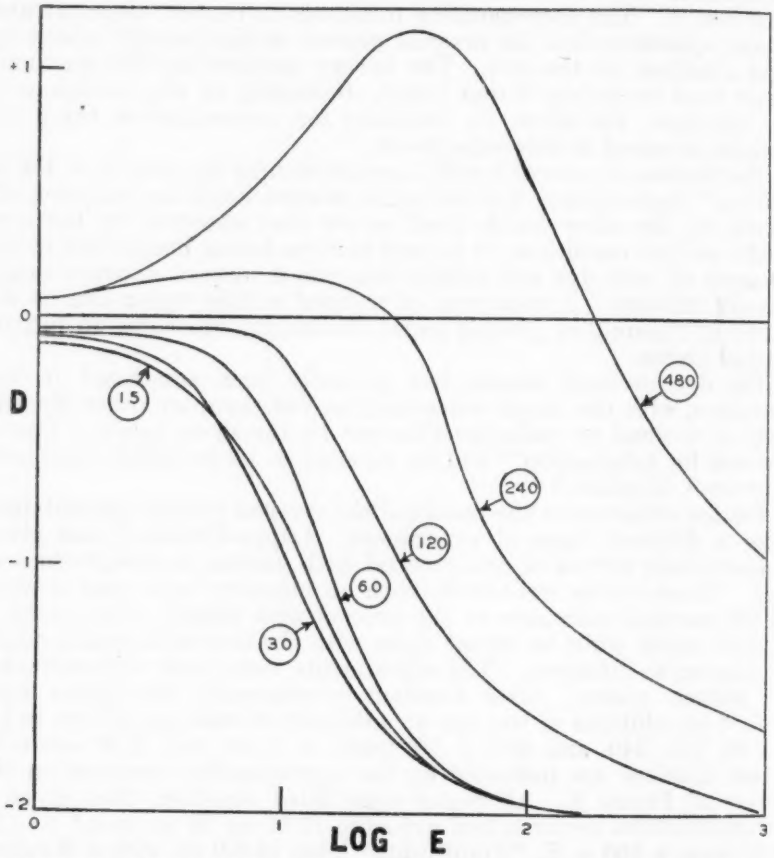

FIGURE 8.—*Characteristic curves of reversal process with safranine-dyed plates, made by time-scale exposures*

Densities on curves are changes from value produced from original uniform exposure. Numbers on curves multiplied by 10^3 indicate dilution of safranine.

it is faintly visible in Figure 6. No indications of this second negative were found in these time-scale exposures; it is possible that it might have occurred if the exposure could have been sufficiently prolonged, but at the lower dilutions of dye the minimum density was maintained without change over a range of exposure of more than 10 times.

The dye at a dilution of 15×10^3 produced slightly less effect than at the next higher dilution. Lüppo-Cramer [18] has frequently observed

[17] Lüppo-Cramer, Zeit. f. wiss. Phot., vol. 26, p. 350, 1929. Camera, vol. 6, p. 182, 1928.
[18] See footnote 16, p. 459.

that the more concentrated solutions may produce less effect, and has explained this on the basis of the mutual replacement of adsorbed dye and bromide ions on the silver halide with varying concentrations. It is not excluded, however, that in the plates bathed with the stronger solutions the excess unadsorbed dye may act as a filter to reduce the light absorbed by the dyed silver halide.

III. DISCUSSION

The outstanding feature of these data is the excellent correspondence between the energy absorbed by the dyed silver bromide and the reversal.

It must be remembered that any photochemical process is necessarily the result of absorption of radiant energy by the reacting system. In the plates as exposed in the spectrograph there are three materials possessing selective absorption in the visible spectrum and near infra-red. These are the silver halide, the dye, and the products of the first exposure (probably, but not positively identical with the latent image). Absorption by silver sulphide (sensitivity nuclei) may also reasonably be included with the products of exposure. Silver halides have strong selective absorption for radiation of wave lengths less than 500 mμ; the dyes have strong selective absorption for regions depending on the dye; and the products of exposure, plus silver sulphide, have selective absorption for the red and near infra-red,[19] which is extremely weak because of the minute traces present. Energy absorbed by any of these three from radiation in or near the visible region is a potential source of photochemical reaction in the plate, since the absorbing molecules must thereby become "excited" or "activated." The energy of activation may simply be transformed to heat, without reaction; an unknown proportion is so lost in the plates under discussion. A chemical reaction may follow activation either because the activated molecule itself breaks down, or because the energy of activation is transferred [20] to some other species of molecule, causing it to be chemically activated and therefore to react. This second process is commonly termed sensitization or photochemical catalysis. The spectral sensitivity of the plate will be determined by the primary process, the absorption of energy; but the photochemical yield from a given energy absorption (expressed when possible in terms of molecules reacting per quantum of energy absorbed) depends enormously on secondary chemical processes following the primary absorption; that is, on the chemistry of the system in which the absorption takes place.

Assuming anything like equal yield in terms of molecules reacting per quantum of light absorbed in different parts of the spectrum, we would therefore expect a marked reaction to be produced by the spectral regions absorbed by the silver bromide and the dye, respectively, and a very slight one in the red where the selective absorption by the latent image is strongest. The observed photographic reversal corresponds to this assumption. The plates bathed with fuchsin and safranine, on which the two main regions of absorption are far enough

[19] See footnote 12, p. 456.

[20] This process in gases occurs largely by "collision of the second kind." This same term has been applied by Leszynski and others to hypothetical energy transfer from sensitizing dyes to silver halide; without denying the possibility of such energy transfer in photographic sensitization, it seems quite undesirable in the present state of our knowledge to apply the term of "collision" to a process occurring in the solid state.

separated so that they can be clearly distinguished, were most sensitive in the region around 420 to 430 mμ, since the reversal was as strong as in the longer wave lengths, while the energy received on unit area was much less. As the absorption could not be measured quantitatively in the plates, it is impossible to estimate the relative quantum yield in the two regions.

In the opinion of the writers, the results given by Mauz [21] are in agreement with ours, in spite of their superficial differences. His use of a prism spectrograph with an incandescent source of about 2,850° color temperature caused a great concentration of energy in the red end of the spectrum. A simple calculation from the scale of his published figures and the energy distribution of such a source shows that the plates received about 85 times as much energy per unit area in the spectral region 600 to 700 mμ as in the region 400 to 420 mμ, as against a ratio of 6 for the same regions in our instrument. His exposures were, furthermore, so long as to produce reversal over the entire visible spectrum in every case, thus tending to obscure the differences between the plates bathed in different dyes. However, the influence of the absorption by the dye is clearly evident from his figures. The plates bathed with fuchsin and phenosafranine have marked maxima in the red which are not shared by the other dyes. That bathed with pinakryptol yellow has its strongest reversal between 400 and 500 mμ. The results with pinakryptol green are more difficult to interpret, but the appearance of the plates between 400 and 500 mμ, where the central part of the spectrum is dark and the edges light, is most probably explained by a maximum sensitivity in this region, combined with overexposure sufficient to produce the second negative. The light edges are the result of reversal in the region of irradiation from the more strongly exposed central portions. A similar effect may be detected in spectrum 8 (fig. 2) of the paper by Carroll. In Figure 2 of Mauz's paper the reversal in the region of absorption by the silver halide, where it is distinct from that of the dye, was obscured by the low intensity incident on this portion of the plates, but a secondary maximum is detectable at about 460 mμ.

Conclusions based on a process as complicated as this must be accepted with considerable caution, but the field for speculation is extensive and tempting. The theory of the true Herschel effect (reversal without dyes) is apparently simple. Absorption of red and infra-red radiation by the products of the first exposure causes them to react, naturally destroying their effectiveness as latent image whether the reaction is regression to the original form or not. The photographic sensitivity is very low, corresponding to very weak absorption; emulsions containing iodide show the Herschel effect with great difficulty because the traces of absorption by brom-iodide in the longer wave lengths cause a reaction (latent image formation) which counteracts the Herschel effect at least photographically, and probably chemically. The Herschel effect may be materially increased by changes in the chemistry of the emulsion, increase in bromide ion concentration and the presence of traces of copper salts being definitely established as promoters of the effect. As alkali bromides have no absorption in the visible region their effect must be on the secondary chemical processes following absorption.

[21] See footnote 4, p. 450.

The possible views of the effect of the dyes on reversal are that: (1) Energy absorbed by the dye is used in the reversal reaction, either directly or indirectly, and (2) the dye, like soluble bromide, increases the effect of absorption of energy by other materials, via the secondary chemical processes; this is the view taken by Lüppo-Cramer.[22] These theories are not mutually exclusive, since the second may apply independent of the first. The tendency to reversal in the presence of the dye certainly exists, since the rate of fading of the latent image in the dark is quite appreciable, especially when soluble bromide as well as desensitizer is present. This is essentially the same reaction, going on slowly under thermal activation of the dye molecules, and rapidly under photochemical activation. Further evidence that the dye causes a tendency to regression independent of its absorption of light comes from the observed reversal by radiation which must be absorbed by the silver bromide itself. In this case, we must assume that the energy absorbed by the silver bromide is transferred to the latent image. This is reasonable, since the converse process—spectral sensitization of silver bromide by colloidal silver—is a well-known phenomenon. Energy absorbed by the products of exposure must be effective in producing reversal in the presence of the dye, but it is nearly negligible in comparison to that acquired by the other absorbents. Our data fail to show that the sensitivity of the dyed plates to the red and infra-red resembles what might be expected if the true Herschel effect played any appreciable part in the reversal process. We accordingly consider that it is unjustifiable to identify the Herschel effect and the dye reversal to the extent which has been common in the literature.

The analogy between sensitization in the ordinary sense and the reversal phenomena under discussion is evident from the data on spectral sensitivity. It receives considerable confirmation from the effect of variables common to the two processes. The most important of these is the silver (or bromide) ion concentration. Increase in silver ion concentration (up to the point where fog interferes) greatly improves[23] the effectiveness of ordinary sensitization; conversely, increase in bromide ion concentration by addition of soluble bromide increases reverals by desensitizing dyes,[24] and decreases sensitization. We have shown in Figure 7 that the action of safranine, as the result of activation by light which it selectively absorbs, may be either, an increase or a decrease in density, depending on the bromide ion concentration of the emulsion. We have already expressed the opinion that the bromide ion concentration alters the oxidation-reduction potential of the silver halide grain with respect to its environment through the varying adsorption of bromide or silver ions to its surface. Further evidence that the reversal is an oxidation process is given by Lüppo-Cramer's observations[25] that photo-silver may be bleached by pinakryptol yellow plus bromide in light, and that under some conditions desensitization and reversal may be appreciably decreased by the presence of reducing agents, such as nitrite. We also have the increase in sensitization (hypersensitization) by reducing

[22] "Die an und für sich, besonders in langwelligen Gebiete vorhandene Tendenz zur Umkehrung der Bromsilberzersetzung (Herscheleffekt) durch die Farbstoffe infolge Keimisolierung unterstützt wird." (Handbuch, vol. 3, pt. 3, p. 285.)
[23] Carroll and Hubbard, B. S. Jour. Research, vol. 9 (RP488), p. 529, 1932.
[24] Lüppo-Cramer, Die Kinotechnik, vol. 11, p. 399, 1929.
[25] Lüppo-Cramer, Phot. Ind., vol. 28, p. 365, 1930.

agents,[26] and the increase in reversal by oxidizing agents.[27] These effects are somewhat erratic and difficult to reproduce, but appear to be real. The evidence establishes a strong presumption that sensitization and reversal by dyes are not only photographically but chemically opposite directions of the same process.

The nature of the characteristic curves with varying dye concentrations, in Figure 8, may be interpreted by the hypothesis that reversal begins when a given oxidation potential is reached. Oxidation potential under constant illumination should tend to increase with increasing concentration of dye, and with increase in latent image. The required potential may then be built up either by more concentrated dye and less image, or by an increase in image with the most dilute dyes. Once the reversal process is started, it may be able to continue without a decrease in reduction potential to the original value, if the quantity of dye is assumed to be chemically equivalent to many times the silver of the latent image.

Sensitization and reversal by dyes may be both brought about by energy absorbed by the dye. The simplest and most probable theory is that the dye, chemically activated by absorption, then takes part in an oxidation or reduction reaction with silver bromide or photo-silver. The evidence from spectral sensitivity, however, does not distinguish between this case and the transfer of the activation energy from the dye to another material which then reacts.

WASHINGTON, February 13, 1933.

[26] Bokinik, Zeit. f. wiss. Phot., vol. 30, p. 330, 1932; Carroll and Hubbard, B. S. Jour. Research, vol. 10 (RP525), p. 211, 1933.
[27] Lüppo-Cramer, Die Kinotechnik, vol. 10, p. 506, 1928.

1, 1-DIMETHYLCYCLOPENTANE AND 2-METHYLHEXANE IN A MIDCONTINENT PETROLEUM [1]

By Johannes H. Bruun [2] and Mildred M. Hicks-Bruun

ABSTRACT

This paper describes the separation and identification of 1,1-dimethylcyclopentane and of 2-methylhexane. The specific gravity, refractive index, boiling point, freezing point, and molecular weight of the isolated hydrocarbons are recorded and compared with the corresponding values for the synthetic hydrocarbons as reported in the literature. The infra-red absorption spectrum of the 2-methylhexane is shown. The 2-methylhexane is estimated to constitute about 0.25 per cent and the 1,1-dimethylcyclopentane not more than 0.04 per cent of the crude oil.

CONTENTS

	Page
I. Historical	465
1. C_7H_{14}, 1,1-Dimethylcyclopentane	465
2. C_7H_{16}, 2-Methylhexane	465
II. Experimental procedure and results	467
III. Discussion of the results	470
1. 1,1-Dimethylcyclopentane	470
2. 2-Methylhexane	471
IV. Acknowledgment	473
V. Bibliography	473

I. HISTORICAL

1. C_7H_{14}, 1, 1-DIMETHYLCYCLOPENTANE

1,1-Dimethylcyclopentane has apparently never been previously isolated from petroleum, nor does it seem that anybody claims to have established the presence of this hydrocarbon in any crude oil.

Synthetic 1,1-dimethylcyclopentane, however, has been prepared by Kishner (1),[3] who has reported values for its boiling point, refractive index, and density.

2. C_7H_{16}, 2-METHYLHEXANE

A study of the physical constants of known hydrocarbons reveals that a number of aliphatic and naphthenic hydrocarbons have boiling points which are near that (90.0° C.) reported for pure 2-methylhexane Because of this fact nobody seems to have succeeded in isolating the above hydrocarbon in a pure state from petroleum.

The presence of 2-methylhexane in petroleum, however, was indicated by the earliest investigators of petroleum, such as Pelouze and Cahours (2), Warren (3), and Schorlemmer (4). Since that time many investigators (5) have confirmed the presence of this isomer of *n*-heptane in petroleum and have also attempted to isolate the pure hydrocarbon. The physical constants of the final fraction, however,

[1] Financial assistance has been received from the research fund of the American Petroleum Institute. This work is part of project No. 6, The Separation, Identification, and Determination of the Constituents of Petroleum.

[2] Research associate representing the American Petroleum Institute at the Bureau of Standards.

[3] Figures in parenthesis here and elsewhere in the text indicate references given in the bibliography at the end of this paper.

indicate clearly that in every case considerable quantities of naphthene hydocarbons were present as contaminations.

Mabery (6) reported the isolation of a sample of "isoheptane" with a boiling range of 90° to 91° C. This sample was the result of 15 careful distillations, but the reported carbon-hydrogen ratio was too large to correspond to that of a pure aliphatic hydrocarbon.

Francis and Young (7) brominated the petroleum fraction which distilled between 93.5° and 102° C. and separated the normal and isoheptylic bromides by distillation under reduced pressure. They reduced the isoheptylic bromide with a zinc-copper couple and obtained a fraction which distilled between 89.9° and 90.4° C. This

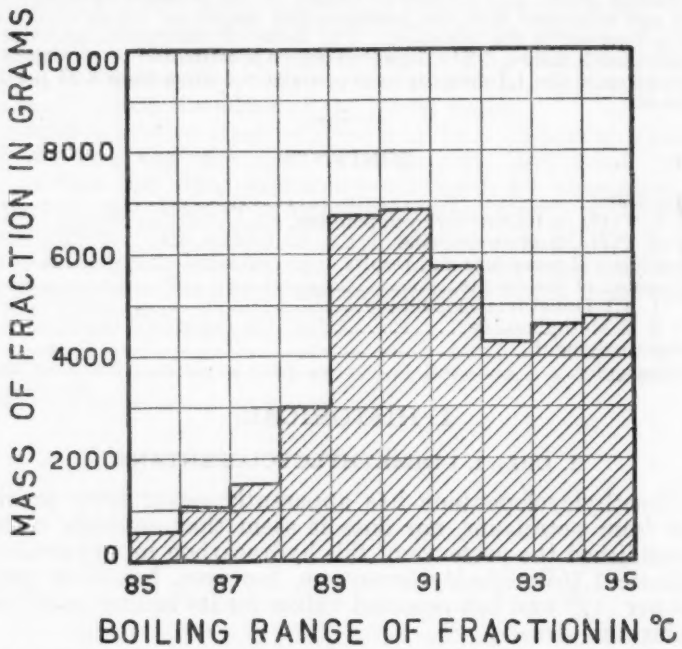

FIGURE 1.—*Distribution of the fractions over their boiling ranges before subjecting them to a nitrating treatment*

Ordinate: Mass of fraction in grams. Abscissa: Boiling range of fraction

had a specific gravity of 0.70670 $\frac{0°}{4°}$ (corresponds to 0.6852 $\frac{25°}{4°}$) as compared with 0.6746 $\frac{25°}{4°}$ for pure 2-methylhexane.

Charitschkow (8) subjected a fraction of Grosny gasoline, with boiling range 90° to 93° C., to a nitrating treatment and subsequent heating with fuming sulphuric acid. He obtained a fraction which distilled between 90.5° to 91.5° C. and which had a specific gravity of 0.7158 $\frac{15°}{0°}$ (corresponds to 0.7079 $\frac{25°}{4°}$). The vapor density agreed with the formula C_7H_{16}.

Later, Costaschescu (9) obtained from Roumanian petroleum by repeated distillation a fraction which he attempted to identify as 2-methylhexane. The boiling range and density of this sample, however, were respectively 91.5° to 92.5° C. and 0.7116 $\frac{0°}{0°}$ (corresponds to 0.6951 $\frac{25°}{4°}$).

Other investigators, who have later attempted to separate compounds from petroleum, have been content to merely comment on

the fact that while the isoheptanes are present in considerable quantity, their boiling points lie close together, and they show a marked tendency to form constant-boiling mixtures with other hydrocarbons and hence can not be isolated by physical methods.

II. EXPERIMENTAL PROCEDURE AND RESULTS

For the present investigation the Oklahoma crude petroleum used was that described in an earlier paper (10). The preliminary distillations[4] of the crude oil and of the fractions dealt with in this paper were carried out as reported in a previous publication (11). As a result of the preliminary distillations the petroleum fraction was distributed over its boiling range in the manner shown in Figure 1.

For the purpose of removing and determining the toluene which was present in the fractions, each cut was subjected to a nitrating treatment (12). The amount of material thus removed, however, was extremely small.

The subsequent final distillations of the fraction having boiling ranges between 85° and 95° C. were done almost entirely in the 11 m jack-chain column (13). About 2,000 ml of material was distilled each time, and the total distilling range for such a charge was often as low as a few tenths of a degree. For this reason special care had to be taken in mixing the distillates (according to their probable composition) for the redistillations. In most cases the boiling point, as well as the refractive index, was determined accurately for each fraction. After a great number of distillations in the 11 m column, a series of 0.1° and 1° C. cuts was obtained. In Figure 2 the distribution of these cuts is plotted against the boiling range. In this graph the amount in grams is given for each 1° C. cut. Thus, for instance, the sum of all of the 0.1° C. cuts with boiling ranges between 90° and 91° C. are shown as a single 1° cut. As shown in the graph, most of the material concentrated between 91° and 92° C., while, on the other hand, the fractions boiling between 85° and 90° and between 92° and 95° C. were comparatively small.

The refractive indices of the fractions, after the final distillations, are plotted against the boiling ranges in Figure 3. As shown by the graph, the highest refractive index (1.4101) was found for the material distilling between 87° and 88° C., while the fraction boiling between 90° and 91° exhibited a minimum (1.3947) in the refractive index graph.

In the case of the 87° to 88° C. cut, the amounts of available material were too small to permit isolation of the pure constituent. This fraction was subjected to a few more distillations in an efficient column, as a result of which the refractive index of the fraction distilling between 87.5° and 87.6° C. was raised to 1.4122. This fraction is discussed in Section III, below.

With regard to the 5,000 g of material with boiling ranges between 90° and 91° C., it was apparent (from the minimum exhibited by this fraction in the refractive index curve) that it consisted mainly of an aliphatic hydrocarbon. The molecular weight of this fraction was determined accurately (for method see (14)) and was found to be 99.6. From this value of the molecular weight, from the refractive index

[4] Acknowledgment is made to S. T. Schicktanz and assistants for all of the distillations referred to in this paper.

(1.3947) and from the boiling range of the material, it was concluded that 2-methylhexane was the major constituent. While pure 2-methylhexane is reported to freeze at −119.1° C. (15), our fraction did not freeze. By cooling, even at a very low rate, the viscosity of the material was tremendously increased, and instead of freezing to crystals a sirupy and glasslike substance was obtained, which could be pulled into long threads by means of a glass rod. In view of

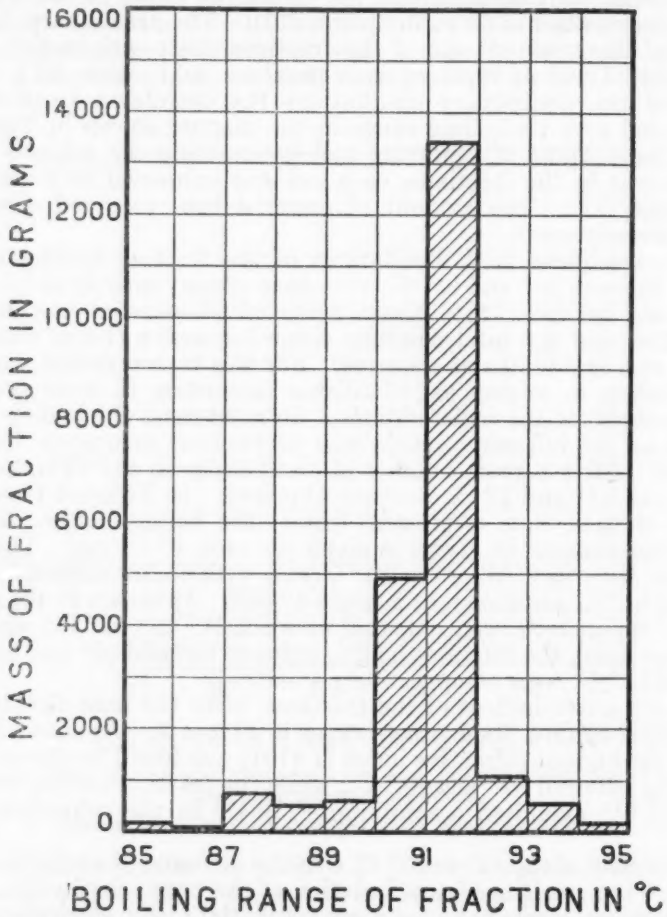

FIGURE 2.—*Distribution of the fractions over their boiling ranges after the final distillation*

Ordinate: Mass of fraction in grams. Abscissa: Boiling range of fraction.

the above fact it was apparent that further purification of the hydrocarbon could not be accomplished by means of simple equilibrium melting (16).

Attempts were made to separate the 2-methylhexane by preferential extraction. Aniline, sulphur dioxide, nitrobenzene, alcohols, and other solvents were tried, but without any appreciable amount of fractionation. Similarly, selective adsorption by means of silica gel, fuller's earth, charcoal, lampblack, and other materials was tried without success.

The method finally employed for the purification of the 2-methylhexane present in the 90° to 91° C. cut was that previously developed by R. T. Leslie (17) for the isolation of 2-methylheptane. The technic used was as follows: 100 ml of material to be fractionated was cooled by means of carbon dioxide slush and mixed with 120 ml of liquid propane. The liquid mixture thus obtained was further cooled by means of liquid air, after which it was slowly poured into

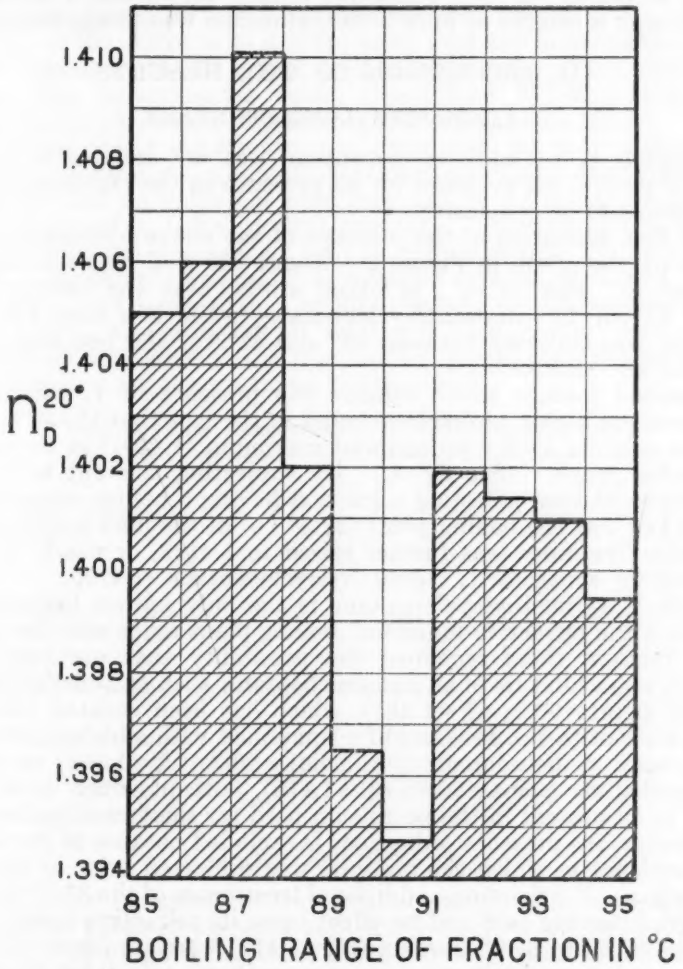

FIGURE 3.—*The refractive indices of the final distillates*

about 100 ml of liquid methane. Crystals would thereupon precipitate and these were separated from the mother liquor. After subsequent evaporation of the propane and methane, two fractions were obtained. The material which separated as crystals in the methane was found to be rich in 2-methylhexane. By systematic application of the above method, fractions of successively decreasing refractive indices were obtained.

As the fractionation proceeded, it was noticed that as soon as the refractive index decreased to below 1.393 the hydrocarbon would no longer form glass upon cooling, but would freeze easily to crystals. This, of course, indicated that the tendency to form a sirupy mass was not a property of the 2-methylhexane, but was caused by the impurities which were present in the 90° to 91° fraction.

The fractions which were obtained by the above method were mixed according to their refractive indices for further purification. In this way a sample of pure 2-methylhexane was finally isolated.

III. DISCUSSION OF THE RESULTS

1. 1, 1-DIMETHYLCYCLOPENTANE

Although 1, 1-dimethylcyclopentane was not isolated in a high state of purity, the evidence for its presence in the Oklahoma petroleum seems to be conclusive.

The first indication of the presence of the above hydrocarbon was shown by the graph in Figure 2. About 750 g of material distilled between 87° and 88° C., in other words, near the boiling point (87.5° C.) of 1, 1-dimethylcyclopentane, while less than 100 g of material was collected between 86° and 87° C., and less than 500 g between 88° and 89° C.

A second feature which renders the presence of 1, 1-dimethylcyclopentane highly probable is found in the fact that the 87° to 88° portion exhibits a very pronounced maximum (1.4101) in the refractive index graph. (See fig. 3.) By subjecting this cut to further distillation and by collecting a fraction having a boiling range of less than 0.1° C. at the boiling point (87.5° C.) of the pure hydrocarbon, the refractive index was further raised to 1.4122, or nearly to that reported for synthetic 1, 1-dimethylcyclopentane (1.4139).

While 1, 1-dimethylcyclopentane is the only known hydrocarbon for which the refractive index and boiling point agree with the petroleum fraction, there remained the possibility that our petroleum fraction was a mixture of an isomeric heptane, such as 2-methylhexane (boiling point = 90.2; $n_D^{20} = 1.385$), which has been isolated from the 90° to 91° cut (see p. 469) and of a compound with a higher refractive index, such as benzene (boiling point = 80.2; $n_D^{20} = 1.501$) or cyclohexane (boiling point = 80.8; $n_D^{20} = 1.476$), both of which have been found to be present in the petroleum used for this investigation.

However, the presence of benzene is excluded because of the nitrating treatment to which the material was subjected prior to the final distillation. Furthermore, additional treatments of the 87.5° to 87.6° cut with nitrating acid had no effect upon its refractive index.

If the 87.5° to 87.6° fraction ($n_D^{20} = 1.412$) were a mixture of cyclohexane and 2-methlyhexane, its composition, calculated from the refractive index, would correspond to 67 per cent of cyclohexane (molecular weight = 84) and 33 per cent of 2-methylhexane (molecular weight = 100). Such a mixture would have a molecular weight of 89.3.

The molecular weight was also calculated upon the previously mentioned assumption that the 87° to 88° cut consisted mainly of 1, 1-dimethylcyclopentane mixed with some 2-methylhexane. The composition of the 87.5° to 87.6° cut, calculated from its refractive index (1.4122) was thus found to be 95 per cent of 1, 1-dimethylcyclopentane (molecular weight = 98.1) and 5 per cent of 2-methyl-

hexane (molecular weight = 100). The molecular weight of this mixture should be 98.3. If other isomeric heptanes with boiling points near 87.5° C., such as 3, 3-dimethylpentane (boiling point 86° C.; $n_D^{20} = 1.391$) or 2, 3-dimethylpentane (boiling point 89.7° C; $n_D^{20} = 1.392$), were present as minor constituents in the petroleum fraction (boiling point 87.5° to 87.6° C.; $n_D^{20} = 1.412$) it is apparent that the percentage of 1,1-dimethylcyclopentane calculated from the refractive index would be less than 95, and consequently a somewhat higher value should be found for the molecular weight.

In view of the above facts it is apparent that any appreciable quantity of cyclohexane would reveal itself in a low value of the molecular weight. The experimental value, determined by measuring the freezing point depression in benzene, was found to be 102 ± 4. This result agrees, within the experimental error, with the above calculated value for a mixture of 1, 1-dimethylcyclopentane and 2-methylhexane.

It seems that no value has been reported in the literature for the freezing point of 1, 1-dimethylcyclopentane. Because of this fact a freezing point was determined for our impure sample of the hydrocarbon. The sample was found to freeze to crystals at −76° C., but it failed to yield more than a slight break in its time-temperature cooling curve. Consequently, it was not of high purity. In Table 1 the physical constants of the fraction are given, together with the reported values for the synthetic hydrocarbon.

TABLE 1.—*Physical constants of 1,1-dimethylcyclopentane*

Sample	d_4^{20}	n_D^{20}	Normal boiling point	Initial freezing point (in dry air)	Molecular weight
			°C	°C	
Synthetic: Kishner (1)	0.7552	1.4139	87.5		[1] 98.1
Petroleum fraction	[2] .7509	1.4122	87.5	−76.4	102±4

[1] Theoretical.
[2] Determined by the section for capacity and density of this bureau.

No definite value can be given for the amount of 1,1-dimethylcyclopentane present in the crude oil (600 gallons) but from the amount of the 87 to 88° cut (about 750 g) it is apparent that the percentage must be less than 0.04.

2. 2-METHYLHEXANE

The physical constants of the isolated sample of 2-methylhexane are given in Table 2, together with the best reported values in the literature. The high value found for the freezing point together with the flatness of the cooling curve (fig. 4) is an index of a high degree of purity.

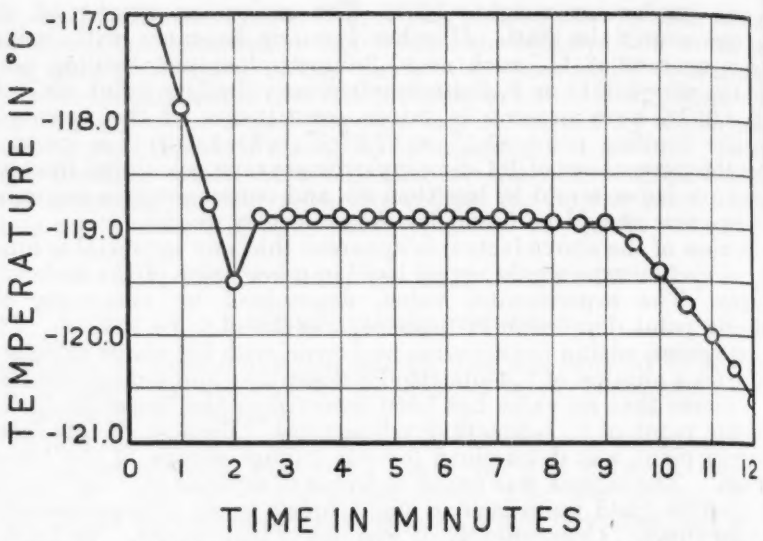

FIGURE 4.—*The time-temperature cooling curve of the 2-methylhexane isolated from petroleum*

TABLE 2.—*Physical constants of 2-methylhexane*

Sample	d_4^{25}	n_D^{20}	Normal boiling point	Freezing point (in dry air)	Critical solution temperature in aniline	Molecular weight
Synthetic:			°C	°C	°C	
Edgar and Calingaert	[1] 0.6746	1.38509	90.0	−119.1	74.1	[2] 100.0
Isolated from petroleum	[3] .67492	1.3850	89.67	[4]−118.90	74.1	[5] 100.0

[1] Computed from Edgar and Calingaert's value $d_4^{20}=0.6789$ and their value $\Delta d/\Delta t$ at 20° C. $=0.000855$.
[2] Theoretical.
[3] ± 0.00001. Determined by the section for capacity and density of this bureau.
[4] Determined by means of a platinum-resistance thermometer.
[5] For method used see (14).

The freezing point, which is about 0.2° C. higher than that reported for the synthetic hydrocarbon, was determined by means of a platinum resistance thermometer calibrated by this bureau in accordance with the international temperature scale (18), as adopted in 1927.

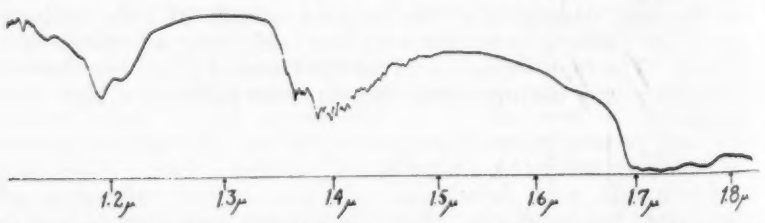

FIGURE 5.—*The energy transmission curve, through a 4 mm cell of 2-methylhexane, of the emission of a tungsten lamp source, recorded on an automatic registering infra-red spectograph*

Characteristic absorption of the hydrocarbon may be seen at 1.2, 1.4, and 1.7 μ. Fine structure bands at 1.1 and 1.4 μ are due to atmospheric water vapor. Recorded by U. Liddel, of the Fixed Nitrogen Research Laboratory of the U. S. Department of Agriculture.

The infra-red absorption spectrum of our best sample was determined by U. Liddel, of the Fixed Nitrogen Research Laboratory of the U. S. Department of Agriculture, and is shown in Figure 5.

From Figure 2 it is apparent that not less than 5 kg of 2-methylhexane was present in the petroleum fractions used for this work. Based upon the total amount of crude petroleum used (600 gallons, specific gravity = 0.9) it is estimated that the percentage of 2-methylhexane is not less than 0.25.

IV. ACKNOWLEDGMENT

The authors acknowledge the technical advice of E. W. Washburn, Director of American Petroleum Institute Project No. 6.

V. BIBLIOGRAPHY

1. Kishner, N. M., Chem. Zentr., vol. 2, p. 2132, 1913.
2. Pelouze and Cahours, Compt. rend., vol. 54, p. 1231; vol. 56, p. 505; vol. 57, p. 62.
3. Warren, C. M., Proc. Am. Acad. Art. Sci., vol. 27, p. 56, 1868.
4. Schorlemmer, C., Ann., vol. 136, p. 257, 1865.
5. References given in Engler-Höfer, Däs, Erdöl, vol. 1, p. 244, 1919, S. Hirzel, Leipzig.
6. Mabery, C. F., Proc. Am. Acad. Art. Sci., vol. 31, p. 55, 1894.
7. Francis, F. E., and Young, S., J. Chem. Soc., vol. 73, p. 921, 1898.
8. Charitschkow, K. W., Chem. Zentr., vol. 2, p. 474, 1899.
9. Costaschescu, N., Chem. Zentr., vol. 1, p. 682, 1911.
10. Washburn, E. W., Bruun, J. H., and Hicks, M. M., B. S. Jour. Research, vol. 2 (RP45), p. 469, 1929.
11. Bruun, J. H., and Hicks-Bruun, M. M., B. S. Jour. Research, vol. 7 (RP360), p. 608, 1931.
12. Bruun, J. H., Leslie, R. T., and Schicktanz, S. T., B. S. Jour. Research, vol. 6 (RP280), p. 364, 1931.
13. Bruun, J. H., and Schicktanz, S. T., B. S. Jour. Research, vol. 7 (RP379), p. 851, 1931.
14. Hicks-Bruun, M. M., B. S. Jour. Research, vol. 5 (RP215), p. 575, 1930.
15. Edgar, G., and Calingaert, G., J. Am. Chem. Soc., vol. 51, p. 1544, 1929.
16. Hicks-Bruun, M. M., and Bruun, J. H., B. S. Jour. Research, vol. 8 (RP432), p. 527, 1932.
17. Leslie, R. T., B. S. Jour. Research, vol. 9 (RP439), pp. 591–599, 1932.
18. Burgess, G. K., B. S. Jour. Research, vol. 1 (RP22), p. 635, 1928.

WASHINGTON, February 6, 1933.

161541—33——4

THE COMBINATION OF SILK AND WOOL WITH POSITIVE AND NEGATIVE IONS

By Milton Harris[1]

ABSTRACT

Wool, with an isoelectric point at pH 3.4, combines with negative ferrocyanide ion in solutions ranging in pH up to about 5.0 and with positive nickel ion in solutions ranging in pH down to about 2.0. Similarly silk, with an isoelectric point of pH 2.5, combines with ferrocyanide ion up to about pH 4.0 and with nickel ion down to about pH 1.8. Evidently these amphoteric proteins combine with both positive and negative ions over a certain range on both sides of the isoelectric point. The extent of this "isoelectric region" depends upon the ions employed as well as upon the protein. The limiting values obtained for the pH at which ions combine with a protein do not necessarily represent the isoelectric point of the protein.

CONTENTS

		Page
I.	Introduction	475
II.	Theoretical	475
III.	Review of previous work	477
IV.	Experimental	478
V.	Conclusions	478
VI.	Acknowledgment	478

I. INTRODUCTION

Quantitative determinations of the combination of proteins with ions are made by electrometric methods. Qualitative determinations are made by employing salts containing colored ions or ions which may form colored compounds on treatment with the proper reagents. Both methods have been used for the determination of the isoelectric point. It is the purpose of this paper to show the possibilities and limitations of such methods.

II. THEORETICAL

A colloidal (or other) particle is at its isoelectric point when the particle is electrically neutral with respect to its surrounding medium. For an amphoteric substance at its isoelectric point, the concentration of the anions is equal to that of the cations. That the sum of the anion and cation concentration is a minimum may be proved as follows:[2,3] Consider an amphoteric electrolyte of the type HROH. The law of mass action gives the following relationship:

$$\frac{[HR^+]\,[OH^-]}{[HROH]}=K_b \tag{1}$$

$$\frac{[ROH^-]\,[H^+]}{[HROH]}=K_a \tag{2}$$

At the isoelectric point $[HR^+]=[ROH^-]$; therefore

$$K_b\frac{[HROH]}{[OH^-]}=K_a\frac{[HROH]}{[H^+]} \tag{3}$$

[1] Research associate representing the American Association of Textile Chemists and Colorists.
[2] W. M. Clark, The Determination of Hydrogen Ions, p. 32, Williams & Wilkins Co., 1928.
[3] L. Michaelis, Hydrogen Ion Concentration, pp. 62-65, Williams & Wilkins Co., 1926.

Since $K_w = [H^+]\,[OH^-]$ then (3) reduces to

$$[H^+] = \sqrt{\frac{K_a}{K_b} \times K_w} \tag{4}$$

From equations (1) and (2) we may write

$$[HR^+] = [ROH^-] = K_b \frac{[HROH]\,[H^+]}{K_w} + K_a \frac{[HROH]}{[H]^+} \tag{5}$$

Let $X = [HR^+] + [ROH^-]$ For X to be a minimum, $\frac{dX}{d[H^+]}$ must equal 0

This condition is fulfilled when $[H^+] = \sqrt{\frac{K_a}{K_b} \times K_w}$ which is the value of $[H^+]$ at the isoelectric point given in equation (4). Therefore X, the sum of the anion and cation concentrations, is a minimum at the isoelectric point.

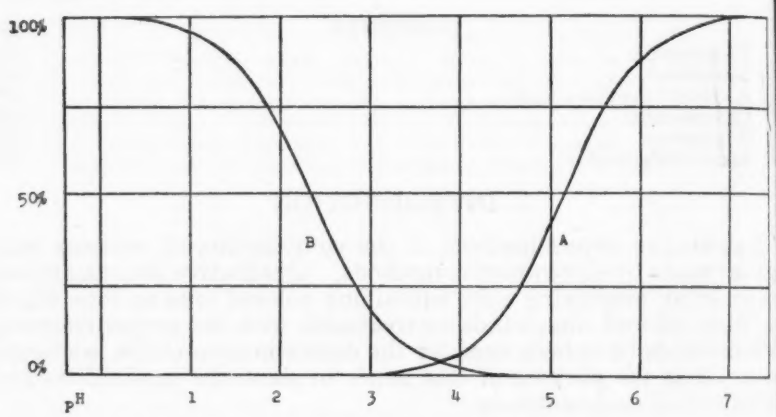

FIGURE 1.—*Dissociation curves of p-amino-benzoic acid*

That the ionization at this point is not zero is clearly shown in the dissociation curves of *p*-amino benzoic acid.[4] (Fig. 1.) They intersect at pH 3.77 which is the isoelectric point of this ampholyte. It is apparent from the curves that *p*-amino benzoic acid combines with positive ions on the acid side of the isoelectric point to about pH 2.7; similarly, it combines with negative ions on the alkaline side to about pH 4.9. These two points are the approximate limits of what may be called its isoelectric range.

If curves *A* and *B* intersected at zero per cent dissociation, the point of intersection would represent the isoelectric point. Moreover, if the two curves are symmetrical the isoelectric point will be the mean of the two limits. Such measurements might therefore be useful for defining approximately the isoelectric point. The suitability of such methods will depend largely on the sensitivity with which the limits of combination of the ions can be determined. The principle is illustrated by the data given on page 477 which show that the mean of the two limits for wool is 3.5 while the isoelectric point determined by migration is 3.4. The agreement for silk, for which the values are 2.9 and 2.5, respectively, is not so good, probably because of the difficulty noted in detecting the limits of combination.

[4] See footnote 2, p. 475.

III. REVIEW OF PREVIOUS WORK

Northrop and Kunitz [5] have contributed considerable data on the mbination of gelatin with cations and anions on both sides of the oelectric point. They used concentration cells and a method based the measurement of membrane potentials for those ions for which electrode was available. They found that gelatin combines appreciably with copper in acid solutions to pH 2 and with calcium to H 2.5, values which are considerably on the acid side of the isoelectic point of pH 4.7.

Pauli and Schön[6] measured the combination of undenatured egg albuin with zinc chloride. Chloride ion was found to be in a bound condion up to about pH 6. This justified Pauli's contention that negatively harged protein was capable of combining with the anion of the salt.

Carroll and Hubbard [7] found that the amount of silver ion comined with gelatin increases with increasing pH, but does not fall to ero on the acid side of the isoelectric point.

Loeb,[8] Speakman,[9] and Denham and Brash [10] have reported values or the isoelectric points of gelatin, wool, and silk, respectively, obtained ualitatively from the reactions of salts with these substances. The alue which Loeb obtained for the isoelectric point of gelatin is in good greement with values obtained by other workers employing various ethods. The values which Speakman and Denham and Brash obained for the isoelectric points of wool and silk are not in good agreeent with those obtained by other workers.[11]

Speakman treated samples of wool with standard potassium errocyanide solutions of known pH. After 24 hours the wool was emoved and carefully washed to remove uncombined ferrocyanide nd then immersed in ferric chloride solution to form the blue ferriferrocyanide. By this procedure he found that when the pH was igh no combination with the ferrocyanide ion occurred; at pH 4.8 ombination began and as the pH decreased the amount of ferroyanide ion absorbed by the wool increased. He concluded from this hat the isoelectric point of wool was in the neighborhood of pH 4.8. n his paper only the combination with negative ferrocyanide ion was eported, no experiments with positive ions being mentioned.

Denham and Brash treated samples of silk with copper acetate, ilver nitrate, and potassium chromate. Using copper acetate, they stimated the isoelectric point of China silk to be at pH 3.9, but with ussah silk they found it to be between pH 3.0 and 3.7. Using silver itrate they found the results to be "less definite but indicated that the

[5] J. H. Northrop and M. Kunitz, Combination of Salts and Proteins, J. Gen. Physiol., vol. 7, p. 25, 1924; vol. 9, p. 351, 1926; vol. 11, p. 481, 1928.

[6] W. Pauli and Schön, Untersuchungen an Elektrolytfreien, Wasserloslichen Proteinen, Biochem. Zeit., vol. 153, pp. 253–284, 1924.

[7] B. H. Carroll and D. Hubbard, The Photographic Emulsion—The Silver Ion-Gelatin Equilibrium, B. S. Jour. Research vol. 7, pp. 811–825, 1931.

[8] Jacques Loeb, Proteins and the Theory of Colloidal Behavior, p. 28, McGraw-Hill Co.

[9] J. B. Speakman, The Behavior of Wool as an Amphoteric Colloid, J. Soc. Dyers and Colourists, vol. 41, pp. 172–179, 1925.

[10] W. Denham and W. Brash, The Isoelectric Point of Silk Fibroin, J. Text. Inst., vol. 18, pp. T520–525, 1927.

[11] L. Meunier and G. Rey, Sur les Propriétés de la Laine, J. Intern. Soc. Leather Trades' Chemists, vol. 11, p. 508, 1927.
H. R. Marston, The Chemical Composition of Wool, Australia, Council Sci. and Ind. Res. Bull., No. 38, 36 pp., 1928.
M. Harris, The Isoelectric Point of Wool, B. S. Jour. Research, vol. 8, pp. 779–786, 1932.
T. G. Hawley and T. B. Johnson, The Isoelectric Point of Silk, Ind. & Eng. Chem., vol 22, pp. 297–299, 1930.
M. Harris and T. B. Johnson, Study of the Fibroin from Silk in the Isoelectric Region, Ind. & Eng. Chem., vol. 22, p. 539, 1930.
L. Meunier and G. Rey, Determination du Point Isoelectrique de la Laine et de la Soie, Compt. Rend., vol. 184, p. 285, 1927.
M. Harris, The Isoelectric Point of Silk, B. S. Jour. Research, vol. 9, pp. 557–560, 1932.

isoelectric point of fibroin lies at pH 4 or at a less pH value." In experiments with potassium chromate they found that the chromate ion was not held by the silk at pH 3.7 and above. They concluded that "the determination of the exact position of the isoelectric point in the ways described is therefore not quite certain apart from the question of an isoelectric range or of more than one isoelectric point," but concluded that that point lies between pH 3.6 and pH 4.0.

IV. EXPERIMENTAL

Samples of wool and boiled-off silk were purified by successive extractions with alcohol and ether until no appreciable residue was obtained on evaporation of the solvent.

The wool samples were treated with a 1 per cent potassium ferrocyanide solution in a pH range from 2 to 7. After 24 hours the wool was removed and each sample washed in a buffer solution of the same pH as the ferrocyanide solution in which it had been soaked. The washing was continued until no ferrocyanide could be detected in the sample treated at pH 7. It was assumed that all ferrocyanide mechanically held by the wool would wash out at the same rate regardless of the pH and only that chemically combined would be retained. The samples were immersed in a 1 per cent ferric chloride solution for one hour after which they were rinsed and dried. The samples treated above pH 5 showed no color; a light blue appeared at pH 5 and increased in depth as the pH decreased.

A second set of wool samples were treated with a 5 per cent solution of $NiCl_2$ in a pH range of 1.2 to 7. After 24 hours the samples were washed with corresponding buffer solutions until no nickel was detectable in the sample at pH 1.2. The wool was then treated with an alcoholic solution of dimethyl glyoxime. Below pH 2 the wool was colorless. At pH 2 a light pink color appeared and increased in samples treated with solutions of increasing pH.

Similar experiments were carried out with silk. Since the acid and basic binding power of silk is very weak, no sharp changes were detectable. The experiments indicated roughly, however, that silk combines with ferrocyanide up to about pH 4 and with nickel down to about pH 1.8.

V. CONCLUSIONS

The results of these experiments are in accord with those obtained by Northrop and Kunitz, Carrol and Hubbard, and Pauli and Schön. Taking the values for the isoelectric points of silk and wool to be at pH 2.5 and pH 3.4, respectively, they show that combination with positive or negative ions may take place within a certain range on both sides of the isoelectric points of these proteins. Consequently, values of the isoelectric points obtained by determining the pH limits of the combinations of positive and negative ions with silk and wool do not necessarily represent the isoelectric points of these substances, but indicate the point above or below which the fiber combines with a given ion. The mean of these limits may give an approximate value for the isoelectric point.

VII. ACKNOWLEDGMENT

This investigation was made possible by a grant to the American Association of Textile Chemists and Colorists by the Textile Foundation. We wish to express our appreciation for the aid given.

WASHINGTON, February 13, 1933.

THE PREPARATION AND CRYSTALLIZATION OF PURE ETHER-SOLUBLE RUBBER HYDROCARBON: COMPOSITION, MELTING POINT, AND OPTICAL PROPERTIES

By W. H. Smith, Charles Proffer Saylor, and Henry J. Wing

ABSTRACT

Rubber hydrocarbon from latex was purified by a method which involved the use of trypsin to remove protein adsorbed on the rubber particles. The natural antioxidants which always occur in crude rubber were used to protect the rubber during purification. The ether-soluble portion of the purified rubber was crystallized from dilute solutions at low temperatures. A special apparatus was devised for the microscopical examination of the crystalline hydrocarbon. By its means, the growth of crystals was witnessed, and the melting point and refractive indices were determined.

The crystals are spherulites composed of many fine needles. They have a consistent melting point at approximately 10° C. The refractive indices are ϵ=1.535 and ω=1.583 at −5° C. The index of the melted crystals is 1.525 at 11° C. Assuming that the molecule contains no more than 100 carbon atoms and that the crystals are a single substance, ultimate analysis indicates that the composition is $(C_5H_8)_x$.

CONTENTS

	Page
I. Introduction	479
II. Purification and crystallization of rubber hydrocarbon	480
1. Purification	480
2. Crystallization	483
III. Microscopical study of crystalline rubber	484
1. The apparatus	484
2. The crystals of ether-soluble rubber hydrocarbon	485
3. Melting point	486
4. Optical properties	487
IV. Determination of the composition of pure ether-soluble rubber hydrocarbon	488
1. Apparatus	488
2. Preparation of the sample	490
3. Balance, weights, and weighing	491
4. Analytical results	491
V. Acknowledgments	492

I. INTRODUCTION[1]

Substantially all of the chemical and physical evidence concerning the nature of rubber is consistent with the chemical formula $(C_5H_8)_x$, and this is the generally accepted formula for "rubber hydrocarbon." An examination of the evidence discloses, however, that the above formula is not the only one which is consistent with this evidence. The difficulty of establishing beyond question the chemical composition of rubber hydrocarbon has been due largely to the lack of efficient physical methods for fractionating the hydrocarbon, of proving that the final fractions are one-component systems, and of chemically identifying these fractions. If, as seems not improbable, rubber hydrocarbon is a mixture of closely related hydrocarbons not all of which can be represented by the formula $(C_5H_8)_x$, no single method of

[1] The introduction is part of a note by E. W. Washburn, Phys. Rev., vol. 38, No. 9, pp. 1790–1791, 1931.

fractionation can be relied upon to separate this mixture into its constituents. The only methods heretofore available for this purpose have been those based upon extraction with different liquids and fractional precipitation. One of the most powerful methods for fractionating a mixture of hydrocarbons is systematic crystallization and the purpose of this investigation was to develop a technic for applying this method to rubber.

II. PURIFICATION AND CRYSTALLIZATION OF RUBBER HYDROCARBON

By W. H. Smith

1. PURIFICATION

Rubber hydrocarbon readily undergoes changes in structure of an unknown character. Light, for example, changes the viscosity of rubber solutions, and the addition of a small amount of mineral acid rapidly decreases it. Crude rubber which is used in the preparation of commercial rubber cements must be masticated before it is dissolved in organic solvents or solution may be incomplete. Busse[2] has shown that the mastication of rubber requires oxygen to produce plasticity. Pure rubber hydrocarbon quickly oxidizes when exposed to air. The natural oxidation inhibitors of Hevea rubber, two sterol-like compounds, have been isolated by Bruson, Sebrell, and Vogt.[3]

Rubber of commerce, which is obtained chiefly from the latex of *Hevea brasiliensis*, contains various other substances in addition to rubber hydrocarbon. These nonrubber materials may be classified as water-soluble, acetone-soluble, protein or other nitrogenous compounds and mineral substances. Reviews of existing methods for preparing pure rubber hydrocarbon are given by Pummerer and Koch,[4] and by Pummerer and Miedel.[5]

Some form of commercial coagulated rubber was the raw material formerly used in attempts to prepare pure rubber hydrocarbon. Pummerer and Pahl,[6] however, used latex, which is preferable to coagulated rubber because the impurities are readily attacked in an alkaline dispersion. In their method, the latex is treated three or more times at 50° C. with a 2 per cent solution of sodium hydroxide to remove protein. After each treatment, the rubber particles coalesce or "cream" in an upper layer, and the impurities in the lower layer are drawn off. At the conclusion of the third treatment, neither the biuret reaction nor the ninhydrin reaction shows the presence of nitrogen in the rubber hydrocarbon. The alkali is finally separated by dialysis. The solutions are saturated with nitrogen during purification to protect the rubber from oxidation.

The use of trypsin to remove protein qualitatively from rubber in latex was first tried by Spence.[7] Later Freundlich and Hauser[8] used it to remove protein in Hevea latex and observed microscopically the disappearance of protein adsorbed on the rubber particles.

---

[2] Busse, W. F., India Rubber J., vol. 82, p. 311, 1931.
[3] Bruson, H. A., Sebrell, L. B., and Vogt, W. W., Ind. Eng. Chem., vol. 19, p. 1187, 1927.
[4] Pummerer, R., and Koch, A., Ann., vol. 438, p. 294, 1924.
[5] Pummerer, R., and Miedel, H., Ber., vol. 60B, p. 2148, 1927.
[6] Pummerer, R., and Pahl, H., Ber., vol. 60B, pp. 2152–63, 1927.
[7] Spence, D., Caoutchouc and Gutta-percha, vol. 5, p. 1632, 1908.
[8] Freundlich, H., and Hauser, E. A., Kolloid Z., 36A, Zsigmondy Festschrift, pp. 15–36, 1925.

Rubber may be separated into two fractions by ethyl ether. Petroleum ether has also been suggested for the purpose by Caspari.[9] The fractions are called, in the literature, alpha and beta, or sol and gel phases. Ethyl ether has been used in the present work, and throughout this paper the fractions are called, respectively, the ether-soluble and ether-insoluble portions of the total rubber hydrocarbon.

When crude rubber of commerce is extracted with ether, the soluble rubber is quite pure, as Feuchter[10] has indicated, and the impurities are concentrated in the insoluble portion.

According to Pummerer,[11] from 65 to 75 per cent of the total rubber is soluble in ether, and Bruson, Sebrell, and Calvert[12] reported that 75 per cent of the material was ether-soluble. They noted also that the "polymers" of rubber formed by treating it with tin tetrachloride could be separated by benzene, and that the ratio of soluble to insoluble "polymer" was 75 to 25. Whitby[13] believes that "the coincidence of these proportions was probably fortuitous." He has noted the wide variation reported in the literature on the relative amounts of soluble and insoluble rubber. The work of the Midgley Foundation[14] on the fractional precipitation of rubber indicated that unmilled pale crêpe contains a single "sol" component, which amounts to more than half of the material.

Pummerer and Koch[15] were the first investigators to report the isolation of crystalline rubber. More recently, however, Pummerer and von Susich[16] have stated that the crystallized material reported by Pummerer and Koch was not rubber but alpha gutta-percha.

In the course of work on the purification of rubber hydrocarbon by the author, several lots of pure material were prepared by the method of Pummerer and Pahl. It was observed that the treatment of latex with a 2 per cent solution of sodium hydroxide at 50° C. causes the ether-insoluble fraction to become partly soluble. At 60° C. the effect is intensified. At 80° C., however, much of the ether-soluble fraction becomes insoluble. This behavior was subsequently confirmed on isolated ether-soluble and insoluble hydrocarbon. Therefore, to separate the two fractions, it is necessary that contact with alkali at 50° C. be avoided, if a partial conversion of the ether-insoluble fraction into an ether-soluble form is to be prevented.

It appeared possible to use trypsin for the quantitative removal of protein. The enzyme mixture in technical preparations of trypsin is effective between pH 8.2 and pH 10.2. A 3 per cent aqueous solution of sodium bicarbonate provides a suitable medium, and a temperature of 38° to 39° C. is satisfactory. It was observed that if digestion of the protein in the latex takes place in the presence of a 3 per cent solution of sodium bicarbonate, the subsequent addition of sodium hydroxide equivalent to a 2 per cent solution causes creaming at room temperature. Under these conditions, the sodium hydroxide solution is used only as a creaming agent at room temperature, in accordance with DeVries and Beumée-Nieuwland's[17] technic, and the action of alkali on latex at 50° C. is avoided.

---

[9] Caspari, W. A., J. Soc. Chem. Ind., vol. 32, p. 1041, 1913.
[10] Feuchter, H., Kolloidchem. Beihefte, vol. 20, p. 434, 1925.
[11] Pummerer, R., Kautschuk, vol. 2, pp. 85–88, 1926.
[12] Bruson, H. A., Sebrell, L. B., and Calvert, W. C., Ind. Eng. Chem., vol. 19, p. 1033, 1927.
[13] Whitby, G. S., Trans. Inst. Rubber Industry, vol. 5, pp. 40–62, 1930–31.
[14] Midgley, jr., T., Henne, A. L., and Renoll, M. L., J. Am. Chem. Soc., vol. 54, p. 3381, 1932.
[15] Pummerer, R., and Koch, A. See footnote 4, p. 480.
[16] Pummerer, R., and von Susich, G., Kautschuk, vol. 7, pp. 117–119, 1931.
[17] DeVries, O., and Beumée-Nieuwland, N., Arch., Rubbercultuur, vol. 9, p. 694, 1925.

With the above observations as a basis, a method of purificatio was developed in which it was sought to maintain unchanged th structure of rubber hydrocarbon and also to permit a sharp separatio of the ether-soluble and insoluble fractions. Throughout the purifi cation, until the coagulated rubber was extracted with acetone, th rubber hydrocarbon was protected against the action of light, whic produces a gel in an ether solution of the hydrocarbon. It was als protected against the action of oxygen by the natural antioxidants which have a powerful protective action. The antioxidants wer extracted from commercial smoked sheet according to the method o Bruson, Sebrell, and Vogt.[18] An amount sufficient to keep the rubbe protected was added to the latex at intervals and later removed from the coagulated rubber by extraction with acetone. The antioxidants were not isolated, but were used in concentrated alcoholic solution after freezing out phytosterol and octadecyl alcohol. The alcoholic solution of antioxidants was kept under nitrogen, to preserve their protective action.

The details of the method of purification are as follows: Four hundred milliliters of 38 per cent commercial ammoniated latex was dialyzed, using a bag of washed cellophane. According to the observation of Beadle and Stevens,[19] from 20 to 25 per cent of the total nitrogen derivatives is dialyzable, and they are consequently removed with the ammonia. Dialysis was continued until the latex was almost free from ammonia. At its conclusion, the latex, already considerably diluted, was further diluted with distilled water to a volume of 2,500 ml. About 80 g of sodium bicarbonate was added to make approximately a 3 per cent solution. The latex was warmed to 38° C. in an oven, after which a filtered aqueous solution of trypsin containing about 2.0 g was added. If the trypsin is added at room temperature, coagulation may occur. The mixture was maintained at 38° C. for 10 hours, and afterward was allowed to cool to room temperature. A solution of sodium hydroxide was added to produce a concentration of 2 per cent. Creaming commenced immediately and after one or two hours the lower layer, containing the impurities but practically free from rubber, was removed. Another portion of 2 per cent sodium hydroxide solution was added and creaming was repeated with subsequent removal of the lower layer. The number of creamings necessary to reduce the impurities to a negligible amount was estimated from the relative volumes of the upper and lower layers, by assuming that the soluble impurities were uniformly distributed between the layers at each washing. After the final washing the creamed rubber was dialyzed through a washed cellophane membrane until neutral to phenolphthalein. A portion of the rubber coagulated as the last traces of alkali were removed. The remainder was in some cases coagulated by adding acetone and passing a brisk current ofnitrogen into the mixture to cause ollision and adhesion of the rubber particles. In other cases the rubber was obtained by electrodeposition. The coagulated or electrodeposited rubber, still containing added antioxidant, was cut into strips and dried in a vacuum at room temperature. It was then cut into small pieces (2 mm ^{3}), extracted with acetone for 20 hours, and dried in a vacuum. The product was transparent and amber colored. The

[18] Bruson, H. A., Sebrell, L. B., and Vogt, W. W. See footnote 3, p. 480.
[19] Beadle C., and Stevens, H. P., Kolloid Z., vol. 13, p. 220, 1913.

mount of nitrogen in the purified total rubber before extraction with cetone was found to vary between 0.008 and 0.02 per cent as deter-ined by the Kjeldahl method. The extracted rubber was free from itrogen when analyzed by the same method.

The total rubber which had been extracted with acetone was ubsequently extracted with ether. This operation was performed at mes in a Soxhlet extractor and at other times in the apparatus sug-ested by Pummerer, Andriessen, and Gündel.[20] In each instance a tream of nitrogen was passed through the ether during extraction. n the course of the work it was observed that when rubber is pro-ected by the natural antioxidant during purification, approximately 5 per cent of the total rubber is soluble in ether. The solution of ubber hydrocarbon, suitably diluted with ether, and saturated with itrogen, was used to obtain crystalline rubber hydrocarbon. These rystallizations were not confined to one lot of material but represent ubber hydrocarbon which was purified at intervals from different hipments of ammoniated latex.

2. CRYSTALLIZATION

The conditions necessary for the formation and growth of crystal-ine particles have been formulated by Tammann,[21] by von Weimarn,[22] nd by others. Purity is necessary, particularly freedom from material which might be adsorbed on the crystal nuclei. With ubber this means freedom from material of a nitrogenous nature. The fluidity should be high enough to provide sufficient mobility for he formation of nuclei, and the solution should be dilute in order to keep the number of nuclei at a minimum. The temperature should e sufficiently low to start the formation of nuclei and to provide a uitable medium for their continued growth.

Solutions of different concentrations of ether-soluble rubber, dis-olved in anhydrous ether, were prepared and subjected to successively ower temperatures, beginning at $-10°$ C. At $-65°$ C., with a con-entration of 1 part of rubber to 2,000 parts of ether, tiny particles of material which were birefringent under crossed nicols, separated after about one hour. The particles grew slowly and formed aggregates. These developed into larger aggregates during a period of several hours, and after about 12 hours the entire mass settled as a clot. Repeated experiments confirmed the observations. Concentrations of 1 part of rubber in 2,500, 3,000, and 3,500 parts of solvent gave similar results but with increasing slowness.

The velocity of formation of nuclei under such conditions is high and crystal habit is not established. Crystal habit is developed by using Tammann's [23] procedure, which permits the formation of only a few nuclei, and these are subsequently grown under conditions such that the formation of new nuclei is at a minimum and the velocity of crystallization is suitable.

Two Dewar flasks were used, one a silvered half-liter flask and the other of 4 liters capacity. The smaller flask was supported in the larger flask, which was inclosed in several layers of insulating felt. Each flask contained acetone at $-58°$ C. A tube containing the

[20] Pummerer, R., Andriessen, A., and Gündel, W., Ber., vol. 60B, pp. 1583–1591, 1928.
[21] Tammann, G., Kristallizieren u. Schmelzen, Johann Ambrosius Barth, Leipzig, 1903.
[22] von Weimarn, P. P., Zur Lehre von den Zuständen der Materie, Theodor Steinkopff, Dresden, 1914.
[23] Tammann, G., Kristallizieren u. Schmelzen, see footnote 21, p. 483.

ethereal solution of the rubber hydrocarbon was cooled to −65° C. for 15 minutes and then allowed to warm to −58° C., at which temperature it was immersed in the acetone contained in the smaller Dewar flask. During a 24-hour interval the temperature increased about 15°. Although the temperature rose, the velocity of crystallization was low and a satisfactory degree of supersaturation was maintained. The rubber deposited on the sides of the tube in small nodules which appeared to have developed radially from a point in the center. By maintaining suitable conditions for a longer period, nodules half a millimeter in diameter or larger are produced. Approximately 95 per cent of the rubber crystallizes at −65° when the initial concentration is 1 part of rubber in 2,500 parts of ether.

Material prepared as nodules was used in the examination of optical properties and in the determination of the hydrogen-carbon ratio.

In addition to the crystals of ether-soluble rubber obtained as described above, crystals of the ether-insoluble form of rubber have also been produced. These latter crystals differ materially from the ether-soluble crystals both in appearance and in melting behavior. They will be discussed in a later paper.

IV. MICROSCOPICAL STUDY OF CRYSTALLINE RUBBER

By Charles Proffer Saylor

The low temperature which is necessary for the nodules of rubber hydrocarbon to be stable in contact with their ether solution makes it impossible to watch their growth or determine their properties by the usual microscopical methods. Several forms of apparatus [24] have been used in the examination of crystals at low temperatures, but, since none of them was entirely suited to the uses described in this paper, an apparatus was designed by means of which the crystallinity of the nodules was established and some properties of the crystals were determined.

1. THE APPARATUS

The apparatus which was employed is illustrated in Figure 1. It departs from that commonly used in photomicrography between crossed nicols chiefly in three particulars: (1) The sample is contained in an unusual form of cell; (2) a Dewar flask with optically plane windows at the bottom holds the cell and its temperature bath; and (3) a long range immersion condenser, capable of focusing the light source on the crystals at the bottom of the cell, is employed. The details of these parts are represented in Figure 2. The cell and Dewar are made entirely of Pyrex glass. The cell is a cylinder with an inside diamater of 12 mm and a height of 10 mm. To its polished upper and lower edges are sealed the ground and polished disks, 0.5 mm thick, which serve as windows. Two tubes for filling and emptying connect with the cylinder. One of them is bent downward inside the cell and nearly touches the surface of the bottom disk. The windows of the Dewar flask, which also are polished, optically plane disks of glass sealed to polished edges on the flask, are 1 mm thick, 30 and 24 mm, respectively, in diameter, and 1 mm apart. When the cell rests on the inner window of the Dewar flask, the distance from the crystals on its bottom to the outside of the flask is 3.5 mm. Therefore,

[24] Such apparatus is reviewed by E. M. Chamot and C. W. Mason, Handbook of Chemical Microscopy, vol. 1, pp. 206-208, John Wiley & Sons (Inc.), New York, 1930.

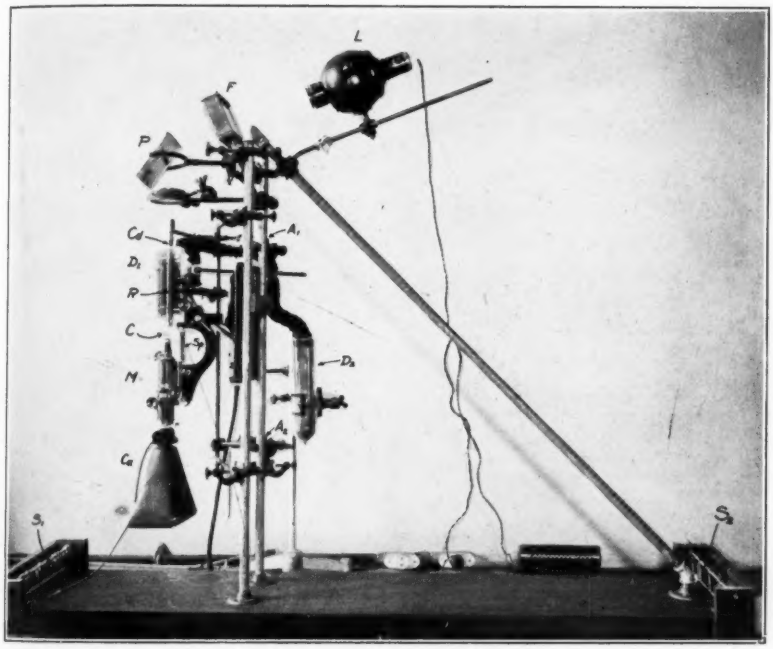

FIGURE 1.—*Assembly of apparatus*

C, cell; D_1, Dewar flask with optically plane windows at bottom; *Cd*, optical condenser; *L*, projection lamp; *F*, light and heat filter; *P*, polarizing reflector; *M*, microscope; *Ca*, camera; D_2, Dewar flask to contain liquid air; *R*, refrigeration coil; *A*, A_2, axis of rotation for D_1, *Cd*, *R*, and *C*; *Sp*, spring to overcome weight of microscope tube; S_1, S_2, spring suspension.

UNIV OF MICH.

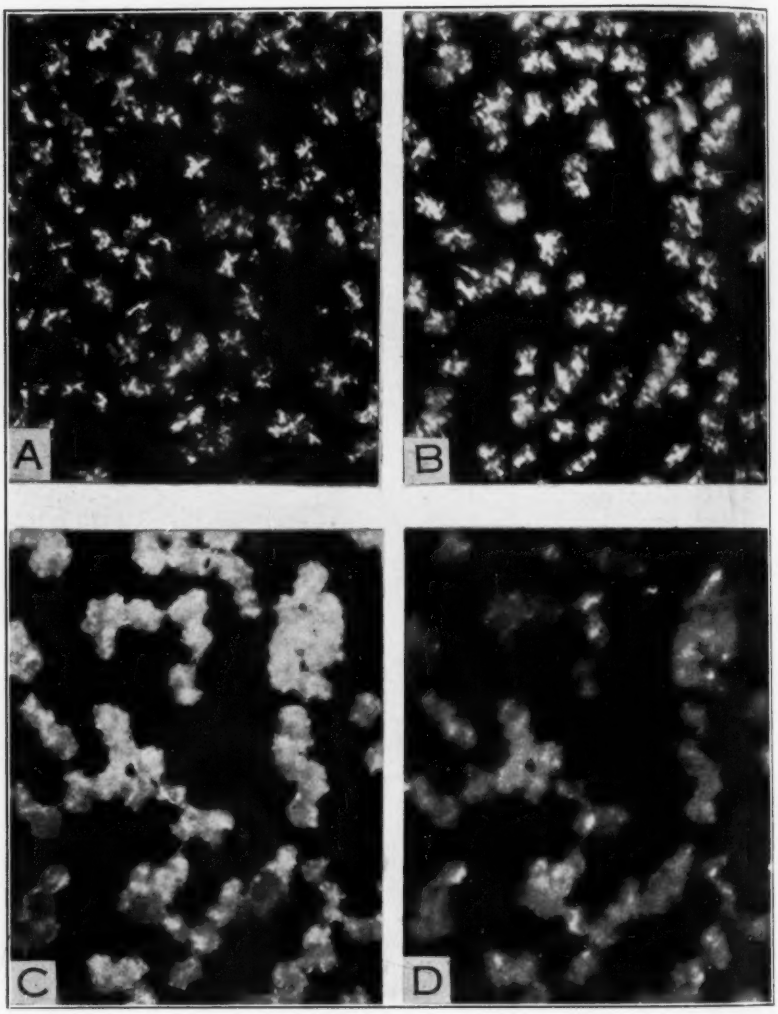

FIGURE 3.—*Photomicrographs showing melting of ether-soluble hydrocarbon crystals*

A, crossed nicols. × 200. Rubber crystals surrounded by mother liquor. They are roughly spherular clusters of birefringent crystals. The brightness of the clusters is created by their optical anisotropy. Temperature, −50° C. Exposure, 1 second.

B, crossed nicols. × 200. A similar field after the mother liquor has been withdrawn. Otherwise, except for optical distortion produced by the adhering liquid, there is no significant difference. The different clusters can be seen in the same position in this and succeeding photomicrographs. Temperature, −45° C. Exposure, 5 seconds.

C, crossed nicols. × 200. Same field as *B*. The ether has all been evaporated by suction. Surface tension has distorted the crystals. As a consequence the brightness of birefringence is less. This is indicated by the greater exposure. Temperature, −40° C. Exposure, 12 seconds.

D, crossed nicols. × 200. Same field as *B*. Just below the melting point. The principal difference between this and *C* arises from differences in the photomicrography. Temperature, +8.4° C. Exposure, 12 seconds.

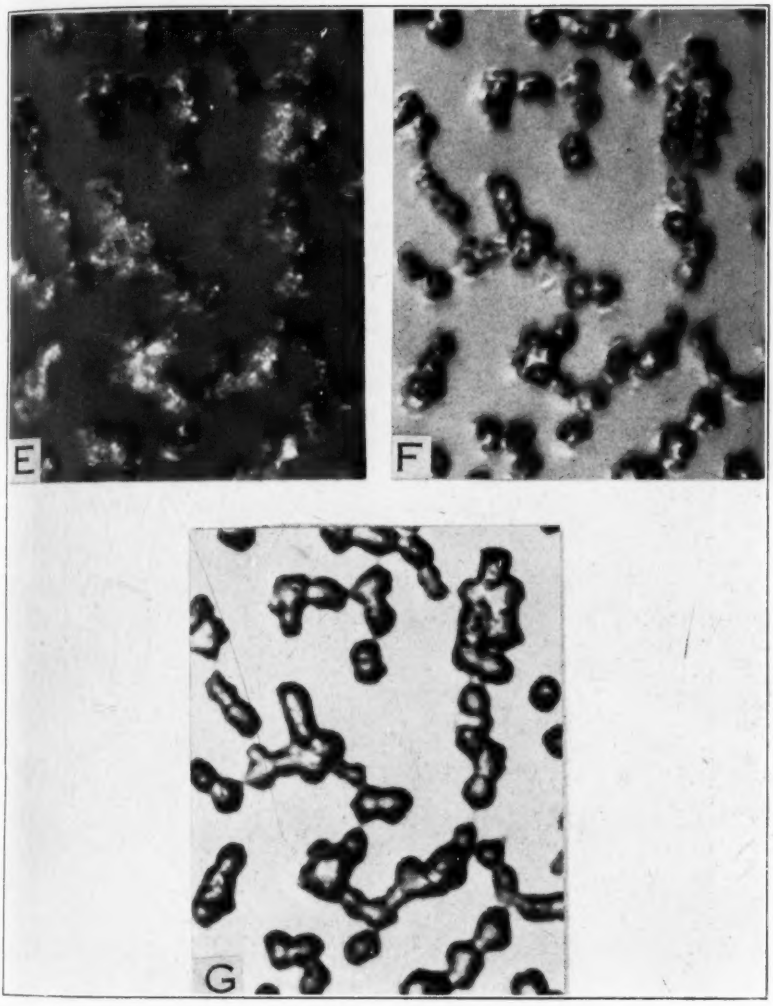

FIGURE 3 (Continued).—*Photomicrographs showing melting of ether-soluble hydrocarbon crystals*

E, crossed nicols. × 200. Same field as *B*. Much of the birefringence has disappeared. It is supposed that the more severely distorted crystals have melted below the true melting point. Those which were less distorted persist unchanged. Temperature .7° C. Exposure, 12 seconds.
F, crossed nicols. × 200. Same field as *B*. Very long exposure so that extinct field appears bright. Birefringence has disappeared. Groups are beginning to flow into globules. Temperature, +11.8° C. Exposure, 1 minute.
G, parallel nicols. × 200. Same field as *B*. Because of the smallness of the clusters, the surface tension forces have been relatively large. Melted ether-soluble rubber hydrocarbon has flowed into rounded globules. Temperature, +12.6° C. Exposure, 1/10 second.

FIGURE 4.—*Crystals of ether-soluble rubber hydrocarbon*

Crossed nicols. × 500. The dark cross which is characteristic of spherulites can be readily observed.

lthough the crystals were viewed at temperatures as low as −90° C, was possible to use a 16 mm objective, N. A. 0.25. An excessive mount of glass intervened between the objective and its focal plane, ut satisfactory images were ormed despite this handicap. he Dewar flask contained ace- one, which was cooled by rawing liquid air from flask, D_2 n Figure 1, through the coil, R, f copper tubing. Temperatures ere determined by means of a riple junction, copper-constantan hermocouple. The condenser, *Cd*, was so designed that it ocused the entire beam from the rojection lamp upon the prep- ration, forming an image the ize of the microscope field. The icroscope, a petrographic model ith a rotating tube analyzer, as bolted by its base to the ertical support. A rotation of 0° at the pillar joint permitted omplete inversion of the instru- ment. Except when refractive ndices were determined, a mul- iple plate polarizer served as he primary nicol. A tube cam- ra with side telescope was used oth for viewing and for photo- graphing preparations in th ecell. he positions of the Dewar flask, he condenser, and the coils of opper tubing were adjusted on a swinging support so that they were coaxial with the microscope when the support was pushed against stops and clamped.

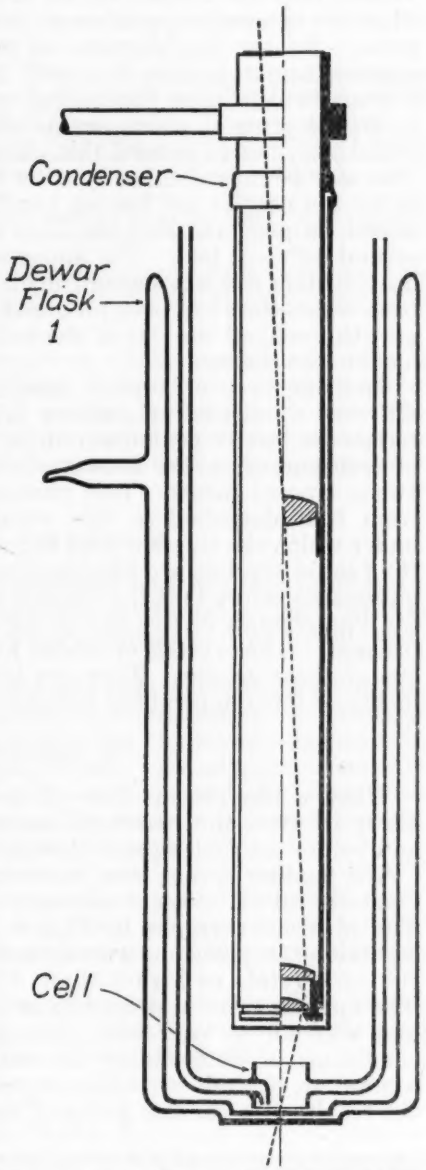

FIGURE 2.—*Cell, Dewar flask, and condenser*

The dotted line indicates the course of a beam of light. It intersects the center line at levels where images of the arc crater are formed

2. THE CRYSTALS OF ETHER-SOLUBLE RUBBER HYDROCARBON

A solution of ether-soluble rubber hydrocarbon was treated as has been described on page 483. This treatment caused the formation of nodules on all walls of the cell. More nodules formed on the bottom of the cell, however, than on any of the other surfaces. If the cell was removed from the bath, the upper surface touched briefly with a finger, and the cell replaced in the bath, the temporary warmth caused the crystals at the spot touched to dissolve but did not disturb those on the bottom of the cell. The alcohol in the Dewar flask

was cooled to −50° C. The cell was transferred to the flask, and the revolving carriage which supports the Dewar flask, cooling coil, condenser, and cell was swung into the optical axis of the microscope. Viewed between crossed nicols, the crystals appear as in Figure 4.[23] They are spherulites, clusters of thin needles radiating from a central point. By the birefringence of its individual needles, the cluster appears bright against the dark background. The best organized clusters tend to show the typical spherulitic extinction, a dark radial cross, the arms of which are parallel to the nicol prisms and rotate with them, but in general this phenomenon is not very well marked. This may be caused either by a low state of organization in the clusters or by the needles not having parallel extinction. It has been mentioned on page 483 that the latex used in this work was obtained in several different lots. The appearance and properties of the spherulitic clusters did not depend upon the sample of ammoniated latex from which they had been prepared, although the conditions of crystal growth modified the size of the individual needles and their arrangement in the cluster.

Birefringence, or optical anisotropy, is characteristic of three different conditions of matter: (*a*) Viscous liquids or colloidal materials are birefringent when under mechanical strain. Thus a sheet of transparent rubber shows polarization colors when stretched between crossed nicols. This phenomenon is fundamentally different from that described in this report. Furthermore, the conditions under which the clusters were formed are unlikely to result in strains. (*b*) Liquid crystals are birefringent. The great amount of structure observable shows that the clusters of Figure 4 are not liquid crystals. (*c*) The crystals of five out of six systems of true crystals are birefringent. The crystals of rubber hydrocarbon undoubtedly belong to one of these groups. They are true crystals and appear to offer a means of purifying rubber hydrocarbon.

3. MELTING POINT

When a birefringent crystal melts, the birefringence disappears abruptly when the structural interrelations of the solid are loosened and before the first signs of flowing can be observed.

The mother liquor was removed from a preparation of rubber crystals and all residual solvent evaporated by evacuating the cell. The photomicrographs in Figure 3 illustrate the changes in these crystals as they became warmer and establish the melting point of the rubber crystals as higher than +9.5° C. and lower than +11° C. The melting point appeared to be independent of the sample of latex and also not to vary with different preparations of crystals. The conditions of determining the melting point influenced the result somewhat, but not more than would be expected. Table 1 indicates the results of a varying group of such determinations.

[23] An earlier photomicrograph of sol rubber crystals was published with the note previously mentioned (see footnote 1, p. 479).

TABLE 1.—*Determinations of the melting point of ether-soluble rubber hydrocarbon*

Melting point (° C.)	Conditions affecting accuracy
5	Evaporation of ether with water-jet pump.
8	Evaporation of ether with an oil pump.
5-11	Very thorough removal of solvent. Evacuation with oil pump continued during entire time that temperature rose. A series of photomicrographs (fig. 3), shows the condition of the crystals at each significant temperature.
0-9.5	Replacement of ether with acetone. Melting of crystals determined under acetone.
8.0-8.8	Replacement of ether with acetone. Replacement of acetone with Sonstadt's solution [1] diluted with acetone. Melting was determined under this mixture in which the crystals had been immersed at a temperature near their melting point for 4 days.

[1] Sonstadt's solution, otherwise known as Thoulet's solution, is a saturated water solution of potassium mercuric iodide. It is used for gravity separations of minerals and occasionally for the determination of refractive indices.

NOTE.—The second and third determinations are believed to be more trustworthy than the others. The third is particularly favored because of the thorough removal of the solvent (the oil pump operated about 3 hours) and because the making of photomicrographs largely removed the personal element from the determination.

That fraction of rubber hydrocarbon which is soluble in ether is therefore a stable liquid at the ordinary temperatures at which rubber is used. Its melting point has not seemed to depend upon whether it represented the whole ether-soluble component or only that which remained in ether solution after a portion had been precipitated with acetone and discarded.

4. OPTICAL PROPERTIES

The largest spherulites which have so far been grown for microscopical examination were about 50 microns (0.05 mm) across. In these clusters the individual particles were needles about 20 μ long and 1 or 2 μ wide.

The refractive indices of the crystals were determined by immersion [26] in aqueous solutions of potassium mercuric iodide. The method of central illumination was used to indicate the relation between the index of a crystal and the immersing liquid. By adjusting concentrations of the iodide solutions each index of the crystals was matched at $-5°$ C. The index of the corresponding liquid was then determined on an Abbe refractometer at the same temperature.

So far as possible, needles were chosen which were somewhat separated from the clusters. Two indices were determined corresponding to the ϵ and ω of uniaxial crystals. It must not be inferred, however, that the rubber crystals are uniaxial. There was no attempt to obtain an interference figure.

The uncertainty of the determinations is greater than equally careful work would yield in ordinary optical determinations. It is believed to be about ± 0.003. The indices found are

$$\epsilon = 1.535 \text{ at } -5° \text{ C.}$$
$$\omega = 1.583 \text{ at } -5° \text{ C.}$$

Determinations of the optical character of elongation were made with the Johannsen wedge. The crystals have negative elongation. This is consistent with the determined values for ϵ and ω.

[26] For a description of the immersion method, the reader is referred to F. E. Wright, The Methods of Petrographic-Microscopic Research, pp. 83 et seq., Carnegie Inst. Washington Pub. 158, Washington, D. C., 1911, or to Albert Johannsen, Manual of Petrographic Methods, 2d ed., pp. 271-275, McGraw-Hill Book Co., New York, 1918.

The temperature was allowed to rise and the refractive index of the rubber was determined after the crystals had melted. The refractive index of melted ether-soluble rubber hydrocarbon crystals was found to be 1.525 at 11° C. This corresponds closely with the value found by McPherson [27] who used large samples of total rubber hydrocarbon.

The microscopical examination of the crystals of rubber hydrocarbon indicates that they are spherulites composed of many fine needles. They have a consistent melting interval of narrow range. The refractive indices of the crystals have been determined. They are higher than the index of the rubber after melting by an amount inconsistent with the "melting" of liquid crystals, but consistent with the melting of true crystals.

V. DETERMINATION OF THE COMPOSITION OF PURE ETHER-SOLUBLE RUBBER HYDROCARBON

By Henry J. Wing

The ratio of hydrogen to carbon in rubber and rubber hydrocarbon has often been determined. Upon these determinations, in large part, has rested the assumption that rubber hydrocarbon is a polymer of isoprene, which may be represented as $(C_5H_8)_x$. However, this assumption is not entirely justified because of the questionable purity of the substances analyzed and the low precision of many of the reported results. The preparation of pure rubber hydrocarbon in this laboratory offered opportunity to make an accurate determination of the ratio of hydrogen to carbon by the usual method of organic combustion.

1. APPARATUS

The combustion furnace and accessories (Fig. 5) were similar to those described by Bruun [28] except that all mercury seals and flow meters were eliminated and all but two of the joints beyond the preheating furnace, *A*, were hermetically sealed. These two, *C* and *D*, were sealed on the outside with DeKhotinsky cement so that the gas stream did not come in direct contact with the cement. In order to obtain suitable blank runs it was found necessary to run the preheating furnace, *A*, at a higher temperature than that of the combustion furnace, *B*.

The absorption tubes were two 75 mm Schwartz U tubes fitted with ground joints on the side arms so that no rubber connections were used. In order to avoid loss due to the action of hot water on the greased joints, the exit tube, *E*, from the combustion tube was bent in a U and a small bulb was blown on the outflow side of this U. Most of the water from the combustion condensed in the bend of the U. The oxygen was allowed to pass until all this water was transferred to the weighing tube in the form of vapor. The weighing tubes were weighed filled with dry hydrogen both before and after the combustion. This made any correction for air buoyancy unnecessary.

A silica-glass sample tube was used in making the combustions instead of an open boat in order to prevent too rapid burning of the rubber. One end of the tube was open and unconstricted. The other end was closed except for a pinhole of such size that the rubber

[27] A. T. McPherson, B. S. Jour. Research, vol. 8 (RP449), p. 757, 1932, plots the refractive index of purified rubber against temperature. The refractive index interpolated from that curve is 1.5236 at 11° C.

[28] E. W. Washburn, J. H. Bruun, and M. M. Hicks, B. S. Jour. Research, vol. 2 (RP45), p. 487, 1929.

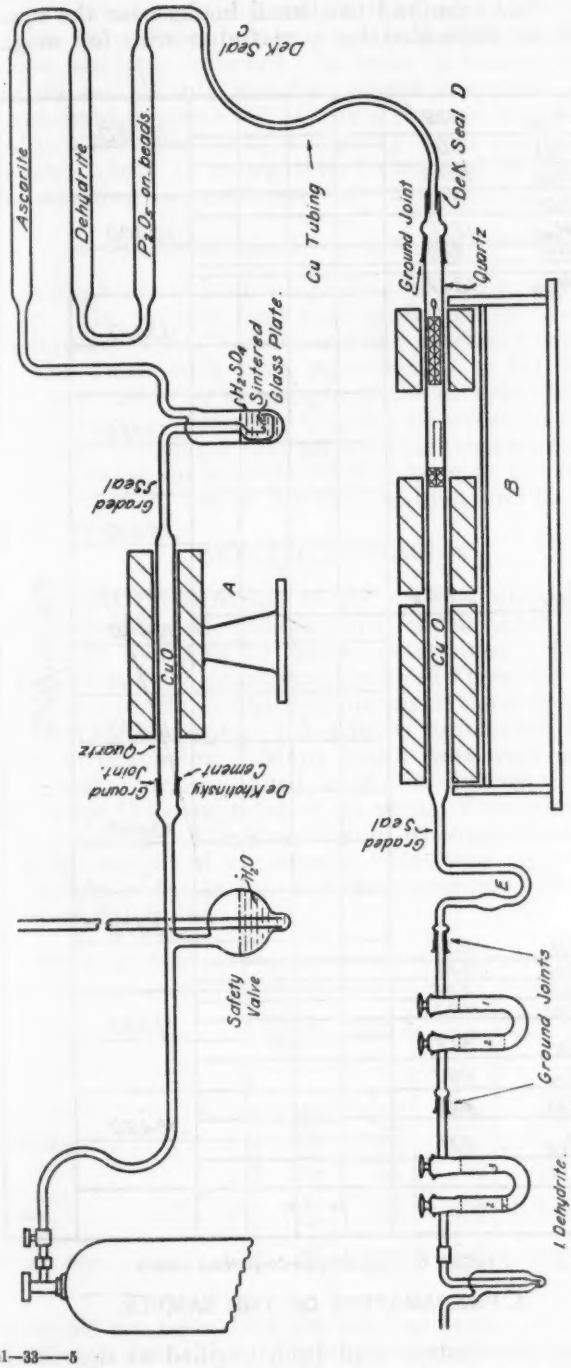

FIGURE 5.—*Combustion apparatus*

solution would not run through, yet in the combustion furnace oxygen could enter. This tube had two small hooks near the open end so that it could be suspended by a platinum wire for weighing and handling.

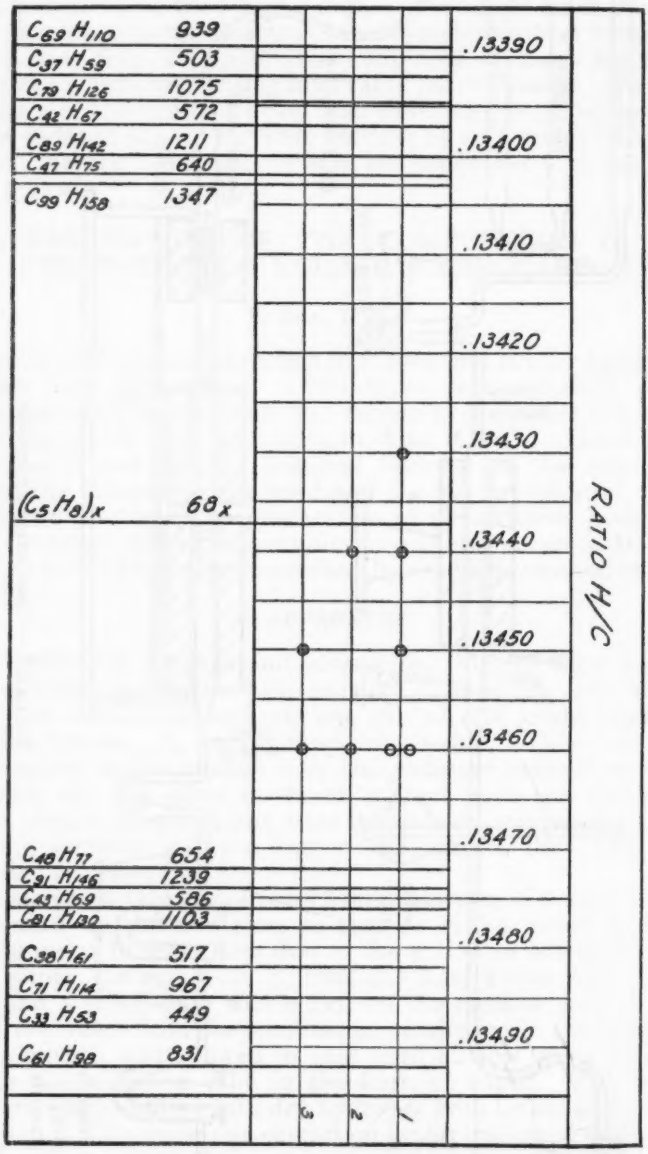

FIGURE 6.—*Hydrogen-to-carbon ratios*

2. PREPARATION OF THE SAMPLE

The material for analysis had been purified as described in the first part of the paper and put into ether solution. A small portion of this solution was placed in the sample tube. The ether was evapo-

rated from this first small quantity of rubber solution by placing the sample tube containing it in a wide test tube and carefully reducing the pressure. This procedure was repeated until about 0.2 g of the hydrocarbon had been collected. In order to remove the last traces of solvent the sample tube was then placed in a small glass chamber which was heated to about 100° C. by a glycerol bath and which was evacuated to a low pressure by a mercury vapor pump. The sample was evacuated about 18 hours, then transferred to the balance case and, after standing about 20 minutes, was weighed.

3. BALANCE, WEIGHTS, AND WEIGHING

All weighings were made on a high grade analytical balance sensitive to 1/20 mg. The weights used were calibrated by the weights and measures division of this bureau, and the necessary corrections were applied. The blank runs were reproducible to 0.1 mg. Vacuum corrections were made on the weight of the sample, assumed to have a density 0.9 g/cm^3. However, this has no effect on the carbon-to-hydrogen ratio. Assuming that all the weighings were made to ± 0.1 mg, then the maximum possible relative error in the percentages of hydrogen and carbon, and in the ratio of hydrogen to carbon would be ± 0.2 per cent.

4. ANALYTICAL RESULTS

Three different preparations of the ether-soluble rubber hydrocarbon, purified as described in Section II of this paper, were analyzed and the ratio of hydrogen to carbon determined. The results are given in Table 2 and are shown graphically in Figure 6. These results are members of a continuous series from which the only omissions were those in which the absorption tubes failed to function either because of stoppage or channeling. Many blank runs were made with the furnace. These were continued until the difference in successive weighings under the conditions of an actual determination was not more than ± 0.1 mg. The final ratio of hydrogen to carbon is independent of the weight of the sample. However, as a check on the result the weight of the sample and the percentages of carbon and of hydrogen were determined.

TABLE 2.—*Determination of the ratio of hydrogen to carbon*

	Hydrocarbon taken	H_2O absorbed	CO_2 absorbed	Hydrogen found	Carbon found	H/C ratio
	g	*g*	*g*	*Per cent*	*Per cent*	
Original preparation	0.2009	0.2127	0.6481	11.84	87.98	0.1346
	.2328	.2462	.7516	11.83	88.05	.1344
	.2598	.2732	.8345	11.77	87.66	.1343
	.2358	.2496	.7606	11.84	87.97	.1346
	.2320	.2450	.7475	11.82	87.87	.1345
Crystallized once	.2107	.2232	.6799	11.85	88.01	.1346
	.2390	.2525	.7709	11.82	87.97	.1344
Crystallized three times	.1365	.1448	.4417	11.87	88.25	.1345
	.2373	.1349	.4111	11.86	88.07	.1346

These results are figured on the ash-free basis. In every case the ash content was less than 0.1 per cent, practically at the limit of the accuracy of the weighings. The difference between the sum of the

hydrogen and carbon percentages and 100 per cent is probably due to the presence of oxygen. Some of the samples were exposed to the air longer than others, which may account for the difference in the sums.

The first step in the interpretation of these results should be the determination of the number of possible compounds which, if subjected to combustion analysis, would give results somewhat in accord with those found.[29]

If we assume for simplicity that the compound does not have more than 100 carbon atoms in the molecule, then the number of possible compounds may be confined to reasonable limits. The ratio of hydrogen to carbon in isoprene or any of its isomers or polymers is 0.13437 based on the International Table of Atomic Weights for 1932. A number of hydrocarbons are possible having less than 100 carbon atoms in the molecule and a ratio of hydrogen to carbon very near to that of the $(C_5H_8)_x$. The diagram (fig. 6) shows all the possible hydrocarbons in this region. The horizontal scale represents ratio of hydrogen to carbon. Each of the labeled vertical lines represents an individual hydrocarbon. The groups of points in circles represent analyses of different preparations of the ether-soluble rubber hydrocarbon. Group 1 shows the results of analyses of the purified hydrocarbon; group 2, material which had been crystallized once; and group 3, that which had been crystallized three times.

The distribution, in the neighborhood of the C_5H_8 and its polymers, of the hydrocarbons having less than 100 carbon atoms, is fortunately unique. It so happens that none of these hydrocarbons has a ratio of hydrogen to carbon very close to that of C_5H_8 as is shown in Figure 6. The difference in the ratio of the nearest hydrocarbon on either side of C_5H_8 is $0.13472-0.13403=0.00069$. This offers the possibility of identifying the rubber hydrocarbon as a polymer of C_5H_8 provided it has less than 100 carbon atoms in the molecule and that the analysis is of the required accuracy. If, however, the molecule contains more than 100 carbon atoms, there still remains the possibility that it may not be a polymer of C_5H_8. Only reliable molecular weight determinations can decide this question.

At present it is not possible to say definitely that the rubber hydrocarbon has a molecule of less than 100 carbon atoms. However, the fact that the material as prepared and used in this laboratory crystallizes readily indicates that the molecule is possibly much smaller than has been frequently assumed.

V. ACKNOWLEDGMENTS

The authors acknowledge the technical advice of E. W. Washburn, chief of the chemistry division, throughout the course of this investigation. Harry L. Fisher, of the United States Rubber Co., has furnished us from time to time authentic samples of Hevea latex, and his courtesy is appreciated.

WASHINGTON, February 11, 1933.

[29] E. W. Washburn, B. S. Jour. Research, vol. 4 (RP145), p. 221, 1930.

WIND PRESSURE ON A MODEL OF THE EMPIRE STATE BUILDING

By Hugh L. Dryden and George C. Hill

ABSTRACT

Measurements have been made of the distribution of wind pressure over a model of the Empire State Building for the purpose of comparing the results of model tests with measurements on the actual building now in progress under the direction of the Research Committee of the American Institute of Steel Construction. This paper describes the results of measurements on the model.

The pressure was measured at 102 stations on the model, 30 of which represent stations in the actual building, at 11 wind directions. In addition, the overturning moments were measured for the same wind directions. The results show that the pressure varies from point to point, and that reduced pressure is found over the larger part of the model. The greatest loads on the building occur when the wind blows directly against one face. A suitable value of the pressure for use in the design of tall buildings is 0.0038 V^2 (in lbs./ft.^{2}) where V is the wind speed in miles per hour against which provision is to be made.

It was found that the speed of the air rushing by close to the building is greater than that of the approaching wind. Hence, an instrument mounted 15 feet above the top of the building reads too high by a factor 1.23.

An outline is given of a method of procedure for the comparison of the results on the model with those on the actual building.

CONTENTS

	Page
I. Introduction	493
II. Measurements of pressure distribution	495
1. Apparatus	495
2. General procedure	497
3. Reduction of observations	498
4. Results	501
5. Discussion	516
III. Measurements of overturning moment	517
1. Apparatus and method	517
2. Results	518
3. Discussion	520
IV. Remarks on the method of comparing model results with full-scale measurements	521
V. Conclusion	523

I. INTRODUCTION

In the design of tall buildings or other structures, the pressure exerted by high winds plays an important rôle. If the structure is designed for a very large wind pressure, the cost is unnecessarily increased, a matter of concern to the owners of the structure. If the design is made for too small a wind pressure, the structure is unsafe, a matter of concern to those living or working in the building and to the general public.

The forecasting of the wind pressure to which a building may be subjected is difficult. It is practically certain that the speed of the wind will exceed 5 miles per hour at some time during nearly every day of the year. In Washington, D. C., the speed exceeds 40 miles per hour about four times a year, and has not reached 100 miles per hour in the 60 years for which records are available. It is a practical

impossibility to design all buildings to withstand the maximum speeds which have ever been experienced anywhere. The line must be drawn at some speed which is not likely to be exceeded in the life of the building.

To obtain information on wind pressure from observations on a building in a natural wind would require years of measurement and a statistical study of the results. The data obtained from such an investigation would not be applicable to buildings of a different shape or to buildings with a different exposure; for example, located in another part of the country. Some better procedure must be adopted.

The only long-continued observations on the wind are those made by the Weather Bureau. These observations give the speed and direction of the wind for different parts of the country. From these observations, the probability that a given speed will be exceeded say once in a hundred years may be computed.[1] To obtain the pressure on the building, the relation between the pressure and the speed must be known. Two methods are available for determining this relation: (1) By experiments on models in wind tunnels, and (2) by observations in natural winds.

Experiments on models have been found invaluable in hydraulics and aeronautics and are well known to engineers working in those fields. Studies of wind pressure have been made by this method in this country and abroad,[2] but full confidence has not been placed in the results, because of some feeling of uncertainty as to the application to buildings in a natural wind. It seemed to us that the next important step in the study of wind pressure was a coordinated program of model and full-scale experiments as applied to some existing structure.

Both methods of experiment have advantages and disadvantages. In wind-tunnel experiments, the speed and direction of the wind are under continuous control. Standard reference speeds and pressures are easily obtainable and the total force on the model may be measured

[1] The Weather Bureau observations give usually only the mean speed, which is exceeded in gusts. For a discussion of this aspect of the subject see S. P. Wing, Proc. Am. Soc. Civ. Eng. 58 p. 1103, 1932. See also R. H. Sherlock and M. B. Stout, Bull. Nat. Elec. Light Assoc., January, 1931, and January, 1932.

[2] The following papers illustrate the variety of publications in this field:

A. Betz (Winddruck) Messungen von Brückenträgern. Ergebnisse der Aerodynamischen Versuchsanstalt zu Göttingen, vol. 3, p. 146, 1927.

British Elect. and Allied Industries Research Assoc. Investigations of Wind Pressure on Poles and Cables for Overhead Transmission Lines, 1925. Interim Report upon Research on Wind Pressure on Latticed Towers, 1928.

H. L. Dryden and G. C. Hill, Wind Pressures on Structures, B. S. Sci. Paper S. 523, Bull. 20, p. 697.

H. L. Dryden and G. C. Hill, Wind Pressure on Circular Cylinders and Chimneys, B. S. Jour. Research, vol. 5 (RP221), 1930.

H. L. Dryden and G. C. Hill, Wind Pressure on a Model of a Mill Building, B. S. Jour. Research, vol. 6 (RP301), 1931.

O. Flachsbart. Winddruck auf geschlossene und offene Gebäude. p. 128. Winddruck auf Gasbehälter p. 134. Ergebnisse der Aerodynamischen Versuchsanstalt zu Göttingen, vol. 4. (R. Oldenbourg, Berlin) 1932.

O. Flachsbart. Winddruck auf Bauwerke. Die Naturwissenschaften, vol. 18, p. 475; 1930.

O. Flachsbart. Der gegenwärtige Stand der Winddruckforschung, Jahrbuch, 1930, d. Deutschen Gesell. f. Bauingenieurwesen, vol. 6, p. 108, 1931.

O. Flachsbart. Grundsätzliches zur Frage des Winddrucks auf Gebäude. Bauwelt., pp. 660 and 692, 1932.

J. O. Irminger and C. Nøkkentved. Wind Pressure on Buildings. Ingeniørvidenskobelige Skrifter, A Nr. 23, København, 1930.

F. Nagel (Winddruck) Messungen von Profilträgern. Ergebnisse der Aerodynamischen Versuchsanstalt zu Göttingen, vol. 3, p. 151, 1927.

C. Nøkkentved. Wind Pressure on Buildings. Int. Assoc. for Bridge and Structural Engineering, Zürich, 1932.

R. L. A. Schoemaker and I. Wouters. Windbelasting op Bouwwerken, Het. Bouwbedrijf, Oct. 21, 1932.

R. Seiferth. Winddruckmessungen an einem Gasbehalter. Ergebnisse der Aerodynamischen Versuchsanstalt zur Göttingen, vol. 3, p. 144. 1927.

H. M. Sylvester. An Investigation of Pressures and Vacua Produced on Structures by Wind. Rensselaer Poly. Inst. Eng. and Sci. Series No. 31, 1931.

as well as the detailed distribution of the pressure. The chief disadvantages are (1) that the fine detail of the actual building can not be reproduced on the model and (2) that the pressure on the full-scale building may be somewhat different than that at the corresponding location on the model because of the existence of a scale effect. It is our belief that the errors due to failure to reproduce the fine detail and due to scale effect are not very large, but until this belief is actually confirmed by full-scale experiments, results from model tests will not command the full confidence of engineers engaged in the design of buildings.

In experiments in natural winds, the conditions are reversed. It is no longer easy to obtain conditions favorable for measurement, in that the speed and direction of the wind change continuously. In addition, it is very difficult to obtain a steady reference pressure, or otherwise expressed, to measure the "normal" atmospheric pressure. On the other hand, there is no question of scale effect or of lack of detail of a model.

When it was announced by the American Institute of Steel Construction that a program of wind-pressure measurements would be conducted on the Empire State Building, the Bureau of Standards saw an opportunity to test the utility and validity of model measurements. Through the cooperation of the engineer, H. G. Balcom, drawings of the building were generously supplied. A model was designed and constructed by the Bureau of Standards, and measurements of wind pressure were made in the 10-foot wind tunnel. The results of measurements on the model are described in this paper. Measurements on the actual building are in progress under the direction of F. H. Frankland, chairman of the Research Committee of the American Institute of Steel Construction. When the results become available, comparisons can be made.

II. MEASUREMENTS OF PRESSURE DISTRIBUTION

1. APPARATUS

The Empire State Building is 1,250 feet high; the model, shown in Figure 1, is 5 feet high. The model is made of rolled aluminum plates one-quarter inch thick, except the tower, which is constructed of wood. It represents the building in external shape except for the minor irregularities of the surface on a scale of 1 to 250. It does not represent the actual building in material, method of construction, or strength. It is not tested to failure, but is used only for measurements of the wind pressure at different wind speeds.

The wind pressure on the actual building is to be measured on the thirty-sixth, fifty-fifth, and seventy-fifth floors by means of pipes running from the outside face of the walls to manometers mounted at suitable observing stations. At the levels on the model corresponding to these floors as shown in Figure 4, 17 pressure stations were prepared as follows: A hole approximately one-quarter inch in diameter was drilled and tapped at each station. A hollow cylindrical threaded plug about five-eighths inch long and closed at one end was screwed into the hole and the closed end carefully worked down so as to make it flush with the outer surface of the model. After polishing, a small hole approximately 0.040 inch in diameter was drilled along the axis of the plug from the outside face inward. By means of rubber tubing,

connection could then be made through the interior of the model from each station to the pressure gauge.

Fourteen of the seventeen stations at each level were located on two adjacent faces of the model as shown by the short solid lines in Figures 2 and 3, stations designated as 1, 2, 3, 4, 5, 7, 8, 9, 11, 12, 13, 15, 16, and 17. Three were located on the other faces. Because of the symmetry of the model, the complete distribution at each wind direction could be obtained by two runs, one with the wind striking the faces containing the large number of stations, the second with the model rotated through 180°. The levels are denoted by the letters *A*, *B*, and *C*, and the stations by numbers from 1 to 34. The short solid lines show stations actually present in the model; the dotted

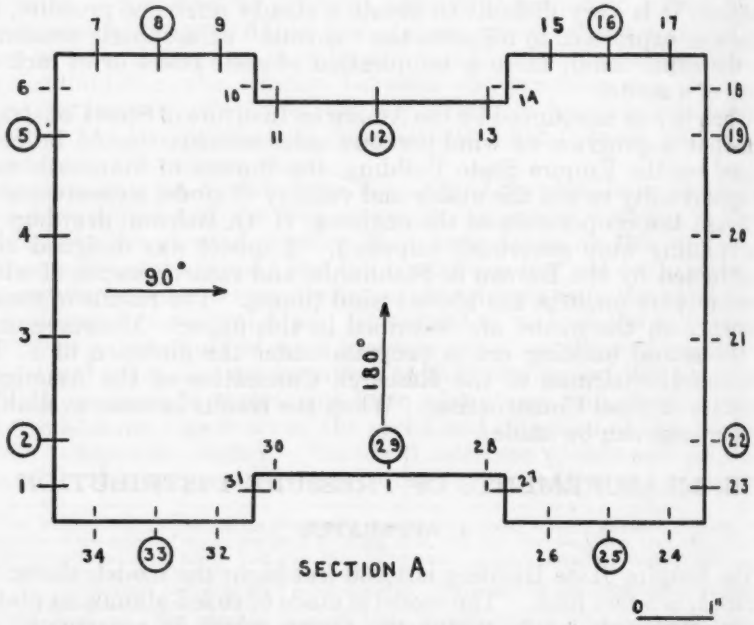

FIGURE 2.—*Location of pressure stations at section A.* (*See fig. 4*)

The solid lines represent stations present in the model, the dotted lines, those for which values are obtained by rotating the model through 180°, the numbers inclosed in circles, those present in the actual building. The designation of wind direction is shown by the arrows.

lines represent stations for which values are obtained by rotating the model through 180°, while the numbers inclosed in circles correspond to stations present in the actual building.

The model rests on and is attached to a circular plate as shown in Figure 1, which also shows the mounting in the wind tunnel. The circular plate can be rotated with respect to a second square plate below, the square plate being fastened to a wooden platform. Since the tunnel is cylindrical, the platform rests on two wooden segments cut to the curvature of the tunnel wall. Both plates have an opening in the center to permit the passage of the 51 connecting tubes from the stations. The circumferential edge of the circular plate is graduated at intervals of 5° and the square stationary plate has an index mark at the center of its upstream face.

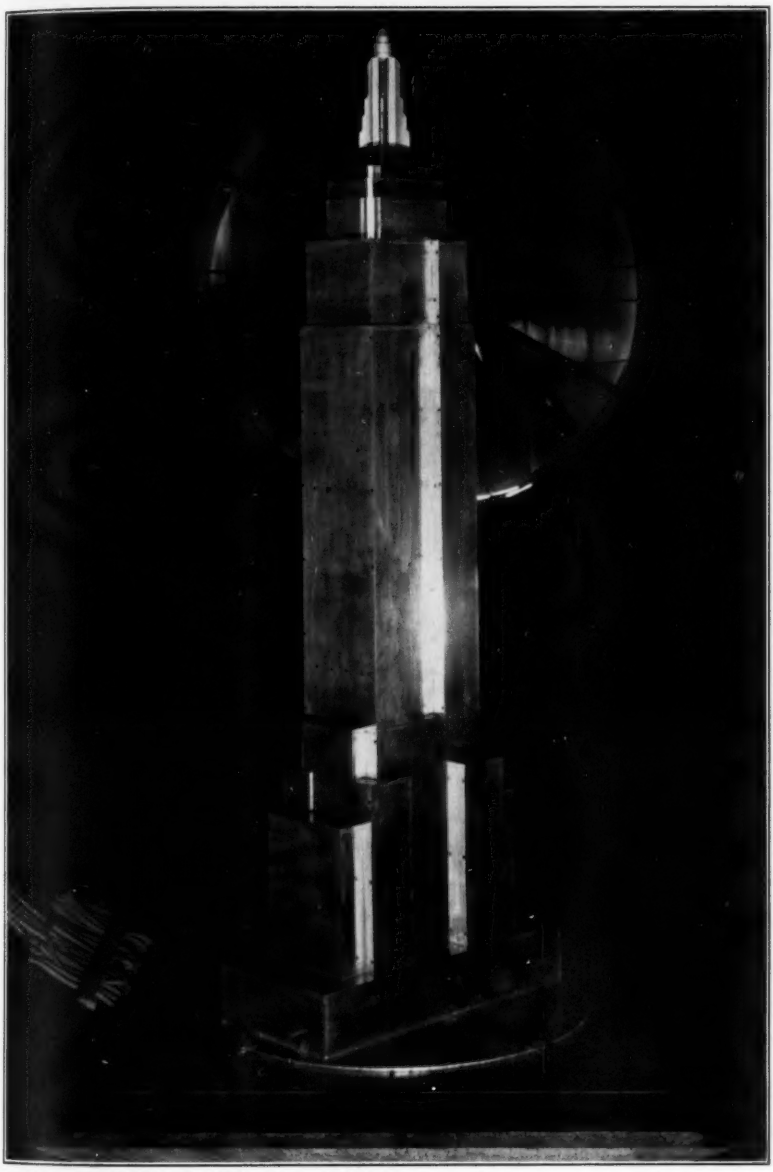

FIGURE 1.—*Model of the Empire State Building in the wind tunnel, looking downstream*

The brass screws holding the model together and the brass plugs in which the pressure holes are drilled appear as dark spots.

UNIV OF MICH

The 10-foot wind tunnel which was used for these measurements has been described in Scientific Paper No. 523. That paper also gives an account of the method of measuring wind speed, and a description of the manometer used for measuring pressures. In the present tests, speeds up to about 55 miles per hour were used.

2. GENERAL PROCEDURE

The general procedure in making the measurements of pressure distribution was as follows: The model was first set with the narrow face containing the five pressure stations normal to the wind direction, an azimuth designated as 90°. Twelve stations were connected to the 12 tubes of a multiple-tube manometer, the reservior of the manometer being connected to a static plate upstream from the model. The pressure at the opening of the static plate served as the

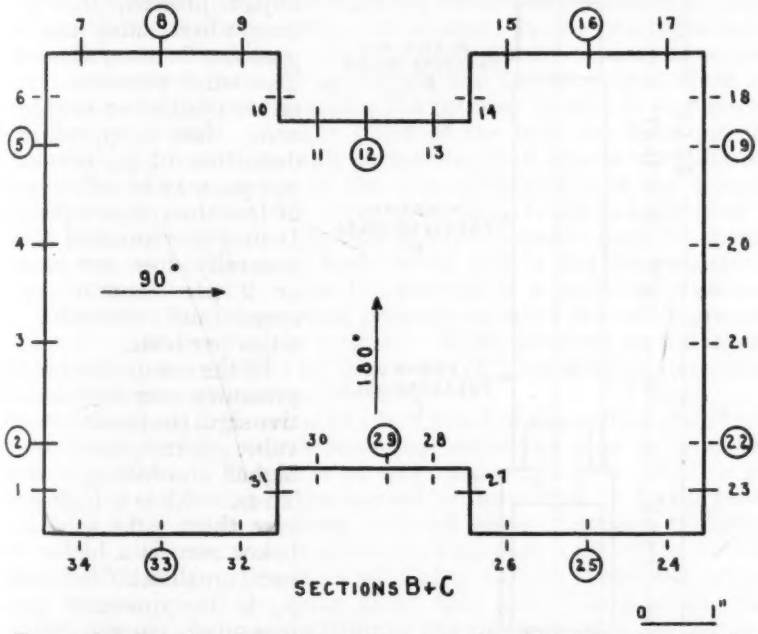

FIGURE 3.—*Location of pressure stations at sections B and C.* (*See fig. 4*)

See note for Figure 2.

base pressure from which all other pressures were measured. At wind speeds of approximately 40, 60, and 80 feet per second (27, 41, and 55 miles per hour), an observer read successively the 12 tubes of the manometer, which gave readings proportional to the differences in pressure between the holes at the surface of the model and the pressure at the static plate. Twelve other stations were then connected, readings taken, and the process repeated until observations were completed for the 51 stations. The model was then turned through an angle of 180° and the series repeated. A complete set of observations at the 102 stations was made for wind directions from 90° to 180° at intervals of 10° and at 135°.

3. REDUCTION OF OBSERVATIONS

When an air stream blows against an object, the pressure, p, at any point on its surface may be regarded as consisting of two parts—the static pressure,[3] p_s, which in a natural wind is the barometric pressure; and the excess, $p-p_s$, caused by the presence of the object. This excess, $p-p_s$, arises solely from the motion of the air with reference to the model. It will be called simply the wind pressure, and will be denoted by p_w. If there is no wind or no object present, then $p=p_s$ everywhere, and the wind pressure is everywhere zero. The wind pressure may be either positive or negative or zero; that is, p, which by definition of p_w is equal to p_s+p_w, may be either greater or less than p_s or equal to it. It may be remarked that p_w generally does not exceed 1 or 2 per cent of p_s for speeds not exceeding 100 miles per hour.

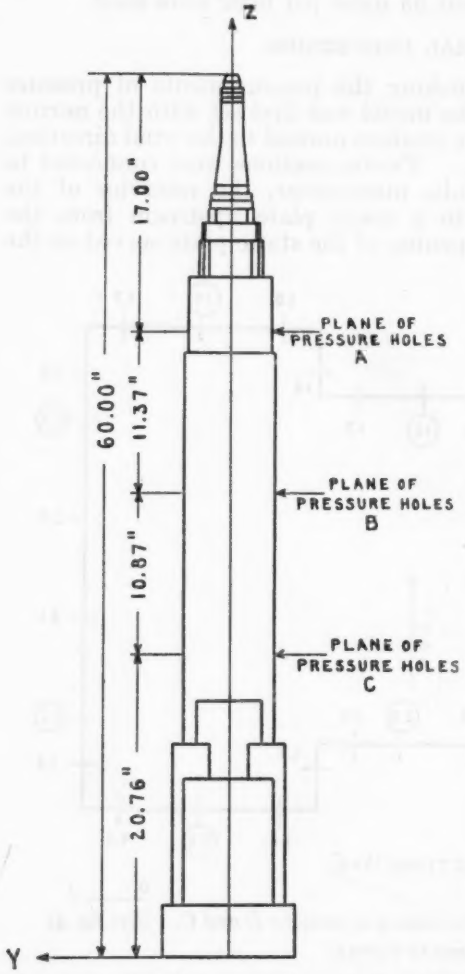

FIGURE 4.—*Location of sections A, B, and C and the axes of reference on the model*

The X axis runs into the plane of the paper at right angles to the Y and Z axes which are snown

In the comparison of wind pressures carrying the negative sign, the lower numerical value corresponds to the higher absolute pressure. Thus, -0.2 is a higher pressure than -0.4 (just as 10° below zero is a higher temperature than 20° below zero). p_w is the quantity usually measured, corresponding to the common practice of using "gauge" pressure in dealing with pressures in steam boilers, compressed air tanks, etc., rather than absolute pressure. Dimensional reasoning teaches that p_w will be given by an expression of the form

$$\frac{p_w}{q}=f\left(\frac{VL\rho}{\mu}\right)$$

where q is the velocity pressure ($\frac{1}{2}\rho V^2$), ρ the air density, V the wind speed, μ the viscosity of the air, and L a linear dimension fixing the

[3] The term static pressure is used to indicate the pressure which would be measured by a pressure gauge moving with the air, and, therefore, "static" with respect to the air. In actual practice the measurement is made by means of holes in the side of a closed tube, the axis of which is parallel to the wind direction. The form of the tube is such that the air flows smoothly past the holes.

scale. The expression applies only to geometrically similar bodies. The wind pressure, p_w could be measured in any convenient units, but there are advantages in using the velocity pressure, $q = \frac{1}{2}\rho V^2$, as the unit. For bodies without curved surfaces and with sharp corners, p_w/q is practically independent of the wind speed and the size of the model (that is, $f\left(\frac{VL\rho}{\mu}\right)$ is a constant for any station), so that from a single value of it for any given shape of body the pressure at the corresponding point on a similar body of any size at any wind speed can be readily computed with the aid of a table of velocity pressures. The ratio is a pure number independent of the units used so long as the pressures are all measured in the same units.

The engineer is in most cases more directly concerned with the resulting forces than with the pressures themselves and their distribution. These resulting forces always involve the pressure acting on the opposite sides of the surface or object. In the case of a hollow object, such as a building, which is open to the outside at various places, air currents are set up within the building, and there is a distribution of wind pressure over the interior as well as the exterior surfaces of the walls. At any point of the wall the force per unit area tending to move the wall normal to itself equals the difference between the wind pressure on the two sides and is in the direction from the higher toward the lower pressure. Little is known at the present time as to the distribution of wind pressure over the interior walls of actual buildings in high winds and in the presentation of data for the distribution over the exterior it is commonly assumed that the interior is at a constant pressure equal to the static pressure, p_s; that is, p_w is zero for the interior. If the pressure on the interior is constant, it has no effect on the resultant force tending to overturn the building, no matter what its value.

By definition, p_s is the same at every point of the surface and, hence, it contributes nothing to the resulting forces and may be ignored in the computations. The force on any element, dA, is equal to pdA and acts in the direction of the normal to the surface.[4] In the case of a building with plane surfaces, with all angles between the planes right angles, the component of force along each axis of the building is readily computed. The faces parallel to an axis contribute nothing to the component of the force along that axis. Each of the faces perpendicular to the axis contributes the summation of the forces on the elements, that is, $\int\int pdA$; but account must be taken of the fact that forces on opposite faces oppose each other. Since the net effect of p_s vanishes, we need only compute $\int\int p_w dA$. Dividing by q, we have the force F given by

$$F/q = \int\int p_w dA$$

It is found convenient to divide this expression by the area of projection, A_p, of the body on a plane normal to the axis under consideration. The quotient $F/A_p q$ is called the force coefficient.[5] It is the average force per unit projected area divided by the velocity pressure; that is, the ratio of the effective resultant pressure on the total projected area to the velocity pressure. The force in any particular case is obtained by multiplying the force coefficient by the projected area and by the velocity pressure.

[4] Excluding frictional effects, which are of importance only in special cases.
[5] The terms "resistance coefficient," "drag coefficient," "shape coefficient" are also used.

In the case of the present model we shall be interested in the average loading at a given elevation. In this case the force per unit length is equal to the summation of $p_w ds$; that is, $\int p_w ds$ where ds is an element of the width of the face. Again it is convenient to divide $\int p_w ds$ by the width and by the velocity pressure q so as to obtain a coefficient applicable to the particular section, giving the average force per unit area per unit velocity pressure.

It will be noted that in all cases, an average value of $\frac{p_w}{q}$ is determined, which if uniformly distributed over the area in question would give the correct value of F/q.

For the convenience of the reader, the relation between the indicated speeds, as measured by 3 and 4 cup U. S. Weather Bureau anemometers, and the true speed is given in Table 1, and the velocity pressures at various true speeds for air of standard density is given in Table 2.

TABLE 1.—*Indicated wind speeds by Robinson cup anemometers* [1]

True speed (miles per hour)	Indicated speed, old 4-cup standard	Indicated speed, new 3-cup standard	True speed (miles per hour)	Indicated speed, old 4-cup standard	Indicated speed, new 3-cup standard
5	5	5	60	78	63
10	11	10	65	85	68
15	17	15	70	91	73
20	23	20	75	98	79
25	30	25	80	105	84
30	37	31	85	112	89
35	44	36	90	118	95
40	50	41	95	125	100
45	57	47	100	132	105
50	64	52	105	138	111
55	71	57	110	145	116

[1] Before Jan. 1, 1928, the U. S. Weather Bureau used the 4-cup instrument; from then until Dec. 31, 1931, the 3-cup instrument. After that date all wind speeds have been corrected before publication, thus giving true speeds.

TABLE 2.—*Velocity pressures at several wind speeds*

True wind speed (miles per hour)	Velocity pressure	True wind speed (miles per hour)	Velocity pressure	True wind speed (miles per hour)	Velocity pressure
	Lbs./ft.²		*Lbs./ft.²*		*Lbs./ft.²*
5	0.064	45	5.179	85	18.48
10	.256	50	6.394	90	20.72
15	.575	55	7.737	95	23.08
20	1.023	60	9.208	100	25.58
25	1.600	65	10.81	105	28.20
30	2.302	70	12.53	110	30.95
35	3.133	75	14.39	115	33.83
40	4.092	80	16.37	120	36.83

NOTE.—Velocity pressure in lbs./ft.²=0.001189 $(V \times 2\frac{3}{4}{}_{(5)})^2$ where V is the true speed in miles per hour, and the density is that at 15° C., 760 mm Hg.

$q = .00257\ V^2$

In an actual structure the wind pressure is modified by the presence of the ground, so that some method must be used in the artificial wind to produce the effect of the ground. In the present experiments the model rested on the floor of the tunnel except for the interposition of a small platform to provide for the curvature of the tunnel wall. In this case the wind is not uniform over the region occupied by the model. Figure 5 shows the measured speed above the tunnel floor

in the absence of the model along the line subsequently occupied by the vertical axis of the model. The speeds are expressed as ratios to the reference speeds given by a Pitot tube located upstream and to one side. The speeds at points within the area occupied by the model are approximately the same at a given elevation. From the curve it is seen that the wind speed above an elevation of 18 inches is approximately uniform. Since the elevation of the lowest pressure holes is 20.76 inches, all pressure stations on the model are within the region of uniform speed. When a speed of 80 feet per second is desired at the model, the reference speed must be set a little lower as indicated by the curve.

The results finally desired are p_w, the changes in pressure produced by the presence of the model. It was necessary, therefore, to measure the difference in pressure between the reference (static plate) pressure and the static pressure in the tunnel (with the model removed) at the place previously occupied by the model and to add this value with proper sign to the observed pressure.

The procedure in reducing the observations was as follows: The readings of the manometer were reduced to absolute pressure differences in pounds per square foot from a knowledge of the slope of the manometer and the density of the liquid used (kerosene).

The pressure differences were then corrected for the difference between the reference pressure and the static pressure and expressed as fractions of the velocity pressure. The values for any one station at the three speeds were, in general, very nearly the same, the variation from the mean in most cases not exceeding 0.03.

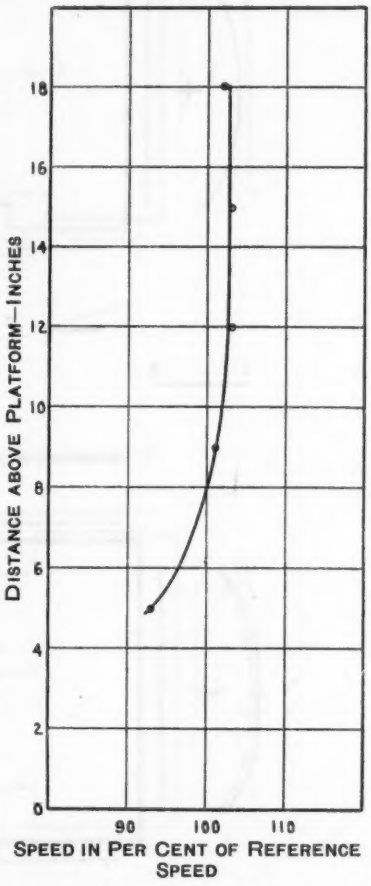

FIGURE 5.—*Variation of wind speed above the platform in the absence of the model*

4. RESULTS

The mean values of p_w/q are given in Tables 3 to 6, inclusive, and plotted in Figures 6 to 16, inclusive. In these figures, two horizontal sections of the model are shown, the upper for elevation A, the lower for elevations B and C. Just outside the section drawings are four fine base lines from which the values of p_w/q are plotted to the scale shown. In the lower plot, the solid curves are for elevation B and the dash curves for elevation C. At each elevation there are four holes in the recesses, and the values of p_w/q for these holes are indicated by the small circles and crosses. In the lower plot, the circles are for elevation B, the crosses for elevation C. The wind direction is

indicated by the arrow, and the number gives the angle which the wind makes with the face containing pressure stations 1 to 6. When p is larger than p_s, p_w/q is positive; when p is smaller than p_s, p_w/q is

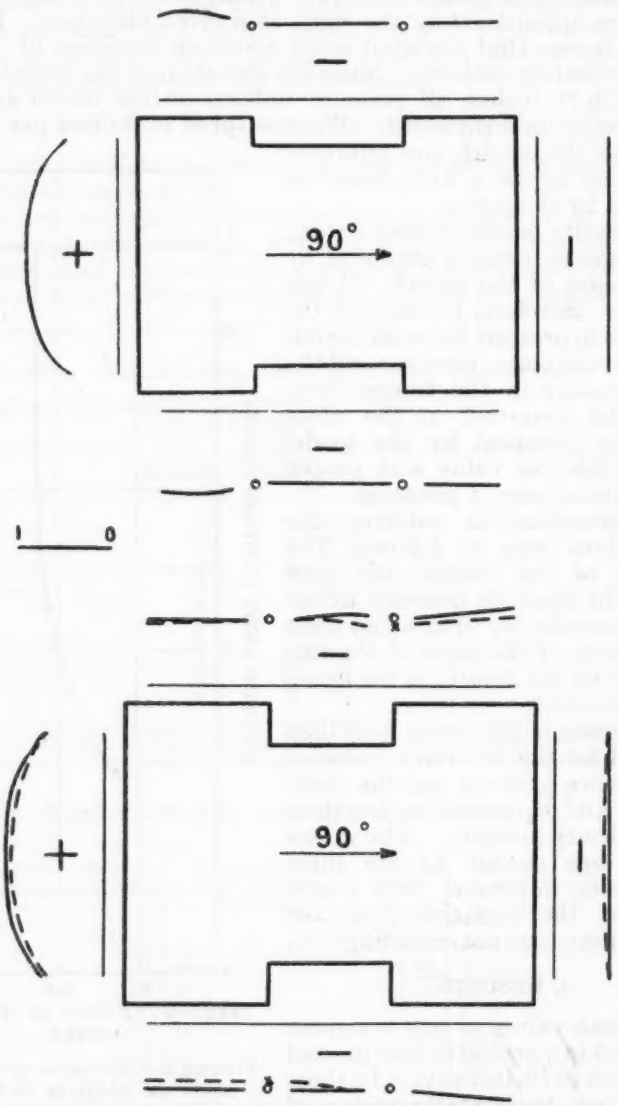

FIGURE 6.—*Distribution of pressure at sections A, B, and C at 90° to the wind*

Above, section *A*; below, solid lines, section *B*; dotted lines, section *C*

The pressures are measured from the static pressure as base and expressed as ratios to the velocity pressure. The ratios are plotted outward from the thin base lines to the scale shown. Minus signs denote that the pressure is lower than the static pressure. The circles and crosses give the values at stations 10, 14, 27, and 31 on the side walls of the embrasures.

negative. Both positive and negative values are plotted outward from the datum line for convenience and are distinguished by the use of plus and minus signs.

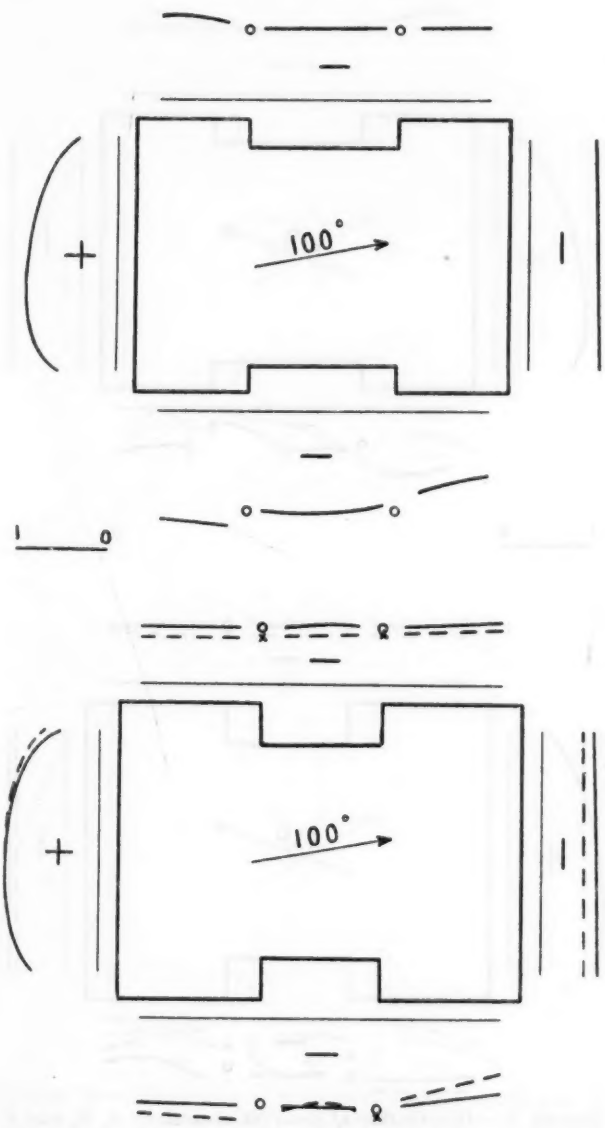

FIGURE 7.—*Distribution of pressure at sections A, B, and C at 100° to the wind*

See legend of Figure 6

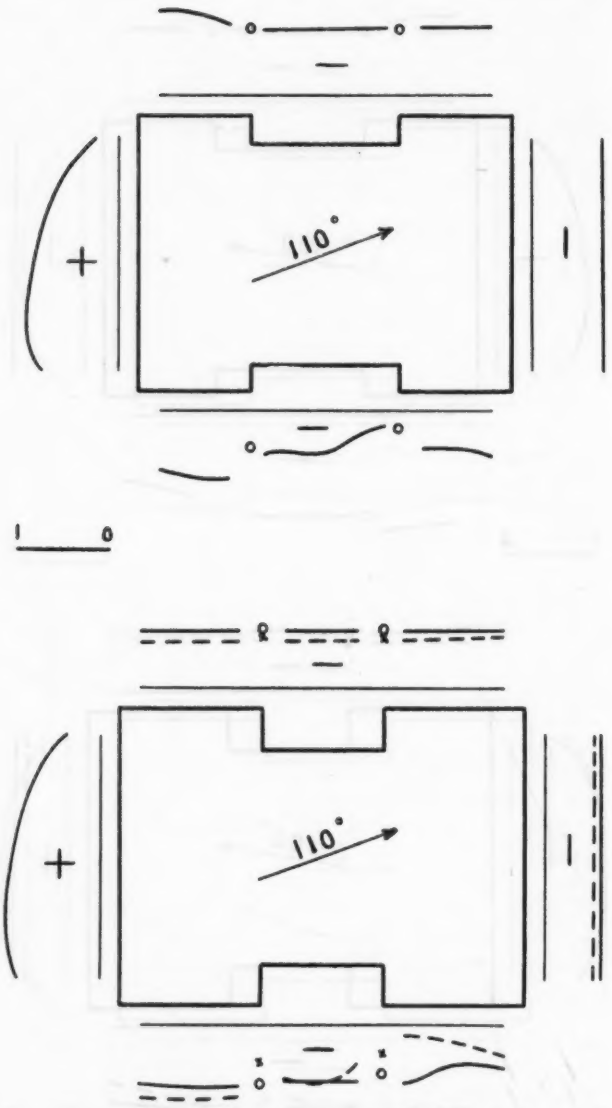

FIGURE 8.—*Distribution of pressure at sections A, B, and C at 110° to the wind*

See legend of Figure 6

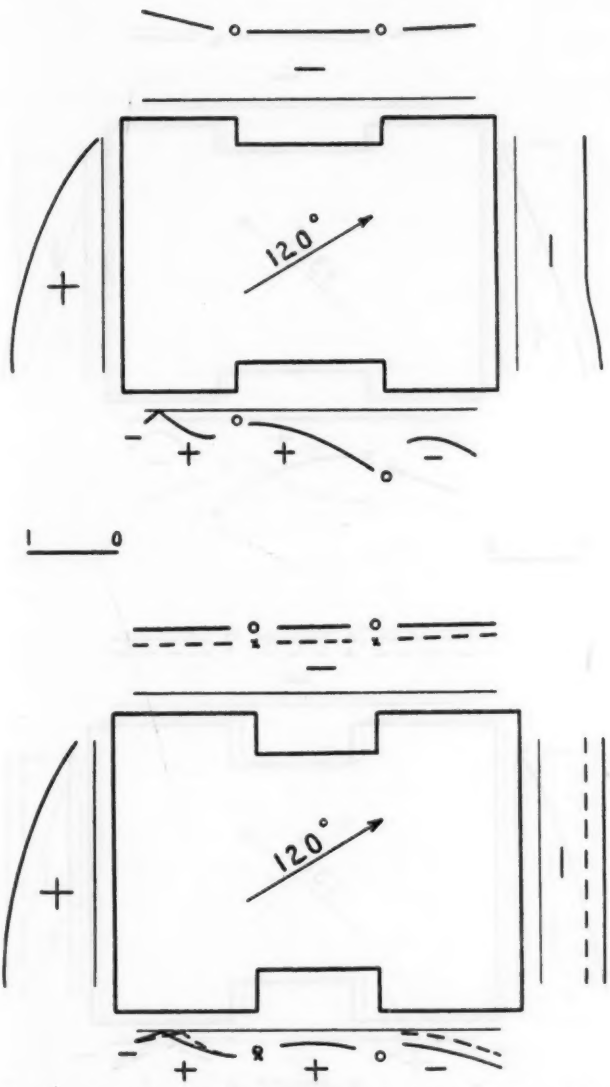

FIGURE 9.—*Distribution of pressure at sections A, B, and C at 120° to the wind*

See legend of Figure 6

161541—33——6

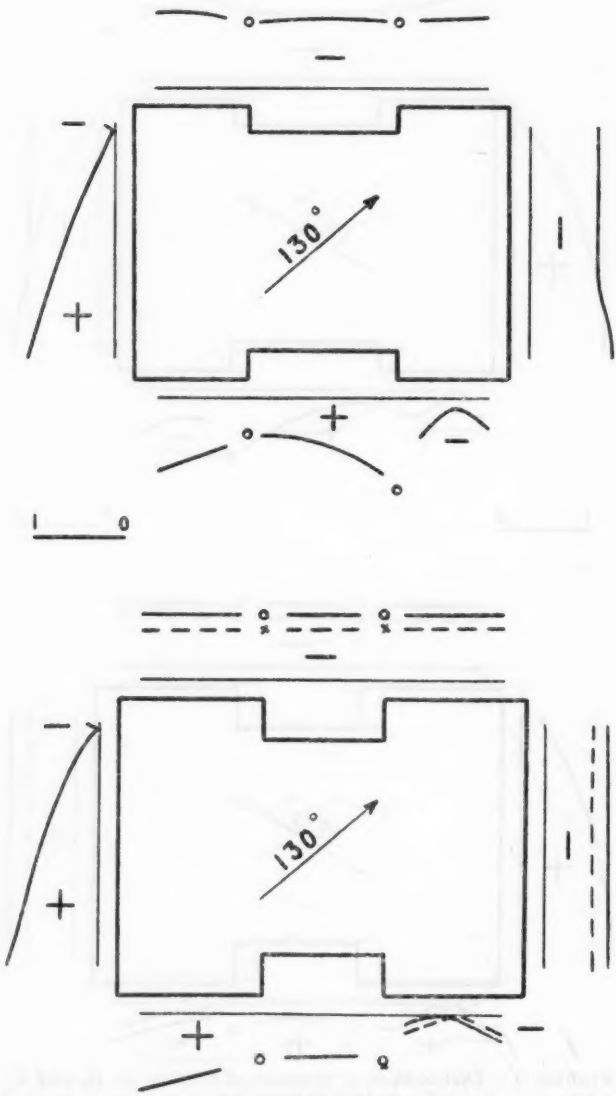

FIGURE 10.—*Distribution of pressure at sections A, B, and C at 130° to the wind*

See legend of Figure 6

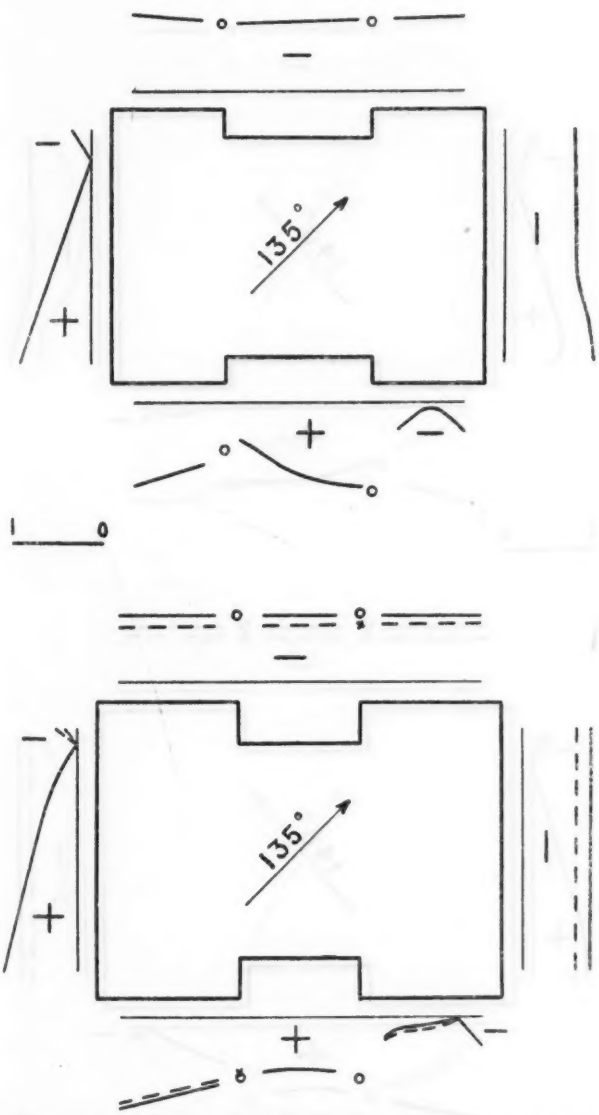

FIGURE 11.—*Distribution of pressure at sections A, B, and C at 135° to the wind*

See legend of Figure 6

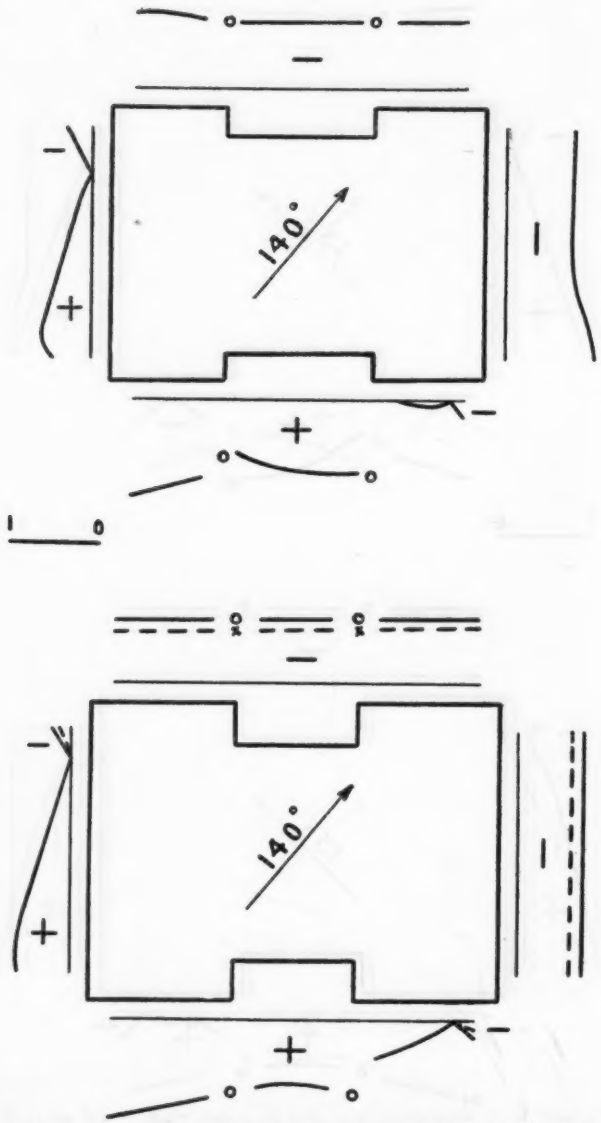

FIGURE 12.—*Distribution of pressure at sections A, B, and C at 140° to the wind*

See legend of Figure 6

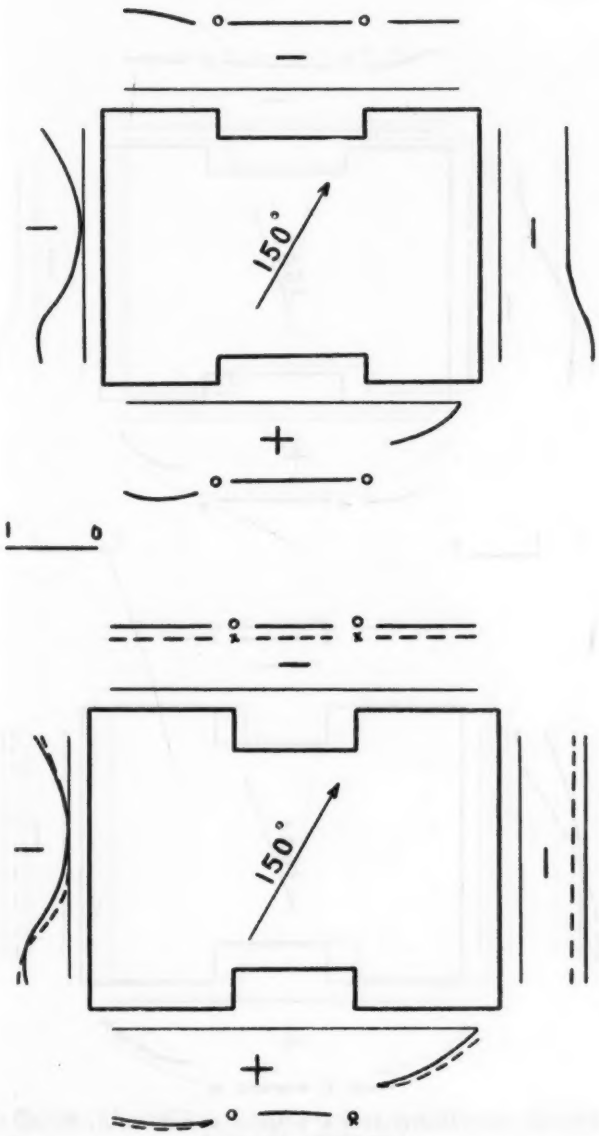

FIGURE 13.—*Distribution of pressure at sections A, B, and C at 150° to the wind*

See legend of Figure 6

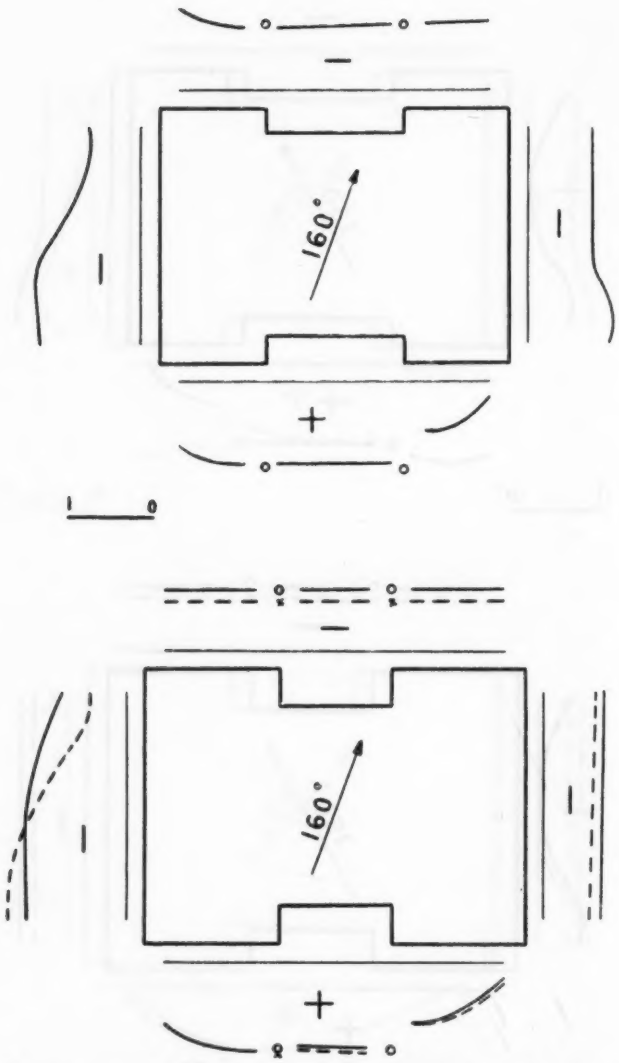

FIGURE 14.—*Distribution of pressure at sections A, B, and C at 160° to the wind*

See legend of Figure 6

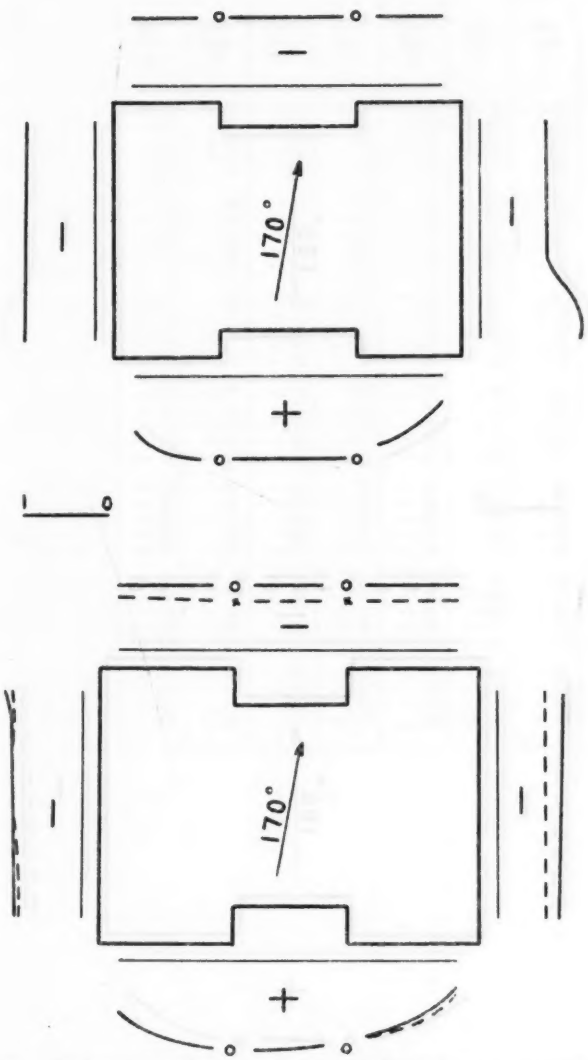

FIGURE 15.—*Distribution of pressure at sections A, B, and C at 170° to the wind*

See legend of Figure 6

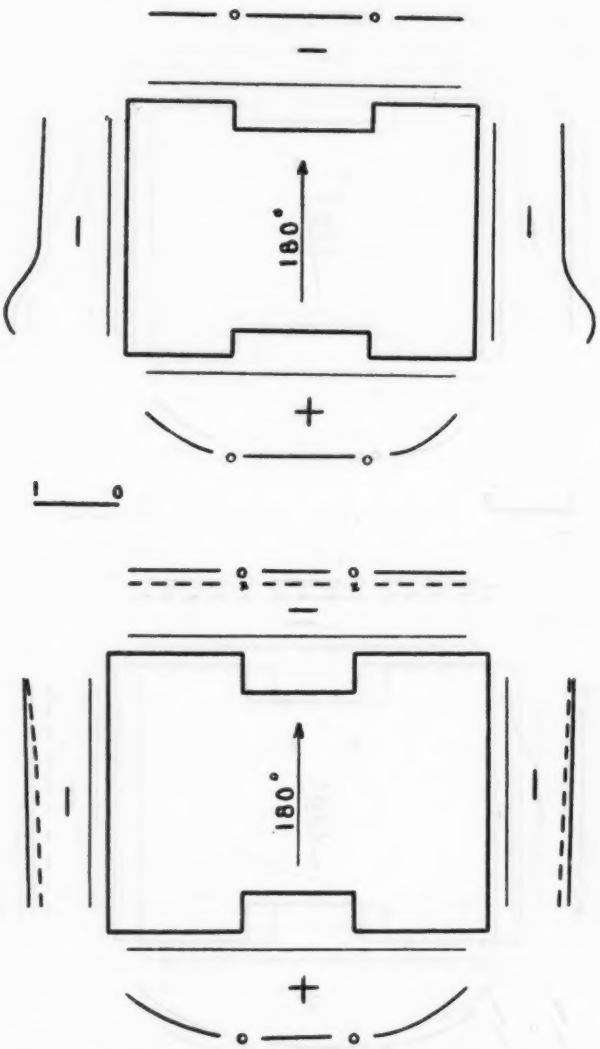

FIGURE 16.—*Distribution of pressure at sections A, B, and C at 180° to the wind*

See legend of Figure 6

TABLE 3.—*Pressure distribution over model, at various angles to the wind*

(See figs. 2, 3, and 4 for position of holes and sections)

p_w/q

Hole No.	90°			100°			110°		
	Section *A*	Section *B*	Section *C*	Section *A*	Section *B*	Section *C*	Section *A*	Section *B*	Section *C*
1	0.52	0.66	0.61	0.62	0.72	0.71	0.84	0.91	0.91
2	.82	.89	.83	.89	.93	.95	1.00	1.02	1.05
3	.98	1.05	.99	.98	1.03	1.03	.97	1.01	1.03
4	.98	1.05	.99	.92	.96	1.00	.83	.89	.89
5	.82	.89	.83	.69	.77	.81	.52	.64	.64
6	.56	.66	.63	.42	.44	.57	.24	.38	.42
7	−.89	−.70	−.67	−.87	−.62	−.51	−.93	−.60	−.50
8	−.94	−.68	−.68	−.91	−.60	−.52	−.92	−.62	−.51
9	−.85	−.68	−.70	−.83	−.61	−.52	−.76	−.63	−.52
10	−.75	−.69	−.68	−.73	−.60	−.50	−.71	−.63	−.52
11	−.79	−.70	−.69	−.76	−.62	−.53	−.70	−.62	−.53
12	−.79	−.73	−.71	−.77	−.64	−.54	−.72	−.63	−.55
13	−.80	−.73	−.64	−.76	−.64	−.55	−.73	−.63	−.52
14	−.78	−.71	−.63	−.73	−.61	−.53	−.70	−.62	−.51
15	−.81	−.72	−.66	−.77	−.62	−.56	−.75	−.63	−.53
16	−.82	−.77	−.71	−.78	−.65	−.58	−.75	−.63	−.55
17	−.83	−.84	−.73	−.79	−.67	−.61	−.75	−.64	−.58
18	−.76	−.60	−.58	−.74	−.58	−.46	−.77	−.62	−.55
19	−.75	−.59	−.56	−.74	−.58	−.45	−.75	−.60	−.55
20	−.75	−.57	−.53	−.75	−.58	−.45	−.75	−.60	−.55
21	−.75	−.57	−.54	−.75	−.60	−.46	−.75	−.62	−.55
22	−.76	−.59	−.56	−.76	−.60	−.46	−.80	−.60	−.54
23	−.76	−.65	−.60	−.78	−.63	−.49	−.80	−.61	−.48
24	−.79	−.82	−.80	−.70	−.77	−.58	−.50	−.46	−.32
25	−.78	−.76	−.76	−.75	−.86	−.71	−.41	−.39	−.15
26	−.78	−.71	−.72	−.88	−.94	−.86	−.40	−.41	−.00
27	−.79	−.70	−.70	−1.08	−.97	−1.05	−.20	−.54	−.32
28	−.78	−.72	−.71	−1.03	−.96	−.98	−.16	−.58	−.38
29	−.79	−.72	−.71	−1.08	−.97	−.87	−.45	−.62	−.62
30	−.75	−.69	−.60	−1.05	−.94	−.97	−.46	−.59	−.55
31	−.78	−.69	−.60	−1.05	−.93	−.93	−.39	−.56	−.40
32	−.83	−.67	−.60	−1.23	−.93	−1.08	−.71	−.65	−.76
33	−.91	−.66	−.59	−1.18	−.91	−1.05	−.69	−.67	−.79
34	−.85	−.65	−.58	−1.15	−.90	−1.03	−.63	−.65	−.77

TABLE 4.—*Pressure distribution over model, at various angles to the wind*

(See figs. 2, 3, and 4 for position of holes and sections)

p_w/q

Hole No.	120°			130°			135°		
	Section *A*	Section *B*	Section *C*	Section *A*	Section *B*	Section *C*	Section *A*	Section *B*	Section *C*
1	1.02	1.00	0.99	0.95	1.02	0.98	0.80	0.83	0.82
2	1.03	1.00	1.00	.86	.91	.91	.69	.74	.74
3	.87	.90	.89	.64	.73	.69	.49	.57	.54
4	.66	.70	.69	.43	.52	.50	.28	.37	.34
5	.33	.40	.43	.13	.22	.22	0	.09	.09
6	.04	.17	.22	−.12	−.07	.02	−.22	−.14	−.24
7	−.96	−.68	−.50	−.80	−.68	−.53	−.83	−.73	−.58
8	−.90	−.66	−.50	−.80	−.67	−.53	−.82	−.71	−.58
9	−.78	−.66	−.52	−.73	−.68	−.54	−.77	−.71	−.60
10	−.74	−.69	−.51	−.69	−.68	−.51	−.73	−.71	−.72
11	−.74	−.67	−.53	−.71	−.69	−.54	−.75	−.72	−.58
12	−.75	−.69	−.55	−.73	−.70	−.56	−.76	−.72	−.60
13	−.74	−.68	−.56	−.71	−.70	−.58	−.76	−.73	−.64
14	−.73	−.70	−.51	−.69	−.71	−.57	−.74	−.74	−.62
15	−.76	−.68	−.56	−.73	−.70	−.57	−.77	−.73	−.63
16	−.77	−.70	−.58	−.75	−.71	−.57	−.78	−.74	−.63
17	−.79	−.72	−.60	−.75	−.72	−.57	−.79	−.74	−.64
18	−.76	−.69	−.50	−.74	−.69	−.53	−.78	−.76	−.59
19	−.75	−.69	−.50	−.73	−.68	−.52	−.77	−.75	−.59
20	−.76	−.70	−.50	−.73	−.68	−.52	−.77	−.74	−.58
21	−.77	−.70	−.49	−.74	−.67	−.52	−.79	−.74	−.58
22	−.87	−.69	−.48	−.87	−.66	−.52	−.94	−.73	−.57
23	−.91	−.70	−.49	−.91	−.70	−.52	−.98	−.73	−.56
24	−.48	−.44	−.30	−.33	−.30	−.21	−.29	−.29	−.31
25	−.30	−.22	−.11	−.08	−.02	.05	−.03	.06	.12
26	−.33	−.13	−.04	−.40	.10	.16	−.28	.22	.25
27	.72	.29	.31	.99	.52	.55	.97	.67	.67
28	.56	.19	.22	.83	.44	.45	.89	.58	.59
29	.26	.15	.17	.54	.43	.41	.77	.56	.56
30	.11	.18	.21	.40	.47	.46	.42	.59	.56
31	.13	.22	.26	.38	.50	.51	.51	.65	.62
32	.25	.28	.31	.55	.58	.58	.65	.70	.69
33	.16	.13	.05	.67	.68	.69	.78	.84	.81
34	−.11	−.10	−.12	.79	.83	.82	.91	.98	.93

TABLE 5.—*Pressure distribution over model, at various angles to the wind*

(See figs. 2, 3, and 4 for position of holes and sections)

p_w/q

Hole No.	140°			150°			160°		
	Section *A*	Section *B*	Section *C*	Section *A*	Section *B*	Section *C*	Section *A*	Section *B*	Section *C*
1	0.39	0.57	0.55	−0.48	−0.46	−0.56	−1.15	−1.16	−1.37
2	.55	.58	.59	−.51	−.49	−.51	−1.22	−1.16	−1.35
3	.36	.42	.40	−.13	−.13	.03	−1.23	−1.18	−1.22
4	.17	.22	.22	−.04	.02	−.02	−.82	−1.11	−.88
5	−.10	−.01	.01	−.26	−.19	−.19	−.55	−.90	−.47
6	−.30	−.20	−.15	−.45	−.35	−.29	−.60	−.73	−.42
7	−.80	−.67	−.54	−.84	−.68	−.54	−.93	−.66	−.55
8	−.79	−.67	−.54	−.79	−.66	−.55	−.75	−.68	−.56
9	−.74	−.67	−.56	−.72	−.66	−.56	−.70	−.68	−.55
10	−.71	−.68	−.54	−.72	−.68	−.53	−.76	−.68	−.55
11	−.71	−.67	−.53	−.71	−.67	−.54	−.69	−.70	−.53
12	−.73	−.68	−.54	−.73	−.67	−.54	−.71	−.68	−.52
13	−.71	−.68	−.58	−.73	−.68	−.56	−.76	−.69	−.55
14	−.70	−.71	−.56	−.74	−.69	−.57	−.76	−.71	−.56
15	−.72	−.68	−.57	−.73	−.67	−.56	−.76	−.69	−.57
16	−.73	−.69	−.57	−.74	−.67	−.56	−.76	−.69	−.57
17	−.73	−.70	−.58	−.73	−.68	−.56	−.77	−.69	−.57
18	−.73	−.72	−.57	−.74	−.71	−.58	−.76	−.71	−.63
19	−.73	−.71	−.57	−.73	−.70	−.57	−.74	−.71	−.61
20	−.72	−.69	−.57	−.73	−.68	−.55	−.75	−.69	−.58
21	−.75	−.69	−.56	−.76	−.68	−.55	−.77	−.69	−.57
22	−.93	−.69	−.53	−1.00	−.68	−.53	−1.01	−.68	−.54
23	−.97	−.69	−.53	−1.02	−.69	−.53	−.96	−.66	−.51
24	−.21	−.16	−.08	−.02	.01	.09	.15	.18	.25
25	.07	.18	.22	.31	.40	.47	.50	.58	.64
26	.01	.36	.39	.45	.59	.58	.57	.72	.70
27	.83	.81	.80	.84	.94	1.00	1.02	1.01	1.00
28	.77	.71	.72	.82	.92	.93	.93	.99	1.04
29	.75	.70	.70	.86	.89	.90	.93	.99	1.04
30	.57	.72	.72	.84	.90	.94	.94	.96	.99
31	.62	.76	.78	.86	.92	.94	.98	.99	1.03
32	.82	.84	.85	.96	.98	1.02	.97	1.03	1.02
33	.94	.95	.95	1.01	1.02	1.07	.94	.98	.99
34	1.04	1.05	1.05	.96	.94	.99	.74	.72	.69

TABLE 6.—*Pressure distribution over model, at various angles to the wind*

(See figs. 2, 3, and 4, for position of holes and sections)

p_w/q

Hole No.	170°			180°		
	Section *A*	Section *B*	Section *C*	Section *A*	Section *B*	Section *C*
1	−0.83	−0.76	−0.73	−1.10	−0.74	−0.58
2	−.85	−.77	−.74	−1.21	−.74	−.59
3	−.84	−.79	−.78	−.84	−.75	−.62
4	−.81	−.80	−.81	−.79	−.77	−.66
5	−.79	−.84	−.80	−.79	−.80	−.72
6	−.81	−.92	−.83	−.78	−.80	−.73
7	−.75	−.74	−.62	−.79	−.74	−.60
8	−.75	−.75	−.58	−.79	−.72	−.58
9	−.75	−.74	−.56	−.79	−.72	−.57
10	−.79	−.72	−.54	−.79	−.71	−.55
11	−.77	−.72	−.54	−.80	−.72	−.57
12	−.78	−.72	−.54	−.81	−.72	−.57
13	−.78	−.74	−.55	−.78	−.72	−.56
14	−.80	−.73	−.56	−.77	−.72	−.56
15	−.78	−.73	−.55	−.79	−.73	−.57
16	−.78	−.74	−.54	−.79	−.72	−.57
17	−.78	−.75	−.56	−.78	−.73	−.60
18	−.79	−.76	−.56	−.79	−.78	−.73
19	−.79	−.75	−.55	−.78	−.78	−.72
20	−.78	−.75	−.62	−.78	−.75	−.68
21	−.81	−.73	−.59	−.82	−.73	−.64
22	−1.20	−.71	−.56	−1.18	−.71	−.61
23	−1.18	−.71	−.56	−1.14	−.74	−.59
24	.26	.29	.37	.42	.44	.49
25	.62	.71	.76	.75	.83	.85
26	.77	.87	.87	.86	.97	.96
27	.95	1.04	1.03	.98	1.04	1.02
28	.96	1.00	1.03	.94	1.02	1.03
29	.97	1.01	1.03	.94	1.02	1.03
30	.97	1.01	1.02	.93	1.01	1.00
31	.96	1.03	1.03	.96	1.03	1.02
32	.96	1.02	1.01	.86	.97	.95
33	.88	.93	.94	.73	.84	.84
34	.63	.63	.64	.44	.51	.51

5. DISCUSSION

Some of the more striking features of the pressure distribution will be described for purposes of emphasis. The greater part of the model is under reduced pressure. The lee faces are subjected to a nearly constant reduced pressure, although the absolute pressure is usually higher at the lower elevation. A fine thread showed that the air passing over the top of the model was deflected downward and that a large eddy is formed behind the model extending downstream some 3 feet. Near the building on the lee side the current is upward as indicated by the pressure distribution.

The behaviour of the embrasures is of interest. In most cases the embrasures carry the pressure of the adjacent wall. When however the embrasure is on the windward side, the pressure is increased relative to that on the neighboring wall. This behaviour is perceptible in Figure 8 for 110° and is very marked in Figure 11 for 135°, especially for elevation *A*.

When a face is struck directly by the wind (figs. 6 and 16), the pressure is greatest in the center, falling off toward the edges. The placing of wind bracing in the end panels alone does not seem to be the most suitable to withstand this type of loading.

III. MEASUREMENTS OF OVERTURNING MOMENT

1. APPARATUS AND METHOD

In addition to measurements of the pressure distribution, the overturning moments were directly measured. For this purpose, the

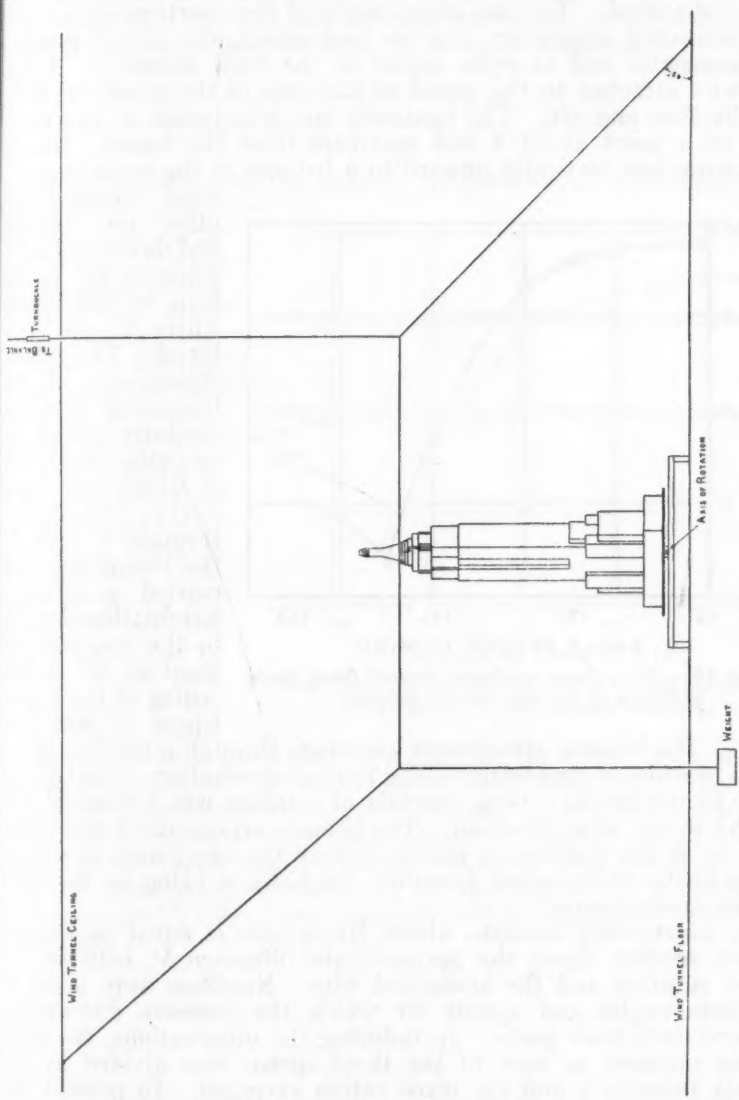

FIGURE 17.—*Diagrammatic sketch of set-up for measurement of overturning moments about a horizontal axis at right angles to the wind direction*

model and attached circular plate were placed on a horizontal bar 1 inch wide and one-half inch thick. The ends of the bar carried the inner races of ball bearings; the outer races of the bearings were supported in housings secured to the platform on the floor of the tunnel. The model and the circular plate could be rotated with

respect to the bar about a vertical axis and held at any desired azimuth as in the pressure distribution tests. (Fig. 17.) For measuring the resultant overturning moment, it was necessary to measure the components about two horizontal axes, one parallel to the wind direction, the other at right angles to the wind direction, since, in general, the resultant force on the model has a component transverse to the direction of the wind. The two components of the overturning moment were measured separately. In the first set-up, the axis of rotation was horizontal and at right angles to the wind direction. A fine steel wire attached to the model at the base of the tower ran horizontally fore and aft. The upstream end was joined to two other wires at a point about 4 feet upstream from the model. One of these wires ran vertically upward to a balance in the room over the wind tunnel; the other ran forward and downward at an angle of 45° to the floor of the tunnel where it was fastened. The downstream end of the horizontal wire was similarly joined to two other wires, one of which ran vertically downward through a hole in the tunnel floor and carried a counterweight; the other ran to the rear and upward at 45° to the ceiling of the tunnel where it was fastened. The balance attachment was made through a turnbuckle by means of which compensation could be made for motion of the balance pan. In the second set-up, the axis of rotation was horizontal and parallel to the wind direction. The balance arrangement was essentially as in the first set-up except that all the wires were in a plane perpendicular to the wind direction, the balance being on the right looking downstream.

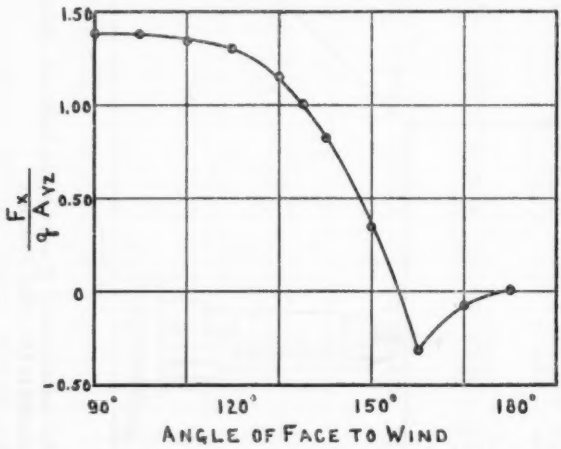

FIGURE 18.—*The x-force coefficient derived from measurements of the overturning moment*

The overturning moment about either axis is equal to the net balance reading times the perpendicular distance h' between the axis of rotation and the horizontal wire. Readings were taken at the same angles and speeds for which the pressure distribution measurements were made. In reducing the observations, the overturning moment at each of the three speeds was divided by the velocity pressure q and the three values averaged. In general, the individual readings were within 2 per cent of the mean value.

2. RESULTS

The moments were measured about axes parallel and perpendicular to the wind direction, to make the balance arrangements as simple as possible. It is more convenient in practice to refer moments to the

principal axes of the building, designated as in Figure 4. (The X axis is directed into the plane of the paper at right angles to the Y and Z axes and is parallel to the wind direction when the model setting is 90°.) At any given angle θ of the model, call F_D and F_{CW} the net balance readings for measurements about the axes perpendicular and parallel to the wind, F_x' and F_y' the values which would have been observed if the wire and balance system had been placed in the YZ and XZ planes, respectively. It is easily seen that

$$F_x' = F_D \cos(\theta - 90°) - F_{CW} \sin(\theta - 90°)$$
$$F_y' = F_D \sin(\theta - 90°) + F_{CW} \cos(\theta - 90°)$$

For comparison with the pressure measurements, it is desirable to divide the overturning moments about the X and Y axes by the areas of the YZ and XZ faces (designated A_{yz} and A_{xz}) and by the distance from the line of action of the resultant force from the axis of rotation. This latter distance is however not known. A suitable conventional distance would be the distance h from the axis to the center of gravity of the area of projection of the model on a plane normal to the wind direction. This distance, however, varies with the angular setting from 25.07 inches at 90° to 22.90 at 180°. The mean value is 23.98 inches or 1.998 feet. The results were finally expressed in terms of coefficients derived from fictitious forces F_x and F_y which if applied at the mean height h of the center of area would give the observed overturning moments. The final coefficients given in the sixth column of Tables 7 and 8 and plotted in Figures 18 and 19 are defined by

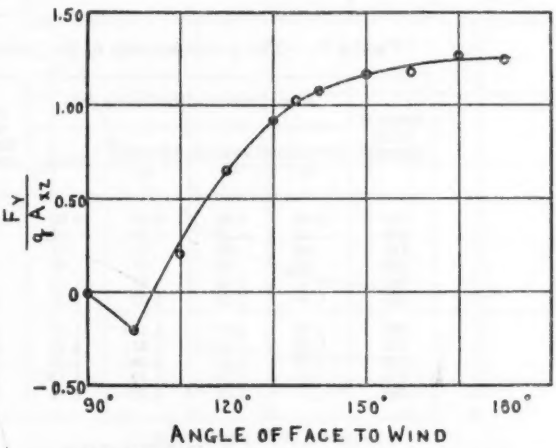

FIGURE 19.—*The y-force coefficient derived from measurements of the overturning moment*

$$\frac{F_x}{qA_{yz}} = \frac{F_x'h'}{qhA_{yz}}$$

and

$$\frac{F_y}{qA_{xz}} = \frac{F_y'h'}{qhA_{xz}}$$

where for the model $h' = 4.413$ feet, $h = 1.998$ feet, $A_{yz} = 2.486$ ft.^{2}, $A_{xz} = 3.915$ ft.^{2}. The overturning moments at a given velocity pressure may be obtained by multiplying the coefficients by the product of velocity pressure, projected area on the vertical plane containing the axis of rotation, and mean distance h from the axis to the center of area.

TABLE 7.—*The x components of the force coefficients*

Angle of wind (degrees)	From pressure distribution data				From overturning moments	Difference
	Elevation *A*	Elevation *B*	Elevation *C*	Mean		
90	1.57	1.48	1.40	1.48	1.38	0.10
100	1.54	1.42	1.31	1.42	1.37	.05
110	1.56	1.44	1.39	1.46	1.34	.12
120	1.56	1.42	1.22	1.40	1.30	.10
130	1.35	1.25	1.08	1.23	1.15	.08
135	1.24	1.16	.99	1.13	1.00	.13
140	1.02	.98	.83	.94	.82	.12
150	.55	.45	.34	.45	.34	.11
160	−.14	−.36	−.39	−.30	−.32	.02
170	.09	−.07	−.21	−.06	.08	.02
180	0	.02	.01	.01	.01	0

TABLE 8.—*The y components of the force coefficients*

Angle of wind (degrees)	From pressure distribution data				From overturning moments	Difference
	Elevation *A*	Elevation *B*	Elevation *C*	Mean		
90	0.00	0.02	0.02	0.02	−0.01	0.03
100	−.21	−.28	−.35	−.28	−.20	.08
110	.29	.07	.04	.13	.21	.08
120	.84	.67	.57	.69	.65	.04
130	1.11	1.05	.93	1.03	.91	.12
135	1.26	1.20	1.02	1.16	1.01	.15
140	1.29	1.27	1.17	1.24	1.07	.17
150	1.44	1.40	1.31	1.38	1.16	.22
160	1.52	1.47	1.36	1.45	1.17	.28
170	1.57	1.56	1.42	1.52	1.27	.25
180	1.57	1.57	1.42	1.52	1.24	.28

3. DISCUSSION

In order to compare the pressure observations with the measurements of the overturning moment, the pressures were integrated by a process of numerical integration, namely, by multiplying the pressure at each hole by the distance between the midpoints of the distances to the two adjacent holes or to the edge of the face for the outer holes. The resulting sums for the X and Y components were divided by the width of the model in the Y and X directions and by the velocity pressure to give coefficients corresponding to those computed from the overturning moments. The coefficients for the three sections and the various angles are given in Tables 7 and 8, columns 2 and 4, inclusive, and the mean values are given in column 5. Since there are no pressure stations on the tower which is of a different shape or on the lower part of the building which is in a region of reduced speed, the mean values in column 5 can not reasonably be expected to give a value representative of the entire building. Moreover, the coefficient from the overturning moment is truly representative only if the pressure is uniformly distributed. Nevertheless, the coefficients determined from the overturning moment are but 0.1 less than the mean value from the pressures measured at three levels for the X direction and but 0.3 less for the Y direction.

From a consideration of the values in the tables, we believe that for design purposes a coefficient of 1.5 is not unreasonable.

IV. REMARKS ON THE METHOD OF COMPARING MODEL RESULTS WITH FULL-SCALE MEASUREMENTS

Although this paper is concerned mainly with the model tests, it appears desirable to indicate the method of application of the results for comparisons with full-scale results and to explain one supplementary measurement made on the model. It has already been pointed out that in measurements in natural winds the wind speed and direction are not under control but vary continuously. Moreover it is certain that in a vertical distance of 1,250 feet there may be great variations of speed and direction at any instant. The only provision at present for measuring the wind speed on the actual building is an anemometer mounted about 15 feet above the top of the mooring tower. A little consideration shows that the indications of this instrument do not give the true speed of the wind approaching the building.

If the anemometer were placed on the windward side of the building on a median line not far from the wall of the building, it is easily seen that the readings would be too low, because the air is slowed up as it approaches the building. Moreover, if the anemometer were placed at the side of the building, it would read too high because the air blocked by the building must escape at higher speeds around the sides. A similar interference effect above the tower has been measured on the model. Figure 20 shows the variation of speed above the top of the tower. From this curve it is estimated that the anemometer on the building gives a speed about 23 per cent greater than the true speed of the approaching wind. When the anemometer reads 100 miles per hour (after correction for purely instrumental errors), the true speed of the approaching wind is 81 miles per hour. This correction must be applied to the readings of the anemometer on the building before comparison with the model tests.

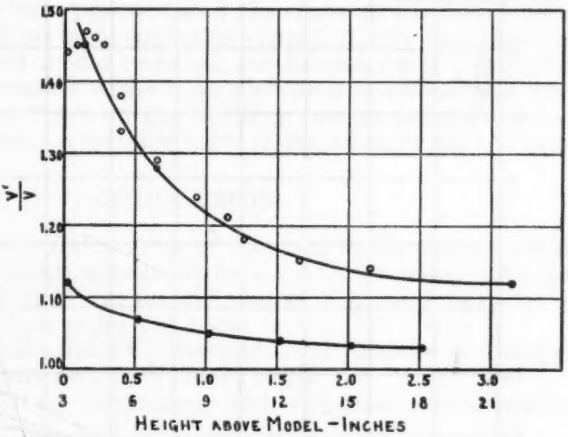

FIGURE 20.—*Distribution of wind speed above the model*
V'=local speed; V=speed at the same place when the model is absent. The fact that the speed V' does not fall to V is due to the blocking of the tunnel cross section by the model

In measurements in natural winds, it is practically impossible to secure a fixed reference pressure. In the case of the installation on the Empire State Building, it is not feasible to measure the pressures at the three levels with respect to the same base pressure. At each level, the base pressure is the pressure at some point within the building at the manometer location on that floor. The model results are expressed in terms of the static pressure and hence the

pressures at the individual stations are not directly comparable with those observed on the building.

Because of this fact and the previously noted variation of wind speed and direction at the different levels on the actual building, it is suggested that the comparison be made by assuming the model results to apply to the building and noting whether this assumption leads to inconsistencies. The procedure recommended is based on the fact that it is possible to choose stations such that certain ratios

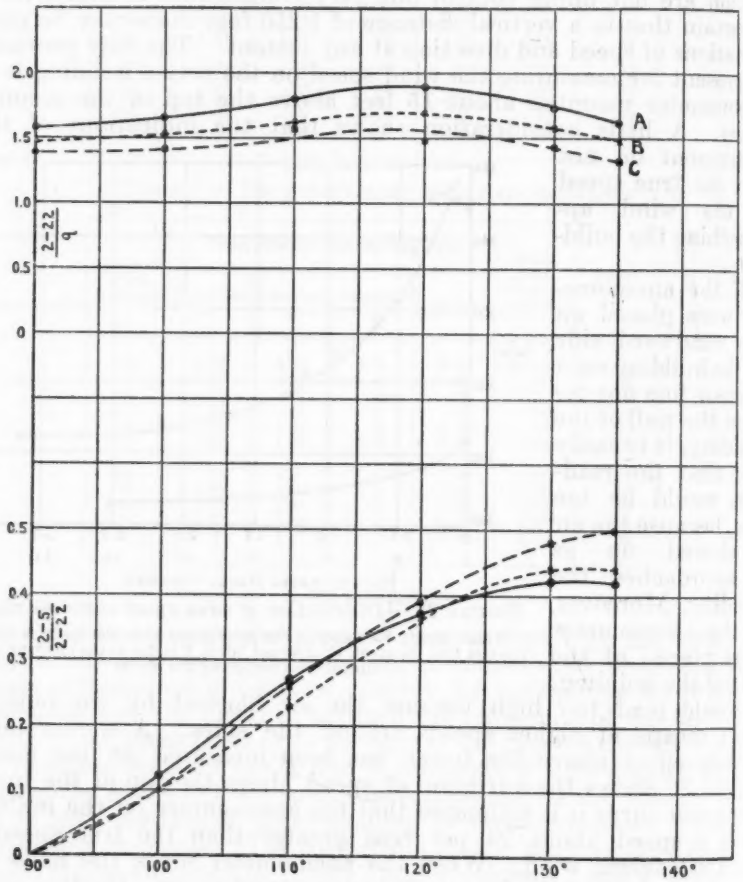

FIGURE 21.—*Diagrams to show method of determining wind speed and direction at various levels on the full-scale building*

The curves are from the model results. 2—5 stands for the difference in pressure between stations 2 and 5, etc.

of pressure differences are very sensitive to changes of wind direction whereas other ratios are insensitive.

The procedure is illustrated for wind directions lying between 90° and 135° in Figure 21. It is found that the ratio of the difference in pressure between stations 2 and 5 to that between stations 2 and 22 varies rapidly with wind direction. This ratio does not depend on the base pressure (if it is the same for the three stations) or on the

wind speed (since all pressures vary in the same ratio with the speed). On the other hand, the ratio of the difference in pressure between stations 2 and 22 to the velocity pressure varies very slowly with the angle. Suppose that observations on the building at elevation B give a value of 0.36 for the ratio $\frac{2-5}{2-22}$. From the lower curve of Figure 21, the wind direction is found to be 120° and from the upper curve $\frac{2-22}{q}$ is found to be 1.7. From the value of $2-22$, q may be found and thence from Table 2 the speed. The value of the speed and direction can be compared with that obtained for the other two levels and the top of the building. Likewise, since the maximum increase in pressure should be equal to q, the difference between the base pressure and the static pressure can be evaluated, the diagrams reduced to the same base pressure, and the shape of the distribution curves compared. If no inconsistencies appear, it may be concluded that the full-scale and model tests are not inconsistent, No better procedure appears possible without an elaborate installation of anemometers at different levels on the building and an expensive interconnection of the reference pressure sides of the manometers by pipes of large diameter.

V. CONCLUSION

To summarize, a reasonable value of the force coefficient for use in the design of tall buildings appears to be 1.5 corresponding to a wind pressure equal to 0.0038 V^2 (in lbs./ft.^{2}) where V is the true speed of the approaching wind in miles per hour.

Data are given for the detailed distribution of pressure at 102 stations for wind directions varying by steps of 10°.

A suggested method of comparison with full-scale measurements is outlined.

WASHINGTON, February 13, 1933.

STANDARD STATES FOR BOMB CALORIMETRY

By Edward W. Washburn

ABSTRACT

An examination of the thermodynamics of the conditions existing in bomb calorimetry shows that the heat of combustion per unit mass of substance burned is a function of the mass of sample used, of the initial oxygen pressure, of the amount of water placed in the bomb, and of the volume of the bomb. In order to eliminate the effects of these at present unstandardized variables and to obtain a more generally useful thermal quantity which characterizes the pure chemical reaction for stated conditions, it is suggested that every bomb-calorimetric determination be first corrected (where such correction is significant) so as to give the value of ΔU_R, the change of "intrinsic" energy for the pure isothermal reaction under the pressure condition of 1 normal atmosphere for both reactants and products.

From this value the more generally useful quantity, Q_p, the heat of the pure reaction at a constant pressure of 1 atmosphere is readily calculable. An equation for calculating the correction is given and illustrated by examples. The magnitude of the correction varies from a few hundredths of 1 per cent up to several tenths of 1 per cent according to the nature of the substance burned and the conditions prevailing in the bomb during the combustion.

It is further recommended that, in approving, for the purpose of standardizing a calorimeter, a particular value for the heat of combustion (in the bomb) of a standardizing substance, such as benzoic acid, the value approved be accompanied by specification of the oxygen concentration and of the ratios to the bomb volume of (1) the mass of the sample and (2) the mass of water, together with appropriate tolerances.

An equation is given for correcting to any desired standard temperature the heat measured in the bomb calorimeter.

CONTENTS

		Page
I.	Nomenclature	526
II.	Introduction	527
III.	Calorimetry and the first law of thermodynamics	528
IV.	The nature of the bomb process	529
V.	Proposed standard states for constant-volume combustion reactions	530
VI.	Comparison of the actual bomb process with that defined by the proposed standard states	531
VII.	The total energy of combustion defined by the proposed standard states	531
VIII.	Definitions of some auxiliary quantities	534
	1. The initial system	534
	2. The final system	534
IX.	Correction for dissolved carbon dioxide	535
X.	The energy content of the gases as a function of the pressure	536
XI.	Correction for the change in energy content of the gases	537
XII.	Calculation of the change in pressure resulting from the combustion	538
XIII.	The negligible energy quantities	540
	1. The energy content of the water	540
	(*a*) The change in the energy content of the water vapor	540
	(*b*) The change in the energy content of the liquid water	540
	2. Combined energy corrections for water vapor and for dissolved carbon dioxide	541

XIII. The negligible energy quantities—Continued. Page
3. The energy content of the dissolved oxygen ... 541
4. The energy content of the substance ... 542
(*a*) The energy of compression of the substance ... 542
(*b*) The energy of vaporization of the substance ... 543
XIV. The total correction for reduction to the standard states ... 543
1. The general correction equation ... 543
2. An approximate correction equation ... 544
XV. The magnitude of the correction in relation to the type of substance burned ... 545
XVI. Computation of the correction ... 545
1. General remarks ... 545
2. Computation for benzoic acid ... 547
3. Computation for a mixture ... 547
XVII. Corrections for iron wire and for nitrogen ... 548
XVIII. Reduction of bomb calorimetric data to a common temperature ... 550
XIX. The temperature coefficient of the heat of combustion ... 551
XX. Standardizing substances ... 552
XXI. Standard conditions for calorimetric standardizations ... 552
XXII. The heat of combustion of standard benzoic acid ... 553
Appendix I. Concentration of saturated water vapor in gases at various pressures ... 554
Appendix II. Empirical formula of a mixture ... 557
Appendix III. Summary of numerical data employed ... 557

I. NOMENCLATURE

(Additional subscripts and superscripts are used in the text as further distinguishing marks)

A	Maximum work.
a, b, c	Coefficients in the chemical formula, $C_aH_bO_c$.
C	Concentration; molal heat capacity.
c	Specific heat.
g	Gram.
(g)	Gaseous state.
h	$=1.70x\ (1+x)$.
g. f. w.	Gram-formula-weight.
(l)	Liquid state.
M	Molecular weight; g. f. w.
m	Mass of sample burned.
m_w	Number of grams of water placed in the bomb.
n	Number of moles or of g. f. w. of substance burned.
n_D	Number of moles of CO_2 in solution in the water in the bomb.
n_M	Number of moles of gas in the bomb after the combustion.
n_{O_2}	Number of moles of O_2 in the bomb before the combustion.
P	Pressure; per cent by weight.
p	Pressure or partial pressure.
p_1	Pressure in the bomb before the combustion.
p_2	Pressure in the bomb after the combustion.
p_w	Vapor pressure of water.
Q	Heat absorbed.
R	Gas constant.
S	Solubility.
s	Heat capacity.
(s)	Solid state.
T	Absolute centigrade temperature.
t	Centigrade temperature.
t_H	Standard temperature °C.
U	Total or intrinsic energy content.

$-\Delta U_B$ Heat evolved during the combustion, per g. f. w. of substance burned.

$-\Delta U_R$ Decrease in intrinsic energy for the pure chemical reaction under standard conditions.

V Volume of the bomb.

v Volume.

W External work.

x Mole fraction of CO_2 in the gases of the bomb after the combustion.

α See p. 555.

Δ Symbol indicating an increase in.

ϕ Number of moles of O_2 consumed to produce nongaseous products.

π See p. 539.

μ See p. 534.

II. INTRODUCTION

The technic of modern calorimetry has been developed to such a degree of precision that it is to-day possible, in some cases, to determine heat of combustion in a calorimetric bomb with a precision approaching 0.01 per cent. If full advantage is to be taken of this degree of precision it is obvious that the process or reaction involved must be defined with the necessary accuracy as regards all factors which can separately or in combination influence the result to this degree of precision. At the present time it is not so defined. In fact, the heat of the bomb process per unit mass of substance burned varies with the actual mass burned and does not belong to any completely defined and clean-cut chemical reaction, and the initial and final states of the system are either incompletely defined or are thermodynamically uninteresting or trivial.

Consider, for example, what takes place in a bomb-calorimetric determination. A certain mass, m, of the substance to be burned is placed in a bomb of volume V (in some cases not stated), together with a small quantity (usually 1 g) of water. The bomb is then filled with oxygen at some pressure, p, and at some temperature, t, neither of which is standardized and one or both of which are, in some cases, not stated. The amount of this initial oxygen is from 3 to 10 times that which is consumed during the combustion. After the completion of the combustion, the system consists of a gaseous phase made up of a mixture of oxygen and carbon dioxide (in some cases in unknown proportions) saturated with water vapor, and a liquid phase which is substantially an aqueous solution of carbon dioxide. These are the conditions for the combustion of substances which contain no elements other than carbon, hydrogen, and oxygen.

The heat obtained in the above process per unit mass of substance burned is a function of the mass of the sample employed, of the volume of the bomb used, of the initial concentration of the oxygen, and of the amount of water initially placed in the bomb. If each of these factors, together with the chemical composition of the material burned, were quantitatively known, the initial and final states of the system would be definite but thermodynamically uninteresting.

If, as is not infrequently the case, the value of some one or more of these factors is not stated by the investigator, the initial or the final state of the system, or both, will be indefinite and the process to which the heat effect belongs will be inadequately defined. It is

obvious from the above picture that the process which takes place within the bomb does not start from a definite and standardized initial condition nor end with a definite final condition, either chemically or physically.

Now the initial condition should obviously be (1) pure substance or definite material in a definite phase state or states (solid and/or liquid); and (2) pure gaseous oxygen at some standard concentration; and the final condition should be pure gaseous carbon dioxide and pure liquid water each under some standard pressure. Furthermore, if the excess oxygen undergoes, as it does, a change in condition which is accompanied by a heat effect, due correction must be made therefor, so that only the oxygen consumed will be involved in the process to which the final heat quantity belongs.

At present the bomb calorimeter appears to have no serious competitor for the precise determination of heat of combustion of organic solids and liquids of low volatility, and the exact standardization of conditions as here proposed is necessary, if one is to take full advantage of the highest precision attainable.

The purpose of this discussion is to propose suitable standard states and to describe methods by which the heat of the bomb process may be corrected so as to yield the total or intrinsic energy change for the reaction defined by these standard states. Without such standardization it is impossible to obtain from the existent precise data of bomb calorimetry the frequently wanted quantity ordinarily called the "heat of the reaction at constant pressure." This is to-day almost universally calculated by the simple addition of a ΔnRT quantity to the result obtained with the calorimetric bomb, a procedure which is thermodynamically inexact when applied to calorimetric data of high precision.

III. CALORIMETRY AND THE FIRST LAW OF THERMODYNAMICS

According to the first law of thermodynamics

$$U_2 - U_1 = \Delta U = Q - W \tag{1}$$

U_2 (or U_1, respectively) is the "total," "internal," or "intrinsic" energy of any system in the state 2 (or 1, respectively). ΔU is the increase in this intrinsic energy which takes place when the system changes from state 1 to state 2 by any path. Q is the quantity of heat absorbed by the system during the process and W is the work done by the system on the surroundings. The quantity ΔU is independent of the path and is completely defined by the initial and final states. For isothermal processes three cases are, for practical or conventional reasons of special interest, as follows:

Case 1. $W=0$. For this case $Q_{W=0}=\Delta U$; that is, the increase in intrinsic energy is equal to the heat absorbed. The heat of a process (any process whatsoever) under these conditions is usually designated by Q_v and is commonly called the "heat at constant volume." This designation is somewhat unfortunate for three reasons: (1) Because in general a constant-volume process is not necessarily a zero-work process (for example, when accompanied by external electrical work); (2) because a zero-work process is not necessarily a constant-volume process (for example, when a gas expands

into a vacuum); and (3) because constancy of volume alone is not a sufficient characterization of an isothermal zero-work process (since the heat of such a process may also be a function of the pressure, for example).

Case 2. $W = \int p dv = p\Delta v$, where Δv is the volume increase under a constant external pressure p. The heat of the process under these conditions is usually designated by Q_p and is commonly called "the heat at constant pressure." This designation is likewise correct and complete only when the value of the pressure is stated or implied and when all of the work done in the surroundings is accounted for by the volume change in the system.

Case 3. $W = W_{max.} = A$, where A is the maximum work or "free energy" of the process. This case is rarely encountered in calorimetry except when it is identical with case 2. The corresponding heat quantity has received no special designation although its ratio to the absolute temperature is the "entropy of the process."

Any one of the above heat quantities is, in principle, calculable from any other, but for conventional reasons the quantity Q_p for $p = 1$ atmosphere appears to be the most wanted one.

It will be advantageous therefore to standardize the initial and final states of bomb calorimetry in such a manner as to facilitate the computation of Q_p for $p = 1$ atmosphere. This can be conveniently accomplished by first correcting the quantity Q_v of the bomb process in such a way as to obtain the quantity ΔU for the reaction standardized for a pressure of 1 atmosphere, from which quantity the value of Q_p can be readily computed.

IV. THE NATURE OF THE BOMB PROCESS

Given a substance (or a material) whose composition is expressed by the empirical formula $C_aH_bO_c$. m grams ($= n$ gram-formula-weights) of this material in a thermodynamically defined physical state or states (solid and/or liquid) are placed in the bomb.[1] m_w grams of water are also placed in the bomb, this amount being at least sufficient to saturate the gas phase (volume $= V$ liters) with water vapor. The bomb is then closed and filled with n_{O_2} moles of oxygen, this amount being at least sufficient to ensure complete combustion.

The above quantities will completely define the initial system and this definition will subsist, if the quantities are all increased in the same ratio; that is, the initial state of the system is completely defined by the specification of the quantitative composition and physical state of the substance, by the temperature, and by three ratios; for example, m/V, m_w/V, and n_{O_2}/V.

When the calorimeter fore period has been established, the charge is ignited with the aid of a known amount of electrical energy. When the after period has been established, the heat liberated is computed, corrected to some definite temperature, t_H, and divided by n so as to obtain the quantity $-\Delta U_B$ which we shall designate as the evolved heat of the bomb process per g. f. w. (gram-formula-weight) of material burned at the temperature t_H. $\Delta U_B = Q_v$.

[1] If the material is volatile, it must be inclosed in a suitable capsule in order to prevent evaporation, and in some cases a combustible wick or admixture with some more easily combustible material must be employed in order to ensure complete combustion. In the latter case we are dealing with a mixture of combustible materials, and the formula $C_aH_bO_c$ should express the empirical composition of this mixture. The heat of combustion of the added material must be separately determined and the two heats are, in principle, not additive in the bomb process.

V. PROPOSED STANDARD STATES FOR CONSTANT-VOLUME COMBUSTION REACTIONS

For the purpose of recording such thermodynamic quantities as heat of formation, free energy of formation, entropy of formation, heat content, etc., for chemical substances, it is necessary to adopt some standard reference state, at least for each of the chemical elements.

From some points of view a logical standard state for each element might be the state of a monatomic gas at zero degrees absolute.[2] For obvious practical reasons, however, it has not hitherto been feasible to advantageously utilize a standard state defined in this way. Most of the compilations of thermodynamic properties of chemical substances define the standard state of a chemical element as the thermodynamically stable form of the element under a pressure of 1 normal atmosphere at the standard temperature (usually 18° or 25° C.).

The immediate requirements of bomb calorimetry will be met, if, in conformity with this general practice, we adopt the following standard states:

1. *For O_2 and CO_2.*—The pure gaseous substance under a pressure of 1 normal atmosphere [3] at the temperature t_H.

2. *For H_2O.*—The pure liquid under a pressure of 1 normal atmosphere [4] at the temperature t_H.

3. *For the substance or material burned.*—In a thermodynamically defined state or states (solid and/or liquid [5]) under a pressure of 1 normal atmosphere [6] at the temperature t_H.

The temperature t_H is the temperature at which the heat of the reaction is desired. For purposes of record this is usually made either 18°, 20°, or 25° C. The utility of thermodynamic data for chemical substances and reactions would be increased, if this temperature could be standardized by international agreement. At all events the temperature coefficient should be stated for each new determination of the heat of a reaction which is recorded in the literature.

The above definitions will make it possible to obtain from the data of bomb calorimetry a clearly defined and generally useful thermodynamic quantity.[7]

---

[2] A still more fundamental (but likewise inaccessible) reference state might be pure proton gas and pure electron gas at zero degrees absolute.

[3] For the purposes of bomb calorimetry this pressure is at present indistinguishable from 1 bar (megabarye).

[4] For a condensed phase not in the neighborhood of its critical temperature this pressure is at present calorimetrically indistinguishable from its own vapor pressure or in fact from zero pressure.

[5] For pure substances only one state, solid or liquid, is involved, but for mixtures more than one state or phase may be present. The gaseous state is excluded from the present discussion for two reasons: First, because the heat content of the gas and of its mixtures with oxygen must be evaluated as a function of the pressure; and second, because the bomb calorimeter is not the best instrument for the determination of heats of combustion of gases (or of volatile liquids). The flame calorimeter is more accurate and convenient for such cases. (See Rossini, B. S. Jour. Research, vol. 6, pp. 1, 37, 1931; vol. 7, p. 329, 1931; and vol. 8, p. 119, 1932.)

[6] See footnote 4.

[7] For purposes of computing heats of formation from heats of combustion it is further necessary to adopt standard states for hydrogen and for carbon, and it would be desirable to agree upon values for the heats of formation of water and of carbon dioxide, such international values being subject to revision when desirable, in the same manner as the atomic weight table. Discussion of these questions is, however, outside the scope of this paper. For the combustion of substances which contain elements other than carbon, hydrogen, and oxygen it is likewise necessary to adopt standard states for these elements and for their products of combustion. These cases will not, however, be discussed in the present paper, which will be confined to materials the composition of which can be expressed by the formula $C_aH_bO_c$.

VI. COMPARISON OF THE ACTUAL BOMB PROCESS WITH THAT DEFINED BY THE PROPOSED STANDARD STATES

As contrasted with the actual bomb process, the nature of which has already been discussed in detail, the analogous process defined by the proposed standard states consists solely in the reaction of unit quantity of the substance with an equivalent amount of pure oxygen gas, both under a pressure of 1 atmosphere and at the temperature t_H, to produce pure carbon dioxide gas and pure liquid water, both under a pressure of 1 atmosphere and at the same temperature t_H, the reaction taking place without the production of any external work.

This process is not experimentally realizable. The intrinsic energy change associated with this process is, however, a definite and useful thermodynamic quantity and is equal to $-\Delta U_R$, the decrease in intrinsic energy for the following reaction at t_H° C:

$$C_aH_bO_{c(s) \text{ or } (l),\ 1\ atm.} + \left(a + \frac{b-2c}{4}\right)O_{2(g),\ 1\ atm.} = aCO_{2(g),\ 1\ atm.} + \frac{b}{2}H_2O_{(l),\ 1\ atm.} \qquad (2)$$

From this quantity, the heat, Q_p, of the isobaric reaction at 1 atmosphere can be readily calculated by adding the appropriate work quantity.

The quantity, $-\Delta U_R$, of course, differs but slightly from $-\Delta U_B$, the heat of the actual bomb process, and for many purposes the difference is of no importance. Indeed, only a few years ago the two were calorimetrically indistinguishable. To-day, however, this is not always the case. The difference, while small, may be many times the uncertainty in determining the heat of the bomb process and may amount to from a few hundredths of 1 per cent up to several tenths of a per cent of this value, depending upon the particular substance and the experimental conditions of the measurement.

To obtain from the heat, $-\Delta U_B$, of the bomb process, the energy quantity, $-\Delta U_R$, for the process defined by the standard states requires the computation of certain "corrections" the nature of which we will now proceed to discuss.

VII. THE TOTAL ENERGY OF COMBUSTION DEFINED BY THE PROPOSED STANDARD STATES

Since the quantity ΔU for any process is completely defined by the initial and final states of the system, the proposed standard states do not define any particular path. In order to arrive at the value of ΔU_R we are therefore at liberty to make use of any desired imaginary process as long as it does nor violate the first law of thermodynamics. The process employed for this purpose should obviously contain the actual bomb process as one of its steps. Its other steps should be selected on the basis of the availability of the necessary data for computing the ΔU terms for these steps.

A review of the available data for various alternative processes indicates that the following process will yield trustworthy values of the ΔU terms. The process is isothermal at the temperature t_H.

Step 1.—n_{O_2} moles of oxygen at $t_H°$ and 1 atm. are compressed into the bomb which contains n g. f. w. of the substance to be burned and m_w g of liquid H_2O. The initial pressure of the oxygen in the bomb is p_1 atm. at $t_H°$.

$$\Delta U_1 = \Delta U_{O_2}\Big]_1^{p_1} + \Delta U_w + \Delta U_{D_{O_2}} + \Delta U_s \tag{3}$$

ΔU_1 represents the value of ΔU for step 1 and the terms on the right obviously have the following significance:

$\Delta U_{O_2}\Big]_1^{p_1}$ is the increase in the total energy of the oxygen which takes place when it is compressed from 1 to p_1 atm. at $t_H°$;

ΔU_w is the increase in the total energy of the water which accompanies its compression and the evaporation of the amount necessary to saturate the bomb volume, V, which is filled with oxygen at p_1 atm.

$\Delta U_{D_{O_2}}$ is the corresponding quantity for the solution of the amounts of oxygen which dissolve in the water and in the substance; and

ΔU_s is the increase in total energy which accompanies the compression of the substance and the evaporation of whatever amount evaporates before the ignition.

Step 2.—The combustion is carried out in the usual way and the quantity $-\Delta U_B$ is calculated for $t_H°$. The final pressure in the bomb is $p_2 + p_w$ atm. at $t_H°$, p_w being the partial pressure of the water vapor in the final system.

$$\Delta U_2 = n\Delta U_B \tag{4}$$

Step 3.—The aqueous solution of $CO_2 + O_2$ is separated from the gas phase and is confined under the pressure $p_2 + p_w$ atm.

$$\Delta U_3 = 0 \tag{5}$$

Step 4.—With the aid of a membrane permeable only to CO_2 the dissolved CO_2 is allowed to escape from its aqueous solution into a space at zero pressure after which it is compressed to 1 atmosphere. The value of ΔU for this process will be called ΔU_D.

$$\Delta U_4 = \Delta U_D \tag{6}$$

Step 5.—The pressure on the water is now reduced to 1 atmosphere and the dissolved oxygen is removed as a gas at 1 atmosphere. At the same time the water vapor present in the bomb at the completion of the combustion is removed in the form of pure liquid water under a pressure of 1 atmosphere.

$$\Delta U_5 = \Delta U'_{D_{O_2}} + \Delta U'_w \tag{7}$$

Step 6.—The gas phase $(O_2 + CO_2)$ in the bomb is now expanded to zero pressure

$$\Delta U_6 = \Delta U_M\Big]_{p_2}^0 \tag{8}$$

in which the subscript M is used to indicate the mixture of O_2 and CO_2.

Step 7.—The O_2 and CO_2 are now demixed at zero pressure

$$\Delta U_7 = 0 \tag{9}$$

Step 8.—The O_2 and CO_2 are each compressed to 1 atmosphere.

$$\Delta U_8 = \Delta U_{O_2}]^1_0 + \Delta U_{CO_2}]^1_0 \tag{10}$$

We started with pure substance, pure water, and pure oxygen at 1 atmosphere and $t°_H$ and we have ended with pure oxygen, pure carbon dioxide and pure water under the same conditions. Consequently ΔU_R for the reaction expressed by equation (2) is given by

$$n\Delta U_R = \Delta U_{O_2}]_1^{p_1} + \Delta U_w + \Delta U_{D_{O_2}} + \Delta U_s + n\Delta U_B + 0 + \Delta U_D + \Delta U'_{D_{O_2}}$$

$$+ \Delta U'_w + \Delta U_M]^0_{p_2} + 0 + \Delta U_{O_2}]^1_0 + \Delta U_{CO_2}]^1_0 = n\Delta U_B + \Delta U_{corr.} \tag{11}$$

and

$$\Delta U_R = \Delta U_B\left(1 + \frac{\Delta U_{corr.}}{n\Delta U_B}\right) \tag{12}$$

The percentage correction which must be applied to ΔU_B in order to obtain ΔU_R is therefore given by

$$(\text{Per cent corr.})_{\text{Total}} = \frac{100\Delta U_{corr.}}{n\Delta U_B} \tag{13}$$

The quantity $\Delta U_{corr.}$ is given by

$$\Delta U_{corr.} = \Delta U'_{corr.} + \Delta U''_{corr.} \tag{14}$$

where

$$\Delta U'_{corr.} = \Delta U_{O_2}]_1^{p_1} + \Delta U_M]^0_{p_2} + \Delta U_{O_2}]_0^1 + \Delta U_{CO_2}]_0^1 + \Delta U_D \tag{15}$$

and

$$\Delta U''_{corr.} = \Delta U_w + \Delta U'_w + \Delta U_{DO_2} + \Delta U'_{DO_2} + \Delta U_s \tag{16}$$

The quantity $\Delta U''_{corr.}$, will be found to be negligibly small in most actual combustions. We shall therefore neglect it in the first instance and return to it later.

The quantity $\Delta U'_{corr.}$ can be written

$$\Delta U'_{corr.} = \Delta U_{gas} + \Delta U_D \tag{17}$$

where

$$\Delta U_{gas} = \Delta U_{O_2}]_1^{p_1} + \Delta U_M]^0_{p_2} + \Delta U_{O_2}]_0^1 + \Delta U_{CO_2}]_0^1 \tag{18}$$

We shall therefore continue our discussion under the following topics:

1. Definitions of some auxiliary quantities.
2. The energy content of the dissolved CO_2. This will give us the quantity ΔU_D.
3. The energy content of the gases. This will give us the quantity ΔU_{gas}.
4. The negligible energy quantities. This will deal with the quantity $\Delta U''_{corr.}$

VIII. DEFINITIONS OF SOME AUXILIARY QUANTITIES

1. THE INITIAL SYSTEM

Given a bomb of volume V liters in which are placed n_{O_2} moles of oxygen and n g. f. w. of the substance or mixture having the composition expressed by the formula $C_aH_bO_c$ and whose heat of combustion in the bomb is $-\Delta U_B$ energy units per g. f. w. There are also placed in the bomb m_w grams of water, a quantity sufficient to saturate the oxygen.

The gram-formula-weight (g. f. w.) of the substance is evidently

$$12a+1.0078b+16c \tag{19}$$

The number of moles of oxygen required for the combustion is

$$n_r=\left(a+\frac{b-2c}{4}\right)n+\phi \tag{20}$$

where ϕ is the oxygen consumed in producing nongaseous products other than CO_2 and H_2O; for example, HNO_3, Fe_2O_3, etc. The initial oxygen pressure in the bomb will be

$$p_1=\frac{n_{O_2}RT(1-\mu_{O_2}p_1)}{V} \tag{21}$$

in which $\mu_{O_2}p_1$ is a small correction term calculable from the equation of state. At 20° C.

$$\mu_{O_2}=0.0_3732-0.0_5225_6p \tag{22}$$

For O_2 pressures between 20 and 40 atmospheres (the range ordinarily met with in bomb calorimetry) this relation may be replaced by the following approximate but sufficiently exact equation:

$$\mu_{O_2}=0.0_3664 \tag{23}$$

2. THE FINAL SYSTEM

After the combustion, the bomb will contain $(n_{O_2}-n_r)$ moles of O_2, n_{CO_2} $(=an)$ moles of CO_2, and $(\frac{1}{2}bn+\frac{1}{18}m_w)$ moles of water. Part of the water will be in the gaseous state and part of the O_2 and CO_2 in the dissolved state in the liquid water. As explained in steps 3 and 5 of the preceding section, all of the water and the dissolved CO_2 are removed from the bomb leaving a gas phase which contains

$$n_M=n_{O_2}-n_r+n_{CO_2}-n_D \tag{24}$$

moles of gas, where n_D is the number of moles of dissolved CO_2 removed with the liquid water. The dissolved O_2 may be neglected in equation (24).

$$n_M=n_{O_2}-\left(\frac{b-2c}{4}\right)n-n_D-\phi \tag{25}$$

The mole fraction of the CO_2 in the gas phase will be

$$x=\frac{an-n_D}{n_{O_2}-\left(\frac{b-2c}{4}\right)n-n_D-\phi} \tag{26}$$

The pressure of the mixture will be

$$p_2 = \frac{n_M RT(1-\mu_M p_2)}{V} \tag{27}$$

At 20° C., μ_M is given by the equation [8]

$$\mu_M/\mu_{O_2} = 1 + 3.21x(1+1.33x) \tag{28}$$

IX. CORRECTION FOR DISSOLVED CARBON DIOXIDE

After the combustion, the bomb contains $m_w + 9bn$ g of water. Of this, the amount (see Appendix I, equation (119), p. 556).

$$VC_w = 0.0173V + (0.0_455 + 0.0_328x)p_2V, \text{ g} \tag{29}$$

is in the vapor state at 20° C. Since this will in general be only about 1 per cent of the total, we may substitute the average values $p_2 = 30$ atm., and $x = 0.15$, and the above equation may, with sufficient accuracy for our present purposes, be written

$$VC_w = V[0.0173 + (0.0_455 + 0.0_328 \times 0.15)30] = 0.02V, \text{ g} \tag{30}$$

and the amount of liquid water will be

$$m_w + 9bn - 0.02V, \text{ g} \tag{31}$$

This amount of liquid water will be saturated with CO_2 at the partial pressure p_2x.

For the range of p_2x values encountered in bomb calorimetry (1 to 8 atmospheres) it will be sufficiently accurate, for the purpose of correcting for dissolved CO_2, to assume that the solubility is proportional to the partial pressure, using a proportionality constant computed from the solubility of CO_2 at about 7 atmospheres. (See fig. 1.) With this assumption the number, S_{CO_2}, of moles of dissolved CO_2 per cm³ of liquid water will be

$$S_{CO_2} = 0.0_3038_2 p_2 x, \ M/\text{cm}^3 \text{ at } 20° \text{ C.} \tag{32}$$

The total number, n_D, of moles of dissolved CO_2 will therefore be

$$n_D = 0.0_3038_2 p_2 x(m_w + 9bn - 0.02V) \tag{33}$$

Now the total energy of vaporization of CO_2 from its aqueous solution at 20° C. to produce pure CO_2 gas at 1 atmosphere is 181 liter-atm. per mole.[9] For the n_D moles of dissolved CO_2 we have, therefore,

$$\Delta U_D = 181 \times n_D, \text{ liter-atm.} \tag{34}$$

Since, as will appear later, this term is a small part of the total correction, we may write with sufficient accuracy

$$p_2x = anRT(1-\mu_M p_2)/V \tag{35}$$

From equations (23) and (28) we have for $x = 0.15$, $\mu_M = 10^{-3}$. Hence for 20° C. and $p_2 = 30$ atm.

$$p_2x = an \times 24.05(1 - 10^{-3} \times 30)/V \tag{36}$$

---

[8] From unpublished measurements in this laboratory by the method described by Washburn, B. S. Jour. Research, vol. 9, p. 271, 1932.

[9] Computed from the temperature coefficient of the solubility of CO_2 in water.

and equation (33) becomes

$$n_D = 0.0_3 9\ an(m_w + 9bn - 0.02V)/V \tag{37}$$

or putting $m_w = 1$ g, $9bn = 0.55$ g, and $V = 1/3$ liter

$$n_D = \text{(approx.)},\ 0.0_3 9an(1 + 0.55 - 0)/0.33 \tag{38}$$
$$= 0.004an\ \text{(approx.)} \tag{39}$$

for average calorimetric conditions.

The discussion of this correction is continued on page 541.

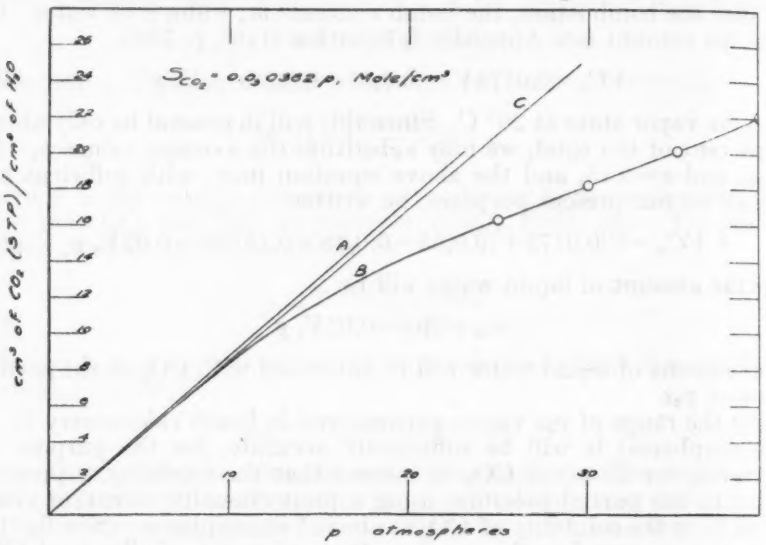

FIGURE 1.—*Solubility of CO_2 in H_2O as a function of the pressure at 20° C.*

The points indicated are taken from International Critical Tables, vol. 3, p. 260. The line *A* is determined by the values at 0 and 1 atmosphere. The locus of the curve *B* is estimated. The line *C* is drawn so as to pass through 0 and the point for 7 atmospheres on the curve *B*. The equation of this line is that shown.

X. THE ENERGY CONTENT OF THE GASES AS A FUNCTION OF THE PRESSURE

Direct calorimetric measurements of $\Delta U]^p_1$ for oxygen and for mixtures of oxygen with carbon dioxide have been made by Rossini and Frandsen.[10] Their results reduced to 20° C. give

$$-\Delta U_{O_2}]^p_0 = 0.0663p, \text{ liter-atm./mole at } 20° \text{ C.} \tag{40}$$

and

$$-\Delta U_M]^p_0 = 0.0663(1+h)p = 0.0663[1 + 1.70x(1+x)]p, \text{ liter-atm./mole at } 20° \text{ C.} \tag{41}$$

Both relations are valid for pressures up to 45 atmospheres and for values of x up to 0.4.

For CO_2 between 0 and 1 atmosphere, we shall employ the relation

$$-\Delta U_{CO_2}]^p_0 = 0.287p, \text{ liter-atm./mole at } 20° \text{ C.} \tag{42}$$

which is derived from the Beattie-Bridgeman equation of state.[11]

[10] Rossini, F. D., and Frandsen, M., B. S. Jour. Research, vol. 9, p. 745, 1932.

[11] See Washburn, B. S. Jour. Research, vol. 9, p. 522, 1932. It is of interest tonote that equation (41) above, when extrapolated to $x = 1$ gives $-\Delta U_{CO_2}]^p_0 = 0.291p$.

XI. CORRECTION FOR THE CHANGE IN ENERGY CONTENT OF THE GASES

We are now in a position to evaluate the quantity ΔU_{gas} as given by equation (18) above, using the number of moles of gas involved. Performing the summation indicated by that equation between 1 and p atmosphere gives us

$$-\Delta U_{gas} = n_{O_2} \times 0.0663(p_1 - 1) + n_M \times 0.0663(1+h)(0-p_2) + n_{CO_2} \times 0.287(1-0) + (n_{O_2} - n_r)0.0663(1-0), \text{ liter-atm.} \quad (43)$$

This may also be written

$$-\Delta U_{gas} = 0.0663 n_{CO_2}\left[\frac{n_{O_2}}{n_{CO_2}} p_1 - \frac{n_{O_2}}{n_{CO_2}} - (n_M/n_{CO_2})(1+h)p_2 + \frac{0.287}{0.0663} + (n_{O_2} - n_r)/n_{CO_2}\right] \quad (44)$$

or putting $x = n_{CO_2}/n_M = n_{CO_2}/(n_{O_2} - n_r + n_{CO_2})$,

$$-\Delta U_{gas} = 0.0663 n_{CO_2}\left[p_1 \frac{(1-x)}{x} - \frac{(1+h)p_2}{x} + 4.33 + \frac{n_r}{n_{CO_2}}(p_1 - 1)\right] \quad (45)$$

If we now introduce the relations

$$n_r = \left(a + \frac{b-2c}{4}\right) n + \phi$$

and

$$n_{CO_2} = an - n_D = 0.996an, \text{ approx.} \quad \text{(See equation (39).)}$$

we have

$$n_r/n_{CO_2} = 1.004\left[1 + \frac{b-2c}{4a} + \phi/an\right] \text{approx.} \quad (46)$$

and

$$-\Delta U_{gas} = 0.0660an\left[p_1 \frac{(1-x)}{x} - \frac{(1+h)\,p_2}{x} + 4.33 + 1.004p_1\left(1 + \frac{b-2c}{4a} + \phi/an\right) - 1.004\left(1 + \frac{b-2c}{4a} + \phi/an\right)\right] \quad (47)$$

$$-\Delta U_{gas} = 0.0660an\left[\frac{p_1 - p_2}{x} - p_1 - \frac{hp_2}{x} + 3.33 + 1.004p_1 + 1.004p_1\left(\left(\frac{b-2c}{4a}\right) + \phi/an\right) - 1.004\left(\frac{b-2c}{4a} + \phi/an\right)\right] \quad (48)$$

$$-\Delta U_{gas} = 0.0660an\left[\frac{p_1 - p_2}{x} - \frac{hp_2}{x} + 0.004p_1 + \frac{1.004\,(p_1-1)\,(b-2c+4\phi/n)}{4a} + 3.33\right] \quad (49)$$

and

$$(\text{Per cent corr.})_{gas} = \frac{100\Delta U_{gas}}{n\Delta U_B} = \frac{6.60a}{-\Delta U_B}[(p_1 - p_2)/x + 0.004p_1 - p_2h/x + 1.004\,(p_1-1)\,((b-2c)/4a + \phi/an) + 3.33] \quad (50)$$

Since one unit in the first decimal place of the terms within the brackets corresponds to less than 0.001 per cent of ΔU_B and since $p_1 \not> 45$ atmospheres, it will be sufficiently accurate for all purposes to write

$$(\text{Per cent corr.})_{\text{gas}} = \frac{6.60a}{-\Delta U_B}\left[-\Delta p\left(\frac{1}{x}+\frac{h}{x}\right)-p_1 h/x+ (p_1-1)\left((b-2c)/4a+\phi/an\right)+3.47\right] \quad (51)$$

which is valid for p_1 and Δp, $(=p_2-p_1)$, in atmospheres and ΔU_B in liter-atmosphere/mole.

XII. CALCULATION OF THE CHANGE IN PRESSURE RESULTING FROM THE COMBUSTION

For computing small pressure changes in the neighborhood of any pressure between 25 and 45 atmospheres, at room temperatures, the pressure of a gas can be taken as given by the relation

$$p = nRT(1-\mu p)/V \quad (52)$$

in which μ is a constant characteristic of the gas, and the temperature. The drop in pressure following the combustion will therefore be

$$-\Delta p = p_1 - p_2 = p_1 - \frac{n_M RT}{V}(1-\mu_M p_2) \quad (53)$$

If we put (see equation (25))

$$n_M = n_{O_2} - \frac{(b-2c)n}{4} - n_D - \phi = (an - n_D - \phi)/x = an/x \text{ (Approx.)} \quad (54)$$

and

$$n_{O_2} = p_1 V/RT(1-\mu_{O_2} p_1) \quad (55)$$

this becomes

$$-\Delta p = p_1^2\left[\frac{\mu_M - \mu_{O_2} + \mu_M \Delta p/p_1}{1-\mu_{O_2} p_1} + \frac{(1+\Delta p/p_1)x}{p_1}\left(\frac{b-2c}{4a}+\frac{n_D+\phi}{an}\right)\right] \quad (56)$$

and

$$-\Delta p = \frac{p_1\left[p_1(\mu_M/\mu_{O_2}-1)\mu_{O_2} + (1-\mu_{O_2} p_1)x\left(\frac{b-2c}{4a}+\frac{n_D+\phi}{an}\right)\right]}{1+p_1(\mu_M/\mu_{O_2}-1)\mu_{O_2} + (1-\mu_{O_2} p_1)x\left(\frac{b-2c}{4a}+\frac{n_D+\phi}{an}\right)} \quad (57)$$

At 20° C.,

$$\mu_M/\mu_{O_2} - 1 = 3.21x(1+1.33x) \quad \text{(see equation (28).)}$$

$$\mu_{O_2} = 6.64 \times 10^{-4} \quad \text{(see equation (23).)}$$

and the above equation becomes

$$-\frac{\Delta p}{p_1}=\frac{x}{1+x}\left[\frac{10^{-3}p_1 3.21\,(1+1.33x)\times 0.664 + (1-6.64\times 10^{-4}p_1)\left(\frac{b-2c}{4a}+\frac{n_D+\phi}{an}\right)}{10^{-3}p_1 3.21\,(1+1.33x)\times 0.664 + (1-6.64\times 10^{-4}p_1)\left(\frac{b-2c}{4a}+\frac{n_D+\phi}{an}\right)}\right] \tag{58}$$

or

$$\frac{-\Delta p}{p_1}=\frac{\pi}{1+\pi} \tag{59}$$

For $\frac{n_D}{an}$ we have (see equation (37)), for 20° C.

$$\frac{n_D}{an}=0.0_39\,\frac{(m_w+9bn-0.02V)}{V} \tag{60}$$

This gives

$$\pi=x\left[10^{-3}p_1 2.07(1+1.33x)+(1-6.64\times 10^{-4}p_1)\left\{\frac{b-2c}{4a}+\phi/an + 0.0_39(m_w+9bn-0.02V)/V\right\}\right] \tag{61}$$

If $\phi=0$, the second term in the expression for π is positive except when $2c>b$. π and hence also Δp may therefore be either positive or negative according to circumstances.

The term containing $(m_w+9bn-0.02V)/V$ is usually very small, almost negligible in fact. For $V=\frac{1}{3}$ liter, and $m_w=1$g, it ordinarily lies within the range $(42\pm 7)\times 10^{-4}$, and in many cases it will suffice to assume this value for it. In certain particular cases, however, this term is the principal one in the expression for π.

Thus for the case [12] $x=0.149$, $p_1=22$ atm., $\phi=0$, and $\frac{b-2c}{4a}=-1/18$, we have

$$\pi=x[0+0.0_39(m_w+9bn-0.02V)/V]$$

$$=0.149\times(42\pm 7)\times 10^{-4}=0.0_363\pm 0.0_31 \tag{62}$$

and

$$-\Delta p/p_1=\pi/(1+\pi)=0.0_363\pm 0.0_31 \tag{63}$$

This is negligibly small. In fact any value of $\frac{\Delta p}{p_1}$ within the limits ± 0.001, may be taken as zero.

For most cases an approximate form of equiation (61) will be sufficiently exact. This can be obtained by substituting the average values 0.15 for x and 42×10^{-4} for the last term, giving

$$\pi=x\left[2.07\times 10^{-3}p_1(1+1.33\times 0.15)+\frac{b-2c}{4a}+\phi/an+42\times 10^{-4}\right]$$

$$\pi=x\left[2.5\times 10^{-3}p_1+\frac{b-2c}{4a}+\phi/an+42\times 10^{-4}\right] \tag{64}$$

[12] For example, myristicinic acid, $C_9H_8O_3$, or dimethoxydihydroxybenzoic acid, $C_9H_{10}O_4$.

XIII. THE NEGLIGIBLE ENERGY QUANTITIES

1. THE ENERGY CONTENT OF THE WATER

(a) THE CHANGE IN THE ENERGY CONTENT OF THE WATER VAPOR

As a result of the bomb reaction the amount of water present as vapor in the final system at $t_H°$ is greater than that present in the initial system at this temperature. The increase, ΔC_w, in the concentration of water vapor for $t_H = 20°$ C., is given by the equation (see equation (122), Appendix I)

$$\Delta C_w = p_2 x\left[0.0_3 34 - 0.0_3 05_5\left(1 - \frac{\Delta p}{p_2 x}\right)\right], \text{ g/liter} \tag{65}$$

This increase is accompanied by the absorption of $V\Delta C_w \times 22.82$ liter-atm. of heat energy, 22.82 liter-atm. being the total energy of vaporization of 1 g of H_2O. We have, therefore,

$$\Delta U_w^{\text{vap.}} = 22.82 V p_2 x\left[0.0_3 34 - 0.0_3 05_5\left(1 - \frac{\Delta p}{p_2 x}\right)\right], \text{ liter-atm.} \tag{66}$$

An extreme case would be the following: $V = \frac{1}{2}$ liter, $p_2 = 45$ atm., $x = 0.3$ and $-\Delta p = 2$ atm., and this would give

$$\Delta U_w^{\text{vap.}} = 0.043 \text{ liter-atm.} = 1.0_4 \text{ cal.} \tag{67}$$

This will rarely amount to more than 0.01 per cent of the heat of the bomb process and will usually be negligible. Since it is opposite in sign to that arising from the quantity ΔU_D, for the dissolved CO_2, a partial compensation will occur and the expressions for the two corrections may advantageously be combined into a single expression representing the algebraic sum of the two effects. This will be done in section 2, below.

(b) THE CHANGE IN THE ENERGY CONTENT OF THE LIQUID WATER

The increase, ΔU_w^{liq}, in the total energy content of liquid water as a function of the pressure upon it is displayed in graphic form by Bridgeman.[13] At 20° C.and for the pressure range encountered in bomb calorimetry this increase is expressed with sufficient accuracy by the equation:

$$\Delta U_w^{\text{liq.}} = -54 \times 10^{-6} P, \text{ liter-atm./g} \tag{68}$$

In the process defined by the proposed standard states, m_w grams of liquid water are compressed from 1 atmosphere to $(p_1 + p_w)$ atmosphere and $(m_w + 9bn)$ grams are decompressed from $(p_2 + p_w)$ to 1 atmosphere.

Since we are dealing with a very small energy quantity, we will write $p_1 + p_w = p_2 + p_w = \frac{1}{2}(p_1 + p_2 + 2p_w) = P$ and the net change in the energy content of the liquid water becomes

$$-\Delta U_w^{\text{liq.}} = 9bn \times 54 \times 10^{-6} P, \text{ liter-atm.} \tag{69}$$

An extreme case would berep resented by $9bn = 2$g and $P = 45$ atmospheres for which case

$$-\Delta U_w^{\text{liq.}} = 0.005 \text{ liter-atm.} = 0.1 \text{ cal.} \tag{70}$$

[13] Bridgeman, P. W., Proc. Am. Acad., vol. 48, p. 348, 1912.

a wholly negligible quantity. Hence for all practical purposes the quantity $\Delta U_w + \Delta U'_w$ is equal to $\Delta U_w^{\text{vap.}}$ as given by equation (66) above.

2. COMBINED ENERGY CORRECTIONS FOR WATER VAPOR AND FOR DISSOLVED CARBON DIOXIDE

The correction for dissolved CO_2 is (see equations (33) and (34))

$$-\Delta U_D = -181 \times 0.0_3038_2 p_2 x (m_w + 9bn - 0.02V), \text{ liter-atm.} \quad (71)$$

and that for the excess water vapor in the final system is (equation (66))

$$-\Delta U_w^{\text{vap.}} = 22.82\ Vp_2x \left[0.0_334 - 0.0_305_5 \left(1 - \frac{\Delta p}{p_2 x}\right)\right], \text{ liter-atm.} \quad (72)$$

For p_2x we have at 20° C. (see equation (36))

$$p_2 x = 23._3 an/V, \text{ approx.} \quad (73)$$

The sum of equations (71) and (72) combined with (73) and divided by $-0.01n\ \Delta U_B$ will give us the net correction in per cent arising from the two effects in question. We thus obtain the following relation:

$$\text{Per cent corr. } (\Delta U_D + \Delta U_w + \Delta U'_w) = \frac{23._3 a}{0.01 \Delta U_B}\left[-0.0066 + 0.0069\frac{(m_w + 9bn)}{V} - 0.0012_5 \frac{V\Delta p}{23._3 an}\right] =$$

$$\frac{-16.1}{-\Delta U_B/a}\left[-0.96 + \frac{m_w + 9bn}{V} - \frac{0.007_8 V \Delta p}{an}\right] \quad (74)$$

The quantity $-\Delta U_B/a$, the heat of combustion per gram-atom of carbon, will have its minimum value in the case of oxalic acid, say 1,200 liter-atm., and its maximum value for hydrocarbons, say 7,500 liter-atm. The net correction given by equation (74) will therefore vary in practice (for $V = 1/3$ liter and $m_w = 1$ g) only between about -0.06 and -0.008 per cent. In the majority of cases it will be found to lie between -0.01 and -0.03 per cent.

3. THE ENERGY CONTENT OF THE DISSOLVED OXYGEN

At 20° C. the solubility of O_2 in water is approximately [14]

$$S_{O_2} = 1.2 \times 10^{-6} p_{O_2}, \text{ mole/cm}^3 \quad (75)$$

The amount of O_2 dissolved in the initial water will therefore be

$$n_{DO_2} = 1.2 \times 10^{-6} m_w p_1, \text{ moles} \quad (76)$$

and that in solution in the final water will be

$$n'_{DO_2} = 1.2 \times 10^{-6} (m_w + 9bn) p_2 (1 - x) \quad (77)$$

[14] Int. Crit. Tables, vol. 3, p. 257 and Frolich, Tauch, Hogan and Peer, Ind. Eng. Chem., vol. 23, p. 549, 1931.

The total energy of vaporization of O_2 from its aqueous solutions at 20° C. to produce O_2 gas at 1 atmosphere is 115 liter-atm./mole. Consequently, if we neglect the oxygen dissolved or adsorbed by the substance,

$$\Delta U_{O_2} + \Delta U'_{O_2} = 115\ (n'_{O_2} - n_{O_2}),\ \text{liter-atm.} \tag{78}$$

An extreme case would be represented by the following:

$$m_w = 1,\ 9bn = 2,\ p_1 = 45\ \text{atm.},\ p_2\,(1-x) = 30\ \text{atm.}$$

For this case

$$n_{O_2} \text{ is } 55 \times 10^{-6},\ n'_{O_2} \text{ is } 110 \times 10^{-6}$$

and

$$\Delta U_{O_2} + \Delta U'_{O_2} \text{ is } 0.0061 \text{ liter-atm.} = 0.15 \text{ cal.}$$

a negligible quantity. Moreover, this correction is opposite in sign to that arising from the quantity $\Delta U_w^{liq.}$ (equation (69)) and roughly of the same order of magnitude. The two corrections, in addition to being each negligibly small, will therefore substantially cancel each other.

4. THE ENERGY CONTENT OF THE SUBSTANCE

The energy quantity ΔU_s consists of the energy of compression of the substance from 1 to p_1 atmosphere plus the energy of vaporization of whatever amount evaporates before ignition. We shall discuss the two effects separately.

(a) THE ENERGY OF COMPRESSION OF THE SUBSTANCE

By integrating the thermodynamic relation

$$-\left(\frac{\partial U}{\partial p}\right)_T = p\left(\frac{\partial v}{\partial p}\right)_T + T\left(\frac{\partial v}{\partial T}\right)_p \tag{79}$$

between 0 and p atmosphere at any temperature T and reducing the quadratic to the linear equation passing through the value for $p = 30$ atmospheres the following sufficiently exact relation is obtained

$$-\Delta U]_0^p = \alpha p,\ \text{liter-atm./g} \tag{80}$$

in which α is a constant characteristic of the substance and the temperature. In deriving the numerical value for α, the term in the integral which arises from the compressibility $\left(\frac{\partial v}{\partial p}\right)_T$, may be neglected without introducing a significant error for the pressures used in bomb calorimetry.

Table 1 displays the values of α and of $-\Delta U$ for compression to 45 atmospheres, for a number of substances. The last column of the table shows the energy of compression expressed as per cent of the heat of combustion. In all the cases shown the energy of compression is negligible in comparison with the present accuracy with which $-\Delta U_B$ is known.

TABLE 1.—*Energy of isothermal compression*

$-\Delta U]_0^P = \alpha P$, liter-atm./g

[Data taken from International Critical Tables. M=molecular weight]

Substance	t	$10^6\,\alpha$	$-\Delta U]_0^{45} = 45\alpha$	$-\Delta U_B/M$	Per cent corr. $\frac{M\Delta U}{-0.01\Delta U_B}$
	° C.	liter/g	liter-atm./g	liter-atm./g	
H_2O	20	59	2.6×10^{-3}		
n-Heptane	20	540	24×10^{-3}	475	0.005
n-Heptadecane	25	325	15×10^{-3}	467	.003
Naphthalene	25	82	3.7×10^{-3}	403	.001
Methanol	20	420	19×10^{-3}	220	.009
Acetone	25	417	19×10^{-3}	304	.006
Formic acid	25	248	11×10^{-3}	56.4	.02
Acetic acid	20	305	14×10^{-3}	142	.01
n-Capric acid	25	270	12×10^{-3}	348	.003
Oxalic acid	20	127	5.7×10^{-3}	27.6	.02
Benzoic acid [1]	20	121	5.4×10^{-3}	260	.002

[1] Thermal expansion determined by E. R. Smith (B. S. Jour. Research, vol. 7, p. 903, 1931).

(b) THE ENERGY OF VAPORIZATION OF THE SUBSTANCE

The energy of vaporization of the substance must either be made negligibly small, by suitable inclosure of the sample when necessary, or must be computed and corrected for. A safe rule to follow is to inclose every substance whose vapor pressure is more than 1 mm Hg. If it is not so inclosed, the investigator must show that the energy of vaporization is negligible or he must make the necessary correction.[15]

XIV. THE TOTAL CORRECTION FOR REDUCTION TO THE STANDARD STATES

1. GENERAL CORRECTION EQUATION

By adding together equations (74) and (51) and converting to cal. units, we obtain equation (13) in the form

$$(\text{Per cent corr.})_{\text{Tot.}} = \frac{0.160\,p_1}{-\Delta U_B/\text{a}}\left[\frac{-\Delta p}{p_1}\left(\frac{1}{x}+\frac{h}{x}\right)-h/x+(1-1/p_1)\left(\frac{\text{b}-2\text{c}}{4\text{a}}+\phi/\text{a}n\right)-2.4_4(m_w+9\text{b}n)/p_1V+5.8/p_1+\frac{0.019V\Delta p/p_1}{\text{a}n}\right] \quad (81)$$

in which V is the volume of the bomb in liters; p_1 is the initial O_2 pressure at 20° C., p_2 is the final pressure in the bomb at 20° C., both in atmospheres; $\Delta p = p_2 - p_1$; x is the mole fraction of CO_2 in the final system; $h = 1.70x(1+x)$; n is the number of gram-formula-weights of the material, $C_aH_bO_c$, burned; m_w is the mass of H_2O initially placed in the bomb; ϕ is the number of moles of O_2 consumed by auxiliary reactions; and $-\Delta U_B$ is the evolved heat of the bomb process in kg-cal.[15] per gram-formula-weight.

By evaluating this relation for a given combustion we obtain the total correction in per cent which must be applied to the value of $-\Delta U_B$, in order to obtain $-\Delta U_R$, the decrease in intrinsic energy for the chemical reaction, for the standard conditions at 20° C., (equation (2)).

[15] See footnote 5, p. 530.

Because of the small magnitude of this correction and the small temperature coefficient of ΔU_B, the value of ΔU_B used in equation (81) may be the value for any room temperature and the correction given by the equation may for the same reasons be directly applied to the value of ΔU_B at any room temperature, except possibly in certain extreme cases.

In deriving this relation we have neglected ΔU_s, the energy of compression of the substance plus the energy content of its vapor. This energy quantity is at present negligible and is in any case specific for each substance and is not therefore included in equation (81). It may, however, become significant for some substances, if the accuracy of the determination of $-\Delta U_B$ is increased. (See Table 1.)

If the sample is inclosed in a sealed glass capsule which it does not fill, the quantity ΔU_s becomes zero but in its place we would have the probably negligible energy of compression of the capsule.

We have also neglected the heat of adsorption of water by the sample. When the perfectly dry weighed sample is placed in the bomb and the latter closed, the sample is in contact with saturated water vapor. It immediately proceeds to adsorb water and to evolve or absorb heat. The amount of water adsorbed depends upon the nature of the sample, the surface exposed and the time of contact with the water vapor. Presumably the amount thus adsorbed has become substantially constant by the time the calorimeter fore period has been determined. The charge is now ignited and the adsorbed water appears as liquid water in the final system. The observed heat of combustion will therefore be less than the true value by the amount of heat required to convert this adsorbed water into liquid water. Since the correction here involved is specific for the substance burned and varies with the surface exposed and the conditions of the experiment, it can not be provided for in equation (81). For hygroscopic substances it might be very appreciable and difficult to determine and correct for. Such substances should therefore be inclosed in a suitable capsule.

2. AN APPROXIMATE CORRECTION EQUATION

The calculation of the total correction by means of equation (81) is somewhat time consuming and it is desirable for many purposes to have available a simpler equation for rapid calculation. Such an equation can be obtained, with some loss of accuracy and generality, by introducing certain approximations into equation (81) and taking advantage of certain fortuitous compensations for typical calorimetric conditions. In this way the following approximate equation may be obtained, for p_1 in atmosphere, for $-\Delta U_B$ in kg-cal.$_{15}$ per g. f. w., for a bomb volume of ⅓ liter, for $\phi = 0$, and for $m_w = 1$ g.

$$(\text{Per cent corr.})_{\text{Total}} = \frac{0.30 p_1}{-\Delta U_B/a}\left[-1 + 1.1\frac{b-2c}{4a} - \frac{2}{p_1}\right] \text{approx.} \qquad (82)$$

This approximate equation will in general give a value for the $(\text{per cent corr.})_{\text{Total}}$ which is accurate within 15 per cent of itself, a degree of accuracy which is sufficient for correcting most of the now-existing data of bomb calorimetry.

XV. THE MAGNITUDE OF THE CORRECTION IN RELATION TO THE TYPE OF SUBSTANCE BURNED

It will be noted that of the terms in the parenthesis of equation (82), only the second depends upon the nature of the substance burned. The extreme values possible for this term are: (1), 1.1×0.5 for all hydrocarbons and mixtures of hydrocarbons whose net composition is approximately expressed by the empirical formula C_aH_{2a}; and (2), 1.1 (−0.75) for oxalic acid; with the value zero for all carbohydrates, carbon itself, and certain aldehydes.

The magnitude of the correction for these three types of substances is illustrated in Table 2 for three different values of the initial O_2-pressure.

TABLE 2.—*Illustrating the magnitude of the correction for reducing the data of bomb calorimetry to the proposed standard states*

$$\text{Per cent corr.}_{\text{Approx.}} = \frac{0.30p_1}{(-\Delta U_B)/a}\left[-1+1.1\frac{b-2c}{4a}-\frac{2}{p_1}\right]$$

Type of substance	$\frac{b-2c}{4a}$	$\frac{(-\Delta U_B)}{a}$	Per cent correction for		
			$p_1=20$	$p_1=30$	$p_1=40$ atm.
		kg-cal.$_{18}$			
Hydrocarbons of the types $CaH_{2a\pm\gg2}$	0.5	150	−0.02$_2$	−0.03$_1$	−0.04$_0$
Carbohydrates, certain aldehydes, etc	.0	110	− .06$_9$	− .08$_7$	− .11$_4$
Oxalic acid	−.75	30	− .3$_3$	− .5$_8$	− .7$_5$

XVI. COMPUTATION OF THE CORRECTION

1. GENERAL REMARKS

In computing the correction for reduction to the standard states, it is necessary to reduce each experimental value separately; that is, before averaging, unless the experimental conditions (values of p_1, m, and m_w) are substantially the same for all experiments. By making these conditions the same (see Table 5), the values of $-\Delta U_B$ may be averaged first and the correction applied to the average, thus greatly reducing the amount of computation required.

Before averaging, each observed value of $-\Delta U_B$ must first be corrected to the same temperature, t_H. The method of making this correction is discussed below. (See Sec. XVIII.)

A convenient computation form is illustrated by the chart of Table 3. The first horizontal section of the chart provides for the entry of the necessary numerical values of the initial conditions. The second section provides similarly for the final conditions. The third section contains the steps in the calculation and the final result to which they lead.

In case the sample is a pure substance, the coefficients a, b, and c in the empirical formula, $C_aH_bO_c$, will be known. If the sample is a mixture, the exact composition of which is unknown, this composition must first be determined. This may be accomplished in all cases by making a combustion analysis, from the results of which an empirical formula for the mixture can be computed. If, as is frequently the case, the mixture is made up of known amounts of two constituents, of known compositions, then the composition of the mixture and its empirical formula are calculable. (See Appendix II.)

TABLE 3.—*Illustrating the computation of the correction for reduction to the standard states*

$$(\text{Per cent corr.}) = \frac{0.160 p_1}{-\Delta U_B/a}\left[\frac{-\Delta p}{p_1}\left(\frac{1}{x}+\frac{h}{x}\right) - \frac{h}{x} + (1-1/p_1)\left(\frac{b-2c}{4a}+\frac{\phi}{an}\right) - 2.44\,(m_w+9bn)/p_1V + 5.8/p_1 + 0.019\,V(\Delta p/p_1)/an\right]$$

1	2	3	4	R. D. and B.	J. and S.	D.	F. and W.	Oxalic acid+kerosene		Kerosene
				5	6	7	8	9	10	11
Initial conditions	1	Substance or material $=C_aH_bO_c$		$C_7H_6O_2$	$C_7H_6O_2$	$C_7H_6O_2$	$C_7H_6O_2$	$CH_{1.624}O_{0.0884}$	$CH_{1.370}O_{1.326}$	$CH_{2.19}$
	2	M=g. f. w.=12a+1.0078b+16c	gram	122.05	122.05	122.05	122.05	27.47	34.59	14.14
	3	m=mass of sample	do	.81±.08	.88	1.51	.9	1.3632	2.287	.45
	4	$n=m/M$		.0066	.0072	.0124	.0074	.0496	.0661	.0318
	5	V=volume of bomb	liter	.3	.280	.275	.275	⅓	⅓	⅓
	6	$-\Delta U_B$=heat of combustion per g. f. w	kg-cal$_{18}$/g. f. w	772	772	772	772	101.8	75.0	156.5
	7	m_w=mass of initial H_2O	g	1	1	1	1	1	1	1
	8	p_T=initial pressure of O_2 at (T°K.=t°C)	Atmosphere	35 (20° C.)	45.5 (20° C.)	30 (20° C.)	45 (20° C.)	35 (20° C.)	35 (20° C.)	35 (20° C.)
	9	$n_{o_2}=p_TV/RT[1+(890-11.3t)10^{-6}p_T]$		.4463	.545	.350	.530	.496	.496	.496
	10	$p_1=n_{o_2}\times 24.05[1-664\times10^{-6}p_1/V$	Atmosphere	35	45.5	30	45	35	35	35
Final conditions	11	an		0.0462	0.0504	0.0868	0.518	0.0496	0.0661	0.0318
	12	$(b-2c)n/4$		.0033	.0036	.0062	.0037	−.00129	−.0212	+.0169
	13	$n_D=0.0390an(m_w+9bn-0.02V)/V$=approx. $0.004an$.	Equation (37)	.00405an	.00444an	.00545an	.00293an	.00464an	.00488an	.00432an
	14	$x=(an-n_D)/[n_{o_2}-(b-2c)n/4-n_D-\phi/an]$	Equation (26)	.1039	.0926	.2513	.0981	.0992	.1274	.0660
	15	$\pi=x[2.5\times10^{-3}p_1+(b-2c)/4a+\phi/an+0.004_2]$	Equation (64)	.01697	.01755	.03782	.01846	.00652	−.02917	.0410
	16	$-\Delta p/p_1=\pi/(1+\pi)$	Equation (59)	.01668	.01724	.03648	.01812	.00648	−.03005	.0394
	17	$-h/x=-1.70(1+x)$	Equation (41)	−1.876	−1.857	−2.129	−1.866	−1.868	−1.917	−1.811
	17a	ϕ/an	Equation (88+89)	Assumed to be negligible						
Computation	18	$(-\Delta p/p_1)(1/x+h/x)$		0.1915	0.2182	0.223	0.2184	0.0774	−0.2930	0.6690
	19	$(1-1/p_1)[(b-2c)/4a+\phi/an]$		.0694	.0698	.0690	.0698	−.0253	−.3113	+.515
	20	$-2.44(m_w+9bn)/p_1V$		−.315	−.266	−.494	−.1824	−.361	−.379	−.336
	21	$5.8/p_1$		.166	.127	.193	.129	.166	.166	.166
	22	$0.019\,V(\Delta p/p_1)/an$		−.0021	−.0018	−.0022	−.0018	−.0008	+.0029	−.0079
	23	Σ Items (17+18+19+20+21+22)		−1.765	−1.710	−2.140	−1.627	−2.012	−2.731	−.805
	24	$0.160p_1/(-\Delta U_B/a)$		.0508	.0660	.0435	.0653	.0550	.0747	.0357
	25	Per cent corr.=item 23×item 24	Per cent	−.0898	−.113	−.093	−.106	−.111	−.204	−.0286
	26	Per cent corr. by approx. equation (equation (82))	do	−.09$_3$	−.11$_9$	−.080$_7$	−.11$_8$	−.11$_2$	−.19$_8$	−.03$_2$

R. D. and B.=Roth, Doepke, and Banse; J. and S.=Jaeger and von Steinwehr; D.=Dickinson; F. and W.=Fischer and Wrede.
NOTE.—Without introducing a significant error, item 13 may in all cases be taken as equal to 0.004an (being in most cases negligible) and item 22 may be taken as zero.

2. COMPUTATION FOR BENZOIC ACID

Columns 5 to 8, inclusive, of Table 3 show the details of the computation for benzoic acid in accordance with experimental data obtained in four different laboratories. In this computation the values shown for p_1 and m are the average values used by the experimenter. The actual values varied somewhat in the different experiments of the same set.

In the computation, the quantity ϕ has been taken as zero, although in each instance some oxygen was consumed in the formation of nitric acid. The inclusion of this quantity would, however, change the final value of $-\Delta U_R$ by less than 0.01 per cent of itself.

For comparison there are entered, as item 26, the values of the (per cent corr.) as computed from the simplified approximate formula (equation (82)).

3. COMPUTATION FOR A MIXTURE

The method of computing the correction for the combustion of mixtures may be illustrated by the case of oxalic acid.

Owing to the low heat of combustion of oxalic acid, the correction for this substance is the maximum which will ever be encountered. The heat of combustion of oxalic acid is however always determined by mixing it with some other material having a higher heat of combustion. The most precise data available for this substance appear to be those of Verkade, Hartman, and Coops,[16] who burned a mixture of oxalic acid with a "paraffin oil" (apparently a kerosene) using varying proportions of the two in different experiments. In order to obtain, from data of this character, the heat of combustion of oxalic acid under standard conditions, it is necessary to reduce to standard conditions the heat of combustion of the mixture and the heat of combustion of the paraffin oil and to take the difference of the reduced values. In Table 4 are given the experimental data and final results of two of the Verkade experiments. The two selected are those representing the extremes of the ratio of oxalic acid to paraffin oil.

TABLE 4.—*Heat of combustion of oxalic acid*

g of oxalic acid m	g of paraffin oil m'	Formula of mixture [1]	Temperature rise Δt_B	Calculated heat of combustion of oxalic acid H	100γ= per cent corr.	True heat of combustion for standard conditions $=-\Delta U_R/M$
1	2	3	4	5	6	7
			° *C.*	*g-cal.* 15/*g*		*g-cal.* 15/*g*
0.96620	0.39700	$CH_{1.836}O_{0.864}$	1.6690	678.8	0.661	674.3
1.97320	.31395	$CH_{1.879}O_{1.326}$	1.5900	676.9	.659	672.4

[1] Calculated on the assumption that the paraffin oil contained 15 per cent of hydrogen. For detail of calculation see Appendix II, p. 557.

The values, H, in column 5 are those computed by Verkade by the customary procedure, namely, by subtracting from the total heat the amount $m'H'$ and dividing the difference by m; H' being the heat of

[16] Verkade, P. E., Hartman, H., and Coops, J., Rec. trav. chim., vol. 45, p. 376, 1926.

combustion, per gram, of the paraffin oil as determined in a separate experiment in which m is made zero and m' such as to give about the same temperature rise, 1.6° C.

Now if 100 γ is the correction in per cent which must be subtracted from the values of H in column 5 in order to obtain the true value for the heat of combustion of oxalic acid under standard conditions, then it can be readily shown that

$$\gamma = \gamma_M + \frac{m'H'}{mH}\left(\gamma_M - \gamma'\right) \tag{83}$$

where 100 γ' is the corresponding per cent correction for the combustion of the paraffin oil alone and 100 γ_M the correction for the mixture of the oxalic acid and the paraffin oil.

In order to compute the corrections γ' and γ_M it is necessary to know the empirical composition of the paraffin oil used. This is not stated by Verkade, and consequently the actual corrections can not be computed. If, however, we proceed on the assumption that the oil is composed of 15 per cent hydrogen and 85 per cent carbon, we will obtain a value for 100 γ which at all events will be of the right order of magnitude and which will serve to illustrate the great importance of the correction in this instance.

In computing the corrections the volume of the bomb used by Verkade will be assumed to be 1/3 liter. The actual volume is unfortunately not stated by Verkade.

The computation of the correction γ_M for the two mixtures shown in Table 4, as well as the computation of γ' for the combustion of 0.450 g of the paraffin oil in the same bomb, is shown in Table 3, columns 9, 10, and 11.

Substituting these values in equation (83) we obtain the values of 100 γ shown in column 6 of Table 4 and the correspondingly corrected values of H shown in column 7.

XVII. CORRECTIONS FOR IRON WIRE AND FOR NITROGEN

Most of the existing heats of combustion have been corrected by the observers for the heats of formation of small amounts of Fe_2O_3 and of $HNO_3aq.$, the latter of which is formed when nitrogen is present in the oxygen used. If we call the corrections (in per cent) thus applied by the observer (per cent corr.$_{Fe}$) and (per cent corr.$_N$), respectively, then the amount of HNO_3 produced must have been

$$n_{HNO_3} = (\text{per cent corr.}_N) \times (-\Delta U_R) n/1{,}455, \text{ mole} \tag{84}$$

where 14.55 kg-cal.$_{15}$ is the total energy of formation, from N_2, O_2 and $H_2O(l)$ of 1 mole of $HNO_3aq.$ at the average normality $\frac{N}{4}$ and $(-\Delta U_R)$ is expressed in kg-cal.$_{15}$/mole.

The formation of this HNO_3 affects the situation principally in three ways. It changes the value of x, it reduces the amount of water vapor in the final system, and it affects the solubility of carbon dioxide in the water.

We shall consider the three effects separately.

The effect on x.—Since the amount of N_2 in the bomb before ignition is almost never recorded by the investigator and is usually not known to him, we shall make use of the approximate equivalence of the molecular weights and energy contents of N_2 and O_2 and shall assume that the N_2, except so far as it combines with the O_2, can be treated as so much excess O_2. Its only effect upon the quantity ΔU_{gas} will therefore reside in its effect upon x. A corresponding effect will also be produced by the combustion of any iron wire. These two effects will combine and equation (26) will read as follows:

$$x \quad \frac{an - n_D}{n_{O_2} - \left(\frac{b-2c}{4}\right) n - n_D - \phi_N - \phi_{Fe}} \tag{85}$$

in which ϕ_N is given by

$$\phi_N = \frac{7}{4} (\text{per cent corr.}_N)(-\Delta U_R) n/1{,}455 \tag{86}$$

and ϕ_{Fe}

$$\phi_{Fe} = \frac{3}{2} (\text{per cent corr.}_{Fe}) \ (-\Delta U_R) \ n/19{,}000 \tag{87}$$

Example

$$\phi_N = \frac{7}{4} (\text{per cent corr.}_N) \left(-\frac{\Delta U_R}{a}\right) an/1{,}455 \tag{88}$$

Put $\quad -\dfrac{\Delta U_R}{a} = 100$ and $(\text{per cent corr.}_N) = 0.2$

Hence

$$\phi_N = 0.024an$$

$$\phi_{Fe} = \frac{3}{2} (\text{per cent corr.}_{Fe}) \times 100an/19{,}000$$

$$= 0.0079 \ (\text{per cent corr.}_{Fe}) \ an \tag{89}$$

Put $(\text{per cent corr.}_{Fe}) = 0.05$.

Hence $\phi_{Fe} = 0.0_34an$.

Total

$$\phi_N + \phi_{Fe} = 0.0244an \tag{90}$$

which may be compared with $n_D = 0.004an$ and $n_{O_2} < 3an$, in equation (85).

It is obvious that the combustion of the iron wire in the amount ordinarily employed is wholly negligible as regards its effect upon x. The effect of the nitrogen on x is appreciable, but also probably negligible for all practical purposes. Since, however, its effect can be readily computed all doubt can be eliminated by computing the quantity x by means of equation (85).

Effect on $\Delta U_w^{\text{vap.}}$.—In the final system in the bomb the concentration of water vapor is (see equation (119), Appendix I).

$$C'_w = 0.0173 + (0.0_455 + 0.0_328x)p_2$$

$$= 0.0173 + 0.0_455 \times 30 + 0.0_328p_2x$$

$$= 0.019 + 0.0_328 \times 24an/V$$

$$= (0.019 + 0.0069an/V), \text{ g/liter} \tag{91}$$

If now the water contains HNO_3 at such concentration (N_{HNO_3} mole/liter) that its partial vapor pressure is reduced by the fractional amount $-\frac{\Delta p_w}{p_w}$, its concentration in the vapor will be reduced by the amount

$$\frac{-\Delta C'_w}{C'_w} = \frac{-\Delta p_w}{p_w} = 0.03 N_{HNO_3} \tag{92}$$

and

$$-\Delta C'_w = 0.03 N_{HNO_3}(0.019 + 0.0069an/V)$$

$$= \frac{[0.03(\text{per cent corr.}_N)(-\Delta U_R)n/1{,}455](0.019 + 0.0069an/V)}{(m_w + 9bn) \times 10^{-3}}$$

$$= \frac{0.0206(\text{per cent corr.}_N)(-\Delta U_R)n(0.019 + 0.0069an/V)}{(m_w + 9bn)}, \text{ g/liter} \tag{93}$$

The energy required to evaporate this water is therefore $22.82 V \Delta C'_w$ liter-atm.

or

$$\Delta(\Delta U_w^{\text{vap.}}) = \frac{0.0114 V(\text{per cent corr.}_N)(-\Delta U_R)n(0.019 + 0.0069an/V)}{m_w + 9bn} \tag{94}$$

or

$$\frac{100\Delta(\Delta U_w^{\text{vap.}})}{(-\Delta U_R)n} = \frac{1.14\ V\ (\text{per cent corr.}_N)\ (0.019 + 0.0069an/V)}{m_w + 9bn} \tag{95}$$

In practice an/V usually varies between 0.1 and 0.3, whence

$$\frac{100\Delta(\Delta U_w^{\text{vap.}})}{(-\Delta U_R)n} = \frac{1.14\ V\ (\text{per cent corr.}_N)\ (0.0203 \pm 0.0_38)}{m_w + 9bn}$$

$$= \frac{(0.023 \pm 0.0_39)\ V\ (\text{per cent corr.}_N)}{m_w + 9bn}$$

For $V = 1/3$ liter, (per cent corr.$_N$) $= 0.2$ and $m_w + 9bn = 1.5$ this gives 0.001 per cent, a wholly negligible quantity.

Effect on the amount of dissolved carbon dioxide.—There are no data on the solubility of carbon dioxide in aqueous solutions of nitric acid for CO_2-pressures of the magnitudes encountered in bomb calorimetry. For pressures in the neighborhood of 1 atmosphere the data in International Critical Tables (vol. 3, p. 279) indicate that the solubility of CO_2 in 1/4 N HNO_3 at 25°C. is about 0.9 per cent greater than in pure water. Such a difference would of course be negligible, since the total CO_2 correction will never exceed 0.06 per cent.

In view, however, of the various corrections and uncertainties introduced by the presence of nitrogen in the bomb it is obvious that in bomb calorimetry of the highest accuracy nitrogen-free oxygen should be employed and the air should be swept out of the bomb.

XVIII. REDUCTION OF BOMB CALORIMETRIC DATA TO A COMMON TEMPERATURE

In the actual calorimetric determination, the calorimeter and its contents undergo a rise in temperature

$$\Delta t_B = t_2 - t_1 \tag{96}$$

as a result of the bomb reaction. In order to obtain, from this observed temperature rise, the heat of the bomb process at some constant known temperature, t_H, it is necessary to know the effective heat capacity, s_I, of the initial system and/or the effective heat capacity, s_F, of the final system. The effective heat capacity of any system, substance or material is the quantity of heat which must be added thereto in order to raise its temperature from t to t', divided by $(t'-t)$.

If s_B is the effective heat capacity of the calorimetric system itself, then the heat evolved by the bomb process at the constant temperature, $t_H°$, will be

$$-\Delta U_B n = s_B(t_2 - t_1) + s_I(t_H - t_1) + s_F(t_2 - t_H) \qquad (97)$$

The temperature, t_H, may be any desired value whatsoever. If, as is usually the case (although not at all necessary), it is made equal to t_1 or to t_2, one of the terms in the above expression reduces to zero.

For use in equation (97) above, the following values (average for 25° C.) for s_I and s_F are sufficiently accurate for any value of Δt_B within the region of room temperatures.

$$s_I = 5.01n_{O_2} + 0.995m_w + 0.7V + \Sigma mc_p + 0.108m_{Fe}, \text{ cal.}_{15} \text{ deg.}^{-1}\text{C} \qquad (98)$$

$$s_F = 5.01n_{O_2} + 0.995m_w + 0.7V + 0.158m_{Fe} + n[(1.77_1 + 0.0112p_2)a + 7.74b + 2.5c] - 34n_{HNO_3}, \text{ cal.}_{15} \text{ deg.}^{-1}\text{C} \qquad (99)$$

in which

n_{O_2} = g-moles of O_2 in the bomb initially.
m_w = g of H_2O in the bomb initially.
V = volume of bomb in liter.
Σmc_p = the total heat capacity, at constant pressure, of the carbonaceous material or materials burned, cal.$_{15}$ deg.$^{-1}$ C.
n = the number of gram-formula-weights of carbonaceous material burned, the total composition of which is expressed by the empirical formula $C_aH_bO_c$.
$p_2 = p_1 + \Delta p$ = final pressure in the bomb.
m_{Fe} = g of iron wire burned to Fe_2O_3.
n_{HNO_3} = gram-formula-weights of HNO_3 formed.
= (per cent corr.)$_{HNO_3}$ $(-\Delta U_B)n/1{,}455$.
(Per cent corr.)$_{HNO_3}$ = per cent correction applied to $-\Delta U_B$ for the heat of formation of a small amount of HNO_3.

In deriving equations (98) and (99) account has been taken of the variation of the heat capacity of the gases and of the liquid water with pressure. The term $0.7V$ takes care of the latent heat of vaporization of the water and the term $34n_{HNO_3}$ of the heat capacity of the dissolved HNO_3.

XIX. THE TEMPERATURE COEFFICIENT OF THE HEAT OF COMBUSTION

Using the specific heat data given in International Critical Tables, the following equation, valid strictly over the interval between 20° and 30° C., but sufficiently accurate for all practical purposes over any temperature interval in the region of room temperatures, can be readily derived

$$\frac{100(\Delta U'_R - \Delta U_R)}{\Delta U_R(t'-t)} = \frac{-100}{-\Delta U_R}(1.78a+7.74b+2.492c-C^s_p), \text{ per cent per deg.} \quad (100)$$

in which $-\Delta U_R$ is the evolved heat of the reaction (decrease in intrinsic energy) for standard conditions and C^s_p the heat capacity (under constant pressure) of the substance, both for 1 gram-formula-weight and in $cal._{15}$ units. A survey of the existing data for CH and CHO compounds shows that in all cases this coefficient is less than 0.01 per cent per degree, and if we assume that it will never be applied over a range of more than 10°, then it is obvious that the allowable error in the coefficient is >0.0005; that is, >5 per cent of the coefficient itself.

The temperature coefficient of $-\Delta U_B$, the heat of the bomb process, differs from equation (100) only to a negligible extent for any temperature range in which it should ever be required. It can be obtained from the difference between equations (98) and (99).

XX. STANDARDIZING SUBSTANCES

The effective heat capacity of a bomb calorimeter is customarily determined by making a series of combustions with a substance for which the value of $-\Delta U_B$ is accurately known. The substance benzoic acid is the working standard chosen for this purpose and the value selected for its heat of combustion at 20° C. is based upon determinations made by several laboratories. The value selected in this way has been approved by the International Union of Chemistry as the official value of $-\Delta U_B$ for benzoic acid.

In specifying this particular value, however, the conditions under which it is valid are, unfortunately, inadequately defined. The conditions under which the various determinations of the value have been made were quite different in several respects, and the rather close agreement obtained by the different laboratories has apparently been interpreted as indicating that specification of these conditions is unnecessary. This, however, can not be the case, as will be shown below, and the close agreement obtained by the various observers must have resulted to a considerable degree from the fortuitous compensation of several influences and to some extent perhaps from an accidental compensation of errors.

XXI. STANDARD CONDITIONS FOR CALORIMETRIC STANDARDIZATIONS

For determining the thermal quantities associated with a chemical reaction or physical process it is essential to so define the initial and final states that the resultant thermal quantities will be utilizable for combining with other available thermodynamic data.

For the combustion of a standard substance used to determine the effective heat capacity of a calorimeter, however, this is not essential. All that is required is a sufficient definition of the initial conditions and a knowledge of the value of $-\Delta U_B$ for the substance under these conditions. For a given standardizing substance, for example benzoic acid, it is sufficient to specify the values of the following ratios: m/V, m_w/V, n_{O_2}/V, and the temperature, t_H.

m/V.—The mass of benzoic acid per liter of bomb space has in practice usually varied between about 1.9 and 3.9 g. Apparently

any convenient value between these limits might be selected as the standard value for this quantity.

m_w/V.—The mass of initial water per liter of bomb space has usually been about 3 g, and this is a satisfactory value.

n_{O_2}/V.—This factor will be completely determined, if the initial oxygen pressure at some temperature is specified. In practice this pressure, at room temperatures, has varied between about 22 and 45 atmospheres. Apparently any value within these limits is sufficient to ensure complete combustion, although more accurate data on this question are needed. Perhaps 30 atmospheres at 20° C. would be a good value to adopt.

Should it ever be necessary or desirable to depart from one or more of these standard conditions in using benzoic acid for standardizing a calorimeter, the corresponding change which should be made in the standard value of $-\Delta U_B$ is calculable.

Once having agreed upon the standard conditions, the tolerance for each value should also be stated. An example is shown in Table 5.

TABLE 5.—*Illustrating standard conditions and tolerances for benzoic acid as a standardizing substance for bomb calorimetry*

Assumed standard conditions	Assumed tolerance ±	Error produced by just exceeding the tolerance. ± per cent of $-\Delta U_B$
p_1=30 atmospheres at 20° C	1.0 atmosphere	0.003₄
$\frac{m}{V}$=3 g/liter	0.5 g/liter	.002₈
$\frac{m_w}{V}$=3 g/liter	0.3 g/liter	.001₁
Maximum error, per cent		.007

XXII. THE HEAT OF COMBUSTION OF STANDARD BENZOIC ACID

The various determinations of the heat of combustion of benzoic acid have recently been reviewed by Roth.[17] After reducing them to the same energy and mass units he finds the following values for 20° C.

	Int. kj. per g
Fischer and Wrede	26.449
Dickinson	26.436
Jaeger-v. Steinwehr	26.437
Roth, Doepke, Banse	26.433

Roth selects the average of the last three values, namely, 26.435, as the "best value."

Now the four determinations in question were obtained under different experimental conditions; that is, with different values of p_1, m/V, m_w/V, and the apparent good agreement is partly fortuitous. In order to compare these values we must first correct them to a common set of conditions. We shall adopt for this purpose the

[17] Roth, Z. physik. Chem., vol. 136, p. 317, 1928.

conditions $p_1=30$ atm., $m/V=3$ g/liter, and $m_w/V=3$ g/liter (see Table 5.) So corrected [18] the values become

	Int. kj. per g
Fischer and Wrede	26. 440
Dickinson	26. 439
Jaeger-v. Steinwehr	26. 427
Roth, Doepke, Banse	26. 430

The agreement is now not so good, but the average of all four is still 26.434 with an apparent uncertainty of not more than 7 joules. There is, therefore, no reason at the present time for changing the value adopted by the International Chemical Union, provided the standard conditions assumed above are also adopted. There is, however, need for new determinations of this important quantity under more exactly controlled conditions than have prevailed heretofore.

If now we assume the value 26.434 kj/g for $-\Delta U_B$ when $p_1=30$ atm., $m/V=3$ g/liter, and $m_w/V=3$ g/liter, then the value of $-\Delta U_R$ for the pure reaction

$$C_7H_6O_{2\,(s),\ 1\ atm.}+7\tfrac{1}{2}\,O_{2\,(g),\ 1\ atm.}=7CO_{2\,(g),\ 1\ atm.}+3H_2O_{(l),\ 1\ atm.}$$

will be 0.08 per cent less (see Table 3) or 26.413×122.05 kj. per gram-formula-weight.

It is, of course, this latter value (or rather the corresponding one for $-Q_p$, the heat of the pure reaction under a constant pressure of 1 atmosphere) which would appear for benzoic acid in tables of heats of combustion of chemical substances. The former value $-\Delta U_B$ is applicable only to the use of benzoic acid as a standardizing substance for bomb calorimetry.

APPENDIX I. CONCENTRATION OF SATURATED WATER VAPOR IN GASES AT VARIOUS PRESSURES

Within the pressure range involved in bomb calorimetry the concentration of saturated water vapor varies with the temperature according to the equation

$$\log_{10}C_w=\frac{A}{T}+I \tag{101}$$

A is a constant characteristic of water and independent of the composition and pressure of the gas phase. (See fig. 2.) I is a function of the composition and pressure of the gas phase.

For water at 25° C. and under its own vapor pressure, we have

$$C_w=\frac{m}{V}=0.02302\ \text{g/liter} \tag{102}$$

and for 70°

$$C_w=0.1967\ \text{g/liter} \tag{103}$$

Hence for equation (101) we find

$$\log_{10}C_{w(\text{g/liter})}=\frac{-2,117}{T}+(I=5.465) \tag{104}$$

[18] An additional correction for temperature has been applied to the Dickinson value since the writer is advised by Doctor Dickinson that this value is for 25° C. (approx.) instead of 20° C.

Within the range of pressures and gas compositions met with in bomb calorimetry the concentration of saturated water vapor varies with the pressure according to the equation

$$C_w = C_0 + \alpha P \tag{105}$$

C_0 is a temperature function only and α varies with the nature of the gas phase. Combining this equation with the preceding one we have

$$\log_{10}(C_0 + \alpha P) = \frac{-2{,}117}{T} + I \tag{106}$$

For N_2 at 50° C. Bartlett [19] found $C_0 + \alpha P = 0.095$ g/liter for $P = 50$ atmospheres

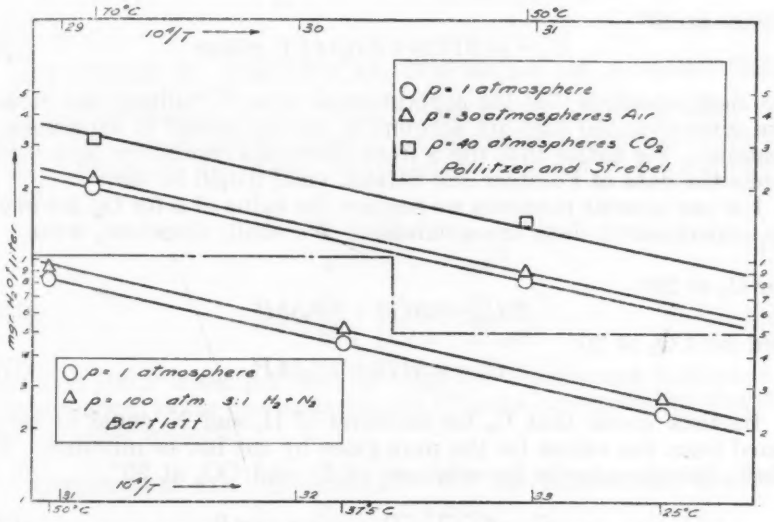

FIGURE 2.—*Temperature variation of the concentration of saturated water vapor in the presence of various gases*

Hence

$$I = 5.530 \tag{107}$$

and at 20° C. and 50 atmospheres

$$\log_{10}(C_0 + \alpha P) = \frac{-2{,}117}{293.1} + 5.530 \tag{108}$$

$$\log_{10} C_0 = \frac{-2{,}117}{293.1} + 5.465 \tag{109}$$

$$C_0 + \alpha P = 1.161 C_0 \tag{110}$$

$$C_0 = 0.01728 \tag{111}$$

$$\alpha = 0.0_4 56 \tag{112}$$

[19] F. P. Bartlett, J. Am. Chem. Soc., vol. 49, p. 65, 1927.

and

$$C_w = (0.01728 + 0.0_456P), \text{ g/liter for } P \text{ in atm.} \quad (113)$$

For air at 49.9° C. Pollitzer and Strebel [20] found

$$C_0 + \alpha P = 0.099, \text{ g/liter for } P = 72.5 \text{ atm.}$$

accuracy about 1 per cent. These data yield

$$C_w = (0.01728 + 0.0_450\ P), \text{ g/liter at } 20° \text{ C.} \quad (114)$$

For CO_2 at 49.9° C., Pollitzer and Strebel found

$$C_0 + \alpha P = 0.1443, \text{ g/liter for } P = 38.7_2 \text{ atm.}$$

Hence at 20°

$$C_w = (0.01728 + 0.0_334P), \text{ g/liter} \quad (115)$$

Bartlett considers that the experimental data of Pollitzer and Strebel are somewhat too high on account of certain errors in experimental technic. We notice that the α from Bartlett's results for N_2 is 0.0_456 while the data of Pollitzer and Strebel yield 0.0_450 for air.

For our present purposes we require the value of α for O_2, for which no experimental data are available. We shall, therefore, write

for O_2 at 20°

$$C_w = 0.0173 + 0.0_455P \quad (116)$$

and for CO_2 at 20°

$$C_w = 0.0173 + 0.0_334P \quad (117)$$

Bartlett found that C_w for mixtures of H_2 and N_2 could be calculated from the values for the pure gases by the law of mixtures. We shall, therefore, write for mixtures of O_2 and CO_2 at 20°.

$$C_w = C_0 + [\alpha_{O_2}(1-x) + \alpha_{CO_2}x]P \quad (118)$$

$$= 0.0173 + (0.0_455 + 0.0_328x)P \quad (119)$$

The quantity C_0 can be obtained from the expression

$$\log_{10} C_0 = \frac{-2{,}113}{T} + 5.453 \quad (120)$$

which is valid for room temperatures, 16° to 30°.

If C_w is the value for O_2 at the pressure p_1 and C'_w the value for an $O_2 - CO_2$ mixture at the pressure $p_2 = p_1 + \Delta p$, then

$$\Delta C_w = C'_w - C_w = \alpha_{CO_2}p_2x - \alpha_{O_2}(-\Delta p + xp_2) \quad (121)$$

$$= p_2x\left[0.0_334 - 0.0_305_5\left(1 - \frac{\Delta p}{p_2x}\right)\right], \text{ g/liter} \quad (122)$$

[20] F. Pollitzer and E. Strebel, Z. physik. Chem., vol. 110, p. 768, 1924.

For $p_2 = 22$ atm., $-\Delta p = 3$ atm., and $x = 0.3$, this being the most unfavorable case which could occur in bomb calorimetry when $\phi = 0$, we have

$$C'_w - C_w = 0.00171 \pm 3 \text{ per cent} \tag{123}$$

the uncertainty of 3 per cent arising from an estimated uncertainty of 10 per cent in the value assumed for α_{O_2}. From this it may be seen (p. 540) that the uncertainty in the value of α_{O_2} is of no practical importance.

Since (see equation (36))

$$p_2 x = \frac{RT}{V}(1 - 0.03)an \text{ (approx.)}$$

$$V\Delta C_w = 0.080T \times an\left[0.0_3 34 - 0.0_3 05_5\left(1 - \frac{\Delta p}{p_2 x}\right)\right], \text{ g; (approx.)} \tag{124}$$

at T°K.

APPENDIX II. EMPIRICAL FORMULA OF A MIXTURE

If two substances or materials containing no elements other than C, H, and O are mixed together in the proportions, m grams of the one and m' grams of the other, the empirical formula of the mixture is CH_bO_c

$$c = \frac{3(P_O m + P'_O m')}{4(P_C m + P'_C m')} \tag{125}$$

$$b = \frac{12}{1.008}\,\frac{(P_H m + P'_H m')}{(P_C m + P'_C m')} \tag{126}$$

in which 100 P is the per cent by weight of the element (indicated by the subscript) in the one material and P' is the corresponding quantity for the other material.

APPENDIX III. SUMMARY OF NUMERICAL DATA EMPLOYED

1. Atomic weights—

   C = 12.000.
   H = 1.0078.
   O = 16.

2. Coefficient μ in the equation $p = \frac{nRT(1 - \mu p)}{V}$ —

   For O_2 at 20° C, $\mu = 0.0_3 664$.
   For $O_2 - CO_2$ mixtures at 20°C., $\mu = 0.0_3 664[1 + 3.21x(1 + 1.33x)]$ where x is the mole fraction of CO_2.

3. Fractional vapor pressure lowering for aqueous solutions of strong electrolytes at 20° C. and N equivalents per liter

$$\frac{-\Delta p}{p} = 0.03N$$

4. Concentration of saturated water vapor in contact with gases at various pressures. (See Appendix I, p. 555.)

Total energy of vaporization at 20° C.—

$H_2O = 22.82$ liter-atm/g.

Dissolved gases from an aqueous solution at 20° C.—

CO_2—181 liter-atm/mole.

O_2—115 liter-atm/mole.

5. Total energy of compression as a function of the pressure (in atmospheres), at 20° C.

Units, liter-atm/mole.

O_2, $\Delta U]^p_0 = 0.0663p$.

CO_2, $\Delta U]^p_0 = 0.287p$.

$O_2 - CO_2$ mixtures, $\Delta U]^p_0 = 0.0663[1 + 1.70x(1+x)]p$, where x is the mole fraction of CO_2.

For solids and liquids. (See Table 1, p. 543.)

6. Total energy of formation at 20° C.—

$Fe_2O_{3(s)}$ from its elements = 190 kg-cal.$_{15}$/mole.

$\frac{1}{4}N$ $HNO_3aq.$ from $O_{2(g)}$, $N_{2(g)}$, and $H_2O_{(l)}$ = 14.55 kg-cal.$_{15}$/mole.

7. Heat capacity at constant volume and 30 atm.

O_2 at 25° C.—

$C_v = 5.01$ g-cal.$_{15}$/mole.

8. Solubility in water at 20° and a pressure of p atm.—

For O_2, $S_{O_2} = 1.2 \times 10^{-6} p$, mole/cm^3.

For CO_2, $S_{CO_2} = 0.0_3038_2 p$, mole/cm^3.

WASHINGTON, February 13, 1933.

THE INFLUENCE OF pH ON THE DETERIORATION OF VEGETABLE-TANNED LEATHER BY SULPHURIC ACID

By R. C. Bowker and E. L. Wallace

ABSTRACT

Thirteen different lots of vegetable-tanned leather were prepared, treated with varying amounts of sulphuric acid, tested for tensile strength, and placed in storage for two years, after which strength tests were again made. The loss in strength on aging was used as a measure of the deterioration, and the results are presented in a series of graphs as a function of the initial pH of the leather. It is shown that all of the leathers started to deteriorate at or near pH 3 regardless of the kind of vegetable-tanning material used, the degree of tannage, the amount of sulphuric acid added to the leather at the critical pH, the aging conditions, and the pH of the original leather before being treated with acid. The hydrolysis of the leathers, as measured by determining the nitrogen extractable with cold water, also increased sharply near pH 3. The results strongly indicate that vegetable-tanned leather will start to deteriorate at about this point whatever the combination of circumstances may be which causes it to have this critical value. Serious consideration of the value of a pH measurement for indicating the harmful acidity of leather is advocated, the limiting values for different leathers to be governed by the length of service expected and the conditions of use.

CONTENTS

	Page
I. Introduction	559
II. Materials and methods	560
III. Results and discussion	561
IV. Summary	565

I. INTRODUCTION

The determination of the acid content of leather has been a major research subject for many years. Since 1895 no less than 16 analytical methods have been proposed for directly determining this constituent of leather. The Proctor and Searle method, which involves ashing the leather with a substance capable of combining with sulphuric acid, is the chief one used in this country at the present time. In general, the recognized limitations of this method are: (1) The total acid present may not always be determined, (2) sulphur from any source present in the leather may be determined as acid, and (3) no indication is obtained relative to the presence of strong organic acids which may be harmful.

These limitations became of much greater importance as the development and increased use of sulphonated and sulphited leather-making materials proceeded. In this connection sulphonated oils, sulphited vegetable tanning materials, sulphite cellulose extract, and synthetic tanning materials (sulphonated condensation products from coal-tar crudes) may be mentioned. The use of these materials and also certain finishing products which contain strong organic acids or salts of these acids has made increasingly doubtful the value, by itself, of any of the known direct analytical methods for indicating the true acidity of leather.

The situation has logically led to an examination of pH methods for indicating the acidity of leather. Kohn and Crede [1] suggested making pH measurements of water solutions in equilibrium with finely divided leather and plotting neutralization curves for a sufficient number of leather samples of known tannage and wearing quality so as to establish a permissible upper limit for acidity. They further stated that all good leather samples tested in this way showed an initial pH value of about 3 or only slightly below 3. Since that time Pickard and Caunce,[2] Bradley and Cohen,[3] Innes,[4] Atkins and Thompson,[5] and Kubelka and Wolmarker,[6] have devised methods which involve the measurement of the pH values of leather and water systems.

An investigation of the effects of sulphuric acid on different vegetable-tanned leathers during storage has been in progress at this bureau for some years, and a number of reports have been issued [7] in which the deterioration of the leather measured by its loss in strength on aging, has been expressed as a function of the sulphuric acid present in the leather. As a part of this investigation pH measurements were made on all samples of leather before they were placed in storage. Data are now available for 13 different lots of vegetable-tanned leather, each treated with varying amounts of sulphuric acid and aged for two years, for an expression of deterioration as a function of the pH of the leather. It is the purpose of this report to present this information as additional evidence of the substantial value of pH measurements for evaluating leather with respect to acidity.

II. MATERIALS AND METHODS

The leather used in this work consisted of lot Nos. 1 to 12, inclusive, and lot No. 14. The method of preparing these leathers and the procedure followed in making aging tests have been adequately described in previous reports,[8] which also contain the chemical analyses and aging test results for lots Nos. 1 to 11, inclusive. No previous report has been made on lots Nos. 12 and 14, which were tanned with mangrove bark and sumac extracts, respectively. The chemical analyses of these two leathers are given in Table 1.

The A. L. C. A. methods were used for all analytical work on the leather excepting for the determination of the pH values and the amount of sulphuric acid added. The latter was checked by a modified wuensch method previously reported.[9]

The pH measurements were made in a water solution in equilibrium with finely divided leather, 4.9 g of dry leather being weighed into a beaker and 100 ml distilled water added. The system was allowed to stand overnight in order to reach equilibrium conditions; that is until no further variation in the pH value was observed on longer contact of the leather with water solution, before making a reading.

[1] The Acidity of Vegetable Tanned Leather, J. Am. Lea. Chem. Assoc., vol. 18, p. 189, 1923.
[2] J. Int. Soc. Lea. Tr. Chem., vol. 8, p. 156, 1924.
[3] J. Int. Soc. Lea. Tr. Chem., vol. 8, p. 340, 1924.
[4] J. Int. Soc. Lea. Tr. Chem., vol. 12, p. 256, 1928.
[5] J. Int. Soc. Lea. Tr. Chem., vol. 13, p. 300, 1929.
[6] Collegium, p. 96, 1931.
[7] J. Am. Lea. Chem. Assoc., vol. 23, p. 82, 1928; vol. 26, p. 444, 1931; vol. 26, p. 667, 1931; vol. 27, p. 81, 1932; vol. 27, p. 158, 1932.
[8] See footnote 7.
[9] See footnote 7.

Hydrogen electrodes of the Hildebrand type were used. A fresh electrode was used for making each pH measurement. This limitation on the use of the electrodes was necessary because of the poisoning effect of copper which was in the tanning extracts. The apparatus has been described in a previous report.[10]

TABLE 1.—*Chemical analyses of leathers*

[Results expressed in per cent, excepting for degree of tannage and pH values]

Tanned with—	Lot No. 12, mangrove	Lot No. 14, sumac
Water solubles	10.28	6.74
Hide substance	48.42	49.68
Grease (P. E. E.)	4.23	3.03
Moisture	9.70	7.49
Insoluble ash	.08	.15
Combined tannin [1]	27.29	32.91
Total	100.00	100.00
Degree of tannage [2]	56.40	66.50
Soluble tans	8.02	4.47
Soluble nontans	2.26	2.40
Total ash	.15	.14
Acid (P and S)	.12	.36
pH value [3]	5.19	3.71

[1] Determined by difference.
[2] Ratio of combined tannin to hide substance.
[3] 4.9 g of dry leather in 100 ml distilled water.

III. RESULTS AND DISCUSSION

The data compiled in this study are presented in Figures 1 to 4, inclusive. The arrangement is such that the ordinates show the percentage of the original strength of the leather after aging for two years, the amount of sulphuric acid added, and the original pH value of the leather before aging. The storage conditions, unless otherwise noted on the graphs, were constant at 65 per cent relative humidity and 70° F., in a room illuminated solely by electricity. Each point on the pH-strength curves represents the average of strength determinations on six specimens after aging compared with the average strength of six specimens cut from the same sample before aging. The points in some cases scatter badly until an apparent critical position is reached after which the downward trend, representing loss of strength, is clearly defined. The initial scattering of the points is characteristic of the strength variations of normal leather and emphasizes the advisability of using a large number of samples.

A glance at the pH-strength curves immediately reveals the important fact that each of the 13 leathers begins to show deterioration due to acid at or near pH 3, below which value the deterioration steadily increases. There is a well-defined break in the curves in every case near pH 3. It is important to note that this apparent critical point is common to all of the leathers without relation to the kind of tanning material used, the aging conditions, the amount of acid added to the leather, originally, the initial pH of the leather, or the degree of tannage. The extent of the variation of these factors may be observed readily on the graphs. It is of particular interest

[10] E. L. Wallace and John Beek, jr., A Comparison of the Quinhydrone and Hydrogen Electrodes in Solutions Containing Tannin, B. S. Jour. Research, vol. 4 (RP176), p. 737, 1930.

to note the acid added to bring the various leathers to pH 3. This varies from about 0.4 per cent for lot No. 4 to about 1.8 per cent for lot No. 3.

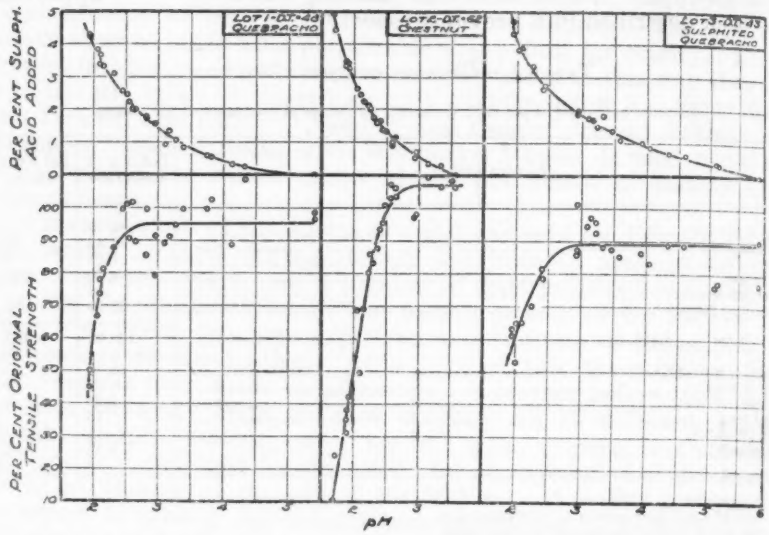

FIGURE 1.—*Results for lots Nos. 1, 2, and 3, showing acid added and loss of strength on aging as a function of pH*

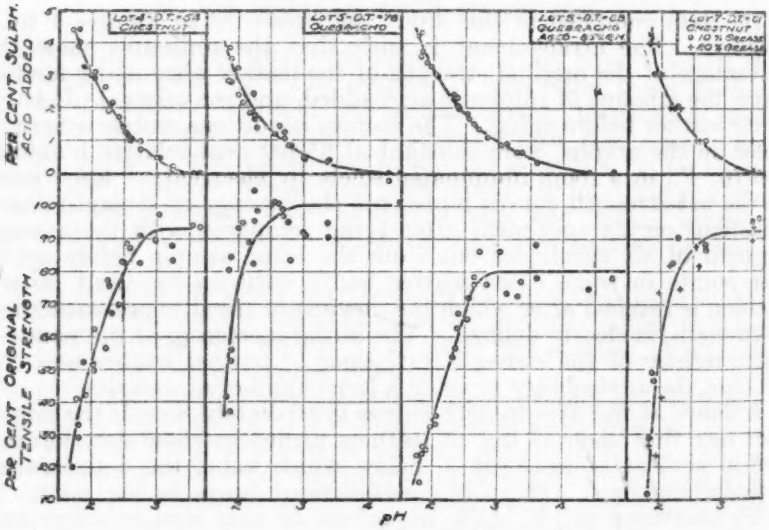

FIGURE 2.—*Results for lots Nos. 4, 5, 6, and 7, showing acid added and loss of strength on aging as a function of pH*

Since the pH at which deterioration starts appears to be independent of the above-mentioned variables it was considered that the critical point might be better located by averaging the results of all the 13 lots. This is done in the last graph of Figure 4 after moving the parts of the curves for zero per cent acid to a uniform base of 100.

Here again it is clear that deterioration starts at or near pH 3. This curve may be said to be typical of the shape of a pH-deterioration curve for any vegetable-tanned leather containing sulphuric acid al-

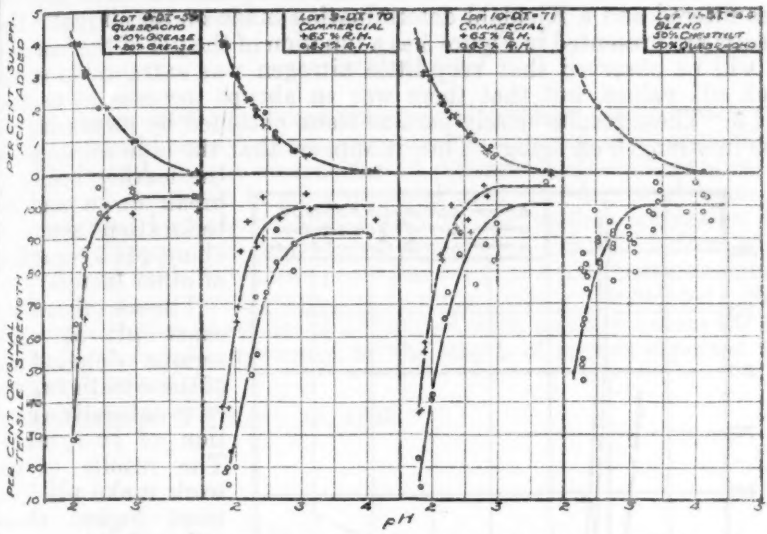

FIGURE 3.—*Results for lots Nos. 8, 9, 10, and 11, showing acid added and loss of strength on aging as a function of pH*

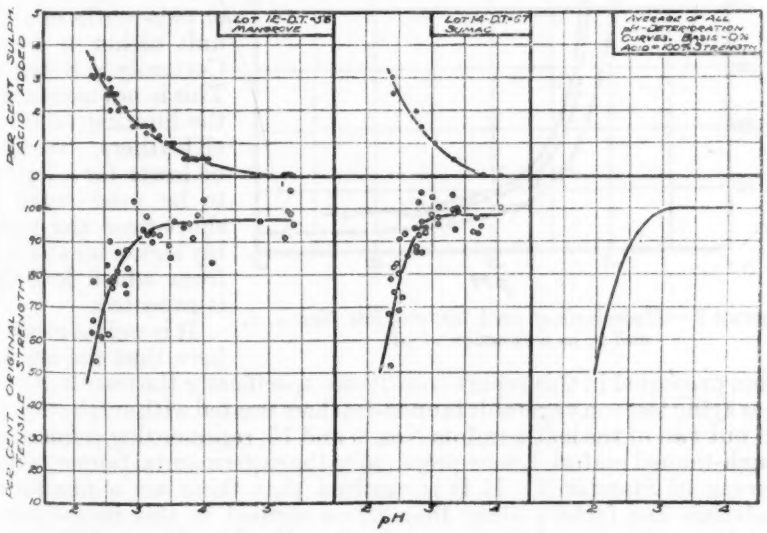

FIGURE 4.—*Results for lots Nos. 12 and 14, showing acid added and loss of strength on aging as a function of pH. Also average pH-strength curve for all lots*

though the portion of the curve below pH 3 may vary in its slope due to a difference in the rate of deterioration.

Since deterioration of all the leathers starts at about the same pH, it appears that the hide substance itself exerts the major influence.

Three of the aged leathers, lot No. 4 (chestnut), lot No. 6 (quebracho), and lot No. 9 (commercial), were examined for extractable nitrogen. Twenty-gram samples were extracted with 200 ml of distilled water in a shake-bottle for four hours at room temperature. The solution was filtered and a Kjeldahl determination made on an aliquot. The results are presented in Figure 5 as a function of the pH of the leathers. It will be observed that very little nitrogen was extractable at the high pH values, but that there was an abrupt increase at or near pH 3. These results closely parallel those obtained by measuring the loss in strength on aging. Thus it appears that the hide substance in the leather begins to break down and deterioration starts at about pH 3 regardless of other factors.

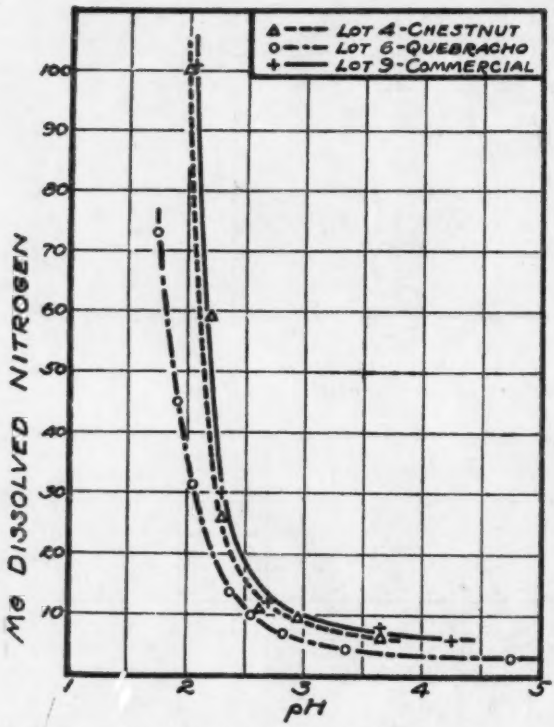

FIGURE 5.—*Hydrolysis of aged leathers, lots Nos. 4, 6, and 9, as a function of pH*

The selection of the exact pH at which serious deterioration of these leathers started is naturally a question of judgment. The results of this work make pH 3 the most logical choice atlhough it is conceivable that the actual value might be one- or two-tenths of a pH unit higher or lower. Certainly it is near 3. This is not necessarily the limiting value for all leathers. It might be lower for a leather to be used within a short time and possibly higher for a leather from which long life is expected.

It is well to mention here that the information presented in this report constitutes specifically the results of two-year aging tests on vegetable tanned-leathers treated with sulphuric acid. All but two of the leathers, lots Nos. 9 and 10, representing commercial rough-tanned material, were prepared in the experimental tannery at the Bureau of Standards. It is recognized that there are a number of materials and factors other than those studied in this investigation which may have an influence upon the pH of leather and the value of such a measurement for indicating harmful acidity. In this connection we now have in progress aging tests on typical leathers to determine the effect of sulphuric acid when sulphite cellulose extracts, synthetic tanning materials, sulphonated oils, glucose, and Epsom salts are also present. Typical leathers containing oxalic acid are also being studied. The results obtained thus far in a study of the

basic materials used in making leather substantiate the inference of Kohn and Crede that the minimum pH of good leather must be around 3, and appear to justify serious consideration of a pH measurement as a more reliable indication of harmful acidity in leather than any direct method now any use.

IV. SUMMARY

It is shown that pure vegetable-tanned leathers treated with sulphuric acid and aged for two years start to deteriorate at or near pH 3. This was found to be true for 13 different leathers regardless of the kind of vegetable tanning material used, the degree of tannage, the amount of sulphuric acid added to the leather originally, the aging conditions, and the pH of the original leather before being treated with acid. Thus the potential value of a pH measurement for evaluating leather with respect to harmful acidity is indicated. Serious consideration of its use is advocated with limiting values for different leathers to be governed by the length of service expected and the conditions of use.

WASHINGTON, February 13, 1933.

AN APPARATUS FOR MAGNETIC TESTING AT HIGH MAGNETIZING FORCES

By Raymond L. Sanford and Evert G. Bennett

ABSTRACT

Description of an apparatus suitable for general magnetic testing in the range of values of magnetizing force from 100 to 1,000 oersteds. Specimens of rectangular cross-section from one-half inch (1.27 cm) to 1½ inches (3.8 cm) in width and any thickness up to three-fourths inch (1.9 cm) can be tested with an accuracy estimated to be within 2 per cent. The apparatus is convenient and simple to operate, and does not heat the specimen.

CONTENTS

	Page
I. Introduction	567
II. Experimental investigation of the magnetic circuit	568
III. Description of apparatus	570
IV. Performance	571

I. INTRODUCTION

As a result of recent developments in magnetic materials, it has become necessary to increase the maximum value of magnetizing force used in magnetic testing. Whereas, previously, a maximum value of 300 oersteds was ample, forces up to 1,000 oersteds are now required. In the design of apparatus to work at these higher values of magnetizing force, two points in particular must be kept in mind if satisfactory results are to be obtained. First, the magnetic circuit must be of such a form that uniform magnetization is produced in the part of the specimen under test. Failure to meet this condition results in errors in the observed values of both magnetizing force and induction. Second, the apparatus should be so designed that heating of the specimen is avoided. The current required for the application of high magnetizing forces produces a considerable amount of heat which should not be allowed to raise the temperature of the specimen by as much as 5° C., since it is well known that even small changes in temperature alter the magnetic properties to an extent that can not be neglected.

The most obvious way to obtain uniform magnetization is by surrounding the specimen with the magnetizing coil. If this is done, however, some means of keeping the specimen cool, such as a water jacket, must be provided. This is not convenient and it seems better to adopt an arrangement based on the well-known isthmus method, with a magnetic circuit such as to give uniform magnetization.

An apparatus previously described[1] meets the requirements, but is not convenient for routine testing because a separate set of pole pieces and test coils is required for each different size of specimen. The present investigation was undertaken to see if it might not be possible to design a single set of pole pieces and test coils for this

[1] Sanford, A Method for the Standardization of Permeameters at High Magnetizing Forces, B. S. Jour. Research, vol. 6 (RP279), p. 355, 1931.

apparatus which would give satisfactory results for a considerable range of sizes of specimens. The final result was an apparatus capable of testing specimens of rectangular section from one-half inch (1.27 cm) to 1½ inches (3.8 cm) in width and any thickness up to three-fourths inch (1.9 cm). The accuracy is sufficient to meet ordinary commercial requirements in the range of magnetizing force values from 100 to 1,000 oersteds.

II. EXPERIMENTAL INVESTIGATION OF THE MAGNETIC CIRCUIT

The magnetic circuit is shown in Figure 1. The test specimen is clamped in pole pieces between two similar U-shaped yokes of laminated silicon steel upon which are wound the magnetizing coils. In the previous apparatus pole pieces 1 cm thick surrounded the test specimen at each end. In the present arrangement these pole pieces are replaced by simple laminated blocks of rectangular section 5 cm wide, 3 cm thick, and 12 cm long as shown in the figure. This change

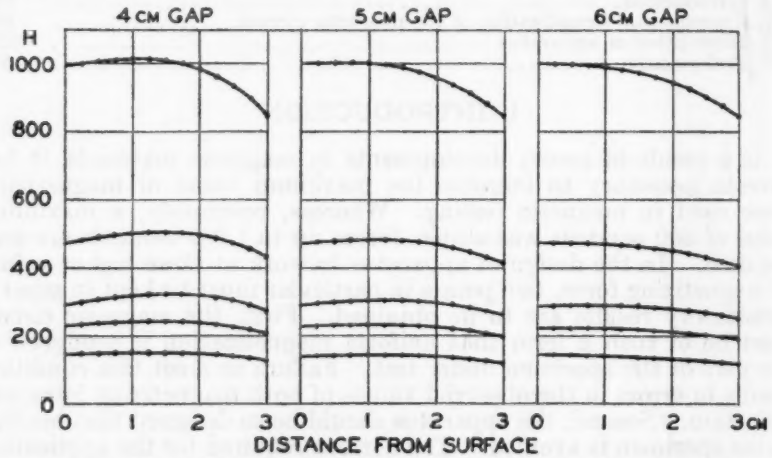

FIGURE 2.—*Radial distribution of the field for different lengths of gap*

was made so as to obviate the necessity of providing a separate set of pole pieces for each size of specimen to be tested.

In order to determine whether or not this circuit would prove to be satisfactory, and, if so, to fix upon the best gap length and test coil dimensions, the field between the ends of the pole pieces was explored by means of a small test coil.[2] Various gap lengths and thicknesses of specimen were used. The distribution of induction along the length of the specimen between the pole pieces was also determined for each condition.

Typical results of this exploration are shown in Figures 2 to 5. Figure 2 shows the radial distribution of the field with a specimen one-half inch thick. The 4 cm gap is evidently too short to obtain uniformity. However, for gaps of from 5 to 6 cm, the field is substantially uniform for a distance of at least 1 cm from the surface of the specimen. Figure 3 shows the longitudinal distribution of the

[2] A preliminary check on the uniformity of the field was made by means of an "iron-filing diagram" using "Magnaflux" iron powder. The diagram obtained is shown in Fig. 1.

B. S. Journal of Research, RP548

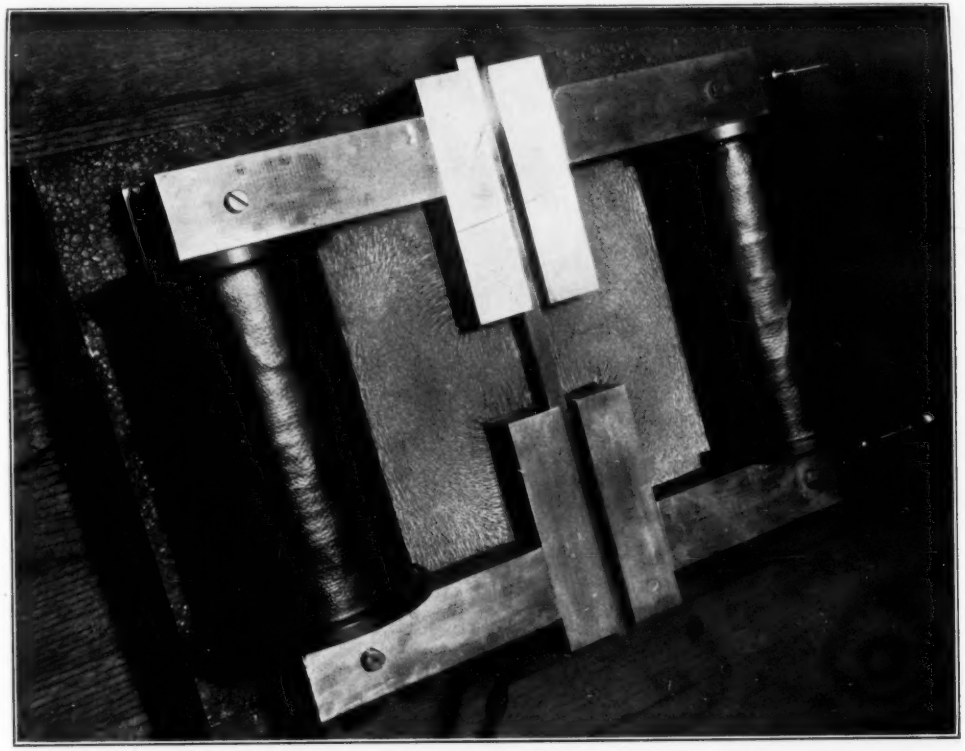

FIGURE 1.—*Magnetic circuit*

Uniformity of field is shown by the "iron-filing" diagram.

shows the longitudinal distribution of B for the different gaps. From these results it was concluded that with a test coil 1 cm long extending not over 1 cm from the surface of the specimen, the value of magnetizing force could be measured with a satisfactory degree of accuracy for a specimen one-half inch thick.

In order to determine the effect of variation in thickness of specimen, the tests were repeated with specimens one-fourth and three-fourths inch in thickness, respectively. The values obtained for the 5 cm gap are shown in Figure 5. There is some variation due to difference in thickness but not enough to cause an appreciable error.

III. DESCRIPTION OF APPARATUS

In the apparatus as finally constructed, each pair of pole pieces on the same side of the specimen is rigidly fastened together with brass strips above and below. The gap length is thus fixed at 5.5 cm

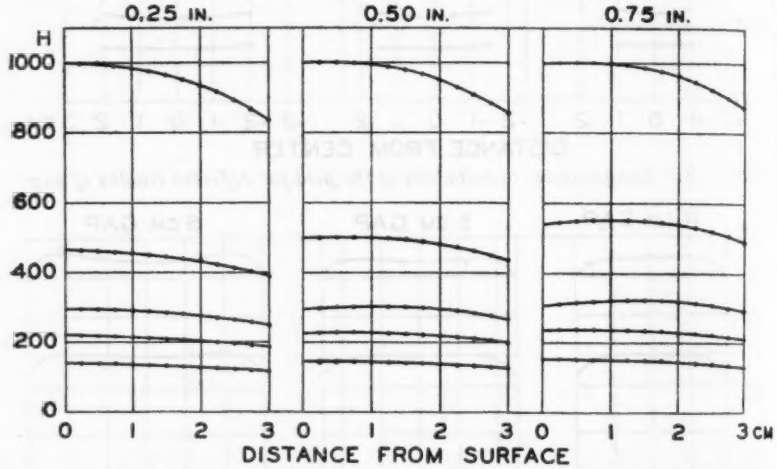

FIGURE 5.—*Radial distribution of the field for specimens of different values of thickness*

which appears to give the best average results. Between the brass strips on one side is mounted the test coil system.

The test coil system consists of three coils—a B coil, an H coil, and a compensating coil—each 1 cm long. The B coil of 25 turns is wound on a split brass form with hard rubber flanges. The coil opening is 2 by 4 cm. One vertical side is in line with the edge of the pole pieces so that a specimen clamped in place comes just in contact with the side of the coil. The H coil is wound on a solid hard rubber form 2.5 by 7.5 mm in cross section. The coil has 725 area turns which gives ample sensitivity. The compensating coil is wound over the H coil and has a number of area turns equal to that of the B coil with which it is connected in series, opposing. The function of this compensating coil is to eliminate the large air correction which would result from the use of a B coil of much larger area than that of the specimen. The combination of H coil and compensating coil is placed adjacent to the B coil so that the H coil comes within the uniform part of the field. The whole combination extends only slightly more than 1 cm from the surface of the specimen. The arrangement of the pole pieces and test-coil system is indicated in the diagram of Figure 6.

The pole pieces are not fastened to the yokes and can be removed so that the yokes can be used for other purposes.

The rest of the apparatus consists of a heavily over-damped ballistic galvanometer with the usual calibrating inductor, reversing switches, rheostats, etc.

IV. PERFORMANCE

After the apparatus was assembled in its final form, several tests were made to check its accuracy and to determine the influence of various factors encountered in general testing.

Check tests with the previous form of pole pieces and concentric test coils gave agreement within the experimental error and demon-

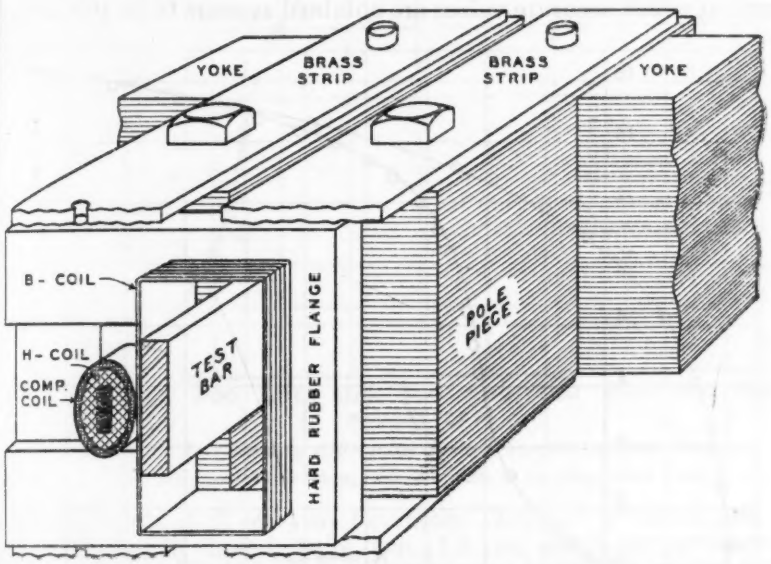

FIGURE 6.—*Arrangement of pole pieces and test coil system*

strated that the degree of reproducibility was satisfactory. It seemed desirable, however, to obtain a comparison with some entirely independent method of known accuracy. Fortunately, there was available a bar of hardened cobalt magnet steel 112 cm long. This bar which was furnished through the courtesy of L. E. Howard, director of research of the Simonds Saw & Steel Co., had been used in previous investigations and was known to have a satisfactory degree of uniformity along its length. The cross-section was approximately 1 by 2.5 cm. A 25-turn B coil was wound directly on the bar at the middle. A thin H coil was placed against this and a test made in a straight solenoid 90 cm long. The values thus obtained were taken as correct. The bar was then tested in the new apparatus and the results were compared. Figure 7 shows the agreement obtained. The full lines represent the results obtained with the solenoid and the circles indicate points obtained with the new apparatus. While the agreement is not perfect the differences do not exceed 1 per cent. It would have been desirable to repeat the tests with other bars of different cross sections but, unfortunately, satisfactory specimens were not available.

In order to determine the effect of the length of the specimen, a test was made on a bar 25 cm long. Equal lengths were then cut off from each end making the specimen only 7.5 cm long. This gave only 1 cm length of contact at each end. Some difference was noted in the steep part of the curve, but there was exact agreement in the upper part of the curve. The short length gave about 1 per cent higher value of residual induction and the same value of coercive force as found for the full length.

The lower limit of magnetizing force was determined by testing several uniform standard bars calibrated by means of the Burrows permeameter. For the low part of the curve the apparatus gives values of H which are too high. In all cases, however, the curves coincided for magnetizing forces of 100 oersteds or over so the lower limit at which accurate values are obtained appears to be 100 oersteds.

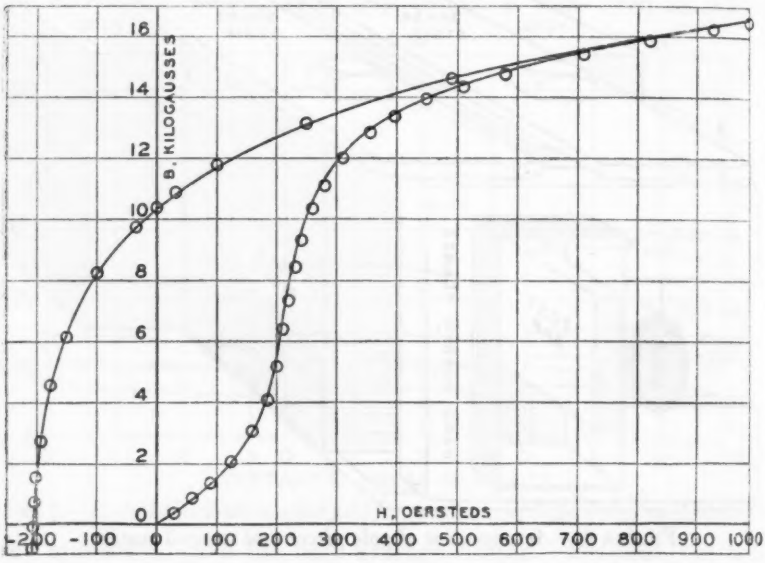

FIGURE 7.—*Comparison of results obtained by a long solenoid and by the new apparatus*

Full lines represent solenoid values; circles are points by the new apparatus

One possible source of error, especially for specimens of small cross section, is lack of uniformity of field throughout the area inclosed by the B coil. This would lead to incorrect compensation with a consequent error in the observed value of the induction. In order to determine the magnitude of this effect under the most unfavorable conditions, a test coil was wound directly on a specimen one-fourth inch thick and the results obtained with this coil were compared with those obtained with the compensated system. The compensated system gave values of induction slightly lower than those obtained with the coil wound on the specimen, but the difference was nowhere as great as 1 per cent. In Figure 8 the full line represents the curve obtained with the coil on the specimen and the circles represent points obtained with the compensated B coil.

In the light of these results, it appears that the apparatus is suitable for general magnetic testing within the range of magnetizing force values from 100 to 1,000 oersteds. The symmetrical magnetic circuit and absence of heating are distinct advantages. The apparatus is convenient and simple to operate and gives results on specimens from

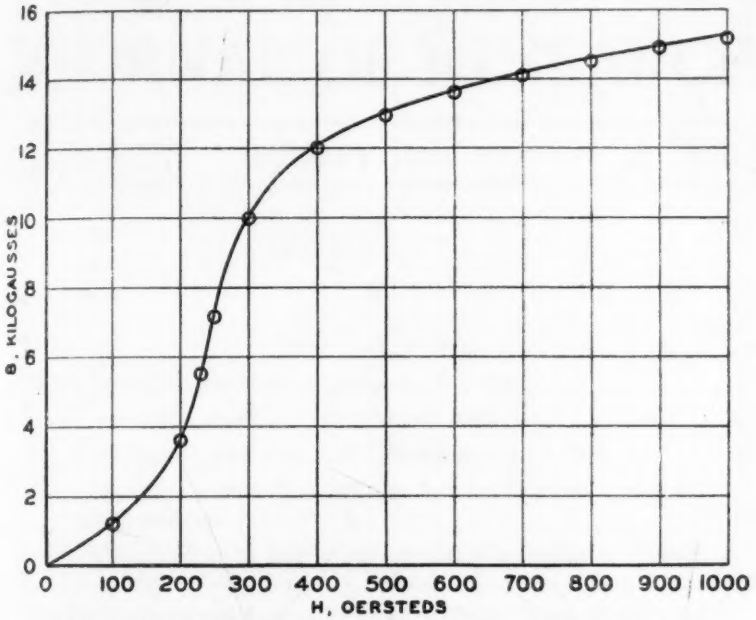

FIGURE 8.—*Showing differences due to imperfect compensation*
Full lines represent true values; circles are points by the compensated *B* coil

one-half inch (1.27 cm) to 1½ inches (3.8 cm) in width and any thickness up to three-fourths inch (1.9 cm) which are estimated to be accurate within 2 per cent. It has been adopted for routine testing in the magnetic measurements section of the Bureau of Standards.

WASHINGTON, January 31, 1933.